An investigation into the influence of local barometric stress upon xenobiotic percutaneous penetration

Dias Pereira Inacio, Ricardo Alexandre

Awarding institution:
King's College London

An investigation into the influence of local barometric stress upon xenobiotic percutaneous penetration

---

A thesis submitted by

Ricardo Alexandre Dias Pereira Inacio

In fulfilment of the requirement
for the degree of Doctor of Philosophy (PhD)
in Pharmaceutical Sciences

Department of Pharmacy
King's College London

October, 2015

Para ti Dianinha…

I thereby declare that the work described in this thesis is the result of my own independent investigation, unless otherwise stated.

This work has not been previously submitted for any other degree and is not being concurrently submitted in candidature for any other degree.

Ricardo Alexandre Dias Pereira Inacio

Abstract

Local barometric pressure changes at the apical surface of the skin have been reported to alter the mechanical and physiological properties of the cutaneous tissue. However, how skin changes induced by barometric pressure alter percutaneous penetration require further investigation. The aim of this study was to understand the effects of local barometric pressure changes upon cutaneous drug delivery with a view to understand if such an approach could be used to design a novel medicinal product. To accomplish this, one of the most widely used test systems for studying *in vitro* skin permeability, the Franz diffusion cell, was adapted to operate under sub-atmospheric pressure. Three relevant agents (tetracaine, diclofenac diethylamine and aciclovir) were selected, based upon their different physicochemical properties, and a suitable analytical method was developed for each molecule. The model agents were shown to aggregate in solution and the process of aggregation appeared to retard penetration into the skin. *In vitro* hypobaric driven delivery was shown to be an effective means to achieve 'targeting' of diclofenac diethylamine and aciclovir within the epidermal tissue after topical application of the aggregated agents. The calculated epidermal 'targeting' potential was 4 and 1.4 for each model agent, respectively. The mechanical and morphological changes in the hypobaric stressed skin showed that the 'targeted' drug deposition to the epidermal layer was accompanied by an enlargement of the follicular infundibula ($p < 0.001$), reduced corneocyte size ($p < 0.001$) and skin thinning ($p < 0.05$). These findings suggested that both enhanced follicular and passive *stratum corneum* transport played a role in the manner which hypobaric pressure improved cutaneous penetration. Local hypobaric stress application to the skin was also shown to induce a haemodynamic response (i.e. a significant increase in blood flow ($p < 0.001$)), which together with the ability to alter skin drug diffusion significantly enhanced cutaneous and systemic bioavailability ($p < 0.01$) of a model macromolecule. These results demonstrated that the application of topical barometric stress represented a promising technology to deliver molecules into the skin and it was thought worthy of further evaluation.

Acknowledgements

First I would like to express my gratitude to my supervisors for their continuous guidance and support with this project. I am extremely grateful to Dr Stuart Jones for his constructive advice and encouraging words that pushed me to work to my best ability. I am also extremely obliged to Dr Julie Keeble for her ongoing help and valuable input throughout the PhD process.

I would also like to thank my fellow PhD students of the Drug Delivery Research Group for their time and help, in particular to Jesmine Cai for her valuable expertise in AFM microscopy, Chen Hanpeng for his help in the lab and Simon Cleary for the support with the skin histological examinations. I wish also to acknowledge all the assistance from the pharmacy technicians and staff, especially Steve Ingham and Dan Asker for their much appreciated help. I am also particularly grateful to Dr Simon Poland for his guidance with multiphoton microscopy analysis, Dr David Barlow for the support with molecular dynamic studies and Dr Xiaole Kong for the help with pKa measurements.

I would like to thank my dearest parents for their patience, support and motivation. I also would like to give much appreciation to my family and friends in particular to Nuno, Carla and Paulo (para os Inacios).

Thank you Diana for your patience and love which has helped me to complete another step of our journey.

Table of Contents

List of Figures

List of Tables

List of Equations

List of Abbreviations

α_s	Thermodynamic activity
ΔC_s	Concentration gradient
ΔC_v	Concentration gradient
A	Skin area
ACN	Acetonitrile
ACV	Aciclovir
AFM	Atomic Force Microscopy
APC_s	Antigen-presenting cells
AUC	Area under de curve
A_s	Peak symmetry
CAC	Critical aggregation concentration
CaF_2	Calcium fluoride
C_{max}	Maximum blood concentration
C=O	Carbonyl group
C-O-H	Hydroxyl group
D	Diffusion coefficient
DDEA	Diclofenac diethylamine
Da	Dalton
D_2O	Deuterium oxide
FLPI	Full-Field Laser Perfusion Imaging
FTIR	Fourier Transform Infrared spectroscopy
HPLC	High Performance Liquid Chromatography
HPMC	Hydroxypropyl methylcellulose
^{1}H-NMR	Proton Nuclear Magnetic Resonance
h	Path length/ barrier thickness

ICH	International Conference on Harmonisation
J_{max}	Maximum rate of diffusion per unit time
J_{ss}	Steady-state flux
kp	Permeability coefficient
L	Lag time
LOD	Limit of detection
Log D	Distribution coefficient
Log *kp*	Skin permeability coefficient
Log P	Partition coefficient
LOQ	Limit of quantification
mBar	milibar
MeOH	Methanol
MW	Molecular Weight
NaCOOH	Sodium acetate
N-H	Amine group
PCS	Photon correlation spectroscopy
Q	Amount of solute
SC	*Stratum corneum*
SD	Standard deviation
S_s	Maximum solubility of a solute
TC	Tetracaine
TCH^+	Tetracaine tertiary amine
TCH_2^{2+}	Tetracaine secondary amine
TEWL	Transepidermal water loss
T_{max}	Time that a drug is present at the maximum concentration in the blood
VE	Viable epidermis
UV	Ultraviolet

CHAPTER ONE

Introduction

1.1 General introduction

Drug delivery via the skin is one of the most commonly employed routes of medicinal compound administration (Cross and Roberts, 2004). The cutaneous tissue can be used to deliver therapeutic agents within the skin strata (topical delivery) and to the systemic circulation (transdermal delivery). This route of administration offers several attractive traits such as the provision of a drug reservoir that can be removed from the body and the possibility of a convenient and pain free means to provide controlled release of a drug over 24 h from a single application (Guy and Hadgraft, 2003; Williams, 2003; Prausnitz *et al.*, 2004; Bronaugh and Maibach, 2005; Joshi and Raje, 2002; Roberts *et al.*, 2002).

Despite its frequent use in modern medical practise, drug delivery via the skin has yet to achieve its full potential (Prausnitz and Langer, 2008). This is due to the fact that the skin's stratified structure provides a formidable resistance to drug movement and currently available formulation technologies still struggle to provide targeted drug administration. The skin's main function is to prevent xenobiotic permeation and regulate transcutaneous water loss (Potts and Francoeur, 1991; Delgado-Charro and Guy, 2001). The outermost "horny layer" of the skin, the *stratum corneum* (*SC*), confers the greatest regulation potential for most agents due to its anatomy. In the *SC*, corneocytes are embedded within a lipid matrix and the architecture of this skin layer is commonly associated with a "brick and mortar" wall, as it gives a sense of both the *SC*'s structure and function. The *SC* and the multiple layers which are formed in the underlying epidermal tissue exhibit a selective permeability that only allows relatively small lipophilic compounds to efficiently penetrate into the dermis (< 500 Da, Log P 0.8 - 3 (Naik *et al.*, 2000; Barry, 1983)). The development of mathematical models to describe and predict skin permeability has strengthened the knowledge of how the

chemistry of drugs can be manipulated to increase passive permeability of agents into the skin. In addition, these models have contributed to the development of a broad range of strategies which facilitate compound penetration into the skin, including passive enhancement delivery methods (e.g. chemical enhancers, supersaturated systems) and physical enhancement methods (e.g. iontophoresis, sonophoresis). However, even using these drug delivery technologies trying to preferentially locate an agent in specific strata of the skin remains a challenge.

The ability to enhance drug delivery into the skin and then localise agents within specific strata of the cutaneous tissue (where the site of action lies) is desirable in a wide range of clinical conditions, including the treatment of neoplasias, inflammatory conditions or microbial infections (Brown *et al*., 2006). Inducing barometric stress to the apical surface of the skin affects its mechanical properties and the local vasculature and these changes could have a significant impact upon drug diffusion and localisation within the cutaneous tissue (Wojciechowski *et al*., 1985; Arora *et al*., 2008; Banga, 2011). Childers *et al*., (2007) has already demonstrated that a sub-atmospheric pressure of 500 mBar resulted in thinning of the epidermis and enlargement of blood vessels embedded in the dermis, hence this may be one means skin strata localised drug delivery could be achieved. However, the potential of this technology to enhance drug delivery via the skin is at the present poorly understood and this field warrants further investigation. It was the aim of this PhD project to investigate this area in greater depth and to facilitate this, the first task was to review the current understanding of the fundamental physiology of the skin layers and the manner in which drug transport is controlled across this barrier.

1.2 Skin structure and routes of permeation

The skin's highly complex structure and physiological organization dictates the pathway for drug permeation across the different strata. Therefore, several methods of enhancing drug delivery into the skin, including using barometric pressure, attempt to induce reversible alterations in the skin's structure. Hence, it is thought to be a valuable activity to review the current understanding of the skin structure and function at the start of the PhD project.

The skin is the largest and most readily accessible organ of the human body with a total weight of more than 3 kg and a surface area of 1.5 - 2 m^2 (Cevc, 1997). The main function of the skin is to act as a protective barrier from the outside environment. This protective function is achieved mainly by its physiological structure. The skin is a multilayered organ that structurally comprises two distinct main components: a stratified avascular outer cellular epidermis (*SC* and viable epidermis (VE)) and an underlying acellular dermis consisting of connective tissue (Figure 1.1). The properties of the skin strata are different and hence drug permeation through these barriers differs. The knowledge of the specific anatomy helps the design of a strategy to target cutaneous delivery.

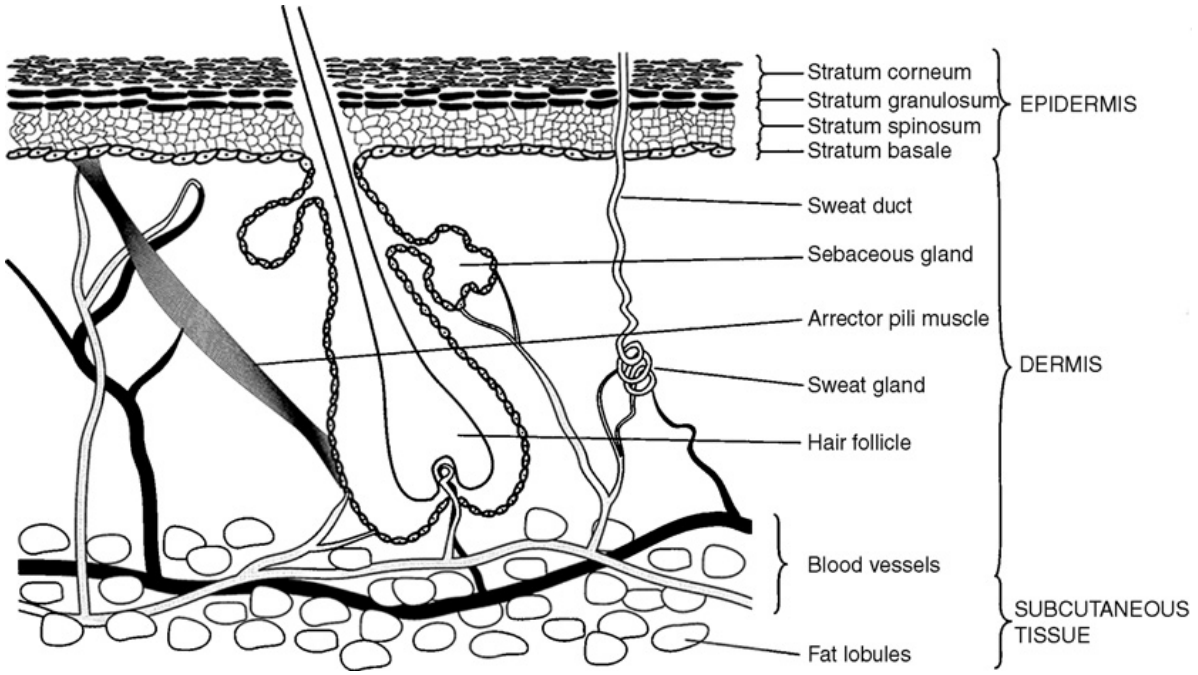

Figure 1.1. A diagrammatical representation of a cross-section through human skin showing the different cell layers and appendages, taken from (Williams, 2003).

1.2.1 Stratum corneum

The *SC*, or horny layer, is the outermost layer of the epidermis, which is often the focus for most delivery strategies that attempt to increase percutaneous penetration, as it presents a highly restrictive barrier. The thickness of this layer ranges between 10 and 20 μm (Bouwstra *et al.*, 2003; Huang *et al.*, 2005). Its "brick and mortar" structure (Figure 1.2) consists of 10-25 rows of dead keratinocytes (corneocytes) embedded in a lipid matrix (Bouwstra *et al.*, 1997; Norlen, 2008). The corneocytes represent the "bricks", which are flattened, elongated, dead cells, lacking nuclei and other organelles (Benson, 2005). It is important to note that the corneocytes are not brick shaped, but rather are polygonal, elongated and flat (0.2 -1.5 μm thick and 34 – 46 μm in diameter) (Benson, 2005).

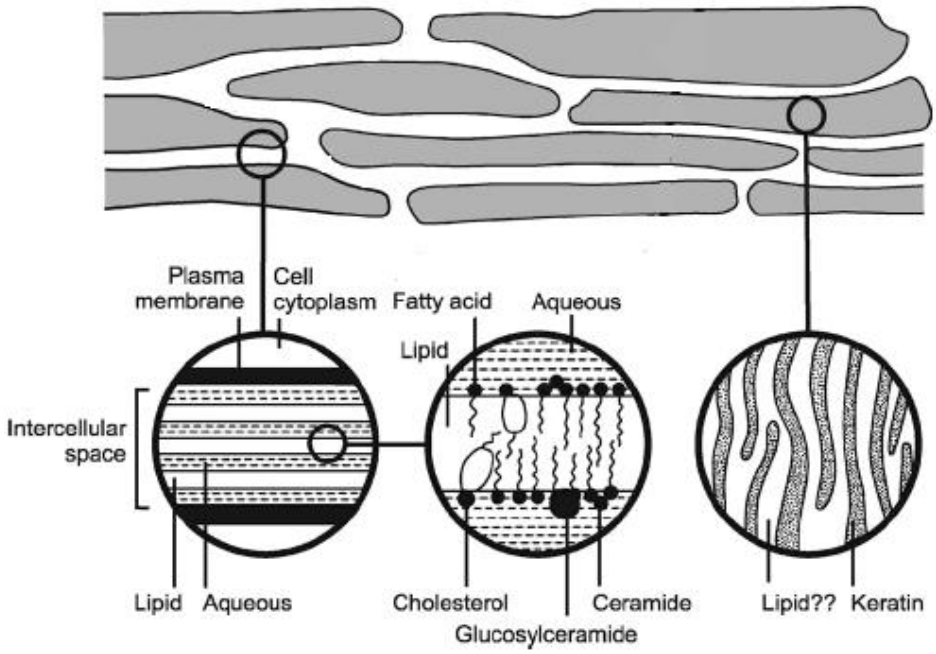

Figure 1.2. The "brick and mortar" structure of the *SC*, modified from (Williams and Barry, 1992).

The cells are joined together by desmosomes that maintain the cohesiveness of this layer (Menon, 2002). The heterogeneous structure of the *SC* is composed of approximately 75 - 80 % proteins, 5 – 15 % lipids and 5 – 10 % unidentified on a dry weight basis (Williams, 2003). The intercellular lipid matrix provides the "mortar" for the "bricks". This mortar chiefly comprises of ceramides, cholesterol, triglycerides and fatty acids, arranged into lipid lamellae. These lamellae are predominantly organised into bilayers (Michaels *et al*., 1975). The "brick and mortar" structure is primarily responsible for the *SC*'s ability to act as the main barrier of the skin. It functions to regulate both the permeation of xenobiotic compounds into the skin and endogenous compounds out of this tissue (Elias, 2005), but simply crossing the *SC* does not lead to strata localisation of therapeutic agents as increasing transport across the *SC* can result in more drug passage to the epidermal and dermal tissue.

Drug diffusion across the *SC* is achieved via an intercellular (i.e. restricted to the lipid matrix) or transcellular (i.e. through the corneocytes and lipid matrix) transport (Figure 1.3). Diffusion through these routes is dependent upon the drug's affinity with the lipid matrix, with the internal environment of the corneocyte and upon the ability to permeate the corneocyte envelop (Barry, 1987; Friberg *et al.*, 1990). The intercellular route is believed to be the dominant means of entry for most drugs (Yotsuyanagi and Higuchi, 1972; Potts and Francoeur, 1991; Tanner and Marks, 2008). However, via both routes penetration of the *SC* is a multistep process that involves partitioning into, diffusion through and partitioning out of the tissue. The transcellular route provides a larger area for diffusion and at the same time a shorter route to bypass the *SC*, but it also involves more partitioning and diffusion steps than the intercellular route. After partitioning into and diffusing through the relatively aqueous corneocytes, the drug following the transcellular route must partition into the surrounding lipid envelope and subsequently partition in and out of the multiple lipid bilayers that separate the corneocytes (Hadgraft and Guy, 1989). Drug enhancement strategies such as barometric stress can alter these passive diffusion pathways via the *SC* and/or it can modify the transappendageal cutaneous route (Figure 1.3) as discussed later. If passage of a molecule through the *SC* is successful then encounters the viable epidermis (VE).

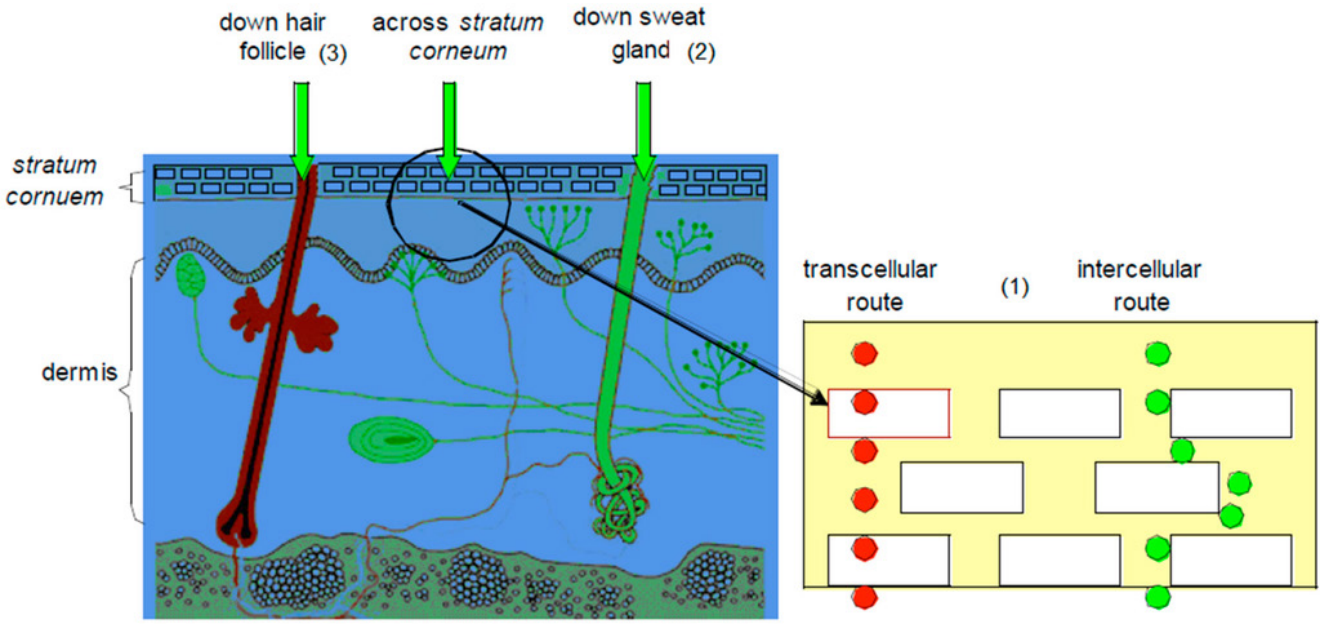

Figure 1.3. Permeation routes through the *SC*: 1) via the lipid matrix between the corneocytes (i.e. intercellular route) and across the corneocytes and lipid matrix (i.e. transcellular route), 2) via the sweat glands and 3) via de hair follicle (taken from (Daniels, 2007)).

1.2.2 The viable epidermis

Strategies to enhance drug delivery rarely act directly upon the VE as it lies below the *SC*, but this layer is the main site of action for a wide range of drugs applied to the skin for local action (Brown *et al.*, 2006). Its properties are different to the *SC* and therefore if one wishes to localise a drug in this strata, its anatomy and penetration routes must be compared to the *SC*.

The VE consists of a keratinized stratified squamous epithelium. The thickness of the epidermis ranges from 100 to 150 μm (Menon, 2002). The predominant cells are the

keratinocytes (Menon, 2002), which produce sulphur containing proteins, keratins and various lipids while differentiating and then gradually converting from live to dead fully keratinised cells as the cells move towards the skin's surface (Huang *et al*., 2005). The other non-keratinocyte cells present in the VE are the Langerhans' cells, which are involved in keratinocyte proliferation and skin sensitisation, and melanocytes, which generate and supply melanin granules to the keratinocytes (Barry, 2007). The keratinocytes are organized in layers above the basement membrane, reaching to the outer surface, which correspond to the consecutive steps of the vectorial process of keratinocyte maturation/differentiation (Figure 1.1). *The stratum basale* is a single layer of columnar or cuboid cells that are attached to the underlying irregular basement membrane by hemidesmosomes and laterally to each other and to the overlying *stratum spinosum* cells by desmosomes. The basal cells are constantly undergoing mitosis causing the off-spring to be displaced outward to keep the epidermis replenished as the *SC* cells are constantly being sloughed from the surface epidermis. This continual renewal of the epidermis takes place every 20 – 30 days (Delgado-Charro and Guy, 2001). The succeeding outer layer is the *stratum spinosum*, which consists of several layers of irregular polyhedral cells that become flattened as they reach the surface. These cells are connected to the adjacent *stratum spinosum* cells and the *stratum basale* cells below by desmosomes (Huang *et al*., 2005). The presence of numerous tonofilaments differentiates them morphologically from the other cell layers. The subsequent layer is the *stratum granulosum,* which comprises of numerous layers of flattened cells lying parallel to the epidermal - dermal junction. This layer contains irregularly shaped keratohyalin granules (Huang *et al*., 2005). These granules are thought to play a role in keratinization and barrier function. Another characteristic of this stratum is the presence of lipid containing lamellar granules. The three strata described above form the VE. Then, the *stratum lucidium* is the transition layer that consists of thin, translucent and homogenous strata. It is found only in

distinct anatomical areas of exceptionally thick skin and in hairless regions (e.g. plantar and palmar surfaces). It is formed of several layers of fully keratinized, closely compacted, dense cells devoid of nuclei and cytoplasmic organelles. Their cytoplasm contains protein-bound phospholipids and a keratin-like protein (Huang *et al*., 2005). Most researchers tend to view the *stratum lucidum* as the lower portion of the *SC* and thus bracket them together (note: Figure 1.1 does not show the *stratum lucidum*).

The fact that drug diffusion across the VE is heavily influenced by diffusion through an aqueous domain that is restricted by proteins and keratinocyte tight junctions (Bazzoni and Dejana, 2002; Brandner *et al*., 2006) means that hydrophobic drugs can be trapped in the *SC* without the ability to penetrate into the epidermis. It is primarily the higher water content of these strata that makes it a more efficient barrier to lipophilic permeant ingress (Scheuplein, 1971). Other factors may have a significant impact upon the penetration and retention of agents within this layer including drug metabolism and binding to cellular components (Liu *et al*., 1991; Hikima *et al*., 2002; Roberts *et al*., 2005). For example, Bhatt *et al*., (2008) reported a higher than expected amount of a lipophilic pesticide in the epidermal tissue (after a 48 h exposure) due to protein binding. The contribution of such processes is not always very clear, however it is generally accepted that they can have a significant impact on the amount of drug that can permeate into the underlying dermal tissue. Altering skin thickness and cutaneous blood flow by modifying barometric pressure applied to the skin may modify the properties of the VE and hence this could facilitate drug localisation in this layer or enhance penetration into the dermis.

1.2.3 The dermis

Immediately beneath the epidermis sits the dermis, which is the thickest component of the skin, up to 1 - 2 mm in depth (Bouwstra *et al.*, 2003). Its upper layer, the 100 - 200 μm thick papillary dermis, consists of thin collagen bundles, elastin fibres, fibrocytes, water, electrolytes, plasma proteins and polysaccharides - polypeptide complexes (Jakubovic *et al.*, 1992). Below this layer is the thicker reticular dermis, made up predominantly of collagen and elastin networks (Jakubovic *et al.*, 1992). While collagen bundles provide structural support, elastin fibres are more flexible and serve to anchor the epidermis to the dermis. The elastin adherence helps the skin to return to its original morphology after being stretched. Protected by the epidermal layer, the dermis houses the blood vessels, lymphatics and peripheral nervous system network within the skin, as well as the various skin appendages (Jepps *et al.*, 2013). Underneath the reticular dermis lies the hypodermis (subcutaneous fat tissue), which may have a thickness of up to several millimetres (Jepps *et al.*, 2013). It consists of fat microlobules and collagen bundles; it also houses the blood vessels, lymphatics and nerves. Its main functions are to store energy, to provide thermal insulation and to connect the skin to the underlying structures of the muscle and bone (Ritschel and Hussain, 1988; Jakubovic, 1992; Grams *et al.*, 2005). The dermal layer is the site of absorption of permeated solutes into the systemic circulation. Microvascular flow through the skin can vary by 100-fold depending on exogenous conditions, making it one of the most highly perfused organs in the body. The structural organization of the dermal microvasculature has been described in detail in the literature (Braveman, 1990).

Drug diffusion across the dermis is achieved in the same manner as described above for the VE, it acts as an aqueous barrier. However, the high vascularization of this layer has a

significant impact upon drug transport and localization of actives. In addition, to the local vasculature, the dermis presents several sites for binding and retention of molecules. The co-administration of vasoactive agents (known to alter drug absorption into the systemic circulation) has provided further knowledge of the function of the local vasculator in drug penetration and distribution (Riviere *et al.*, 1991; Singh *et al.*, 1994). Theoretically, vasodilatation should allow a greater absorption of drug into the systemic circulation and vasoconstriction is expected to have a contrary effect. Such effects have been experimentally confirmed for a variety of drugs such as lidocaine and flurbiprofen when co-administered with vasoactive agents (Riviere *et al.*, 1991; Sugibayashi *et al.*, 1999). Increased drug distributions at contralateral sites due to vasodilation (Cross *et al.*, 1999) and the opposite effect due to vasoconstriction (Higaki *et al.*, 2005) have also been reported. The skin appendages located within the dermal tissue may play a significant role upon percutaneous penetration; hence it is thought to be a valuable activity to review their anatomy and physiology.

1.2.4 Skin appendages

The skin appendages present a desirable means to target drug delivery directly to the epidermal and dermal tissue due to the possibility of avoiding the tortuous route through the *SC* (Delgado-Charro and Guy, 2001) (Figure 1.3). There are three main types of skin appendages, which traverse the skin and terminate in the dermis: hair follicles, sebaceous glands and sweat glands (eccrine and apocrine). The follicular opening extends to the sebaceous duct that connects the follicle with the sebaceous gland (Figure 1.1). This gland produces sebum that consists of free fatty acids, cholesterol, cholesterol esters, squalene, waxes and triglycerides (Valiveti *et al.*, 2008) that fills the infundibulum and serves different

roles such as lubricating the skin surface and maintaining the surface pH at around 5 (Williams, 2003; Barry, 2007). The follicle is covered by an epithelium layer that is a continuance of the *SC* and its thickness is gradually reduced along the structure (Scheuplein *et al.*, 1971; Grams *et al.*, 2005; Schaefer *et al.*, 2001). The heavily vascularized network that surrounds the follicular structure could have a significant impact upon drug diffusion of a permeant following this route (Jepps *et al.*, 2013; Jacobi *et al.*, 2006). Eccrine sweat glands are tubular structures which possess a coiled section located at the lower dermis (Figure 1.1). These glands produce sweat to help cool the body by evaporation, improve grip and sensitize the skin (Ritschel and Hussain, 1988; Jakubovic *et al.*, 1992; Montagna *et al.*, 1992). The apocrine glands resemble the eccrine glands however they are ten times larger than the latter and open to the infundibulum (Washington, 2001). Both the eccrine and apocrine glands are highly vascularized (Ellis, 1961; Hurley, 2001).

Among the different transappendageal pathways (Figure 1.3), the follicular route has been shown to provide encouraging results upon epidermal and dermal drug targeting and hence has received a great deal of attention over the past 10 years (Knorr *et al.*, 2009). Initially, these appendages were regarded to not significantly contribute to drug penetration because they represent only 0.1% of the total surface of the skin (Scheuplein, 1967). However, the low percentage of the available surface area is an underestimation of the actual surface area available for permeation, since the hair follicles extend deep through the skin surface past the dermis and hence allow drug delivery to this skin strata (Babiuk *et al.*, 2000). In addition, the possibility of interfollicular drug diffusion directly into the viable epidermis and the presence of a heavily vascularized network around the follicular route may have a significant impact upon drug localisation within the cutaneous tissue (Jepps *et al.*, 2013; Jacobi *et al.*, 2006; Rancan *et al.*, 2009). In fact, there have been some reports that suggest that the

transappendageal route may play an important role upon the permeation of actives, especially hydrophilic and large molecules (Huang *et al*., 2005; Wilke *et al*., 2006).

1.3 Parameters that influence percutaneous penetration

1.3.1 The influence of permeant characteristics

The permeant characteristics play an important role in the process of traversing the cutaneous tissue and mainly it is the interaction between the permeant and the tissue that dictate the rate of penetration and residence of the drug in a particular skin strata. The journey across the cutaneous tissue for many xenobiotics is not exclusively by one route; rather it involves utilisation of the intercellular, transcellular and transappendageal pathways to varying extents. The permeant characteristics influence the way the molecules approach the process of skin penetration and therefore this has an impact on any strategies to enhance transport and localise agents within specific strata of the cutaneous tissue.

The effect of partition coefficient (usually expressed as Log P, defines the ratio of partition between octanol/water), molecular size, hydrogen bonding and solubility have been considered to be the major characteristics that influence cutaneous drug delivery (Scheuplein and Blank, 1971; Michaels *et al*., 1975; Roberts, 1996). However, the relationship between permeant's physicochemical characteristics and hypobaric driven delivery has not yet been reported in the literature and this is one aspect of percutaneous administration that warrants further investigation. Hence, an understanding of the principal physicochemical characteristics that may influence drug permeation through the skin is required. There has been much academic debate as to which of these physicochemical characteristics are the most

important when one wishes to design a drug that will traverse the skin effectively. Barry, (1987) reported that the route of permeation through the skin is mainly determined by the permeant's partition coefficient as this is a good prediction of the route a molecule may move through the skin. Polar or hydrophilic molecules (Log P < 1) are thought to transport through the skin via the transcellular route (Williams, 2003) whereas lipophilic compounds (Log P > 1) are expected to travel along the intercellular route (Williams, 2003; Hadgraft *et al*., 1998). For highly hydrophilic, charged and large molecules the transappendageal route may be of more importance (Huang *et al*., 2005; Wilke *et al*., 2006). To achieve a good level of skin permeation an intermediate partition coefficient (Log $P_{octanol/water}$ between 1 and 3) has been reported to be ideal since it allows drug diffusion through the lipophilic lipid matrix of the *SC* and subsequent clearance into the lower hydrophilic VE and dermis. Molecular size has also been reported to be an important drug characteristic that influences the diffusion coefficient of a permeant (Potts and Guy, 1992). An inverse relationship between molecular size and percutaneous permeation has been established and some studies suggest that molecular size is the main determinant of permeant diffusion across the skin (Magnusson *et al*., 2004). It has been proposed that ideally a drug administered to the skin should display a molecular size of less than 500 Da (Bos and Meinardi, 2000). The hydrogen-bonding capacity of drugs has also been considered to have a significant role to play in percutaneous permeation (Roberts, 1976). The introduction of one hydrogen bounding group to a permeant was reported to significantly limit its ability to cross the skin, whereas the addition of extra groups resulted in less pronounced effects relative to the first binding site (Roberts, 1996).

Another important characteristic of a permeant is the solubility in the application vehicle. Since most topical products are formulated with a polar external phase, a certain degree of aqueous solubility is usually required since the flux of a drug moving across the cutaneous

tissue is dependant to some extent on the drug concentration in the application vehicle (as described in Section 1.5). In some cases, however, drug flux can still be obtained with only a small amount of dissolved drug in a topical delivery system, as this can be in equilibrium with precipitated drug within the vehicle. The undissolved drug can provide a drug reservoir at the apical surface of the skin because the movement through the barrier is typically quite slow, hence a constant rate of delivery can be achieved (Gupta *et al*., 1992).). The degree of ionisation of the permeant in the application vehicle can also influence percutaneous penetration. Unionized microspecies permeate easily through the *SC* due to their hydrophobic characteristics, whereas the ionized form displays low affinity to lipid domains and this usually results in poor permeation as described by the pH-partition hypothesis (Shore *et al*., 1957). However, despite the lower affinity of the ionised molecules to the *SC*, such molecules have been shown to pass through the skin and this may be related to their high aqueous solubility which may help the permeation through the cutaneous tissue (Barry, 2007). In addition, charged molecules can cross the skin via the transappendageal route (Horita *et al*., 2014; Barry, 1987). It is important to either measure or predict the manner in which the inherent properties of a drug will influence its transport through the skin, as normally it is difficult to change these characteristics without creating a new drug entity. Therefore, any attempts to enhance drug delivery or target specific skin strata must be tailored to the particular drug which wishes to be administered.

1.3.2 The influence of temperature, skin anatomy and physiology

Temperature, hydration of the *SC* and regional variation can also affect cutaneous penetration and localisation of a therapeutic agent within specific skin strata. One approach to enhance skin permeability is the application of heat (Mitragotri, 2006). For example, exposure to

prolonged moderate heating has been reported to enhance fentanyl skin penetration by 4-fold (Shomaker *et al*., 2000). However, controlling the application of heat during medical practise can be problematic and some heat patches have caused burning due to extreme variations of temperature in the products (Park *et al*., 2008). Hydration of the skin caused by topical formulation or transdermal patch occlusion of the skin tissue has been reported to increase skin permeability by 5 to 10-fold due to increasing the fluidity of the cells within the *SC* (Van Den Merwe and Ackermann, 1987). This effect can also be observed indirectly by an increase in the movement of water from the VE to the *SC*, commonly defined as transepidermal water loss (TEWL) (Blank *et al*., 1984). Other factors, such as drug metabolism, protein binding and blood flow can influence skin penetration and residence of actives within specific skin strata (as seen in Section 1.2). In addition, a different *SC* thickness, variation of the density of sebaceous glands, hair follicles and water content may result in different transport rates across several areas of the body. Prausnitz *et al*., (2012) suggested the rank of regional permeability to be as follows: << palm/sole < trunk/extremities < face/scalp << scrotum.

1.4 The prediction of percutaneous drug delivery

The evaluation of the effects of topical barometric stress upon percutaneous penetration and drug residence within specific skin strata should ideally be assessed under similar circumstances to those observed when administering a formulation to a patient. However, this approach would be extremely complicated and costly. The fundamental linking of the skin structure and the factors that alter drug penetration and residence within the cutaneous tissue drove the need for the development of predictive models and experimental methodologies (*in vitro* and *in vivo)* to determine the ability of novel technologies to enhance drug delivery via

the skin. As such, a series of laboratory based methods to determine the effects of hypobaric driven delivery upon percutaneous penetration including mathematical modelling, *in vitro* and *in vivo* techniques were employed in this project.

1.4.1 Mathematical models

The passive transport rate of a therapeutic agent through a confluent barrier can be described by mathematical representations of the chemical penetration process. Although the latter is typically measured at a set barometric pressure, this term is not typically included within the standard mathematical models that aim to describe drug passage across the cutaneous tissue. Nevertheless, the effects of skin changes (e.g. membrane thinning and blood flow) induced by barometric stress upon cutaneous drug penetration may be understood through mathematical representation of this process.

Although the penetration of therapeutic agents through the heterogeneous structure of the skin is a multifactorial process, scientists have simplified the approaches taken to understand the transport process (Barry, 1983). For example, one approach is to suggest that the main barrier for skin permeation lies in the non-viable *SC* and since solute transport across this layer is primarily by passive diffusion (Scheuplein and Blank, 1971) then solute mass transfer across the cutaneous tissue can be described by Fick's first law. This equation relates the amount of solute (Q), that is transported across the skin barrier of area, A, over a period of time, T, with a constant concentration gradient, ΔC_s, the diffusion coefficient in the skin barrier, D, and the path length, h (equation 1.1).

$$Q = DAT\Delta Cs/h \qquad \text{(Equation 1.1)}$$

The main assumptions of this model are that the *SC* barrier is a pseudo-homogeneous membrane and that its intrinsic barrier characteristics do not change during the solute transfer process. In the percutaneous penetration process, steady-state can only be achieved after the lag time (L) for permeant diffusion has passed. The lag time can be determined by the x-intercept of the linear portion of the cumulative solute amount as a function of time (Figure 1.4) and is dependent upon the diffusion coefficient in the skin barrier (D) and the barrier thickness (h) and is given by (equation 1.2) as demonstrated by Crank, (1975).

$$L = h^2/6D \qquad \text{(Equation 1.2)}$$

Equation 1.1 is often represented as steady-state flux, J_{SS}, as follows (equation 1.3).

$$J_{SS} = Q/(AT) = D\,\Delta C_s/h \qquad \text{(Equation 1.3)}$$

In vitro experiments are performed to generate J_{ss} as displayed in Figure 1.4. Using equation 1.3, other indices may then be derived.

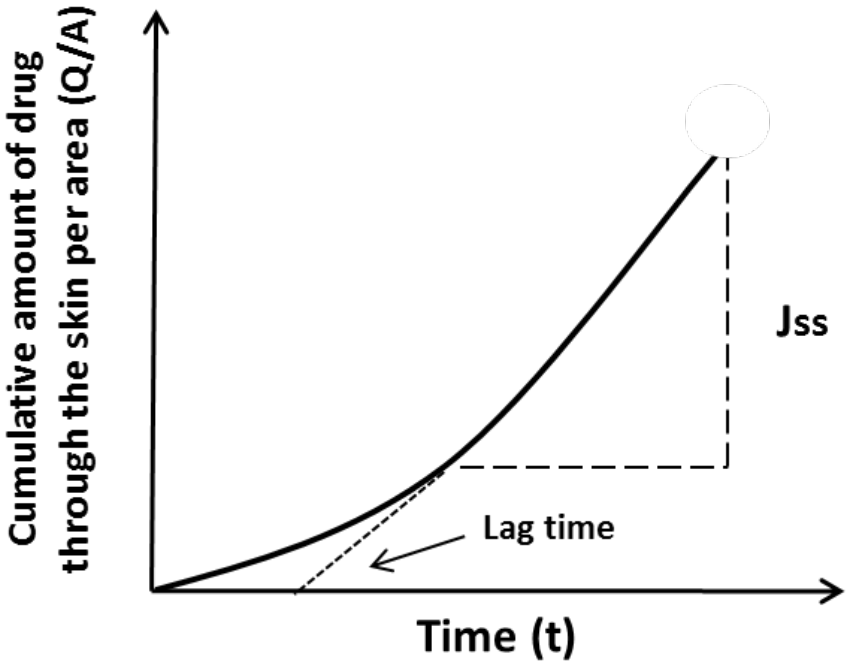

Figure 1.4. The cumulative mass per area (Q/A) permeating the skin as a function of time (t), may be modelled using equation 1.3 to obtain steady-state flux (J_{SS}). The lag time can be determined by the x-intercept of the linear portion of the cumulative amount (J_{SS}) as a function of time.

With the acknowledgment that solute mass transfer across the skin can be described by Fick's first law, Higuchi work revealed the significance of the thermodynamic activity of the permeant agent (Higuchi, 1960; Higuchi, 1961). This laid down a seminal principle for modern theories to follow in subsequent years. It was proposed that assuming that there is so little drug present on the basolateral side of the cell line that diffusion is occurring under 'sink conditions' the maximum rate of diffusion per unit time, (J_{max}), is proportional to the thermodynamic activity (α_s) of the compound and not its concentration (equation 1.1). The latter can be rewritten in terms of thermodynamic activity, where *D* is the diffusion

coefficient of the drug, S_s is the maximum solubility of a solute in the *SC* and h is the barrier thickness (Higuchi, 1961).

$$J_{max} = DS_s/h \quad \text{(Equation 1.4)}$$

According to this relationship, the flux of a compound from saturated solutions is constant, regardless of the saturated concentration in a given vehicle because all saturated solutions have a thermodynamic activity of 1 (Bronaugh and Maibach, 1989). However, this transport model makes several assumptions, including: mass transfer occurring under sink conditions, membrane rate controlled movement, the application vehicle does not affect the barrier, thermodynamic activity is homogenous throughout the formulation and only one compound is transported across the membrane (Higuchi, 1960). It is important to consider that non-linearity is likely to occur due to the heterogeneity of the cutaneous tissue that permits at least two possible routes (polar and non-polar). Several workers have built mathematical models that consider two diffusional layers: the non-viable lipophilic *SC* and the viable hydrophilic tissue that presents non-polar and polar routes (Chien, *et al.*, 1989; Anissimov and Roberts, 1999).

Quantitative structure-permeation relationship (QSPR) models attempt to determine the permeability coefficient (commonly presented as k_p) which represents the ratio of the steady-state flux of a permeant (J_{ss}) and the concentration gradient (ΔC_v), (equation 1.5).

$$k_p = J_{ss}/\Delta C_v \quad \text{(Equation 1.5)}$$

In most cases, the quantity of drug present on the basolateral side of the cell line is so little that k_p is represented by the ratio of J_{ss} and C_v. If one considers that the *SC* is the main barrier for drug permeation, k_p is represented by the product of the partition coefficient, *K* (*SC*/vehicle) and diffusion coefficient of the drug (*D*), normalized by the barrier thickness (*h*) as proposed by Crank, (1975) (equation 1.6).

$$k_p = K \,.D/h \qquad \text{(Equation 1.6)}$$

Many of the proposed QSPR models are based on the extensive dataset gathered and reported by Flynn, (1990). In this work, skin permeability coefficients were obtained from a simple algorithm derived from their octanol-water partition coefficients and molecular weight. Potts and Guy (1992) when analysing Flynn's dataset developed the QSPR that is now the most commonly used to estimate skin permeability. This mathematical model correlates skin permeability coefficient, *log* k_p, with the permeant's partition coefficient in octanol-water, *log* $P_{oct/w}$, and molecular weight, MW (equation 1.7).

$$\log \mathrm{K_p} = -6.3 + 0.71 \,.\log \mathrm{P_{oct/w}} - 0.0061 \,.\mathrm{MW} \quad (r^2 = 0.67,\ n = 93) \qquad \text{(Equation 1.7)}$$

Other mathematical models have been generated including parameters such as hydrogen bonding (Abraham *et al.*, 1997; Buchwald and Bodor, 2001), melting point (Barrat, 1995) and group contribution approaches (Pugh *et al.*, 1998). These additional factors can be more descriptive of the partition coefficient and hence, result in better fits of the model. Recent equations to predict skin permeability are based on empirical modelling, primarily using molecular descriptors. For example, neural networks are a good predictor for non-linear modelling of causal-effect relationships (Lim *et al.*, 2002).

1.4.2 In vitro methodologies

Different *in vitro* techniques have been employed to investigate drug percutaneous penetration and localisation within different skin strata. These approaches commonly involve the use of diffusion cells fitted with suitable membranes (e.g. silicone membrane, porcine skin) that operate under atmospheric pressure conditions. As such, to accomplish the aim of this PhD project, these methodologies needed adapting to operate under sub-atmospheric pressure and hence allow the transport of permeants across hypobaric stressed skin to be investigated.

Percutaneous penetration through a membrane fitted in a diffusion cell can be determined by measuring the cumulative drug appearance in the receptor cell (Figure 1.5) as a function of time (as shown in Figure 1.4), or a concentration-depth profile of the permeant within the different cutaneous layers can be evaluated to determine drug residence within specific skin strata. The most commonly employed diffusion cells are the static diffusion upright cells commonly designated as "Franz" type diffusion cells (Franz, 1975; Franz, 1978) (Figure 1.5). The donor solution traditionally consists of the test permeant in a vehicle (e.g. aqueous, buffer or formulation), which is applied to the apical surface of the membrane in order to initiate the permeation experiment. The receptor compartment contains the receiver solution that is a good solvent for the permeant and does not induce any alteration to the barrier properties of the selected membrane (Howes *et al.*, 1996). The receiver solution should also allow sink conditions (i.e. not exceeding 10% of the donor concentration and permeant saturated concentration in the spent receiver fluid) as this maintains a concentration gradient between the donor and receiver solution and hence, providing the driving force for the permeation process through the controlling barrier (Howes *et al.*, 1996). To aid the

maintenance of sink conditions throughout the experiment, stirring of the receiver solution is employed. The receiver solution should be at 37 °C in order to achieve a skin surface temperature of 32 °C (to mimic *in vivo* skin surface temperature (Maddock *et al*., 1933)). The amount of formulation applied in the donor compartment is either an infinite dose (i.e. > 10 $mg.cm^{-2}$), typically used when analysing the fundamental permeation behaviour of a test molecule or finite dose (i.e. between 2 and 10 $\mu g.cm^{-2}$) typically used to mimic the clinical application of a topical formulation (Howes *et al*., 1996). To ensure infinite dose throughout the duration of the study, fine suspensions of the permeant are often employed in the donor chamber of the Franz diffusion cell, to avoid any drug depletion and hence, guarantee a constant concentration gradient over a significant period of time. The selection of the vehicle to administer the test compound to the apical surface of the Franz cells is important because this process can have a large effect on the results obtained by this method. For most of the *in vitro* experiments aqueous based vehicles are employed because there is little deleterious influence of the vehicle upon the structure and barrier properties of the skin. However, buffering may be needed when there are issues related to the permeant ionization. The kinetic permeation profile is achieved by sampling the receiver fluid at defined time points and determining the amount of permeant in the receiver fluid using accurate and sensitive methods. Chromatographic methods (e.g. High Performance Liquid Chromatography) are most commonly used; however, when the detection sensitivity is a problem radiolabelled permeants (e.g. tritium ^{3}H and ^{14}C) can be employed. Skin components may leach during permeation studies due to the close contact with the receiver solution and hence, any analytical perturbation should be avoided.

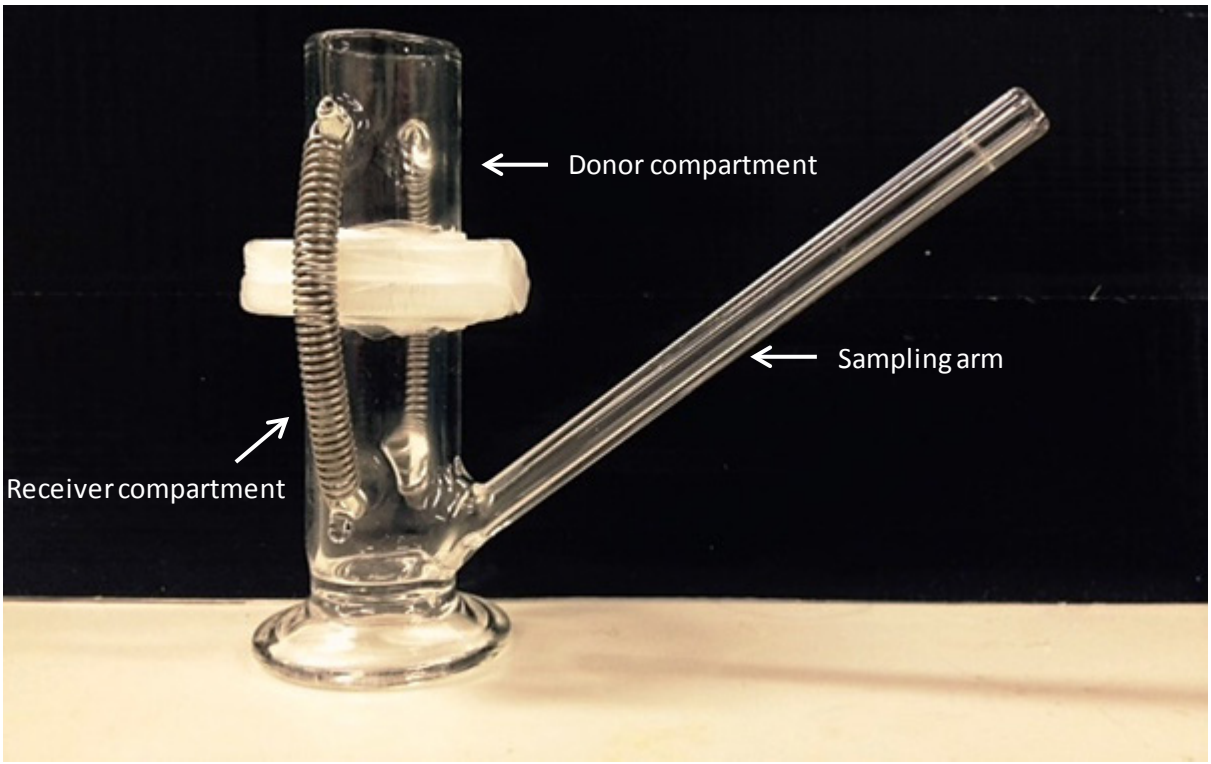

Figure 1.5. A "Franz" type diffusion cell. The formulation is placed in the donor compartment and the diffusion of the drug through the membrane into the receptor is measured by taking samples at different time points through the sampling arm. The receptor phase is constantly mixed with a magnetic flea during this procedure.

Since the structure and barrier properties of the skin are maintained following excision (Franz, 1975; Franz, 1978; Howes *et al*., 1996), *ex-vivo* Franz cell models using human tissue have been developed and shown to provide a reliable prediction of the dermal absorption in man. Human skin is the most relevant membrane to predict drug delivery across the cutaneous tissue; however, due to the cost and lack of availability and variability, alternatives have been employed to mimic the skin barrier properties. Investigations employing diffusion cells fitted with artificial membranes have been widely used to study the *in vitro* percutaneous penetration behaviour and the impact of the formulation composition upon the

flux rate of a test compound (Twist and Zatz, 1986; Feldstein *et al*., 1998; Houk and Guy, 1988). This technique is cost-effective, the isotropic nature of the membrane results in higher reproducibility and the permeation kinetics can be described by simple mathematical models. The most commonly used are the polydimethylsiloxane membranes (e.g. silicone) that provide a non-porous hydrophobic confluent barrier, which allows the diffusion of water and hence, mimicking the TEWL process during permeation studies. Several animal membranes have also been used *in vitro* (Twist and Zatz, 1986; Feldstein *et al*., 1998; Houk and Guy, 1988). Due to its availability, rodent and porcine skin are commonly used to perform *in vitro* permeation studies. Porcine skin is the most relevant animal model (apart of primates) to human skin *in vitro* due to its similar histological and biochemical properties, albeit the diameter of the follicular opening to the surface is larger (Gray and Yardley, 1975; Jacobi *et al*., 2007). Permeation profiles obtained across porcine skin have been reported to be in good agreement when compared with those generated through human skin (Schmook *et al*., 2001; Singh *et al*., 2002). Among rodents, rat skin has more anatomical similarities to human skin; however, rodent skin normally shows higher permeation rates than human skin (Sato *et al*., 1991; Nicoli *et al*., 2008). Other alternatives such as skin equivalents (Schmook *et al*., 2001; Godin and Touitou, 2007; Roy *et al*., 1993), human reconstructed epidermis (Netzlaff *et al*., 2005; Schmook *et al*., 2001; Godin and Touitou, 2007) and lipids from the *SC* (Matsuzaki *et al*., 1993) have recently been employed as model membranes to mimic human skin *in vivo*.

The amount of permeant detected in the receiver solution allows the assessment of the penetration process across the skin. In addition, the concentration-depth profile of the drug within the different strata of the skin may be used to determine the kinetics and contribution of each diffusional layer to the permeation process. Drug deposition profile is time dependent and varies with the permeant's physicochemical properties. Different techniques have been

employed and described in the literature to determine the amount of drug retained in the *SC*, VE and dermis, but the most reported one is tape stripping, which determines drug concentration within the *SC* (Pellett *et al.*, 1997; Shah, 1998; Pershing *et al.*, 1990; Stinchcomb *et al.*, 1999). During tape stripping of the skin the *SC* layers are progressively removed by successive tape applications. The drug is extracted from the strips using a suitable solvent and quantified using an appropriate sensitive analytical method such as HPLC or scintillation counting (Tsai *et al.*, 1999; Schwarb *et al.*, 1999; Wester *et al.*, 1998). This procedure is non-invasive and has been employed in bioequivalence testing (Pershing *et al.*, 1994; Shah *et al.*, 1998). In order to remove the *SC* homogeneously, a roller (Weigmann *et al.*, 1999), a constant weight (Shah *et al.*, 1998) or a spatula (Marttin *et al.*, 1996) can be used to allow the application of the tape under similar pressure conditions, as this improves the contact between the tape and the *SC*. In addition, the velocity of tape stripping should be maintained constant throughout the procedure to ensure that the amount of *SC* adhered to the tape is uniform (Landemann *et al.*, 2009). The first strip is often discarded since this represents unabsorbed drug on the skin surface (Landemann *et al.*, 2009) and the drug is quantified. After removal of the *SC* by tape stripping the VE is separated from the dermis, each skin layer is finely minced with scissors or using a tissue homogenizer and the drug is extracted using a suitable solvent. Then, the amount of drug is quantified with an appropriate sensitive method (e.g. HPLC or scintillation counting for radiolabeled compounds). Several techniques to separate the epidermis from the dermis have been reported such as by gentle teasing with the needle-type forceps (Lehman *et al.*, 1988; Lehman and Malany, 1989), with a scalpel (Surber *et al.*, 1991; Ferreira *et al.*, 1995; Ayub *et al.*, 2007; Argenta *et al.*, 2014) and employing a freezing microtome (Kammerau *et al.*, 1975; Schaefer and Stuttgen, 1976). Every method employed should be shown to be reproducible and the drug recovery extraction procedures need to be developed and validated prior to the start of the experiments. The

regulatory guidelines define 100 ± 15% as of the drug amount that should be recovered at the end of each experiment (Health and consumer protection directorate-general, 2006). The *in vitro* assessment of cutaneous drug delivery is often used to support *in vivo* measurements because it is cheaper, faster and there are no concerns with ethical issue or housing animals (Russell and Guy, 2009). However, it is recognized that *in vivo* studies usually must be completed to validate science concepts, such as the effects of topical barometric stress described in this PhD thesis, as they provide realistic measurement of the penetration process in intact skin (e.g. the cutaneous microvascular flow is present).

1.4.3 In vivo methodologies

Inducing barometric stress to the apical surface of the skin affects the cutaneous microcirculation and local blood flow changes could have a significant impact upon drug diffusion and localisation within specific skin strata (Wojciechowski *et al.*, 1985; Arora *et al.*, 2008; Banga, 2011; Childers *et al.*, 2007). Animal models provide a useful tool to access the effects of the cutaneous blood flow upon xenobiotic penetration into the cutaneous tissue (Godin and Touitou, 2007). Briefly, the formulation is administered during a fixed period of time to a specific area of the skin and the cutaneous absorption is determined by measuring the amount of drug present in the skin layers and/or in the blood or urine. The data can be used to determine the systemic bioavailability of the drug and/or its metabolites in the plasma or urine (Akrill *et al.*, 2002; Brooke *et al.*, 1998; Roberts and Cross, 1999; Singh and Roberts, 1994).

Other method that has been proposed to study the pharmacokinetics of cutaneous absorption is microdialysis (Kreilgard, 2000; Morgan *et al.*, 2003; Schnetz *et al.*, 2001). The technique

consists on the passive diffusion through a semipermeable dialysis membrane of a microdialysis probe that is inserted into the dermis parallel to the site of interest. The probe is slowly perfused with a site compatible physiological solution, mimicking the blood flow (Kreilgard, 2000; Morgan *et al*., 2003; Schnetz *et al*., 2001). The technique presents several advantages such as avoidance of reference exposure, possibility to study skin metabolism and several sampling sites can be studied at the same time (Kezic, 2008). However, this technique is not suitable for the study of large or highly protein-bound compounds due to the low recovery rates (Kezic, 2008). Further, the insertion of the probe causes a skin reaction that may influence the cutaneous absorption process (Kezic, 2008).

Tape stripping can also be employed to study *in vivo* topical absorption. The fundamentals of this methodology are similar to that previously described in *in vitro* studies (Section 1.4.2). Since the *SC* is the main barrier for drug absorption, it is anticipated that the pharmacokinetics of cutaneous absorption across this layer are related to topical bioavailability (Russell and Guy, 2009). Different topical administration times may be employed or stripping of the *SC* delayed after removal of the formulation to assess *SC* clearance and derive pharmacokinetic parameters (Russell and Guy, 2009). A good relationship has been demonstrated between the reservoir effect of the *SC* and percutaneous absorption of drugs (Rougier *et al*., 1983). In addition, this effect was found to be independent of the main factors likely to influence cutaneous absorption such as contact time, animal species or dose applied (Rougier and Lotte, 1993).

Another commonly used *in vivo* technique to predict cutaneous absorption is to assess a biological/pharmacological response (Mckenzie and Stoughton, 1962; Barry and Woodford, 1976; Pershing *et al*., 2002; Mura *et al*., 2007). A drawback of employing this methodology

is that it is only appropriated for drugs that exhibit an easily measurable response. One example of a pharmacological response is the effect of an anti-inflammatory drug on the carrageenan induced paw edema (Halici *et al*., 2007). Several spectroscopic methods such as attenuated total reflectance Fourier transform infrared spectroscopy (Klimich and Chandra, 1986; Naik *et al*., 1995), remittance spectroscopy (Feather *et al*., 1989; Sennhenn *et al*., 1993), fluorescence spectroscopy (Sennhenn *et al*., 1993; Jansen *et al*., 1974) photothermal spectroscopy (Sennhenn *et al*., 1993; Kolmel *et al*., 1986) and confocal Fourier transform Raman spectroscopy (Caspers *et al*., 2002) have also been employed *in vivo* to determine the kinetics of dermal absorption.

1.4.4 In vitro vs in vivo data

The relationship between *in vitro* and *in vivo* diffusion studies is of fundamental importance to evaluate the effects of the physiological processes (e.g. cutaneous microcirculation under differential barometric pressure) that dominate the diffusion partition process *in vivo*, since these processes are not apprehended employing *in vitro* methodologies. Several workers have attempted to establish the relationship between *in vivo* and *in vitro* data by performing the comparison between the amount of permeant detected in the receiver solution in *in vitro* studies and comparing to the amount of drug absorbed and eliminated in the urine in the *in vivo* studies (Bronaugh and Maibach, 1985; Bronaugh and Franz, 1986; Wester *et al*., 1992; Dick *et al*., 1995; Dick *et al*., 1997; Cnubben *et al*., 2002; Mavon *et al*., 2007; Griffin *et al*., 1999; Griffin *et al*., 2000). Generally, in these comparative studies there is a good agreement between *in vitro* and *in vivo* data; however some of the *in vitro* results were shown to underestimate *in vivo* cutaneous absorption (Bronaugh and Maibach, 1985; Bronaugh and Franz, 1986; Cnubben *et al*., 2002; Wojciechowski *et al*., 1985). These results were coupled

with the lack of the physiologic processes that have a significant impact in the *in vivo* situation such as the local vasculature (Wojciechowski *et al*., 1985), the existence of a lag time in the drug excretion process (Cnubben *et al*., 2002) and drug metabolism (Bronaugh and Maibach, 1985; Bronaugh and Franz, 1986). On the other hand, an overestimation of the *in vivo* permeation absorption was reported in some studies. This was linked with an *in vivo SC* drug reservoir effect that prevented drug absorption (Griffin *et al*., 1999; Griffin *et al*., 2000; Dick *et al*., 1997) and drug permeation through the subcutaneous fatty layer (Griffin *et al*., 1999; Griffin *et al*., 2000).

1.5 Strategies to enhance percutaneous drug delivery

In this PhD project, barometric pressure has been proposed as a new method to enhance cutaneous drug delivery. To move this concept forward, it is important to acknowledge the considerable efforts that have already been made to overcome this barrier such that best practise in the evaluation of the new technology is taken onwards. Many of the challenges related with the development of percutaneous enhancement strategies already published in the literature are associated with achieving an appropriate balance between effective delivery and safety. Often, this requires "targeted" localisation and this is not easy to achieve using a delivery system that is low cost and easy to use for patients (Prausnitz and Langer, 2008). The strategies that have been documented to date in research publications can be broadly classified accordingly to their overall approach, namely: chemical, biochemical and physical percutaneous drug delivery enhancement strategies such as the application of topical barometric stress. Each of these will be described in the text below in order to contemplate the position of barometric pressure among the other technologies.

1.5.1 Chemical enhancement

Mass transport across the skin can be altered by chemical enhancers that aim to manipulate the environment in which the permeant crosses the skin and they generally influence one or more than one of the parameters described by Equation 1.4 and 1.6. For example, chemical penetration enhancement can be achieved by increasing the partitioning into the *SC*, the solubility in the vehicle (*K*), the ability of the permeant to diffuse through the membrane (*D*) or the drug thermodynamic activity. The major benefits of chemical enhancers are their cost-effectiveness; their easy incorporation into a topical formulation and the lack of dependence of a delivery device. The primary limitation of chemical enhancers is related to the skin's response to the application of the chemicals, as these agents can alter the barrier properties and cause local sensitization, irritation and occasionally systemic toxicity. Chemical enhancers are known to be effective for the delivery of small molecules, but they have a limited capacity to enhance the passage of large molecules into the skin. However, drug enhancement strategies such as barometric stress may overcome this issue by promoting percutaneous penetration of macromolecules, as discussed later.

The most widely used chemical penetration enhancer is water. Formulations with high water content or systems that encourage skin hydration via occlusion have been shown to enhance the permeation of both hydrophilic and hydrophobic drugs (Williams, 2003; Bronaugh and Maibach, 2005). However, the mechanism by which water promotes increased percutaneous permeation is not fully understood. Several mechanisms have been proposed such as an increased mobility of the lipid bilayers (Barry, 1987), the existence of a water phase within the intercellular domain or water uptake by the corneocytes, but no firm conclusion has been made about the activity of this molecule (Marjukka *et al.*, 1999). Chemical enhancers are

commonly divided in different classes including solubilizers (e.g. propylene glycol and ethanol), fatty acids or esters (e.g. oleic acid), surfactants (e.g. sodium lauryl sulphate) and terpenes (e.g. menthol). The enhancement of drug solubility is often fundamental to the mechanism of action of penetration enhancers in the case of poorly soluble permeants. This is of importance as low solubility in the donor vehicle can lead to drug depletion (Williams, 2003) as described previously in Section 1.5.2. Ethanol and propylene glycol are commonly used as solubilizers. These two molecules can also act as chemical enhancers by increasing *SC* permeability and hence, enhancing drug partitioning through the skin (Megrab *et al.*, 1995). Oleic acid is one of the most cited chemical enhancers and it has been shown to increase the permeation of molecules such as 5-aminolevulinic (Pierre *et al.*, 2006) and 6-mercaptopurine (Koyama *et al.*, 1994). The permeation enhancement effect of oleic acid is proposed to be coupled with an interaction with the *SC* lipids resulting in increased bilayer fluidity (Ongpipattanakul *et al.*, 1991). Sodium lauryl sulphate is an anionic surfactant that has been reported to enhance cyclosporin A deposition within the skin (Liu *et al.*, 2006) and lorazepam transdermal permeation (Nokhodchi *et al.*, 2003). This enhancement effect has been shown to be elicited by disrupting proteins and lipids of the *SC* (Barry, 1987). The most widely terpene employed as a chemical enhancer is menthol. Terpenes are non-aromatic compounds derived from essential oils that display relatively high Log P values (Trommer and Neubert, 2006). Menthol has been reported to enhance transdermal delivery of several molecules such as propanol hydrochloride (Kunta *et al.*, 2000) and testosterone (Kaplun-Frischoff and Touitou, 2000). Its mechanism of action is suggested to be attributed to a reversible disruption of the intercellular packing of *SC* lipids (Kang *et al.*, 2007; Williams and Barry, 1991). Liposomes, emulsions, micelles and deformable vesicles have also been employed as “chemical” enhancers with a supramolecular structure that can be used to

increase drug solubility in the formulation and facilitate partitioning into the skin (Prausnitz and Langer, 2008).

1.5.2 Biochemical enhancement

Biochemical approaches increase skin permeability by targeting the lipid matrix of the *SC* or by altering its metabolism. The majority of the published work in this field has used peptides that disrupt or penetrate the outermost layer of the skin. For example, the use of an 11-amino acid synthetic peptide identified by phage display screening has been reported to increase the transdermal delivery of insulin and human growth hormone in an animal model (Chen *et al*., 2006). These workers suggested that its main mechanism of action was related to an enhanced transappendageal peptide transport that led to an improved drug deposition within the cutaneous tissue. Magainin, a naturally occurring pore-forming peptide was reported to increase skin permeability by selectively disrupting the lipid bilayers of the *SC* (Kim *et al*., 2007; Kim *et al*., 2008). The use of a polyarginine heptamer has been reported to enhance cyclosporine A topical delivery by acting as a transporter and localizing the drug within the epidermis and dermis (Rothbard *et al*., 2000). The use of metabolic inhibitors aim to increase the efficacy of standard enhancers by biochemically inhibit the metabolic process *in vivo* and hence delaying barrier recovery (Prausnitz *et al*., 2012). As a consequence, these approaches raise some concerns regarding skin integrity and reversibility and to date, their contribution to medical practise has been limited due to safety issues. Nevertheless, the emergence of such approaches could offer an exciting prospect in the future of percutaneous drug delivery enhancement.

1.5.3 Physical enhancement

Since the main obstacle to achieve an effective xenobiotic percutaneous penetration resides in the *SC*, significant efforts have been made to overcome and/or circumvent this barrier by physical manipulation, such as the application of mechanical barometric stress described herein. The main benefit of such approaches is the opportunity to significantly expand the range of drugs that can be delivered (Arora *et al.*, 2008; Banga, 2011), but the physical manipulation of the skin generally requires a device that can be costly to produce and pose potential constraints for self-administration by patients. In addition, avoiding damage to deeper tissue layers remains a problem when physically manipulating the skin with a device and this has limited the use of these technologies in medical practise. It is suggested in this PhD that the application of topical hypobaric stress could potential represent a cost-effective and simple to use safe technology to enhance percutaneous drug penetration. Physical enhancement methods can be classified accordingly to their overall mode of action, namely: electrically assisted delivery, miscellaneous and mechanical methods.

1.5.3.1 Electrically assisted delivery

Iontophoresis and electroporation are two examples of electrically assisted physical enhancement methods that have been employed to deliver small molecules and macromolecules through the *SC* (Banga, 1998). Iontophoresis uses a continuous low voltage current field that provides an electrical driving force for mass transfer across the *SC* (Banga, 1998; Kalia *et al.*, 2004). Enhanced drug delivery is achieved by one or a combination of the following mechanisms: electro-osmosis (neutral molecules), electro-repulsion (charged molecules) or electro-perturbation (both neutral and charged molecules). An amplification of

mass transport via the follicular route is believed to be the primary mechanism of action for iontophoretic drug delivery (Batheja *et al*., 2006). The main benefit of iontophoresis is the possibility of tightly modulating the rate of drug delivery over time. It has been applied in clinical practise for the delivery of lidocaine and fentanyl in pain management (Mayes and Ferrone, 2006) and water to treat hyperhidrosis (Kreyden, 2004). In contrast to iontophoresis that utilizes low voltage, electroporation applies relatively high voltage pulses for very short periods of time in order to temporarily increase skin permeability by the formation of aqueous pores (Prausnitz *et al*., 1993; Denet *et al*., 2004). Mass transport through the pores is achieved by three mechanisms: iontophoresis during the pulse, electro-osmosis or by simple diffusion across the pores (Williams, 2003). Electroporation is currently being employed in clinical practise for the delivery of therapeutic agents to treat skin cancer (Gehl, 2008). However, both approaches involve the use of costly devices that are often cumbersome and need to be operated by trained personnel and therefore pose problems regarding patient self-administration and compliance.

1.5.3.2 Miscellaneous methods

Ultrasound utilises high frequency acoustic waves to deliver drugs across the skin. Enhanced transdermal delivery is accomplished by two mechanisms: thermal and non-thermal. Skin absorption of ultrasonic energy leads to an increase skin temperature that may facilitate drug permeation and increase microvascular blood flow (Mitragotri, 2005). The non-thermal mechanism is believed to be the most prominent in increasing skin permeability. It forms gaseous cavities that lead to the disruption of the *SC* (Mitragotri, 2005). In a similar approach, pulses from a high power laser and high frequency alternating current have been employed to create sub-microscopic defects within the *SC* to increase skin permeability

(Doukas and Kollias, 2004; Sintov *et al*., 2003). Ultrasound is currently being used in clinical practise as a pre-treatment in local anaesthesia as it improves the onset time of lidocaine action (Spiliopoulos *et al*., 2011). The major drawbacks of such approaches are similar to that previously described above for electrically assisted delivery (Section 1.5.3.1).

1.5.3.3 Mechanical methods

Microneedle based devices provide a very effective means of delivering drugs across the *SC* with minimal discomfort for the patient, which avoid the inherent disadvantages commonly associated with needles (i.e. needle phobia, pain). This technology creates micro-scale perforations that are large enough to allow mass transport of small molecules, macromolecules and nanoparticles (Wermeling *et al*., 2008; Cosman *et al*., 2010; McAllister *et al*., 2003). Despite offering compelling opportunities in the transdermal delivery field some issues still need to be addressed. For example, the long-term effect of repeated application of these devices and the potential of increased susceptibility to bacterial infection remains unclear. Skin stretching after the pre-treatment with a microneedle device has been proposed to enhance transdermal drug delivery (Cormier *et al*., 2001, Neukermans *et al*., 2001). These workers suggest that a tension of ca. 0.01 to 10 mP generates the transient formation of micropathways that allows drug movement across the barrier, but the sole use of the expandable skin stretching technique was described as being inefficient as an enhancing method. Tape stripping (described in Section 1.4.2) and skin abrasion represent simple techniques that have been employed to remove the outermost layer of the skin. The removal of successive layers of the *SC* by an adhesive tape has been reported to enhance *in vivo* dermal permeation of several molecules such as 5-aminolevulinic acid and hexyl aminolevulinate (van den Akker *et al*., 2000). Although cost-effective such an approach is

considered to have poor patient acceptability and this has limited its clinical use. Skin abrasion using sandpaper has also been shown to be an effective and simple method to facilitate vaccine delivery across the skin, but again similar patient acceptability issues exist (Prausnitz and Langer, 2008). The application of local hyperbaric pressure (e.g. 250 mBar) has also been shown to enhance the skin permeability (Trefel *et al.*, 1993). However, no mechanistic studies were reported. The application of topical hypobaric stimuli has been typically used to generate a suction blister that allows the removal of the epidermis while leaving the dermal layer intact (Svedmann, 1995). Since the dermal local vasculator and nociceptor nerves are not affected by this technique, transdermal invasivity is thus avoided. Clinical studies have shown the possibility of trans-epidermal delivery of morphine and vasopressin using this technique. The pharmacokinetic profile evaluation of both drugs was reported to be in good agreement to that registered by continuous intravenous injection (Svedmann *et al.*, 1996; Svedmann *et al.*, 1991). Laser Doppler measurements of the de-epithelialised dermis also revealed a marked increase in the skin microvascular blood flow. This effect was considered to further contribute to the efficient transdermal delivery of the test compounds. The de-epithelialised skin area was reported to recover its normal appearance within 6 weeks without any sign of tissue trauma. The approximate 2.5 h time length that is required to induce a suction blister (Gupta *et al.*, 1999) is one of the major limitations of this method. However, this can be reduced to 15 - 70 min by warming the skin to 38 °C (Svedmann *et al.*, 1996). If this system was as fast and efficient as intravenous catheter insertion its application in medical practise would be practical. Moreover, the risk of epidermal infection is less serious than the consequences of systemic sepsis (Down and Harvey, 2003). However, the effect of local hypobaric pressure upon xenobiotic penetration into the cutaneous tissue has not yet been reported in the literature. Therefore, the ability of this technology to deliver therapeutic agents into the skin requires further investigation.

1.6 Aim and Scope

The exposure of humans to barometric pressure changes (normally ca. 1010 mBar) can be considered both on the macro (whole body exposure) and micro scale (i.e. application of suction). Whole body exposure changes in atmospheric pressure are more common than may be first perceived. For example, passengers on commercial air flights are exposed to hypobaric pressure, approximately 820 mBar, for the duration of the flight. Although aircraft vary in size and flight altitudes the lowest levels of pressure that a human should experience during a commercial flight is 750 mBar (Muhm *et al*., 2007). The greater the altitude the more extreme the pressure changes and therefore space flight simulations use hypobaric pressures of 15 mBar to understand the physiological changes that humans experience during this process (Baisch *et al*., 2000). Physiological changes in blood circulation and respiration under hypobaric pressure have been well documented as a consequence of the humans exposure to whole body barometric pressure changes, but the influence of these changes on the barrier physiology and the bodies natural defence mechanism to xenobiotic insult does not appear to have been studied. Whole body exposure to barometric pressure changes would be expected to have very different effects to local hypobaric pressure changes induced by methods such as suction because the latter generates a pressure differential which could draw molecules across the barrier and have less profound effects on whole body physiology.

There have been reports of how local air suction effects cutaneous microvascular flow and the mechanical properties of the skin. For example, Childers and his colleagues (2007) demonstrated that a hypobaric pressure of ca. 500 mBar resulted in thinning of the epidermis and enlargement of blood vessels embedded in the dermis. Pedersen and Jemec (2006) applied hypobaric pressures between 400 and 600 mBar generated from a suction cup device

and reported a significantly increased TEWL with concomitant decrease in the *SC* water content. In another study, a marked increase in TEWL, disorganization of the intercellular lipid bilayers and rupture of the corneosomes was shown after stretching of the skin (Rawlings *et al*., 1995; Leveque *et al*., 2002). However, a link between skin changes induced by barometric pressure alteration and xenobiotic percutaneous penetration needs further study.

As such, the aim of this study was to investigate the effects of local barometric pressure changes upon percutaneous penetration with a view to understand if such an approach could be used to design a novel medicinal product. In order to achieve this aim four objectives were defined: 1) to build a pressure diffusion cell that could generate a barometric pressure change at the skin surface, 2) to determine the effects of local barometric pressure changes upon the mechanical and physiologic properties of the skin, 3) to investigate the relationship between *in vitro* cutaneous bioavailability under differential barometric pressure and the drug's physicochemical properties and 5) to assess the *in vivo* effects of local barometric pressure changes upon microvascular blood flow, drug pharmacokinetics and tissue distribution. To achieve these objectives there was initially a need to select the test agents, develop analytical assays and an *in vitro* transport methodology and hence this is where this PhD thesis will begin.

CHAPTER TWO

Analytical verification of HPLC methods and transmembrane transport method development

2.1 Introduction

In order to assess the effects of local barometric pressure changes upon xenobiotic percutaneous penetration three model agents were selected from distinct therapeutic classes, namely: tetracaine (local anaesthetic), diclofenac diethylamine (Cox-2 inhibitor) and aciclovir (nucleoside analogues). These agents were selected based upon their different physicochemical properties, their ease of assay and cost. The strategy of employing penetrants that display a range of physicochemical properties to assess the ability of different methodologies to enhance membrane permeability has previously been described in the literature (Guy and Hadgraft, 1988; Aungst *et al*., 1990). For example, a series of proteins, peptides and oligonucleotides have been employed to investigate skin permeation enhancement by high velocity powder injection (Burkoth *et al*., 1999) and the flux of model compounds with different degrees of lipophilicity, including indomethacin and nalbuphine has been used to determine transdermal drug delivery enhancement by the application of a erbium:YAG laser (Lee *et al*., 2001). Using more than one model penetrant allows a more complete understanding of how novel technologies designed to facilitate barrier transport function work by establishing any relationships between the physicochemical properties of a penetrant and its transmembrane flux.

Tetracaine is an effective amino ester type local anaesthetic that is indicated for anaesthesia before venepuncture or venous cannulation (Scott *et al*., 1972). Tetracaine has been shown to pass through the skin (Liu *et al*., 2005; Foldvari, 1994). As a powder tetracaine is a white or light yellow waxy solid and it is very slightly soluble in water and soluble in organic solvents. It has pKa's of 2.24 and 8.39 (Iglesias-Garcia *et al*., 2010).

Table 2.1. Physicochemical properties of the model penetrants used in the present study and their chemical structures. Log P (o/w) octanol-water partition coefficient; TC – tetracaine; DDEA – diclofenac diethylamine; ACV – aciclovir.

Penetrant	Log P (o/w)	Molecular Weight	Potency (μM)	Chemical Structure
TC	2.64	264.36	3.5 (Andrade *et al.*, 2011)	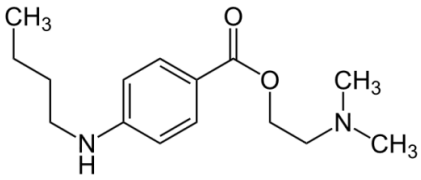
DDEA	0.85	369.29	0.03 (Cordero *et al.*, 2011)	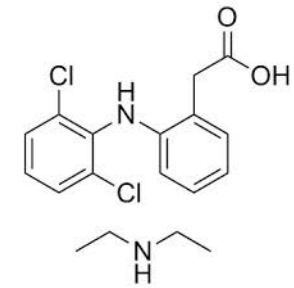
ACV	-1.14	225.21	0.09 (Brand *et al.*, 2001)	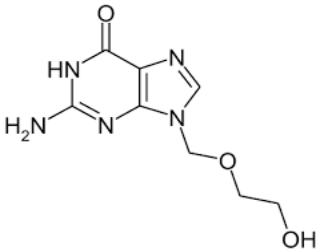

Diclofenac diethylamine is a non-steroidal and anti-inflammatory drug and it is prescribed for patients affected by dermatitis (Stuttgen, 1988) and rheumatic diseases (Heyneman *et al.*, 2000). It is classified formally as a non-selective cyclooxygenase inhibitor but it does possess a slightly preferential cyclooxygenase 2 inhibition activity (Giuliano *et al.*, 1988). Diclofenac diethylamine is the most preferable diclofenac salt for percutaneous delivery due to its high solubility in aqueous solutions and has been shown to provide a good permeation rate across skin (Sengupta *et al.*, 2015; Fini *et al.*, 1999). This molecule has a pKa of 4 (Djordjevic *et al.*,

2005). Aciclovir is indicated for initial and recurrent labial and genital herpes simplex infections (Spruance *et al*., 2002) and has been shown to permeate the skin (Yeo *et al*., 1998, Spruance *et al*., 2002, Freeman *et al*., 1986; Piret *et al*., 2000), albeit with difficulty. This molecule is a white to almost white crystalline powder. It is sparingly to slightly soluble in water and dissolves in dilute solutions of mineral acids and alkali hydroxides and has a pKa of 9.25 (Freeman *et al*., 1986).

In order to assess the effects of barometric pressure upon the ability of the three model agents to pass through a membrane an analytical method for each was required and a sound transport methodology needed to be set up for the specific aims of this work. Tetracaine has been previously determined using sequential injection analysis with permanganate induced chemiluminescence detection with a limit of detection (LOD) of 0.1 $\mu g.mL^{-1}$ (Pasekova *et al*., 2000). Elsewhere, a LOD of tetracaine has been reported to be as low as 1.32 $ng.mL^{-1}$ using electrochemistry (Wang *et al*, 2002). Kitade *et al*., (1995) reported a LOD value of 1.26 $ng.mL^{-1}$ when phosphometry was employed as the analytical method. In addition, the LOD has been reported to be 1.20 $\mu g.mL^{-1}$, 50 $\mu g.mL^{-1}$, 0.003 $\mu g.mL^{-1}$, 0.008 $\mu g.mL^{-1}$ and 0.012 $\mu g.mL^{-1}$ using spectrofluorometry, capillary electrophoresis, resonance Rayleigh scattering, frequency doubling scattering and second-order scattering, respectively (Nevado *et al*., 2000; Al-Otaibi *et al*., 2009; Qin *et al*., 2009). Likewise, the separation and characterisation of diclofenac diethylamine has been reported in a wide range of matrices such as plasma, blood and pharmaceutical preparations using several techniques such as gas chromatography with electron capture detection, gas chromatography/mass spectrometric with selected ion monitoring, protein precipitation and HPLC with electrochemical detection with reported LOD of 0.2 $ng.mL^{-1}$, 0.5 $ng.mL^{-1}$, 25 $ng.mL^{-1}$ and 10 $ng.mL^{-1}$, respectively (Schneider *et al*., 1986; Borenstein *et al*., 1996; El-Sayed *et al*., 1988; Torrez-Lopez *et al*., 1997). Aciclovir has

been quantified in pharmaceutical preparations, plasma and urine by chemiluminiscence, micellar electrokinetic chromatography, capillary electrophoresis and reverse phase HPLC with reported LOD of 0.2 $mg.mL^{-1}$, 3 $\mu g.mL^{-1}$, 0.15 $mg.mL^{-1}$ and 20 $ng.mL^{-1}$, respectively (Yang *et al*., 2004; Neubert *et al*., 1998; Zhang *et al*., 2000; Bangaru *et al*., 2000). Of these previously reported method options, HPLC coupled to ultraviolet (UV) detection was selected as the method to be implemented for each of the three model agents because the quantification of tetracaine, diclofenac diethylamine and aciclovir by HPLC is reported to be reproducible, accurate and sensitive, with sample retention times not longer than 15 min. LOD values for tetracaine in the literature are typically reported to be less than 1 $\mu g.mL^{-1}$ using HPLC-UV and limit of quantification (LOQ) values are reported to be ca. 3 $\mu g.mL^{-1}$ (Wang *et al*., 2003; Al-Otaibi *et al*., 2014; Murtaza *et al*., 2002; Qin *et al*., 2010). Likewise, LOD and LOQ values of 0.25 $\mu g.mL^{-1}$ and 0.75 $\mu g.mL^{-1}$ respectively have been reported for diclofenac diethylamine (Bilal *et al*., 2011). Elsewhere a LOD and LOQ for diclofenac diethylamine has been reported to be 1.1 $\mu g.mL^{-1}$ and 3.38 $\mu g.mL^{-1}$ (Vemula *et al*., 2013). A LOD and LOQ less than 0.8 $\mu g.mL^{-1}$ and 1.5 $\mu g.mL^{-1}$ was reported for aciclovir (Boulieu *et al*., 1997; Darville *et al*., 2007; Tzanavaras *et al*., 2006; Bangaru *et al*., 2000; Basavaiah *et al*., 2003). Despite the higher sensitivity showed by some of the other reported analytical methods, HPLC-UV was deemed to be relatively inexpensive, quick, easy to perform and convenient. The most popular method for the detection of compounds separated by HPLC is UV radiation because of its versatility, reliability, sensitivity, low-cost and suitability for the detection of components that contain a UV active chromophore (Meyer, 2004).

The membrane transport method of choice for topically applied products is currently the Franz diffusion cell (Franz, 1975; Franz, 1978) in a range of pharmaceutical development contexts. They provide a useful tool that allows the systematic investigation of the

permeation process *in vitro* (Reid *et al.*, 2008, Iervolino *et al.*, 2001, Moser *et al.*, 2001). However, significant discrepancies in results are occasionally reported. For example, testosterone steady-state fluxes through sections of a polydimethylsiloxane membrane were reported to have a coefficient of variation of 32% when 63 replicates were tested (Khan *et al.*, 2005). Likewise, sequential intra-laboratory measurements of solute permeation across a silicone membrane resulted in coefficient of variation of 45.5%, 30.7%, 15.1% and 13.1% for adenosine, aldosterone, corticosterone and estradiol, respectively (Frum *et al.*, 2007). In other study involving 18 different laboratories, the steady-state flux of methlyparaben was reported to have a coefficient of variation of 35% (Chilcott *et al.*, 2005). Thus, there is a need to develop experimental Franz cell methods that are robust and that can provide an accurate assessment of transmembrane penetration. For this work, the influence of tetracaine system pre-equilibration time, membrane thickness and degree of ionization of the molecules in the donor solution upon the passive diffusion process was investigated. Only this molecule was used initially to design an optimal method for diffusing testing as it was thought to be the most problematic of the three and hence it was expected that a method for tetracaine could easily be adapted for the other two agents. It has been reported that tetracaine may be prone to hydrolytic degradation (Menon and Norris, 1980), it could interact with membranes (Zhang *et al.*, 2007; Frezzatti *et al.*, 1986; Hata *et al.*, 2000; Racansky *et al.*, 1988) and it has previously been shown to self-associate in solution (Guerin *et al.*, 1980; Umemura *et al.*, 1981). Therefore, the aim of the work presented in this chapter was twofold: first, to demonstrate that HPLC methods for the determination of tetracaine, diclofenac diethylamine and aciclovir were ‘fit for purpose’. Secondly, to investigate suitable conditions to assess the *in vitro* tetracaine permeation through a model membrane in order to subsequently assess the influence of barometric pressure upon percutaneous penetration.

2.2 Materials

Acetonitrile and methanol both HPLC grade, grade A glass pipettes, clear glass HPLC vials crimpable lids and 0.45 μm nylon filter papers were purchased from Fischer Scientific (Leicester, UK). Tetracaine base and aciclovir base both BP grade (99.9%) were supplied by Sigma Aldrich (Dorset, UK). Diclofenac diethylamine BP grade (99.9%) was obtained from Chemos Group (Regenstauf, Germany). Concentrated hydrochloric acid and sodium hydroxide was from Fluka (Dorset, UK). Sodium acetate and potassium dihydrogen phosphate were provided by Alfa Aesar (Heysham, UK). Silicone membranes with a thickness of 0.05, 0.12 and 0.25 mm were purchased from GBUK Healthcare (Selby, UK).

2.3 Methods

2.3.1 HPLC assay method verification

A liquid chromatography pump (P680 HPLC pump, Dionex, Surrey, UK) connected to a UV-visible detector (PDA-100 photodiode array detector, Dionex, Surrey, UK) with an ASI-100 automated sample injector (Dionex, Surrey, UK) was used for the quantitative determination of each drug molecule (Table 2.2). The HPLC system was connected to a computer with Chromeleon software (Dionex, Surrey, UK), which was used to record and analyse the chromatograms.

Table 2.2. HPLC-UV conditions for the model penetrants tetracaine (TC), diclofenac diethylamine (DDEA) and aciclovir (ACV). HPLC – high performance liquid chromatography; UV – ultraviolet; ACN - Acetonitrile; MeOH - Methanol; NaCOOH - Sodium acetate; RT – room temperature.

Parameter	TC	DDEA	ACV
Column specification	Phenomenex® Luna™ 5 µm C18 column (250 x 4.6 mm)	Phenomenex® Luna™ 5 µm C18 column (250 x 4.6 mm)	Phenomenex® Luna™ 5 µm C18 column (250 x 2.0 mm)
Injection volume (µl)	60	60	60
Mobile phase composition	20% ACN, 25% MeOH and 55% (0.1M NaCOOH pH4)	40% ACN, 25% MeOH and 35% (0.1M NaCOOH pH4)	4% MeOH and 96% (0.1M NaCOOH pH4)
Flow rate (ml/min)	1	1	1
Run Time (min)	10	12	13
Temperature (°C)	RT	RT	RT
Detection UV (λ)	310	220	254
Detection sensitivity	0.025	0.025	0.025

Stock solutions of tetracaine, diclofenac diethylamine and aciclovir (100 µg.ml^{-1} in 20:25:55 ACN:MeOH:NaCOOH, 40:25:35 ACN:MeOH:NaCOOH and 4:96 MeOH:NaCOOH, respectively) were prepared by dissolving 10 mg of the solid penetrant in 100 ml of the relevant solvent. From the stock solutions, standard dilutions were made to obtain varying concentrations of each penetrant and calibration curves were produced for the three model agents using five standard concentrations. The mean peak area versus concentration (n = 5)

was plotted for the five concentrations and a regression model was applied. The peak symmetry (A_s) was calculated (n = 15) using equation 2.1.

$$A_s = \frac{W_{0.05}}{2d} \qquad \text{(Equation 2.1)}$$

where $W_{0.05}$ is the width of the peak at one-twentieth of the peak height, d equals the distance between the perpendicular dropped from the peak maximum and the leading edge of the peak at one-twentieth of the peak height. A peak symmetry of 1 was considered ideal as this represents a perfectly symmetrical peak. The theoretical plates (estimation of the column efficiency) for each method were calculated (n = 15) using equation 2.2.

$$N = 5.54\left(\frac{t}{W_{h/2}}\right)^2 \qquad \text{(Equation 2.2)}$$

Where t is the retention time of peak and $W_{h/2}$ equals the width of peak at half the peak height. The LOD (the lowest concentration of analyte in a sample that can be detected but not necessarily quantified) and the LOQ (the minimum injected amount of analyte that gives precise measurements), for each penetrant was calculated according to equations 2.3 and 2.4 respectively.

$$LOD = Y_B + 3s_B \qquad \text{(Equation 2.3)}$$

$$LOQ = Y_B + 10s_B \qquad \text{(Equation 2.4)}$$

Where s_B was equal to the standard deviation of the y estimate and Y_B was the intercept from the regression equation.

The precision of each HPLC method was determined by assay repeatability (intra-day) and assessment of the intermediate precision (inter-day). Intra-day precision was obtained by evaluating the variance between three standard curves assayed from the same standard solutions (five injections per standard) of each model penetrant. The intermediate precision of the test molecules was determined by comparing three calibration curves of each penetrant using independently prepared standard solutions (five injections per standard) on three separate days.

The accuracy of the tetracaine, diclofenac diethylamine and aciclovir HPLC assays were determined by assaying freshly prepared solutions of known concentration. The ability of each assay to quantify the compound was calculated using equation 2.5.

$$\text{Accuracy}(\%) = \frac{A}{T} x100 \qquad \text{(Equation 2.5)}$$

Where A is the actual (measured) concentration and T is equal to the theoretical analyte concentration

2.3.2 Tetracaine chemical stability assessment

The chemical stability of tetracaine was assessed as it was to be used in the transport study method development. Initially the ability of the HPLC method to detect chemical instability was determined using a method to hydrolytically degrade tetracaine. This was achieved by adding a 0.1 mg aliquot of the drug to 0.1 M HCl solution at pH 1.1 (acid degradation solution) and to a 0.1 M NaOH solution at pH 13.2 (base degradation solution). After this

procedure each solution was stored at room temperature and at 90 ˚C in a water bath (Grant Instruments, Cambridge, UK). At regular time intervals, 250 µL of each solution was made up with mobile phase before being analysed by HPLC. The results were interpreted accordingly to the percentage variation in peak area (% Δ) and the appearance of new peaks in the chromatogram which were thought to represent degradation products. The main mechanism for tetracaine degradation in solution is hydrolytic degradation and the main degradation product is p-n-butylaminobenzoic acid (Menon *et al.*, 1981). The HPLC method employed in the analysis was identical to the one described in Section 2.3.1.

2.3.3 Tetracaine permeation studies

The permeation experiments were carried out in previously calibrated upright Franz cells with an average receiver volume of 9.8 mL and an average surface area of 2.1 cm^2 (University of Southampton, UK). Tetracaine saturated solutions at pH 4 and pH 10 with increasing suspension pre-equilibration times were used as the donor solutions (24 h, 120 h and 576 h). Pre-equilibration time corresponded to the period in which the donor solutions were left to equilibrate at room temperature prior to the permeation studies. Different thickness silicone membranes (0.05 mm, 0.12 mm and 0.25 mm) were used as the controlling barrier. The silicone membrane was cut to fit the Franz cell with scissors and mounted on the cell with a 13-mm magnetic flea in the receiver chamber. The top of the cell was positioned over the membrane and the cell was sealed by wrapping parafilm around the two sections. The cell was then inverted, filled immediately with previously sonicated 0.1 M acetate buffer solution (n = 5) and with 0.1 M phosphate buffer solution (n = 5). To ensure there was no leakage, the cells were inverted and visually checked. Leaking cells were excluded from the experiments. Each diffusion cell was placed on a submersible stirring plate in a pre-heated

water bath (Grant Instruments, Cambridge, UK) set at 37 ˚C, to obtain 32 ˚C at the membrane surface (Maddock *et al.*, 1933). The cells were left to equilibrate for 30 min before application of the donor solution, which consisted of tetracaine saturated solutions at pH 4 (0.1 M acetate buffer solution) and pH 10 (0.1 M phosphate buffer solution). Drug permeation was monitored by removal of 1 mL samples out of the sampling arm of the cell, which was placed into an HPLC vial. One millilitre of thermostatically regulated receptor solution was then added to the diffusion cell receiver fluid to replace the withdrawn sample. Membrane thickness was measured before and after the transport experiments using a Venier micrometer (No. 436.1 Series 0 - 25 mm) purchased from Starrett (Jedburgh, UK), in order to check for swelling which would indicate vehicle-matrix interaction (Dias *et al.*, 2001). Cumulative amounts of drug penetrating the unit surface area of the membrane ($\mu g.cm^{-2}$) were corrected for sample removal and plotted against time (min). Flux (J) was taken from the line of best fit with a linearity of $R^2 \geq 0.99$ over at least five values for determined concentrations which exceeded the HPLC assay limits of detection. Lag time was determined by the intercept of the steady-state flux with the x axis and it was provided in min.

2.3.4 Statistical analysis

Statistical evaluation was carried out using a statistical package for social sciences software (SPSs version 16.0, SPSS Inc., Chicago, USA). All data were checked in terms of normality (Kolmogorov-Smirnov test) and homogeneity of variances (Levene's test) prior to analysis. Permeation results were analysed using one way analysis of variance tests (i.e. one-way ANOVA and one-way AVOVA post-hoc Tukey test). Box plot statistical tests were performed on the permeation data obtained from each cell in a single experiment to identify the outliers which were then removed from the calculation of the average. All other data were

analysed using either two-way ANOVA followed by Bonferroni's comparison post-hoc test or Student's *t*-test. Statistically significant differences were defined when $p < 0.05$. All values were expressed as mean ± standard deviation (SD). The number of replicates was 3 in the chemical stability assessment and 5 in the permeation studies.

2.4 Results and Discussion

2.4.1 HPLC assay method verification

Tetracaine, diclofenac diethylamine and aciclovir displayed well resolved peaks with retention times of ca. 7.6 min, 10.9 min and 8.9 min respectively (Figure 2.1). The mean peak symmetry (A_s) for tetracaine, diclofenac diethylamine and aciclovir was within the recommended limit proposed by the International Conference on Harmonisation (ICH, 1995) (Table 2.5) with values of 1.05 ± 0.2, 0.92 ± 0.1 and 1.21 ± 0.3, respectively (n = 15 ± SD in all cases). The column efficiency (where N represents theoretical plate number) for each model agent was within the limit recommended by the ICH guidelines (Table 2.5) as follows: tetracaine N = 3010 ± 102, diclofenac diethylamine N = 4090 ± 190 and aciclovir N = 2900 ± 98 (n = 15 ± SD in all cases).

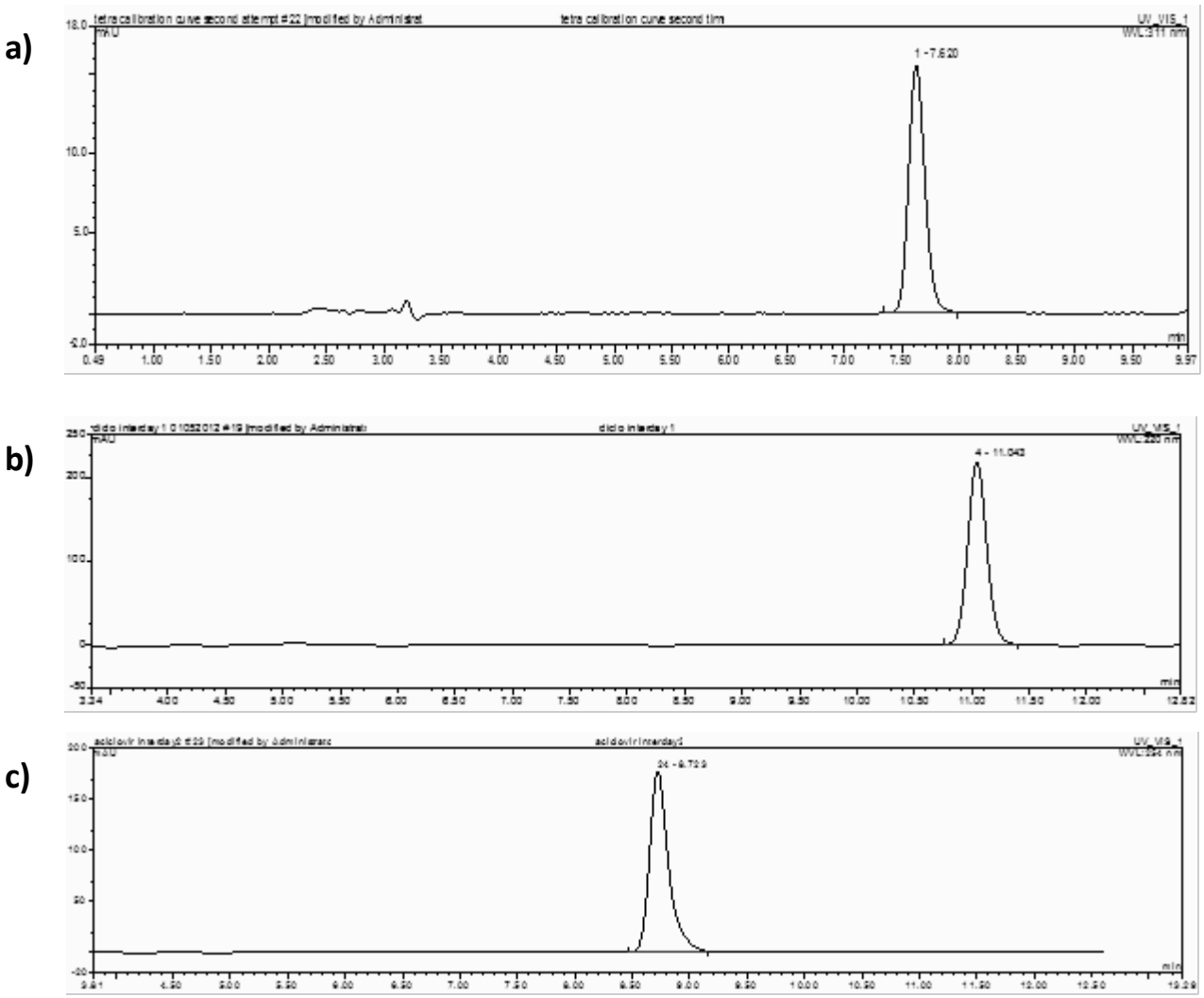

Figure 2.1. Typical liquid chromatographs of a) 100 µg/ml tetracaine (TC) in 20:25:55 ACN:MeOH:NaCOOH, b) 100 µg/ml diclofenac diethylamine (DDEA) in 40:25:35 ACN:MeOH:NaCOOH, and c) 100 µg/ml aciclovir (ACV) in 4:96 MeOH:NaCOOH.

The standard calibration curves of tetracaine, diclofenac diethylamine and aciclovir were linear across the calibration range for each compound ($R^2 \geq 0.99$), as demonstrated in Figure 2.2.

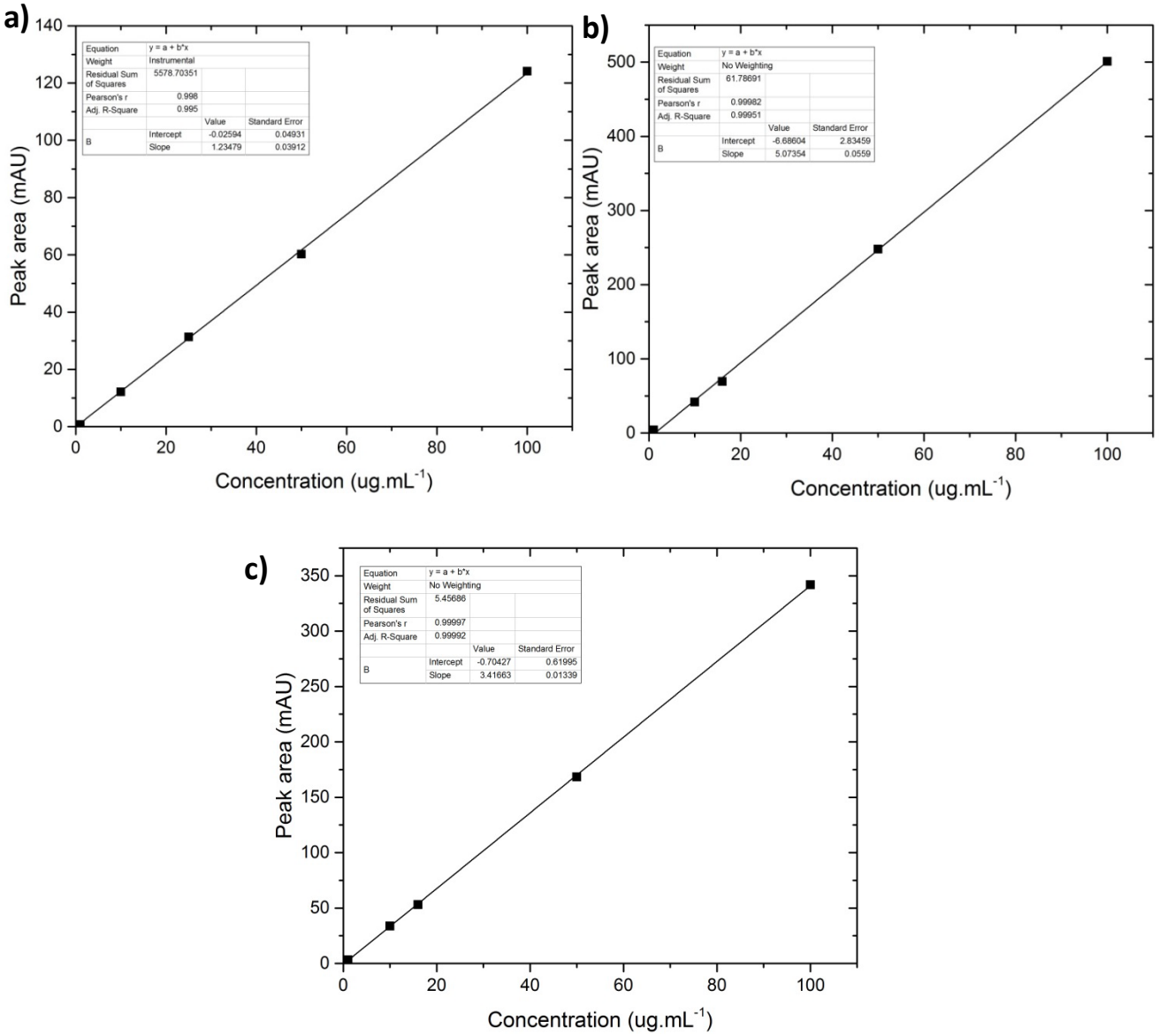

Figure 2.2. Intra-day HPLC calibration curves showing mean peak areas as a function of concentration of a) tetracaine in 20:25:55 ACN:MeOH:NaCOOH b) diclofenac diethylamine in 40:25:35 ACN:MeOH:NaCOOH and c) aciclovir in 4:96 MeOH:NaCOOH. Data represents mean ± SD (n = 18). Error bars represent mean ± SD but are too small to be seen.

This is in accordance with the ICH guidelines that recommend the use of at least a five point calibration curve that displays a linearity > 0.99, to demonstrate the capacity of an analytical

method to generate results that are directly related to the concentration of an analyte present (Table 2.5). The LOD and LOQ values for each compound were calculated from summated intra-day calibration curves (three standard curves). The LOD for tetracaine, diclofenac diethylamine and aciclovir was 3.26 $\mu g.mL^{-1}$, 3.14 $\mu g.mL^{-1}$ and 2.78 $\mu g.mL^{-1}$, respectively whilst the LOQ values were 9.76 $\mu g.mL^{-1}$, 8.92 $\mu g.mL^{-1}$ and 10.58 $\mu g.mL^{-1}$, respectively. The LOQ values calculated in the present study for the three model penetrants were found to be in the same range as those reported in the literature. For example, the LOQ values for tetracaine were reported to be ca. 3 $\mu g.mL^{-1}$ (Wang *et al.*, 2003; Al-Otaibi *et al.*, 2014; Murtaza *et al.*, 2002; Qin *et al.*, 2010), likewise, the LOD for diclofenac diethylamine and aciclovir was found to be in the same range as the published values of ca. 3.38 $\mu g.mL^{-1}$ and 1.5 $\mu g.mL^{-1}$, respectively (Vemula *et al.*, 2013; Boulieu *et al.*, 1997; Darville *et al.*, 2007; Tzanavaras *et al.*, 2006; Bangaru *et al.*, 2000; Basavaiah *et al.*, 2003).

In all cases the differences in peak area for the independently prepared solutions were not statistically different from one another ($p > 0.05$). For tetracaine, diclofenac diethylamine and aciclovir the intra-day and inter-day variability was < 1% and < 2% for all concentrations, respectively (Table 2.3) and these values were below the limits recommended by the ICH guidelines (Table 2.5).The mean accuracy of the tetracaine ($n = 6$), diclofenac diethylamine ($n = 5$) and aciclovir ($n = 6$) assays was 97.9 ± 2.3%, 96.7 ± 0.2% and 99.7 ± 1.1% at the concentrations tested from the calibration range (Table 2.4). The accuracy of the three analytical methods, determined by the extent to which theoretical concentrations of the model agents agreed with the true analyte concentrations was within the ICH guideline recommended values (Table 2.5). As a consequence of this data the three developed and verified HPLC methods were considered to be 'fit-for-purpose'.

Table 2.3. Variance (repeatability and intermediate precision) of the tetracaine (TC), diclofenac diethylamine (DDEA) and aciclovir (ACV) HPLC assays over the calibration range expressed as the coefficient of variation (% CV).

Concentration (µg/ml)	**CV of the intra-day (%, *n* = 15)**			**CV of the inter-day (%, *n* = 15)**		
	TC	**DDEA**	**ACV**	**TC**	**DDEA**	**ACV**
100	0.32	0.42	0.08	0.51	0.61	0.4
50	0.41	1.31	0.3	0.82	2.93	0.5
16	0.45	0.62	0.6	0.91	1.38	0.5
10	0.54	1.11	0.4	1.12	1.33	1.3
1	1.13	1.21	0.02	2.4	2.61	2.5
0.5	1.11	__	0.5	1.3	__	3.5
Mean	**0.66**	**0.93**	**0.31**	**1.17**	**1.77**	**1.45**

Table 2.4. Assay accuracy for tetracaine (TC), diclofenac diethylamine (DDEA) and aciclovir (ACV). Accuracy was determined at 6 concentrations for TC and ACV, and 5 concentrations for DDEA over the calibration range.

TC		**DDEA**		**ACV**	
Concentration ($\mu g.mL^{-1}$)	**Accuracy (%)**	**Concentration ($\mu g.mL^{-1}$)**	**Accuracy (%)**	**Concentration ($\mu g.mL^{-1}$)**	**Accuracy (%)**
100	97.1	**100**	96.4	**100**	99.2
50	98.3	**50**	97.5	**50**	101.2
16	97.9	**16**	97.3	**16**	98.3
10	98.1	**10**	96.4	**10**	98.9
1	98.6	**1**	96.1	**1**	99.5
0.5	97.5	**0.5**	--	**0.5**	101.3
Mean	**97.9**		**96.7**		**99.7**

Table 2.5. A summary of the assay validation data for tetracaine (TC), diclofenac diethylamine (DDEA) and aciclovir (ACV) and comparisons to the ICH guidelines for analytical method validation (ICH,1995).

Validation parameter	**Compound**			**Recommend level/limit by ICH**
	TC	**DDEA**	**ACV**	
System suitability				
Linearity (R^2, n = 3 calibrations, ± SD)	0.998 ± 2×10^{-5}	0.999 ± 4×10^{-5}	0.999 ± 3×10^{-4}	> 0.99
Peak symmetry, A_s (n = 15 ± SD)	1.05 ± 0.2	0.92 ± 0.1	1.21 ± 0.3	< 2, Ideal A_s = 1
Theoretical plate number, N (n = 15 ± SD)	3010 ± 102	4090 ± 190	2900 ± 98	N > 2000
Limit of Detection (μg.mL^{-1})	3.26	3.14	2.78	---
Limit of Quantification (μg.mL^{-1})	9.76	8.92	10.58	---
Precision				
Intra-day variability (repeatability, % CV)	0.58	0.48	0.31	< 1 %
Inter-day variability (intermediate precision)	< 2 %	< 2 %	< 2 %	< 5 %
Accuracy (% ± SD, n = 6 for TC and ACV and n = 5 for DDEA)	97.9 ± 2.3	96.7 ± 0.2	99.7 ± 1.1	95 - 105 %

2.4.2 Tetracaine chemical stability assessment

Forced degradation studies revealed that a degradant was generated upon base hydrolysis of tetracaine (0.1 M NaOH pH 13.2) at room temperature (Figure 2.3) and 90 °C at 30 min, 1h and 24 h sampling time points (Table 2.6).

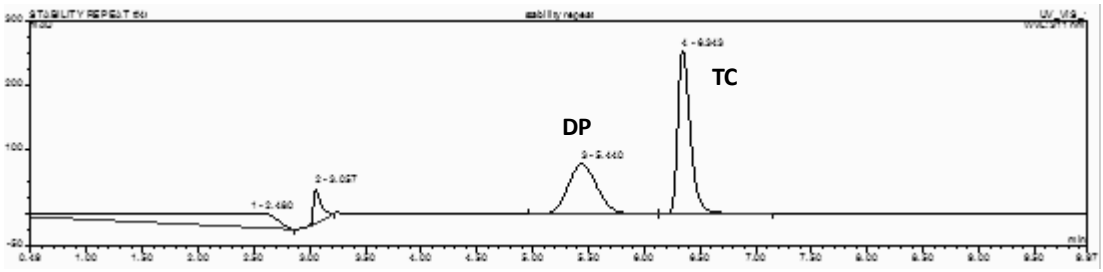

Figure 2.3. Tetracaine (TC) base hydrolysis degradation product (DP) at room temperature at 30 min sampling time.

Upon base hydrolysis at room temperature tetracaine lost 3 % of its original peak area after 30 min, 70 % after 1 h and only the degradation product was eluted after 24 h (Table 2.6). Tetracaine fully degraded to its degradation product for all experiments performed at 90 °C. The retention time for the degradation product and tetracaine was 5.42 ± 0.02 and 6.2 ± 0.016 min, respectively.

Table 2.6. Percentage variation (% Δ) in peak area for tetracaine at different temperatures in 0.1 M NaOH at pH 13.2.

Treatment	Temperature	Duration	% Δ in peak area
0.1 M NaOH	Room temperature	30 min	3
	Room temperature	1 h	70
	Room temperature	24 h	Only the degradation product was eluted
	90 °C	30 min	Only the degradation product was eluted
	90 °C	1 h	Only the degradation product was eluted
	90 °C	24 h	Only the degradation product was eluted

A degradant was also generated upon acid hydrolysis of tetracaine using 0.1 M HCl pH 1.1 at 90°C after 24 h (Figure 2.4).

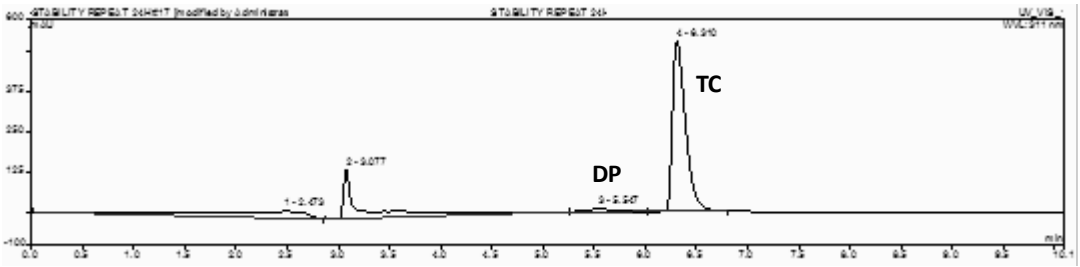

Figure 2.4. Tetracaine (TC) acid hydrolysis degradation product (DP) at 90 °C 24 h sampling time.

Upon acid hydrolysis tetracaine lost 7 % of its original peak area at the 24 h sampling time when stored at 90 °C whereas at room temperature no degradation was detected (Table 2.7). The retention time for the degradation product was similar to that observed upon base hydrolysis at 5.57 ± 0.1 min. It has been reported in the literature that the mechanism for tetracaine degradation in solution is hydrolytic degradation and the main degradation product is p-n-butylaminobenzoic acid (Menon *et al.*, 1981). The HPLC method was able to detect

tetracaine chemical degradation and the fact that the tetracaine peak was sensitive to degradation was deemed suitable to use as an indicator for detecting the chemical stability of the drug in subsequent work.

Table 2.7. Percentage variation (% Δ) in peak area for tetracaine at different temperatures in 0.1 M HCl at pH 1.1. Chemical degradation corresponded to > 2% Δ in peak area.

Treatment	Temperature	Duration	% Δ in peak area
0.1 M HCl	Room temperature	1 h	No significant variation
	Room temperature	2 h	No significant variation
	Room temperature	24 h	No significant variation
	90 °C	1 h	No significant variation
	90 °C	2 h	No significant variation
	90 °C	24 h	7

2.4.3 Tetracaine permeation studies

In order to assess percutaneous penetration of a model compound through a controlling barrier, mass transport studies should be conducted under sink conditions (i.e. not exceeding 10% of the donor concentration and permeant saturated concentration in the spent receiver fluid). These conditions are deemed essential since they guarantee a concentration gradient between the donor and receiver solution and hence, the driving force for the permeation process through the barrier (Howes *et al.*, 1996). The analysis of membrane thickness and donor solution pre-equilibration time effects on drug passive transport was limited to some extent, which resulted in receiver fluid saturation going beyond 10 % on occasion and an inability to measure permeation lag time on other occasion.

At pH 10, sink conditions were exceeded when a 0.12 mm thick silicone membrane was employed as the controlling barrier (14.4% of saturated solubility was recorded) (Table 2.9), but sink conditions were maintained in the receptor fluid at pH 4 for all test systems (a maximum of 0.36% of the drugs saturated solubility was recorded at the end of the study) (Table 2.8). The rapid transport through the 0.05 mm thick silicone membrane at both pHs did not produce a reasonable lag time and hence, this data was considered unreliable as an equilibrium that could generate a steady-state flux. As a consequence of these issues, only the transport data generated through a 0.25 mm thick silicone membrane was used to optimise the transport method in the Franz cells.

The overall passive transport during steady-state through the 0.25 mm thick membrane of unionised tetracaine (pH 10) was significantly higher ($p < 0.05$) than that of ionised tetracaine (pH 4). For example, at 24 h donor solution pre-equilibration time, steady-state flux across a 0.25 mm thick membrane was 18.7 ± 2.14 $\mu g.cm^{-2}.min^{-1}$ vs 2.6 ± 0.5 $\mu g.cm^{-2}.min^{-1}$ at pH 10 and 4, respectively (Table 2.8 and 2.9). The difference in permeation in the two different pH environments was suggested to be attributable to the different ionisation of tetracaine in the vehicles employed for the transport studies. The silicone membrane used in these experiments was lipophilic and as at pH 10 the calculated distribution coefficient (Log D) of tetracaine is significantly higher than at pH 4 (Log D of 2.78 and -0.77, source: Marvin Sketch, ChemAxon, Cambridge, USA) it is expected that the transport at pH 10 will be higher. Interestingly, lag time was significantly greater ($p < 0.01$) at pH 10 despite its better partition and penetration through the barrier when compared to that registered at pH 4 (Figure 2.5). Moreover, lag time was statistically higher ($p < 0.01$) at pH 4 with an increase in donor solution pre-equilibration time from 24 h to 120 h (Figure 2.5). A further increase in donor fluid equilibration time provided no more increases ($p > 0.05$) at either 120 h or 576 h.

Table 2.8. Summary indicies for Franz cell permeation studies at pH 4. Data represents mean ± SD (n = 5).

Pre-equilibration time (h)	24	24	24	120	576
Membrane thickness (mm)	0.05	0.12	0.25	0.25	0.25
Flux (µg /cm^2 /min)	4.0 ± 0.3	3.8 ± 0.4	2.6 ± 0.5	1.5 ± 0.3	1.6 ± 0.9
Lag time (min)	none	5 ± 1.1	4 ± 1.1	7 ± 0.8	10 ± 0.5
Sink conditions	Fulfilled	Fulfilled	Fulfilled	Fulfilled	Fulfilled
Chemical degradation	Not detected	Not detected	Not detected	Not detected	Not detected

Table 2.9. Summary indicies for Franz cell permeation studies at pH 10. Data represents mean ± SD (n = 5). Chemical degradation corresponded to > 2 % of the total tetracaine peak area

Pre-equilibration time (h)	24	24	24	120	576
Membrane thickness (mm)	0.05	0.12	0.25	0.25	0.25
Flux (µg /cm^2 /min)	7.28 ± 1.8	24.4 ± 2.9	18.7 ± 2.14	16 ± 1.3	__
Lag time (min)	none	7 ± 1.1	16 ± 2.3	13 ± 3.1	__
Sink conditions conditions	Fulfilled	Not fulfilled	Fulfilled	Fulfilled	__
Chemical degradation (%)	2.6 ± 0.9	4 ± 0.7	2.8 ± 0.4	3.4 ± 0.8	__

The reasons behind the changes in steady-state flux with an increase in pre-equilibration time were difficult to explain. For example, the rate of mass transfer during steady-state at pH 10 was statistically equivalent ($p > 0.05$) across a 0.25 mm thick silicone membrane when equilibrated at either 24 h (18.7 ± 2.14 µg. cm^{-2}. min^{-1}) or 120 h (16 ± 1.3 µg.cm^{-2}.min^{-1}) (Figure 2.5). However, the rate of mass transfer during steady-state at pH 4 was significantly higher ($p < 0.05$) across a 0.25 mm thick silicone membrane when pre-equilibrated at 24 h (2.6 ± 0.5 µg. cm^{-2}.min^{-1}) compared to 120 h (1.5 ± 0.3 µg.cm^{-2}.min^{-1}) (Figure 2.5). A further increase in pre-equilibration time did not result in a significantly different ($p > 0.05$) rate of mass transfer at pH 4 (1.6 ± 0.9 µg.cm^{-2}.min^{-1} at 570 h vs 1.5 ± 0.3 µg.cm^{-2}.min^{-1} at 120 h). Chemical degradation was not observed at pH 4 throughout the experiments, but it was observed at pH 10 (Table 2.8 and 2.9). The base derived hydrolysis product was shown in the chromatograms, albeit this was believed not to have a significant impact in the analysis of the transport data since the hydrolysis product corresponded to < 4% of the total tetracaine peak area.

Drug permeation across a confluent barrier such as the silicone membrane employed in this study can be described by Higuchi's equation of mass transport (Section 1.4.1). This equation states that all saturated solutions of the same drug should provide the same rate of transport given that: mass transfer occurs under sink conditions, the membrane is the rate controlling barrier, the application vehicle does not affect the barrier, thermodynamic activity is homogenous throughout the formulation and only one compound is transported across the membrane.

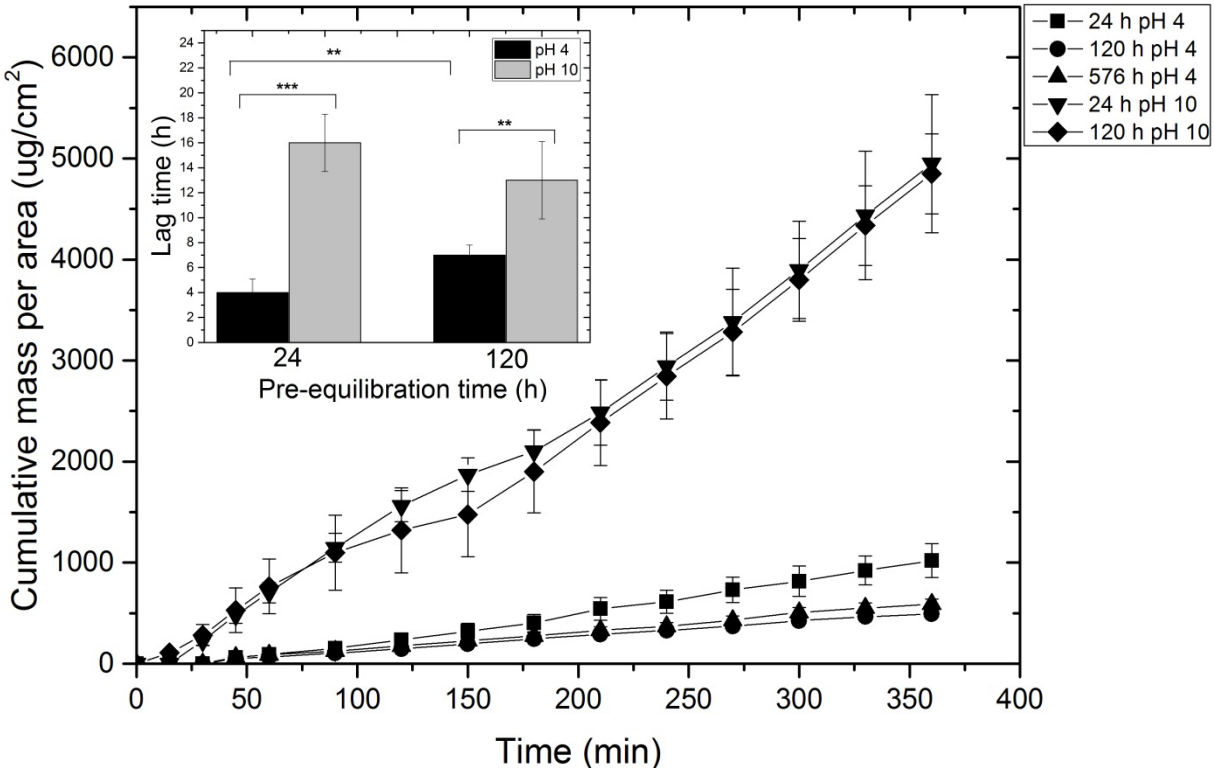

Figure 2.5. Tetracaine permeation profiles across a 0.25 mm silicone membrane at increasing suspension pre-equilibration time at pH 4 and pH 10. The inset graph represents lag time versus pH. Each point represents mean ± standard deviation (n = 5). ** $p < 0.01$ and *** $p < 0.001$ (Two-way ANOVA with Bonferroni post-hoc test).

The experimental setup was designed to investigate the conditions where tetracaine permeation could be explained by the Higuchi model. However, the lower transport rate with an increased donor solution pre-equilibration time (from 24 h to 120 h) did not follow this theoretical model. This was not thought to be due to violation of sink conditions, as they were maintained when the 0.25 mm silicone membrane was employed in the transport studies (no more than 10% of the total drug solubility was exceeded during the permeation studies (Howes *et al.*, 1996)). All the saturated donor solutions with increasing pre-equilibration time

showed linear permeation over the time period studied and this indicated that the membrane was the rate limiting step of the drug flux (Davis and Hadgraft, 1991). Membrane thickness was checked after the transport studies and found to be statistically equivalent ($p > 0.05$) when compared to that registered before the experiments. Hence, water permeation into the silicone membrane was thought to be negligible and did not appear to alter its properties significantly; therefore the vehicle was unlikely to affect the barrier (Dias *et al*., 2001). Only one drug compound was transported across the membrane and the thermodynamic activity was homogenous throughout the formulation as tetracaine donor solution remained saturated (as a fine suspension) at the two pHs throughout the permeation study. One hypothesis that could explain the decrease in permeation across the greater pre-equilibration time and the differences in lag time at both pHs is molecular aggregation. It has been reported in the literature that the interaction of tetracaine with lipophilic membranes is complicated by its detergent and self-association properties (Frezzatti *et al*., 1986; Zhang *et al*., 2007). Tetracaine like other local anaesthetics has a high tendency to self-associate in concentrated solutions due to formation of intermolecular hydrogen bonds (Guerin *et al*., 1980; Umemura *et al*., 1981). In addition, it has been described that the ability of a molecule to cross membranes decreases when intermolecular association occurs by hydrogen bonding (Matsukawa *et al*., 1991).

2.5 Conclusions

Three ‘fit-for-purpose’ HPLC methods were reported in this Chapter. Their use in subsequent parts of the thesis was underpinned by experimental results that demonstrated sound calibration curve linearity, specificity, repeatability and precision in accordance with the

guidelines set by the ICH. The verified tetracaine HPLC method was therefore used to develop the *in vitro* permeation assay. A 120 h donor solution pre-equilibration time and a 0.25 mm thick silicone membrane were considered to be the optimal conditions to determine tetracaine transport because using this setup the data was not limited by drug depletion, receiver fluid saturation or chemical degradation. It was hypothesized that molecular aggregation was influencing tetracaine transport permeation behavior and the next phase of this work was designed to investigate how the effects of drug-drug interaction influenced transmembrane transport.

CHAPTER THREE

The effects of molecular aggregation upon transmembrane permeation

3.1 Introduction

Pharmacologically active compounds can display amphiphilic properties and this can lead to molecular aggregation in solution. Aggregate formation can have a significant impact on the pharmacological effects of a molecule as it can alter the passive diffusion process, thus modifying its ability to localisation at a receptor site. The aggregation of amphiphilic molecules occurs above critical aggregation concentration (CAC) and it generates a cluster of molecules which can present different physicochemical properties to the parent entity (Florence and Attwood, 1998; Potts and Guy, 1995). Diffusion speed is typically retarded and interactions with administration vehicles and biological membranes can be altered when a molecule aggregates (Schreier *et al*., 2000; Rossetti *et al*., 2011; Ueda *et al*., 2012). However, the physical interactions between the aggregated and non-aggregated entities, the multiple routes molecules can take through a barrier and the potential for both the unaggregated and aggregated drug to pass through the barrier means that that influence of molecular aggregation upon membrane transport is a complex field of study that warrants further investigation.

One example of a molecule that is known to aggregate in solution is tetracaine. Its self-association is thought to be driven by intermolecular tertiary amine hydrogen bonding and amine-ester hydrogen bonding (Guerin *et al*., 1980). Tetracaine topical bioavailability is reported to be relatively good for a skin product at 15% (Hadgraft, 1999; Thomas and Finnin, 2004; O'Brien *et al*., 2005), but it has a slow onset of topical anaesthesia (30 to 60 min) which hinders its effective clinical use in certain contexts (Lubens *et al*., 1974; Escribano *et al*., 2005; Heavner, 2008). Attempts to enhance tetracaine diffusion across the skin have been reported in the literature (Sang-Chul *et al*., 2004; Liu *et al*., 2005; Chao *et al*., 2008; Swayer

et al., 2009), but there has been very little investigation into how molecular aggregation influences the drug passive diffusion and hence how this contributes to its speed of onset is therefore unknown.

Tetracaine is commercially available as a 4% gel (formulation pH ~ 9) and can exist in solution as three different microspecies depending on the pH. Tetracaine base (TC) has been shown to penetrate the skin (Chekirou *et al*., 2012), and it is the dominant microspecies above pH 9. Below pH 6.5 both the tertiary (TCH^+) and secondary amine (TCH_2^{2+}) are protonated, the former of these microspecies (TCH^+) prevail at physiological pH of the skin (4.2 - 6.5) (Figure 3.1). It is generally accepted that the tetracaine tertiary amine binds to the sodium channels, blocking the sodium influx and inhibiting nerve cell depolarization that prevent the propagation of nerve cell impulses (Iglesias-García *et al*., 2010), but which is the most effective species to gain rapid penetration into the skin remains less clear.

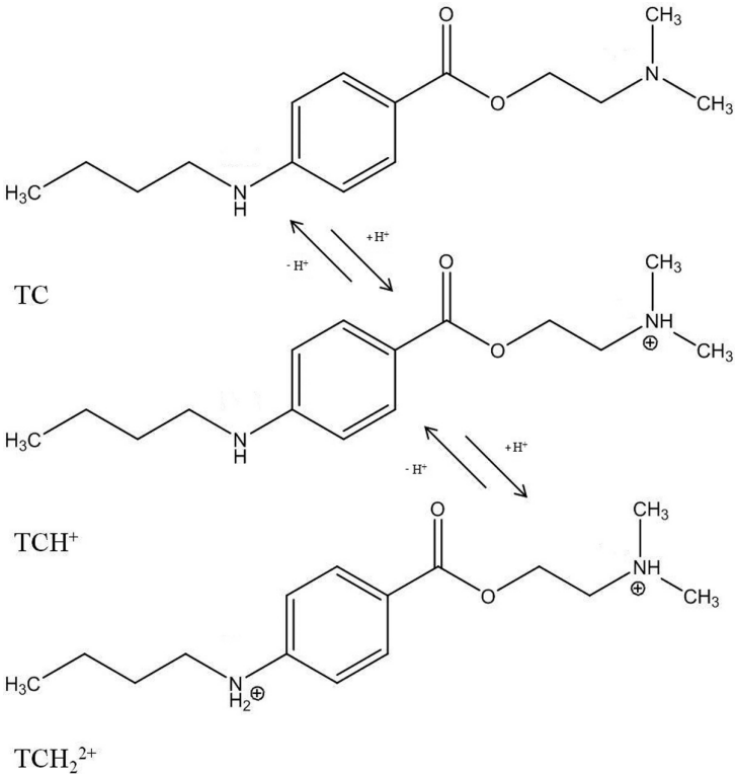

Figure 3.1. Schematic representation of tetracaine (TC) ionization equilibrium, exhibiting two ionisable groups, the tertiary (TCH^+) and secondary amine (TCH_2^{2+}) (Iglesias-García *et al.*, 2010).

The purpose of the work in the current Chapter was to understand the properties of the tetracaine aggregates that may form in topical preparations, in order to gain a better understanding of how the physical attributes of supramolecular masses formed as a consequence of drug aggregation influence hydrophobic membrane transport. Tetracaine amphiphilic characteristics were manipulated by simply altering the pH of aqueous solutions containing the drug when it was above its critical aggregation concentration. This allowed a series of aqueous vehicles where the degree of ionization of both the tertiary and secondary amine was varied to be presented to two hydrophobic membranes, porcine skin and silicone

membrane, in the anticipation that different types of drug aggregates and different transport rates could be recorded and analysed. Photon correlation spectroscopy was employed to determine the critical aggregation concentration at which nanosized aggregates were formed and zeta potential measurements provided details regarding electrostatic interactions. Fourier transform infrared spectroscopy (FTIR) and proton nuclear magnetic resonance (^{1}H-NMR) were employed to investigate the molecular arrangement and intermolecular bonding between the different microspecies in solution.

3.2 Materials

Acetonitrile and methanol both HPLC grade, grade A glass pipettes, clear glass HPLC vials crimpable lids and 0.45 μm nylon filter papers were purchased from Fischer Scientific (Leicester, UK). Tetracaine base BP grade (99.9%) and deuterium oxide (99.9 atom %) were supplied by Sigma Aldrich (Dorset, UK). Concentrated hydrochloric acid and sodium hydroxide was from Fluka (Dorset, UK). Sodium acetate, potassium dihydrogen phosphate and 1-Octanol were provided by Alfa Aesar (Heysham, UK). Silicone membranes with a thickness of 0.25 mm were purchased from GBUK Healthcare (Selby, UK).

3.3 Methods

3.3.1 Tetracaine pKa determination

The automatic titration system used in this study comprised an autoburette (Dosimat 765 liter ml syringe, Metrohm, Buckingham, UK) and pH meter (MP230 Mettler Toledo, Leicester,

UK) with a pH electrode (Metrohm, Buckingham, UK). A 0.1 M KCl electrolyte solution was used to maintain the ionic strength. The temperature of the test solutions was maintained in a thermostatic jacketed titration vessel at 25 °C ± 0.1 °C by using a temperature controller (Techne TE-8J, Sigma Aldrich, Dorset, UK). The solution under investigation was stirred vigorously during the experiment. A pump with speed capability of 20 $mL.min^{-1}$ (Mini-plus, Gilson, Luton, UK) was used to circulate the test solution through a quartz flow cuvette using a cuvette with a path length of 0.1 cm. The flow cuvette was mounted on an UV-visible spectrophotometer (HP 8453, Agilent, Cheadle, UK). All instruments were interfaced to a computer and controlled by a Visual Basic program. Automatic titration and spectral scans adopted the following strategy: the pH of a solution was increased by 0.1 pH unit by the addition of KOH from the autoburette; when pH readings varied by < 0.001 pH unit over a 3 s period the spectrum of the solution was then recorded. The cycle was repeated automatically until the defined end point pH value was achieved. All the titration data were analysed with the pHab program (Gans *et al*., 1999). The microspecies plot was calculated with the HYSS program (Alderighi *et al*., 1999).

3.3.2 Aggregation characterization

3.3.2.1 Photon correlation spectroscopy characterization

Changes in derived count rate and zeta potential of the donor solutions were tracked using photon correlation spectroscopy (Malvern Nanoseries Zetasizer, Malvern Instruments Ltd., Malvern, UK). Measurements were taken at a scattering angle of 173°. Refractive index and viscosity constants were set at 1.33 and 0.88 mPa.s, respectively. Samples were filtered through a 0.45 μm cellulose nitrate filter prior to the analysis. The scattering information was

determined at increasing tetracaine molar concentrations in acetate buffer (0.1 M) at pH 4, 6, 7.6, 9 and 10. Control solutions were prepared in the same manner as for the test systems, but without the addition of drug. The critical aggregation concentration was determined from the discontinuity in the linear model applied to the unattenuated derived count rate data and was confirmed by the application of a second derivative function (OriginPro 9.1 Software, OriginLab, Northhampton, USA). The size of the molecular aggregates was detected by converting the light scattering signal into a hydrodynamic radius using the Stokes–Einstein equation given in equation 3.1, where k is the Boltzmann constant, T is the absolute temperature and η is the solvent viscosity. The size of the molecular aggregates was determined above critical aggregation concentration ca. 87 - 95% of tetracaine saturation in each aqueous vehicle at pH 4, 6, 7.6, 9 and 10. The pH was adjusted to the required value when necessary by adding NaOH (1 M) or acetic acid. The zeta potential of the aggregate containing solutions was determined at pH 4, 7.6 and 9 using the same solutions described above.

$$RH = \frac{kT}{6\pi\eta} \qquad \text{(Equation 3.1)}$$

3.3.2.2 Molecular dynamic studies

Tetracaine self-association was generated from the hydrochloride crystal structure reported by Nowell *et al.*, (2002). The atomic co-ordinates and unit cell parameters were obtained from the Cambridge Structural Database; entry XISVOK (Thomas *et al.*, 2010). The assembly was generated (2 x 2 x 2 unit cells) using the Mercury software (Macrae *et al.*,

2008) and then visualised using Accelrys Viewerlite v5.0 software (Biovia, San Diego, USA).

3.3.2.3 Apparent distribution coefficient

The apparent drug distribution coefficients were measured using a tetracaine saturated acetate buffer solution at room temperature with a second phase composed of 1-octanol. A 0.1 M acetate buffer solution was employed in the studies at a modified pH of 4, 6, 7.6, 9 and 10 as previously described (Valenta *et al*., 2000). After phase separation the aqueous phase was withdrawn and samples were centrifuged at 13000 rpm (Biofuge, Heraeus, Germany) and aliquots of the liquid phase were then transferred into vials. The samples were analysed employing the tetracaine HPLC method described in Section 2.3.1. The apparent distribution coefficient (D) was defined as the ratio of the concentration in octanol (C_0) to the total concentration of ionized (C_i) and unionized (C_u) moiety in the aqueous phase (equation 3.2). The amount of tetracaine detected in the aqueous phase was above the experimentally determined critical aggregation concentration for all the test systems.

$$D = \frac{C_0}{(C_i + C_u)} \qquad \text{(Equation 3.2)}$$

3.3.2.4 Fourier Transform Infrared spectroscopy (FTIR)

Tetracaine solutions at pH 4, 6, 7.6, 9 and 10 were prepared in deuterium oxide (D_2O) at the same concentrations used for molecular aggregates size analysis. D_2O was employed in the solutions as it dampened the solvent signal in the 1700 - 1300 cm^{-1} range. The pH was adjusted with NaOH (1 M) or acetic acid. The samples were loaded into a demountable

universal transmission cell system (Omni-Cell, Specac Ltd., UK) fitted with calcium fluoride (CaF_2) windows and a 25 μm mylar spacer (Specac Ltd., UK). The infrared spectra were recorded from 4500 to 1000 cm^{-1} using a Spectrum One spectrometer (Perkin Elmer Ltd., UK) and spectral analysis was performed with Spectrum software version 5.3.1 (Perkin Elmer Ltd., UK). After normalization of transmittance, background subtraction and baseline correction, the analysis of the spectra was done by analysing the C=O band, as described previously (Popova and Hincha, 2003).

3.3.2.5 ^{1}H-NMR spectroscopy

Tetracaine solutions at pH 4, 6, 7.6, 9 and 10 were prepared in deuterium oxide at the same concentrations used for molecular aggregates size analysis. The spectra of each solution was obtained with a Bruker Avance DRX400 NMR spectrometer (Bruker, Coventry, UK). A 600 μL aliquot of each sample was used for the measurements which were conducted at 400 MHz with 5000 scans. The peaks assignments were made and supported using the predicted spectra (ChemNMR software, PerkinElmer, Beaconsfield, UK).

3.3.3 Tetracaine transport studies

To eliminate any thermodynamic influence on the drug passive transport across both membranes, tetracaine was formulated as a saturated solution, i.e., at a thermodynamic activity of unity (Smith, 1990; Hadgraft, 1996), as previously described in Section 2.3.3. The fine suspension allowed visual verification if drug saturation had been maintained throughout the entire experimental period. The individually saturated solutions at pH 4, 6, 7.6, 9 and 10 were prepared by adding excess tetracaine to acetate buffer (0.1M) and were left to

equilibrate for 120 h. The pH of each solution was adjusted to the required value when necessary by adding NaOH (0.1 M).

Adult pig ears were obtained from a local abattoir. The ears were removed from the carcass after hair removal. Any ears that were obviously damaged were discarded. The ears were cleaned with water, the residual water on the skin surface was immediately removed by blotting with tissue, visible residual hairs were trimmed carefully and the ears were stored at -20 °C (no more than three months before use). Before the experiments the porcine skin was defrosted and the subcutaneous fat carefully removed using a scalpel. Both the silicone membrane (0.25 mm thick, used as obtained) and the porcine skin were cut into pieces of a suitable size and mounted in the Franz diffusion cell (University of Southampton, UK). *In vitro* infinite dose permeation experiments were conducted as method described in Section 2.3.3 over a period of 6 h and 22h (for the silicone and porcine membrane, respectively). The samples were analysed employing the tetracaine HPLC method described in Section 2.3.1.

3.3.4 Statistical analysis

All data were presented as mean ± standard deviation and statistical analysis of data was performed using SPSS version 16.0, as described previously in Section 2.3.4. A statistically significant difference was determined at a minimal level of significance of 0.05 ($p < 0.05$). The number of replicates was 5 in the permeation studies and 3 in the apparent distribution coefficient determination, zeta potential and light scattering studies.

3.4 Results and Discussion

3.4.1 Tetracaine pKa determination

The analysis of the titration data using the pHab program revealed two inflection points at pH values of 2.48 ± 0.03 and 8.56 ± 0.02 in the plots of tetracaine solution UV absorbance versus its pH and these were considered to be the approximate values of tetracaine pKa's (Figure 3.2). The pKa value at 2.48 ± 0.03 was assigned to the protonation on nitrogen of the tertiary amine and the pKa value of 8.56 ± 0.02 was assigned to the secondary amine. There was a good agreement between the experimentally determined values in this work and those described in the literature. For example, Iglesias *et al*., (2012) reported a tetracaine pKa's values of 3.41 and 8.24. Therefore, the percentage of each microspecies in solution (TC, TCH^+ and TCH_2^{+2}) at increasing pH was calculated using the experimentally determined pKa's (Table 3.1). The commercial topical product displayed an apparent pH of ca. 9 and hence it was considered to present tetracaine predominantly as a unionized molecule (TC) when it was used clinically to induce topical anaesthesia.

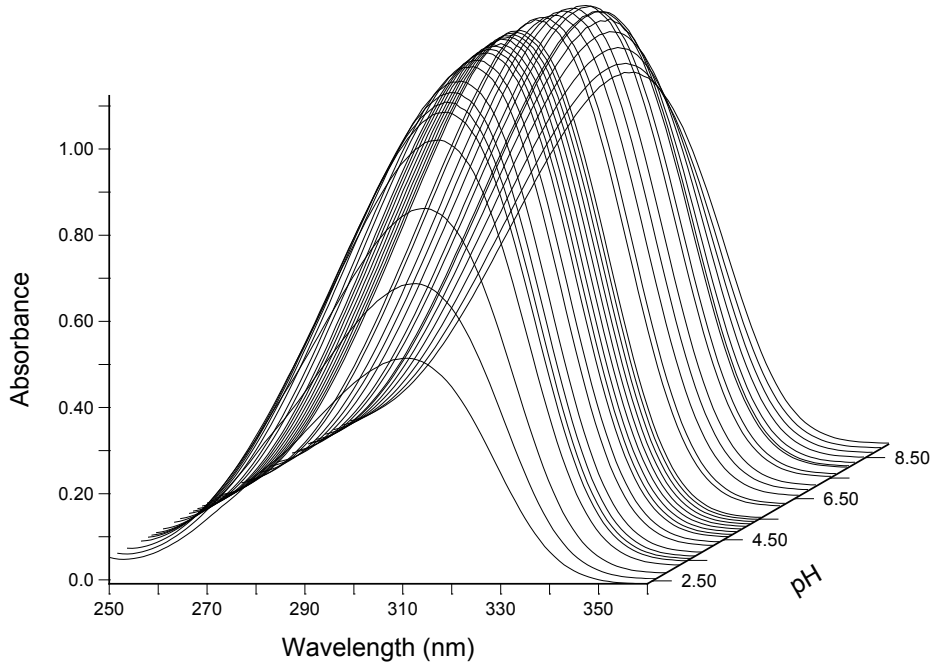

Figure 3.2. UV-spectrum of tetracaine (560 μM) between pH 2.36 to pH 10.94 starting in 20.1 mL of KCL (0.1M) at 25 °C using a cuvette with a path length of 0.1 cm. Total points represented is 44.

Table 3.1. Percentage of the microspecies (TC, TCH^+ and TCH_2^{+2}) in solution with an increasing pH (source: HYSS software (Alderighi *et al.*, 1999)).

pH	**% TC**	**% TCH^+**	**% TCH_2^{+2}**
4	0.03	93.5	6.47
6	0.23	99.7	0.07
7.6	9.88	90.1	0.02
9	73.4	26.6	negligible
10	96.5	3.5	negligible

3.4.2 Tetracaine aggregation characterization

3.4.2.1 Photon correlation spectroscopy characterization

The critical aggregation concentration of the drug solutions was significantly higher ($p < 0.05$) when they contained species with some proportion of both the ionized tertiary and secondary amines, i.e. the critical aggregation concentration was 18 ± 1.4 mM at pH 4 (Figure 3.3) and 3 ± 0.9 mM at pH 7.6 compared to 0.7 ± 0.1 mM at pH 9 and 0.5 ± 0.1 mM at pH 10. The two CAC values recorded at pH 9 and 10 were not significantly different ($p > 0.05$). This trend in the data indicated that the self-association process was more favourable when the unionised tetracaine microspecies were prevalent in the aqueous solutions. Tetracaine is commercially available in a 4% (w/w) gel. The drug is partially precipitated in the product, presumably to promote maximum thermodynamic activity throughout the entire storage and administration period (Escribano *et al.*, 2005; Paudel *et al.*, 2010). It was interesting to note that the 4% (w/w) tetracaine commercial gel not only presented the molecule to the skin using a two phase system, microscopy analysis showed the presence of drug microcrystals (Figure 3.4 a and b), but given the CAC data, it also presented the molecule in the bulk solution in both its aggregated and unaggregated forms.

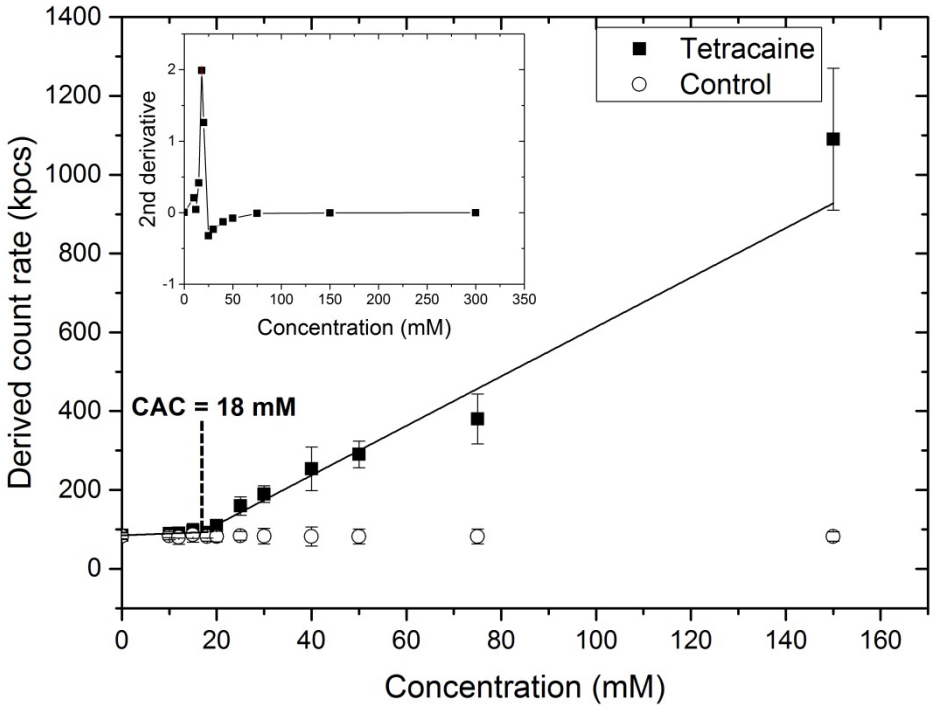

Figure 3.3. Graph depicting the changes in total light scattering for samples at pH 4. Inset graph represents the application of a second derivative function that determined the discontinuity in the slope of the derived count rate data. Each point in represents mean ± standard deviation ($n = 3$).

Miller *et al.*, (1993) reported evidence of significant tetracaine molecular aggregation by three independent methods: surface tension, specific conductivity and pH in propylene glycol and saline (0.9% w/w) vehicles (pH between ca. 6.8 - 8.1). The calculated critical aggregation concentration values ranged from 3 mM to 180 mM. These workers attributed these differences to the broad range over which self-association begins and the way this affects the measured physical properties. Tetracaine self-association in aqueous vehicles at pH 4.5 and 6.5 has been reported to be ca. 34.5 mM and 69 mM by other workers who used light

scattering and surface tension measurements, respectively (Fernandez, 1980; Kitagawa *et al*., 2004).

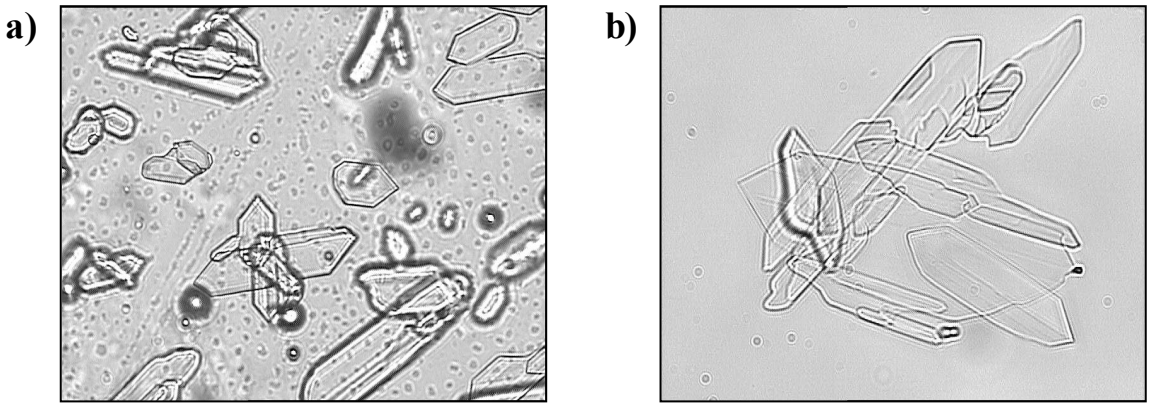

Figure 3.4. Light microscopy (Olympus BX50F, Japan) at a magnification of 40 × a) tetracaine commercial product and b) tetracaine test system at pH 9 above critical aggregation concentration.

The higher critical aggregation concentration values reported in the literature was attributable to a better analytical sensitivity of the technique employed in this work. It should be noted that due to the limit of detection of photon correlation spectroscopy, drug aggregates that displayed a hydrodynamic radius below 2 nm could not be detected and hence the calculated CAC values could be challenged. However, in this case it was assumed that the data collected herein provided a good indication of tetracaine molecular structure changes in solution.

When the donor solutions that were to be subsequently employed in the transport studies were analysed, the size of the aggregates present in solution was shown to be significantly greater ($p < 0.05$) when the charge on the tetracaine was reduced, i.e., the average aggregate size was 114 ± 8.3 nm at pH 4 whilst it was 188 ± 20.4 nm at pH 9 (Figure 3.5 a). The relatively high polydispersity index (≥ 0.25) measured for all test systems can be attributed to the presence of different sized aggregates in solution (Figure 3.5 b, c and d).

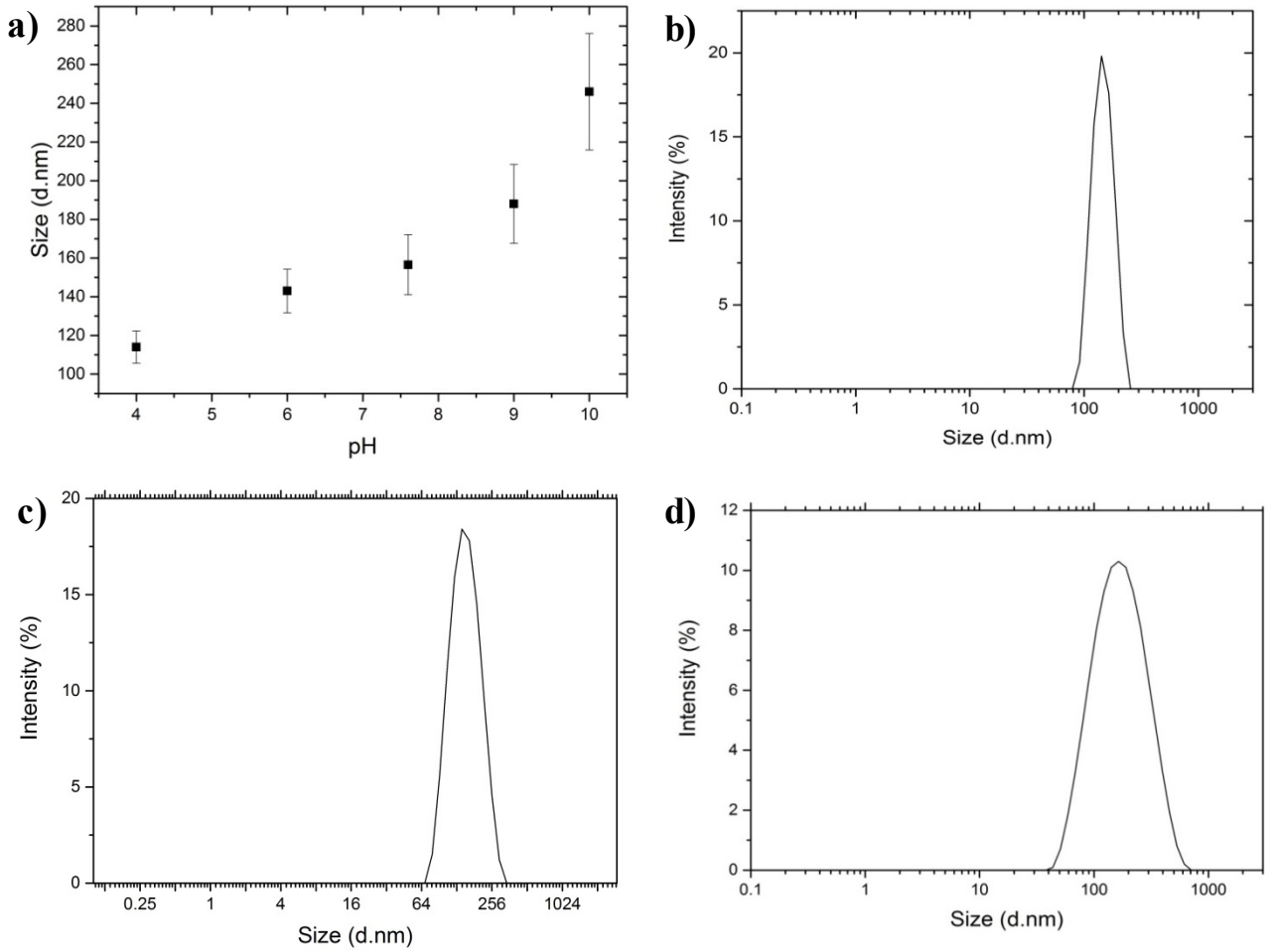

Figure 3.5. Graph depicting the changes in a) molecular aggregates size (nm) at increasing pH of the donor solution and size distribution above critical aggregation concentration b) at pH 4, c) at pH 7.6 and d) at pH 9. Each point represents mean ± standard deviation ($n = 3$).

The zeta potential of the solutions containing more of the charged amine species was also significantly higher ($p < 0.05$) (4.34 ± 1.8 mV at pH 4 vs 0.98 ± 0.2 mV at pH 9). This data suggested that the supramolecular structures formed from the ionised tetracaine microspecies were displaying the charged moiety on its surface. Molecular modelling of the tetracaine aggregate structure using the crystallographic data supported this hypothesis. When tetracaine forms crystals the charged amine is most likely to orientate preferentially at the surface of the structure rather than the interior, as seen by the positioning of the Cl^- ions that form weakly bound pairs with N^+ (Nowell *et al.*, 2002) (Figure 3.6). Whilst it is accepted that the supramolecular formation in solution is not the same process as supramolecular structure formation during crystallisation this was thought to be a rational explanation for the trends in the zeta potential results. It is also important to note that the formation of molecular aggregates by amphiphilic molecules in an aqueous environment is less favoured when electrostatic repulsion between the polar head groups is higher. This results in an increase in the surface area of the molecule that reduces the capability of intermolecular interactions between drug molecules (Tanford, 1980; Israelachvili, 1985). This then correlates well with the size and charge of the tetracaine supramolecular structures in aqueous solution presented herein.

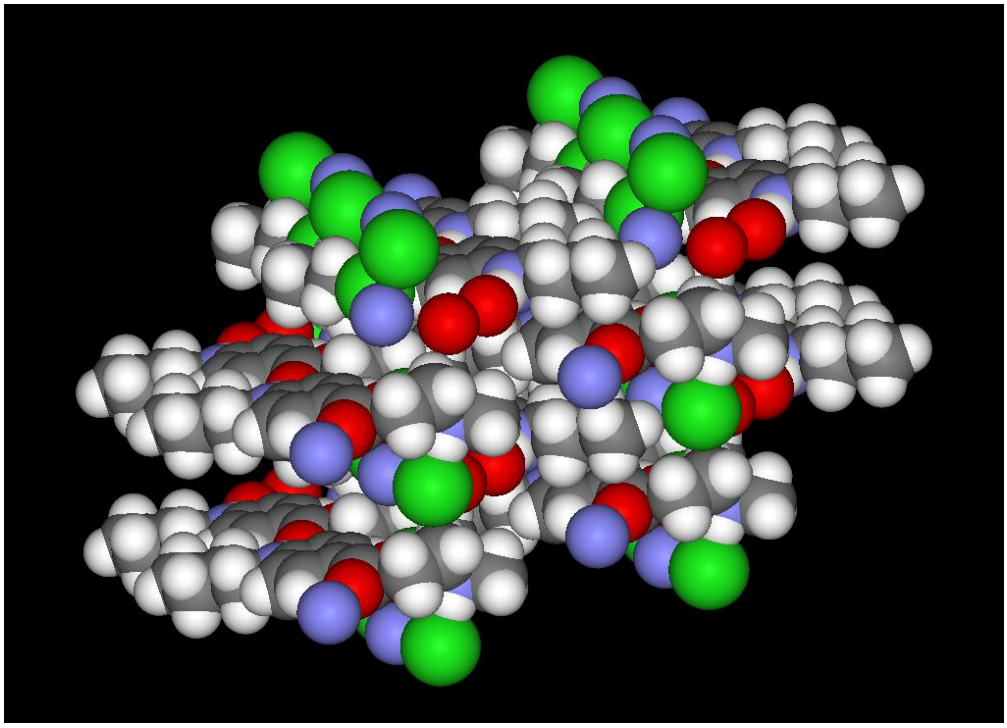

Figure 3.6. Screenshot of a molecular aggregate composed of 16 tetracaine hydrochloride molecules generated from the crystal structure using the Mercury software and visualised using Accelrys Viewerlite v5.0. Atom colour scheme: H = white, C = grey, O = red, N = blue, Cl = green.

3.4.2.2 Apparent distribution coefficient

The experimentally determined Log D values of tetracaine donor solutions at pH 4, 6, 7.6, 9 and 10 showed a good agreement with the calculated values at lower pHs, i.e. when both the tertiary and secondary amine were ionized (Figure 3.7). The most significant differences were surprisingly at the higher pHs of 9 and 10 where the experimental distribution coefficients were recorded as 2.1 ± 0.16 and 2.01 ± 0.18 respectively. As that the amount of tetracaine

detected in the aqueous phase of the partitioning experiments was above the experimentally determined critical aggregation concentration for the entire test systems, it was assumed that the differences in the predicted and measured values were a consequence of supramolecular tetracaine structures. Since the experimental partition coefficient was lower than the predicted value, this indicated that molecular aggregates were in fact more hydrophilic than the unaggregated tetracaine. It was possible that the aggregates ionized amine at pH 9 and 10 was orientated more preferably towards the surface of the supramolecular structure as suggested by the molecular simulation images. As such, it can be hypothesized that the process of aggregation had a negative impact on the hydrophobicity of the molecules presented to the water/oil interface used to determine the distribution coefficient. The presence of an organized cluster where the polar region groups are displayed to the outer region may provide a higher aqueous solubility due to a decrease in the interfacial tension between the aggregate surface and water as previously described for other molecules by Kronberg *et al.*, (2014) and therefore explain the lower experimental Log D values compared to the predicted ones.

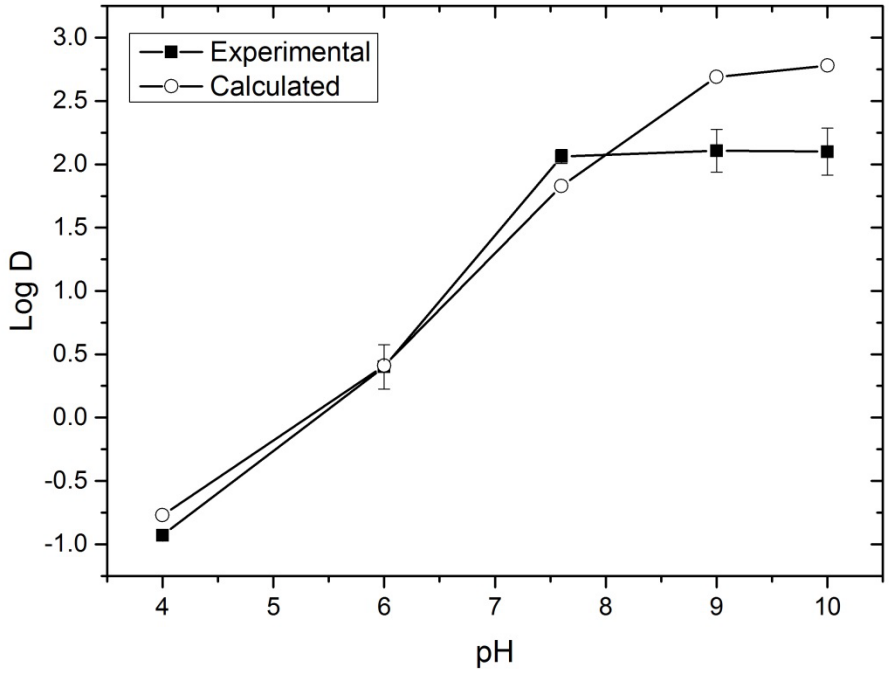

Figure 3.7. Experimental and calculated (Marvin Sketch, ChemAxon, Cambridge, USA) distribution coefficients values (Log D) for tetracaine above critical aggregation concentration using n-octanol in acetate buffer (0.1 M) at pH 4, 6, 7.6, 9 and 10. Each point represents mean ± standard deviation for the experimental data (n = 3).

3.4.2.3 Fourier Transform Infrared spectroscopy

The FTIR spectra at pH 4 was characterized by the presence of the C=O group (1707 cm^{-1}) and two vibrational bands at 1597 cm^{-1} and 1560 cm^{-1} (Figure 3.8). The two bands between 1600 and 1550 cm^{-1} fall within the hydroxyl group absorption frequency and could not be directly assigned to any functional group of the monomeric structure. The 'new' absorption bands were presumably due to intermolecular interactions in solution as a consequence of self-association, which may have generated a cluster of molecules with different physicochemical properties to the parent entity, as previously reported by other researchers

(Florence and Attwood, 1998; Potts and Guy, 1995). The appearance of 'new' absorption bands is not uncommon upon drug-drug interaction and has been shown for other molecules (Hinedi *et al.*, 1993). Above pH 4, the stretching vibrational band assigned to the C=O group was no longer present (Figure 3.8, data at pH 6 and 10 is not shown for greater visual clarity), and there was a significant upfield shift of the vibrational bands assigned to the C-O-H group that resulted in a much broader peak as the vehicle pH increased (e.g. 1473 cm^{-1} at pH 9). This suggested that there was an increasingly favourable environment for aggregation driven by stronger intermolecular interactions in the solutions at a higher pH. The FTIR data suggested that the tetracaine molecules responsible for the supramolecular structure formation utilised hydrogen bonds formed through an N-H-O=C association. It was still considered a possibility that N-H-N-H association could also play a role in the aggregation process (Guerin *et al.*, 1980), but because the IR signals from the amines in water were very weak it was impossible to arrive at firm conclusions with regard to the amine involvement in the tetracaine-tetracaine association.

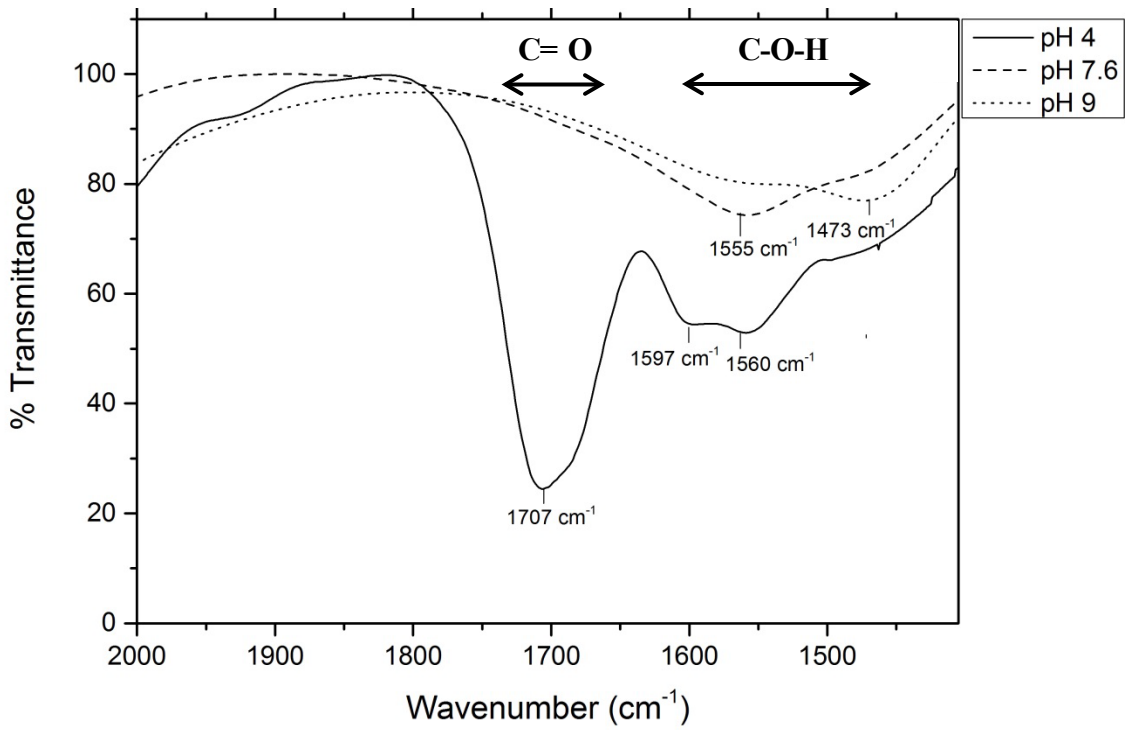

Figure 3.8. Fourier transform infrared (FTIR) transmittance spectra (arbitrary units) of tetracaine in deuterium oxide at pH 4, 7.6 and 9 above the experimentally determined critical aggregation concentration.

3.4.2.4 ^{1}H-NMR spectroscopy studies

There were 9 protons that gave clearly resolved peaks in NMR spectrum (Table 3.2). The resonance of the methylene protons H1, H2, H3 of the alkyl chain of the secondary amine and the methyl group (H9) attached to the tertiary amine remained essentially unchanged regardless of the pH environment of tetracaine. However, the chemical shift of all the other protons tended to shift downfield (deshielding effect) with an increasing pH (Figure 3.9).

Table 3.2. Tetracaine proton chemical shifts in D_2O at 32 °C (ppm) at pH 4, 6, 7.6, 9 and 10. The peak assignment was obtained using (ChemNMR software, PerkinElmer, Beaconsfield, UK). (s) singlet; (d) doublet; (t) triplet and (q) quartet.

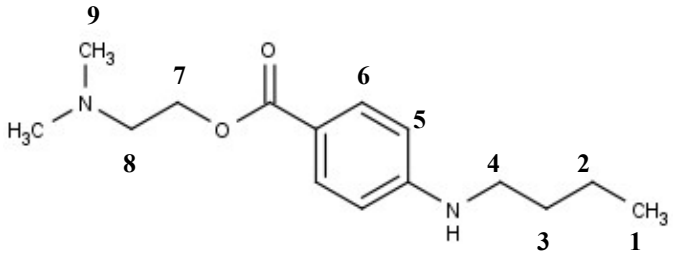

	pH 4	pH 6	pH 7.6	pH 9	pH 10
H1	0.88 (t)	0.88 (t)	0.89 (t)	0.89 (t)	0.89 (t)
H2	1.32 (q)	1.33 (q)	1.33 (q)	1.33 (q)	1.33 (q)
H3	1.47 (q)	1.48 (q)	1.48 (q)	1.48 (q)	1.48 (q)
H4	2.92 (t)	3.12 (t)	3.17 (t)	3.16 (t)	3.15 (q)
H5	6.5 (d)	6.5 (d)	6.73 (d)	6.74 (d)	6.74 (q)
H6	7.68 (d)	7.68 (d)	7.85 (d)	7.86 (d)	7.86 (q)
H7	4.35 (t)	4.3 (t)	4.9 (t)	5.56 (q)	5.51 (t)
H8	3.46 (t)	3.5 (t)	3.57 (t)	3.60 (t)	3.86 (t)
H9	2.87 (s)	2.86 (s)	2.86 (s)	2.87 (s)	2.86 (s)

The methylene protons of the alkyl chain adjacent to the oxygen of the ester group (H7) displayed the largest frequency change of ~ 1.16 ppm as the pH increased from 4 to 10. In addition, both the H6 and H7 protons at either side of the carbonyl group changed in their multiplicity at basic pHs. The other significant proton chemical shift change was the methylene protons adjacent to the tertiary amine (H8) which moved ca. 0.4 ppm as the pH increased from 4 to 10. The chemical shifts of the aromatic protons attached to the benzene

ring and the methylene protons adjacent to the secondary amine changed, but by relatively small amounts, however, there was a change in the multiplicity of these protons at pH 10.

The decrease of the nuclear shielding at increasing vehicle pH could indicate a possible change in the free movement of the tetracaine molecules in solution, suggesting that the rotation of the methylene protons of the lateral alkyl chains was inhibited by intermolecular bonding between tetracaine molecules. Steric hindrance upon molecular interaction between local anaesthetics has been previously reported in the literature (Umeda *et al.*, 2007). This increasing steric hindrance, which increased with pH, indicated in a similar manner to the FTIR data, that when more the non-ionised tetracaine molecules were present in solution a more compact supramolecular structured was formed. Previous studies on the interactions of model polyamines in supramolecular structures have shown similar results (Sassi *et al.*, 1992; Jiang *et al.*, 2002). Both the NMR and IR data suggested that intermolecular interaction was stronger at the high pHs and that the two principal functional groups that facilitated this interaction was the C=O and NH_3^+ and therefore, just like previous work by Guerin *et al.*, (1980), hydrogen bonding was presumed to be the main driver for this interaction.

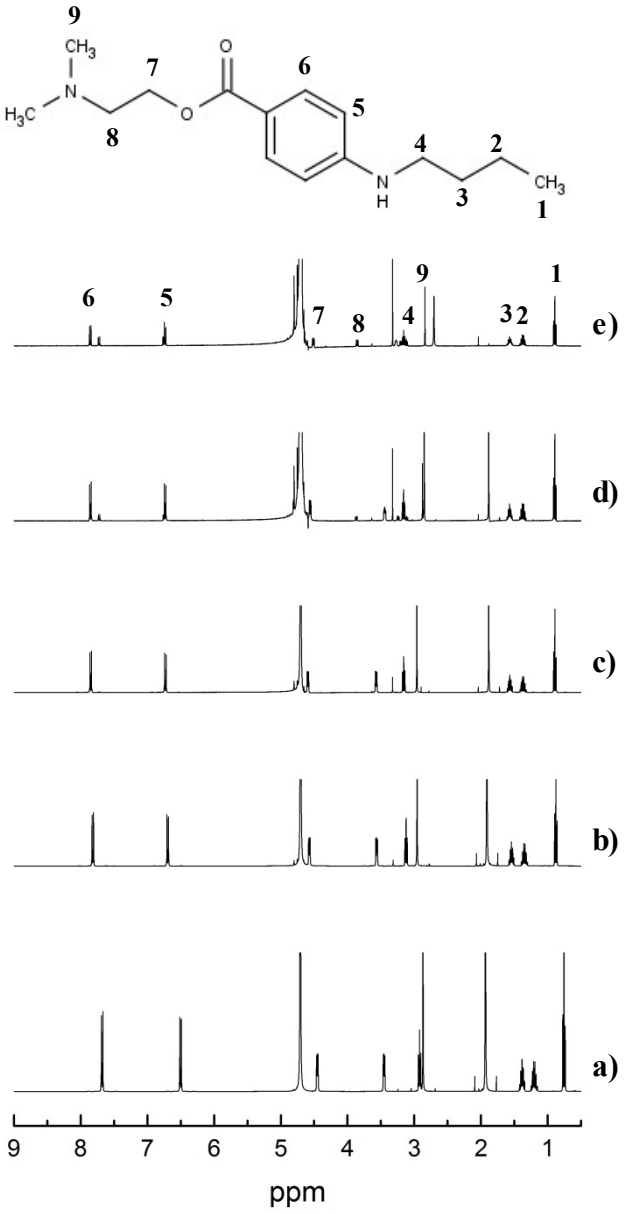

Figure 3.9. ^{1}H-NMR spectra of tetracaine in deuterium oxide above the experimentally determined critical aggregation concentration, a) pH 4, b) pH 6, c) pH 7.6, d) pH 9 and e) pH 10.

3.4.3 Tetracaine permeation studies

Two membranes were used in this work, a synthetic silicone membrane, which presents a homogeneous barrier to diffusion that occurs in the absence of pores (e.g. excluding follicular transport), and porcine skin, which is the typical *in vivo* preclinical model used to characterise topically applied medical products, due to its similar permeability and histological characteristics to human skin (Sekkat *et al.*, 2001; Tiemessen, 1993). Porcine skin allows molecules to pass through its barrier both via the confluent structure presented by the cells in the various skin layers and the pores introduced into the skin tissue (e.g. via hair follicles). In contrast, the synthetic silicone membrane only allows transport through its barrier via the classical partitioning and diffusion process which has been modeled by Higuchi (Section 1.4.1). By combining the data from a series of test systems using both membranes it was hoped that an understanding of how the molecules passed through the barriers could be obtained.

The data confirmed that at each pH the synthetic membrane (Figure 3.10 a) and porcine skin (Figure 3.10 b) were acting as a rate limiting barrier and hence, the linear portion of the permeation data was adequate to calculate steady-state permeation. The experiments applied an infinite dose of the drug that was saturated in an aqueous solution which is known not to interact with the membrane (as demonstrated in Section 2.4.3) and as the calculation of the total drug transport through the membrane in each experiment suggested that no drug depletion occurred, it was thought that tetracaine was constantly supplied in the transport studies at unity to the barrier. Sink conditions in the receiver compartment were maintained for each experiment, i.e., tetracaine concentration in the receiver fluid did not exceed 10% of the saturated solubility at each experimental pH (Howes *et al.*, 1996). Therefore, it was

assumed that the cumulative rate of drug passing the membrane could be considered to be the steady-state flux in the exponential portion of the cumulative drug concentration vs time plots.

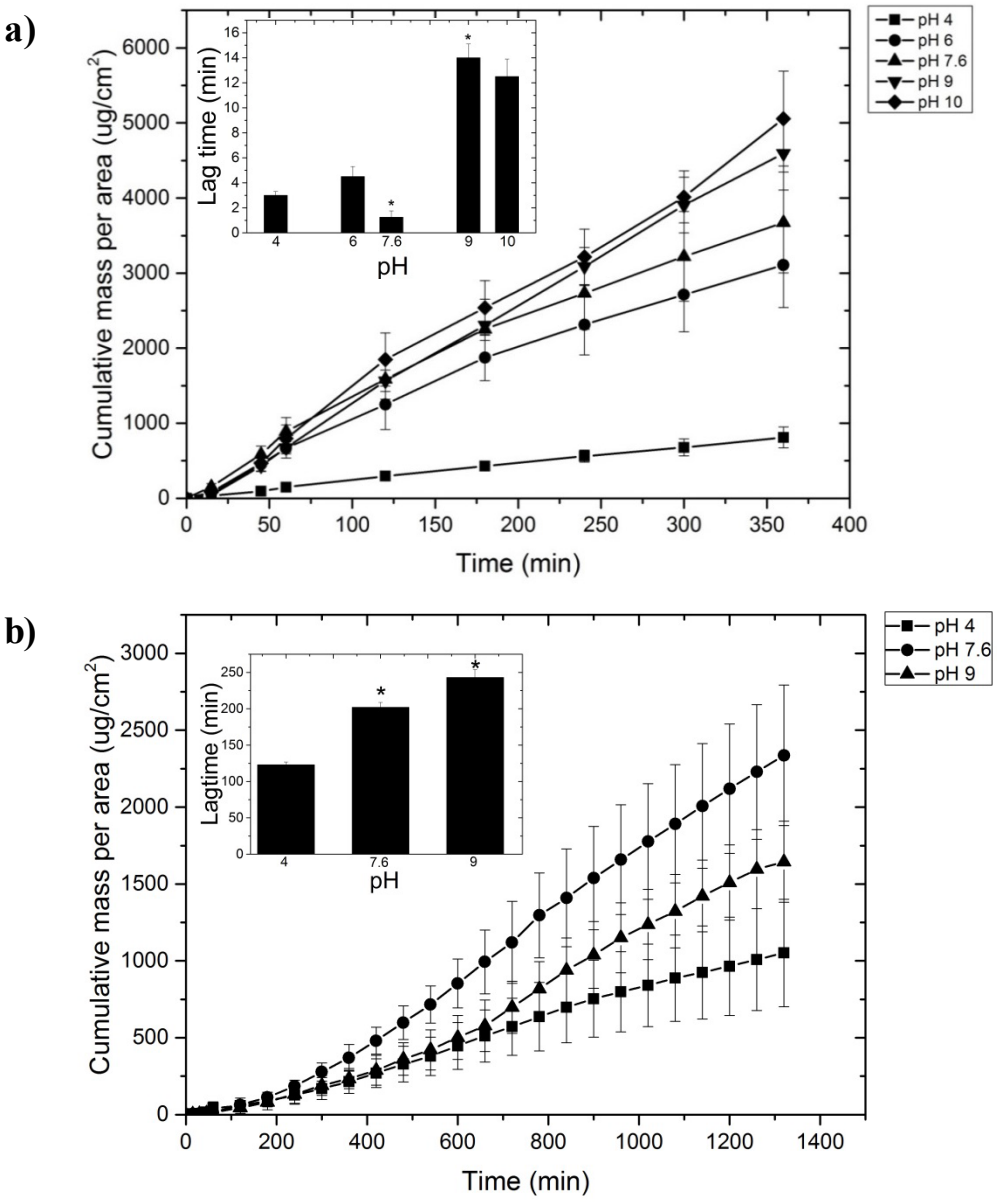

Figure 3.10. Tetracaine permeation profiles through a) silicone membrane using an infinite dose of aggregated drug at pH 4, pH 6, pH 7.6, pH 9 and pH 10 and through b) porcine skin using an infinite dose of aggregated drug at pH 4, pH 7.6 and pH 9. The inset graph represents lag time versus pH. Each point represents mean ± standard deviation (n = 5). * $p < 0.05$ (One-way ANOVA with Tuckey's HSD test).

The transport data showed in general that the drug flux and penetration lag time increased as the solution pH of the donor solutions was increased (Table 3.3 and 3.4). This increase in drug flux was thought to be a consequence of the increase in the percentage of unionized tetracaine in the donor solution, which had a greater affinity for the membrane. This hypothesis correlated well with the distribution data and it suggested that the main mechanism of transport was passive diffusion through the confluent barrier presented by the cells of the skin rather than transport via the follicular route (Figure 3.10). However, in a non-aggregated system where the drug does not interact with the membrane, Higuchi and other workers have shown that when the permeation rate of a drug increases the membrane penetration lag time decreases (Higuchi, 1961; Williams, 2003), in the present study the lag time increased. For example, when the unionized fraction increased in the donor solution from 0.03% to 73.4% (pH 4 and pH 9 respectively) there was a significant increase ($p < 0.05$) in lag time from 3.1 ± 0.8 min to 14.2 ± 1.1 min through the synthetic membrane (Table 3.3) and 123 ± 3.9 to 243 ± 10.9 min through porcine skin (Table 3.4).

Table 3.3. Summary indicies for tetracaine transport studies through a synthetic silicone membrane. Data represents mean ± SD ($n = 5$). $^{**}p < 0.01$, $^{***}p < 0.001$ when compared with following experimental setup (One-way ANOVA with Tukey's HSD test).

pH	Steady-state flux ($\mu g.cm^{-2}.min^{-1}$)	Lag time (min)	Diffusion coefficient ($\times 10^{-3}$ $cm^{-2}.min^{-1}$)
4	2.5 ± 0.3	3.1 ± 0.8	2 ± 0.8
6	11.1 ± 3***	5.2 ± 0.7**	1.6 ± 0.3
7.6	13.6 ± 2.1	1.3 ± 0.4***	5.3 ± 0.9***
9	14.6 ± 1.2	14.2 ± 1.1***	0.51 ± 0.04***
10	17.1 ± 3.3	13.6 ± 0.9	0.63 ± 0.08

Table 3.4. Summary indicies for tetracaine transport studies through porcine skin. Data represents mean ± SD (n = 5). *p < 0.05, ***p < 0.001 when compared with following experimental setup (One-way ANOVA with Tukey's HSD test).

pH	Steady-state flux ($\mu g.cm^{-2}.min^{-1}$)	Lag time (min)	Diffusion coefficient ($\times 10^{-3}$ $cm^{-2}.min^{-1}$)
4	0.96 ± 0.3	123 ± 3.9	0.016 ± 0.003
7.6	2.17 ± 0.2***	202 ± 6.7***	0.001 ± 0.0002***
9	1.59 ± 0.3*	243 ± 10.9***	0.008 ± 0.0001

This data was thought to be a consequence of the supramolecular structuring of tetracaine having a significant functional effect on the drug transport kinetics. The two most likely causes of the increases in lag time were considered to be specific interactions between the drug and the barrier (Zhang *et al*., 2007; Frezzatti *et al*., 1986; Hata *et al*., 2000; Racansky *et al*., 1988) and/or the different availabilities of membrane transportable species. However, as the aggregate characterization data had already shown that larger, more tightly formed drug supramolecular complexes were formed at high pHs, it was assumed that the restriction of the freely rapidly diffusing unionized microspecies of tetracaine by the large hydrophobic masses that displayed a significantly lower diffusion coefficient (p < 0.001) (Table 3.3 and 3.4), which may themselves have difficulty in passing through or leaving the barrier, was the main cause of the general trend of an increased lag time as pH of the donor solutions increased as previously suggested by Scheuplein *et al*., 1969.

There was an interesting exception in the general trend of an increase of membrane penetration lag time as the donor solution pH was increased, i.e., when tetracaine showed the lowest penetration lag time at pH 7.6 through the synthetic membrane. This effect was not

observed in the porcine skin. However, as the light scattering data, the partitioning data, the IR and the NMR data did not show anything particular in the tetracaine solutions at pH 7.6 the reason for this effect could not be derived from the current data set. It was therefore assumed that at pH 7.6 in the membrane silicone transport data where the optimal self-assembly configuration of tetracaine was achieved to make a rapidly diffusing species of tetracaine available for transport. The discrepancy in the skin and silicone membrane data regarding the ability of tetracaine when presented in an aqueous which adjusted to pH 7.6 to produce a rapidly penetrating form of the molecule suggested that the manner in which the drug was passing the biological barrier was a little more complex that traversing the confluent barrier posed by the various strata presented within the skin. This accords with previous work which has shown that ionic drug aggregates have the potential to pass the skin via the follicular route (Horita *et al*., 2014; Desai *et al*., 2010). In the porcine skin the availability of multiple transport routes could have resulted in the shorter membrane penetration lag time shown in the membrane due to multiple routes of transport permeation in this more complex barrier (Magnusson *et al*., 2004; Zhang *et al*., 2009; Potts and Guy, 1992).

3.5 Conclusions

A series of test systems where both tertiary and secondary amine ionization was varied were used to investigate the properties of tetracaine aggregates and to assess how the aggregation process influences the diffusion behavior through the skin. The results from this Chapter demonstrated that the aggregation process was more favourable in the aqueous vehicles at pH 7.6, 9 and 10 and resulted in a different supramolecular structure formation in solution when compared to the aqueous vehicles at pH 4 and 6. The type of structure formed in the application vehicle appeared to be linked to the production of more rapidly diffusing species

that were initially retarded by their tendency to self-assemble into large hydrophobic structures which predicted not to penetrate the barrier directly via the traditional transcellular or intercellular routes of skin penetration. The data generated herein supports the hypothesis from Chapter 2 that tetracaine self-association affects the partition-diffusion process of this agent through a confluent barrier. Although the pH of the commercial formulation favours good partition and effective transport through the skin, larger and more compact aggregates were more easily formed at pH 9 and this resulted in a slower onset of percutaneous penetration. As such, a compromise between aggregate formation and permeation rate for this molecule is required or a strategy to modulate drug aggregation should be implemented for the commercially available product to improve its delayed onset of action and thus, its clinical efficiency. One possible strategy that has received little attention in research is hypobaric driven delivery. Therefore, the next phase of this work was designed to determine the effects of hypobaric stress upon drug delivery into the skin.

CHAPTER FOUR

Modifying xenobiotic passage into the skin through the application of local hypobaric stress

4.1 Introduction

Depositing therapeutically relevant levels of drugs into the epidermis of the skin remains a challenge due to its highly stratified structure which is not conducive to the formation of epidermal depots of xenobiotics (Elias, 2005; Michaels *et al*., 1975). The *SC* and the multiple layers which are formed in the epidermis exhibit selective permeability that only allows relatively small lipophilic compounds to penetrate into lower layers (< 500 Da, Log P 0.8 - 3 (Naik *et al*., 2000; Barry, 1983)). In an attempt to localize drugs in the epidermal tissue, several strategies have been adopted, including sonophoresis, combined with chemical enhancers, mechanical abrasion and electrical charge (Mitragotri, 2006; Megrab *et al*. 1995; Prausnitz *et al*. 2004; Arora *et al*. 2008; Kalia *et al*. 2004). These approaches have been shown to facilitate cutaneous drug diffusion paths (by a transient alteration of the barrier properties and/or manipulation of drug/skin/vehicle interactions), but are often associated with skin safety issues which hinders their clinical impact (Prausnitz and Langer, 2008). However, to date the effects of local barometric pressure changes on chemical transport through the skin seem to be less well characterised.

The application of local hyperbaric pressure (e.g. 1250 mBar) has been shown to enhance the skin permeability of caffeine (Trefel *et al*., 1993), but no mechanistic studies were performed to explain these results. There have been some reports of how local hypobaric pressure affects the mechanical properties of the skin. For example, Childers *et al*., (2007) demonstrated that the topical application of a sub-atmospheric pressure of ca. 500 mBar resulted in thinning of the epidermis and enlargement of blood vessels embedded in the dermis. Moreover, it has been reported that the application of local hypobaric pressure between 400 and 600 mBar generated from a suction cup device significantly increased

TEWL with concomitant decrease in the *SC* water content (Pedersen and Jemec, 2006). In another study, a marked increase in TEWL, disorganization of the intercellular lipid bilayers and rupture of the corneosomes was shown after stretching the skin (Rawlings *et al.*, 1995; Leveque *et al.*, 2002). However, a link between skin changes induced by barometric pressure alteration and the penetration of xenobiotics into the cutaneous tissue has not been reported and hence the potential of this method to target topically administered agents into the skin has not been broadly considered.

The purpose of the work in this Chapter was to assess the influence of locally applied hypobaric stress upon drug deposition within the cutaneous tissue. Tetracaine was chosen as the model compound because this molecule is expected to pass into the skin via transcellular, intercellular and follicular pathways (Woolfson and McCafferty 1993; McCafferty *et al.*, 1988; Miller *et al.*, 1993; Foldvari, 1994; Horita *et al.*, 2014; Doliwa *et al.*, 2001). Tetracaine donor solution was set above critical aggregation concentration in the transport studies to allow the formation of drug nanosized molecular aggregates with an average size of ca. 156.5 ± 15.5 nm (Section 3.4.2.1). The pH was fixed at 7.6, to allow the formation of the ionic form (TCH^+) and non-ionised form of the drug (TC), since the balance between both microspecies in solution resulted in a better permeation through the skin in Chapter 3. It was anticipated that at pH 7.6 the molecule would pass into the skin via transcellular, intercellular and follicular routes, therefore the effects of barometric pressure in all these routes could be picked up in the transport studies. The work adapted one of the most widely used test systems for studying *in vitro* skin permeability, the Franz diffusion cell (Franz, 1975) to operate at a sub-atmospheric pressure of 500 mBar. The Franz diffusion cell transport protocol was verified using a porous (porcine skin) and non-porous membrane (silicone membrane) as the controlling barrier and comparative transport experiments were conducted with the verified

experimental set up using porcine skin, as its permeability and histological characteristics more closely resemble that of human skin (Sato *et al.*, 1991; Fujii *et al.*, 1997; Dick *et al.*, 1992; Robert *et al.*, 1991). To confirm if the follicular transport was enhanced by the application of barometric stress, *ex vivo* permeation studies were conducted through rat skin in order to study the diffusion behavior of a hydrophilic large molecular weight compound fluorescein isothiocyanate-dextran FD-4, M.W.; 4.4 kDa (hydrodynamic radius of 0.45 nm (Yuan, 2007)) and FD-10S, M.W.; 10 kDa (hydrodynamic radius of 1.9 nm (Chouinard-Pelletier *et al.*, 2012)). Rat skin was chosen because this was the animal model selected for the subsequent *in vivo* studies (Chapter 6). Drug transport was understood through comparison of the data with multiphoton microscopy, light microscopy and atomic force microscopic images to provide information of the mechanical and morphological properties of the hypobaric stressed skin. In addition, the mechanism by which hypobaric driven delivery promoted drug passage into the cutaneous tissue was further elucidated by fluorescence microscopy.

4.2 Materials

Acetonitrile and methanol both HPLC grade, grade A glass pipettes, clear glass HPLC vials crimpable lids, DPX mounting medium and xylene were purchased from Fischer Scientific (Leicester, UK). Tetracaine base BP grade (99.9%), formalin solution neutral buffered 10%, DAPI medium, ethanol and FTIC-dextran with average molecular weight of 4 kDa (FD-4) and 10 kDa (FD-10S), used without any further purification steps were supplied by Sigma Aldrich (Dorset, UK). Concentrated hydrochloric acid and sodium hydroxide was from Fluka (Dorset, UK). Sodium acetate was provided by Alfa Aesar (Heysham, UK). Silicone

membranes with a thickness of 0.25 mm were purchased from GBUK Healthcare (Selby, UK). Deionised water was obtained by purification using an Elgstat water purifier (Elga Ltd, Buckingham, UK). Phosphate buffered saline (Dulbecco A) tablets were obtained from Oxiod Limited (Hampshire, England). The Tissue-Tek® O.C.T™ compound was purchased from VWR International (Leuven, Belgium).

4.3 Methods

4.3.1 Tetracaine permeation studies

A standard Franz diffusion cell (Franz, 1975) was attached to an in-house designed aluminium support frame (Figure 4.1) that was able to pressure seal the donor compartment. Hypobaric pressure was generated by removing a known volume of air using a syringe and changes in barometric pressure were recorded with a manometer (Omni Intruments Ltd., Dundee, UK) (Figure 4.2). The system was not completely airtight as the recover chamber sampling port was left open and hence, hypobaric pressure was shown to decrease overtime (183 ± 5.8 mBar over 420 min). A second syringe was used to correct for pressure decrease during the experimental period at ca. 45 min intervals resulting in a barometric pressure that displayed a 15 ± 4.8% variance during the experiments.

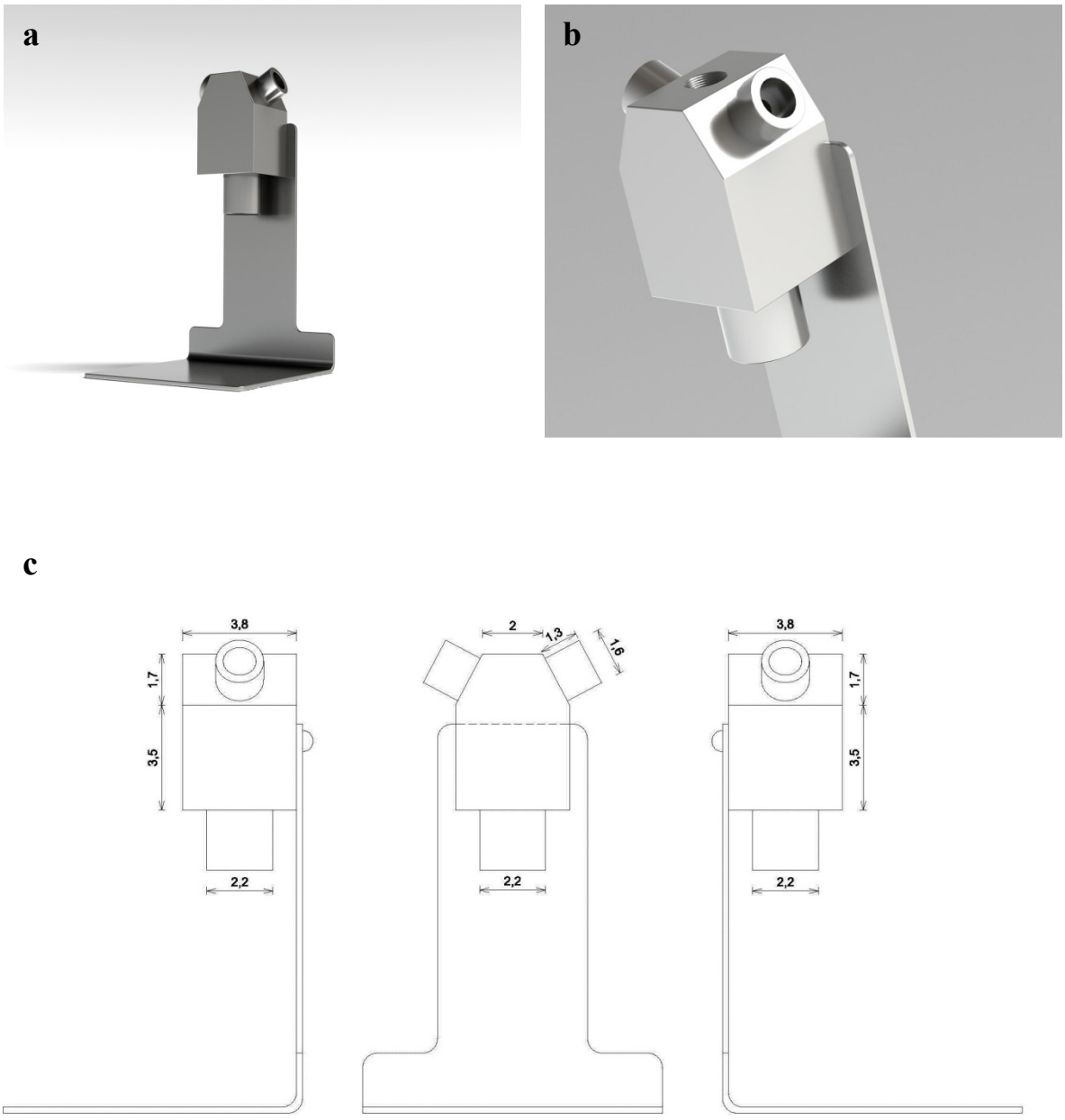

Figure 4.1. Pressure diffusion Franz cell 3 D and 2 D drawings generated in AutoCad LT software (Autodesk, Farnborough, UK), a) front view, b) hypobaric chamber, c) front and lateral views with measurements presented in cm.

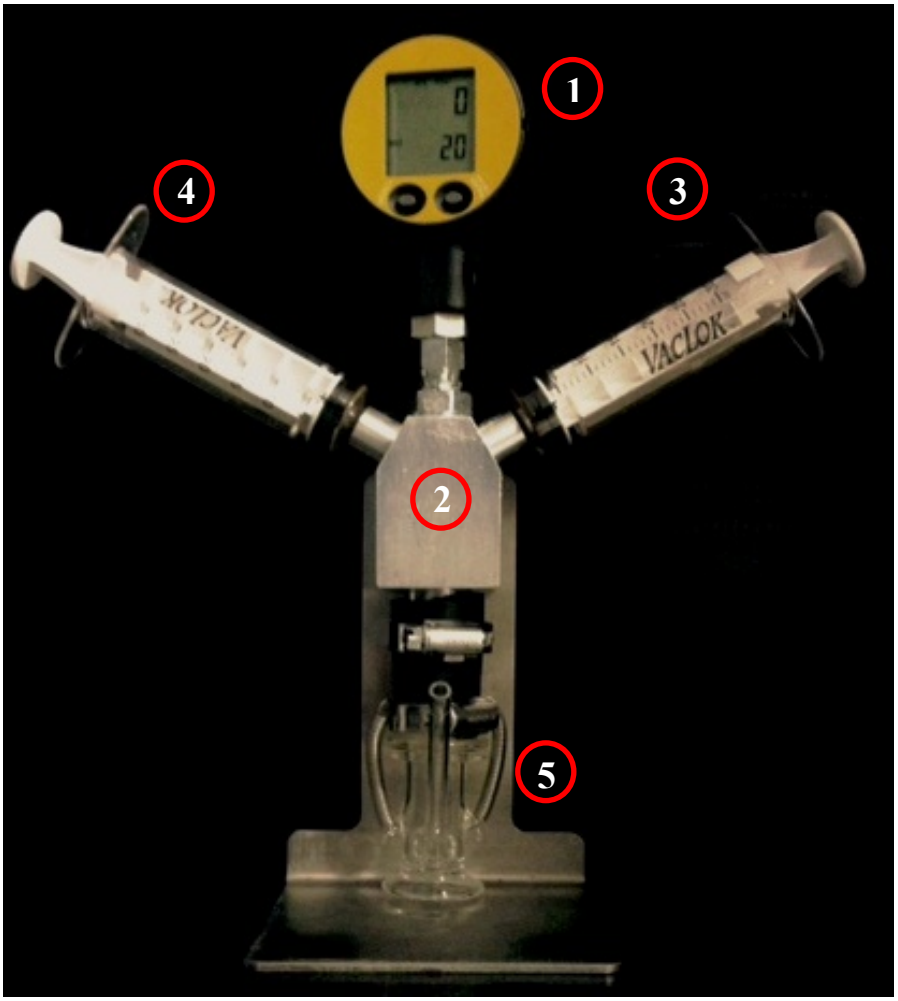

Figure 4.2. In-house developed pressure cell set up. Hypobaric pressure was created by removing a known volume of air using a syringe and changes in barometric pressure were recorded with a manometer.

To develop a sound experimental protocol using the in-house developed pressure cell set up a series of transport experiments were performed over a 7 h period using donor solutions that were prepared by adding excess tetracaine to acetate buffer (75 mM, final pH 7.6 ± 0.3). Porcine skin isolated from pig ears sourced from a local abattoir and silicone membranes were used as the controlling barrier. The pig ears were cleaned with water prior to use. The

residual water on the skin surface was immediately removed by blotting with tissue, visible residual hairs were trimmed carefully and the ears were stored at -20 °C (no more than three months before the experiments). Freezing has been previously shown not to compromise the permeability of porcine skin (Weber, 1993). Porcine skin was defrosted and the subcutaneous fat carefully removed using a scalpel. Both the silicone membrane (0.25 mm thick) and the porcine skin were cut into pieces of a suitable size and mounted in the Franz diffusion cell (University of Southampton, UK). *In vitro* infinite dose permeation experiments were conducted as method described previously in Section 2.3.3 under atmospheric pressure (1010 mBar) and under hypobaric pressure (500 mBar) using the pressure cell assembly. The samples were analysed employing the tetracaine HPLC method described in Section 2.3.1. The analysis of the chromatograms showed that matrix interference was negligible (data not shown) and drug degradation was not detected (< 2% change in tetracaine peak area) for the entire duration of the experimental period.

In the pressure cell protocol, the receptor fluid was replaced by a sponge in order to prevent pressure induced solvent back diffusion. The sponge was cut into squares of approximately 4 cm^2 and placed onto the receiver chamber in a manner that ensured intimate contact of the sponge with the skin. An identical transport experimental protocol was performed as explained above to determine the skin layer deposition. At the end of the 7 h transport studies, the skin was removed, washed with distilled water and blotted dry with tissue paper. The *SC* of the skin was removed by tape stripping (ca. 20 strips until the skin was translucent) using adhesive tape (Scotch 845 book tape, 3M, Bracknell, UK) as described by Primo (2008) and the first strip was considered as part of the applied formulation and hence its removal was part of the formulation wash off (Sheth *et al.*, 1987). The remaining tape strips were applied sequentially by pressing the adhesive tape onto the skin using a roller to stretch

the skin surface (Surber *et al*., 2001). Once the strips were removed they were collected together and weighted, to ensure that a uniform amount of *SC* was collected throughout the procedure. Tetracaine was extracted from the adhesive tape by immersing it in a 90% MeOH and 10% NaCOOH (0.1 M at pH 4) solution for 24 h. The adhesive tape was then removed from the drug solvent and discarded. The drug solutions were dried down, the residue was reconstituted using acetate buffer at pH 7.6 and analysed using the tetracaine HPLC method described in Section 2.3.1. The epidermis was separated from the dermis using a scalpel as previously reported in the literature (Surber *et al*., 1991; Ferreira *et al*., 1995; Ayub *et al*., 2007; Argenta *et al*., 2014). Both the epidermis and dermis were homogenized using a tissue homogenizer (Ultra Turrax, Fisher Scientific, Leicester, UK) in a 90% MeOH and 10% NaCOOH (0.1 M at pH 4) solution and left in contact with the extraction solution for 24 h. Samples were then centrifuged at 17000 rpm (Biofuge, Heraeus, Germany) for 15 min, the resultant supernatant was evaporated before the residue was reconstituted using acetate buffer at pH 7.6 and analysed employing the tetracaine HPLC method described in Section 2.3.1. To assess the extraction recovery efficacy, skin samples were spiked with a known amount of drug and the extraction procedure was conducted as previously described. The extraction recovery was measured by comparing the amount of drug added and extracted. Tetracaine extraction procedure from the receptor compartment, tape strips and skin samples was found to have a recovery at 7 h period of 95.3 ± 2.5% , 96.3 ± 4.3% and 98.16 ± 5.8% (n = 5), respectively. Drug extraction was within the 100 ± 15% recovery rates, which was in line with published regulatory guidelines (Health and consumer protection directorate-general, 2006).

The effect of local hypobaric stress upon tetracaine cutaneous bioavailability was represented by an enhancement ratio (ER), which was calculated according to equation 4.1, where C_P and

C_{AT} were the amount of drug (μg) per cm^2 of skin under hypobaric and atmospheric pressure conditions, respectively.

$$ER = \frac{C_P}{C_{AT}} \quad \text{(Equation 4.1)}$$

4.3.2 Dextran permeation studies

All procedures were conducted in accordance with the U.K. Animal Scientific Procedures Act (1986) and Amendments Regulations (2012) and approved by the King's College London Animal Care and Ethics Committee. Sprague-Dawley male rats (6 - 9 weeks old, ca. 220 - 250 g; Charles River, Kent, UK) were caged in groups of 4 with free access to water and food. A temperature of 19 - 22 °C was maintained, with a relative humidity of 45 – 65%, and a 12 h light/dark cycle. Animals were acclimatized for 7 days before each experiment. Rats were killed by intraperitoneal injection of sodium pentobarbital. The dorsal hair was removed using an animal hair clipper and full thickness skin was excised. The excess fat adhering to the dermis side was removed carefully with a scalpel. The hairless rat skin was cut into pieces of a suitable size and mounted with the *SC* facing the donor compartment in the pressure diffusion cell. The receptor phase, consisting of a sponge, was used in order to prevent back diffusion as previously described for porcine skin (Section 4.3.1). A 1 mL aliquot of each donor solution (125 uM of FD-4 and FD-10S in phosphate buffer solution at pH 7.4) was applied to the apical surface of the skin to initiate the transport studies. Five diffusion cells were used for each experiment. *Ex vivo* diffusion studies were performed under atmospheric pressure (1010 mBar) and under hypobaric pressure (500 mBar). The same transport protocol was conducted as described above for porcine skin; however

hypobaric pressure was applied for the first hour of a 20 h permeation study, as this application protocol was shown to not cause irreversible blistering in the fresh rat skin.

The extraction of the dextran from the sponge and tape strips at the end of the transport studies followed the same steps previously described for tetracaine (Section 4.3.1), however in this case, FDs were extracted by immersing it for 24 h in phosphate buffer saline solution (pH 7.4). The dermal tissue was homogenized in the same drug solvent and centrifuged as described above for tetracaine. Extraction procedure for FD-4 and FD-10S at 20 h period from the receptor compartment, tape strips and dermal tissue was found to have a recovery of 92 ± 5.1% and 90.3 ± 6.3%, 89 ± 8.5% and 90.3 ± 7.1%, 92 ± 5.1% and 90.9 ± 4.1% (n = 5), respectively. Drug extraction was within the 100 ± 15% recovery rates, which was in line with published regulatory guidelines (Health and consumer protection directorate-general, 2006). The effect of local hypobaric stress upon dextran cutaneous bioavailability was represented by an enhancement ratio (ER) which was calculated according to equation 4.1.

4.3.3 Dextran quantification

The amount of FDs was quantified using a stand-alone fluorescence spectrometer (Varian Cary Eclipse fluorescence spectrophotometer, Agilent, Cheadle, UK) at an excitation wavelength of 495 nm and fluorescent emission wavelength of 515 nm as previously reported in the literature (Fang *et al.*, 2004; Fujiwara *et al.*, 2005; Lee *et al.*, 2011). The assay was verified as 'fit for purpose' by determination of linearity, precision and sensitivity using the methodology described in Section 2.3.1. Linearity was confirmed for concentrations ranging from 2.4 to 0.02 $\mu g.ml^{-1}$ of standard solutions and correlation coefficients were greater than 0.998. The limit of quantification was 0.089 and 0.258 $\mu g.ml^{-1}$ and the limit of detection was

found to be 0.027 and 0.077 $\mu g.ml^{-1}$ for the FD-4 and FD-10S respectively. Matrix interference was determined to be negligible (i.e., skin lipids that may leach out during the permeation studies).

4.3.4 Fluorescence microscopy

After the dextran transport studies, skin samples were carefully cut in half along the diameter and subsequently embedded in Tissue-Tek O.C.T. before being sectioned in slices of 20 mm thickness in a cryostat microtome (Bright Instruments, Huntingdon, UK). Sectioning was performed from the dermis side towards the *SC* in order to avoid dislocation of the fluorescein isothiocyanate-dextran from the skin surface on the samples. Skin sections were then mounted using mounting medium with DAPI and covered with glass cover slips. Fluorescence photomicrographs were obtained with a Zeiss Axioscope microscope equipped with a Nikon Digital Camera (DXM1200; Nikon, Kingston upon Thames, UK) at a magnification of 10. Images were acquired in two fluorescence channels to allow the visualization of the cellular structures stained by DAPI (blue color) and the dextran fluorescence signal (green color) using a filter set having an excitation of 360 and 490 nm and emission length at 460 and 526 nm, respectively. Samples without the application of fluorescein isothiocyanate-dextran were also tested as controls. Images were processed using Image J Software (National Institutes of Health, Maryland, USA).

4.3.5 Skin morphology and physiology

4.3.5.1 Multiphoton fluorescence microscopy analysis

The multiphoton microscope images were taken using a custom built system developed around a FN1 upright microscope (Nikon Instruments, Melville, USA). The excitation source was a femtosecond pulsed Titanium:sapphire Chameleon Vision S laser (Coherent Inc., Santa Clara, USA) tuned to 800 nm, which was relayed into an afocal galvanometer scanning system. This was then projected onto the back aperture of an infinity corrected Nikon air-objective (NA. 0.5x20; Nikon Instruments, Melville, USA), where it was focused on the sample. The emitted fluorescence was collected onto two detection channels housed in a non-descanned configuration, with bandpass filters of 525 nm ± 30 nm and 593 ± 40 nm, respectively. The detectors used were a HPM-100-50 Hybrid Photomultiplier Tubes (PMTs) (Becker & Hickl, Berlin, Germany) operating in single photon counting mode. The microscope was controlled by a software developed using the graphical based LabVIEW programming language (National Instruments Corporation, Austin, USA). For these experiments the porcine skin was challenged under the same barometric pressure conditions employed in the permeation studies (Section 4.3.1). Upon hypobaric treatment, the skin was immediately mounted on a glass slide with the *SC* facing the objective. Z stacks of the porcine skin samples were acquired using Bio-Rad software (Philadelphia, USA) and were taken from the *SC* to the dermis (1 - 100 μm deep), with steps every 2 μm. Two dimensional images were generated by raster scanning the excitation beam across the skin sample utilizing the afocal scanning system. Measurements of the hair follicle infundibula were performed using an in-house developed software that was based on the graphical based LabVIEW

programming language (National Instruments Corporation, Austin, USA) that allowed the assessment of the length and depth of the follicular structures.

4.3.5.2 Atomic force microscopy analysis

Atomic force microscopy (AFM) has been widely used to characterize the morphology of corneocytes (Ritcher *et al*., 2001; Kashibuchi *et al*., 2002). Corneocytes were collected from the porcine skin surface (n = 6) treated under the same barometric stress conditions employed in the permeation studies by the removal of 4, 6 and 10 tape strips (Scotch 845 book tape, 3M, Bracknell, UK) from the same cutaneous site, a method that had been previously described by Fredonnet *et al*., (2014). The tape was then fixed on a glass slide and atomic force microscopy images were obtained from a Nanoscope V multimode scanning force microscope (Digital Instruments, Bresso, Italy). Imaging was performed in tapping mode in air. Aluminium coated Si_3N_4 cantilevers with integrated pyramidal tips (NSC15/Al, MikroMasch, Wetzlar, Germany) with a reported resonance frequency of 325 kHz and high spring constant of 40 N/m were used. After acquisition, the images were flattened and analysed using section analysis with the Gwyddion software (Czech Metrology Institute, Brno, Czech Republic).

4.3.5.3 Histological studies

Porcine and rat skin samples challenged under the same barometric stress conditions employed in the permeation studies were carefully cut in small pieces and fixed with 10% of buffered formalin during 24 h at room temperature and subsequently embedded in Tissue-Tek-O.C.T. as previously reported (Hoppert, 2003). Cross-section slices of 20 mm thickness

were obtained using a Bright Model OTF cryostat (Bright Instruments, Huntingdon, UK). The samples were stained following the Ellis Hematoxylin and Eosin (H&E) staining protocol (Ellis, 2010) and dehydrated with different volumes of ethanol (75%, 95%, and 100%) and xylene for 5 min each, before being mounted in DPX and covered with glass cover slips. The samples were analysed using a Leica DM 200 Led light microscope (Leica Microsystems, Wetzlar, Germany) equipped with a Leica digital camera (Model DFC 295) at 4, 10 and 40 magnifications. Images were processed using Las v4.4 Imaging Software (Leica Microsystems, Wetzlar, Germany).

4.3.6 Statistical analysis

All data were presented as mean ± standard deviation and statistical analysis of data was performed using SPSS version 16.0, as described previously in Section 2.3.4. In all cases, a statistically significant difference was defined as $p < 0.05$ and denoted as: * $p < 0.05$, ** $p < 0.01$ and *** $p < 0.001$. The number of replicates was 4 or 5 in the permeation studies and drug quantification within the skin layers, 15 in the follicular infundibula characterisation work and 20 in the corneocyte size assessment.

4.4 Results and Discussion

4.4.1 Tetracaine permeation studies

The data confirmed that tetracaine transport rate through the synthetic membrane (Figure 4.3 a) and porcine skin (Figure 4.3 b) were acting as a rate limiting barrier and hence, the linear portion of the permeation data was adequate to calculate steady-state permeation. The experiments applied an infinite dose of the drug that was saturated in an aqueous solution which is known not to interact with the membrane (as demonstrated in Section 2.4.3) and as the calculation of the total drug transport through the membrane in each experiment suggested that no drug depletion occurred, it was thought that tetracaine was constantly supplied in the transport studies at unity to the barrier. Sink conditions in the receiver compartment were maintained for each experiment, i.e., tetracaine concentration in the receiver fluid did not exceed 10% of the saturated solubility at each experimental pH (Howes *et al.*, 1996). Therefore, it was assumed that the cumulative rate of drug passing the membrane could be considered to be the steady-state flux in the exponential portion of the cumulative drug concentration vs time plots.

The transport data showed that tetracaine steady-state permeation was significantly greater ($p < 0.001$) when the silicone membrane was challenged under hypobaric stress (20.2 ± 3.1 $\mu g.cm^{-2}.min^{-1}$ vs 9.5 ± 1.3 $\mu g.cm^{-2}.min^{-1}$ at atmospheric pressure), but this effect was not mirrored in the porcine skin and the rate of mass transfer was found to be statistically equivalent ($p > 0.05$). A steady-state flux of 1.91 ± 0.2 $\mu g.cm^{-2}.min^{-1}$ under hypobaric driven delivery vs and 1.42 ± 0.7 $\mu g.cm^{-2}.min^{-1}$ at atmospheric pressure was obtained. The lack of change in tetracaine permeation through porcine stressed skin was attributed in these

preliminary studies to solvent back diffusion into the donor fluid, which was visually apparent at the end of the experimental period. This led to the use of the sponge in the receiver compartment in the subsequent studies as this negated the back diffusion effects. The observed back flow was thought not to be caused by a disruption of the mechanical integrity of the skin induced by hypobaric treatment, since application of similar sub-atmospheric pressure has been shown not to compromise barrier integrity (Pedersen *et al*., 2006), but a consequence of the presence of a large volume of liquid under the skin which did not represent *in vivo* conditions.

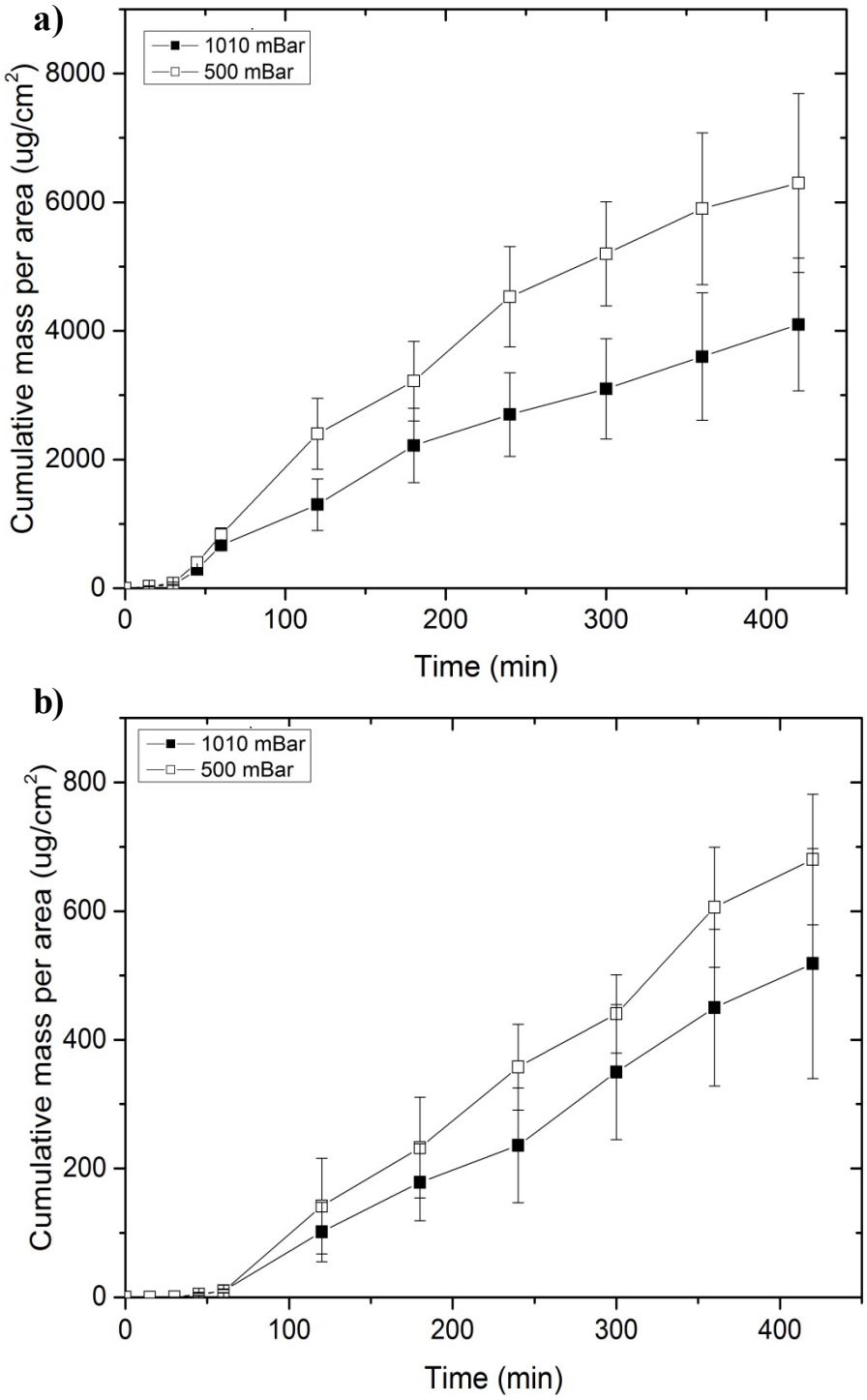

Figure 4.3. Tetracaine permeation profile under atmospheric (1010 mBar) and hypobaric (500 mBar) pressure through a) silicone membrane and b) porcine skin over 7 h. Each point represents mean ± standard deviation (n = 5).

The use of the adapted methodology showed in general that the transmembrane penetration and drug deposition within specific skin strata was increased under hypobaric driven delivery (Figure 4.4). The rate of mass transfer through the biological membrane was found to be 4-fold greater when compared to that obtained under atmospheric conditions. In addition, the ability of hypobaric stress to localise the drug within the epidermal tissue was found to be significantly greater ($p < 0.001$) when compared to the amount found in the *SC* and dermal tissue. It was registered an enhancement ratio of 25.6, 8.8 and 9.9 respectively (Figure 4.4). The enhanced drug deposition within the skin tissue was thought to be caused by a temporary alteration of the skin properties. As such, the mechanical and physiologic changes in the barrier were further investigated and related to the ability of the drug to cross the skin by the transcellular, intercellular and follicular routes.

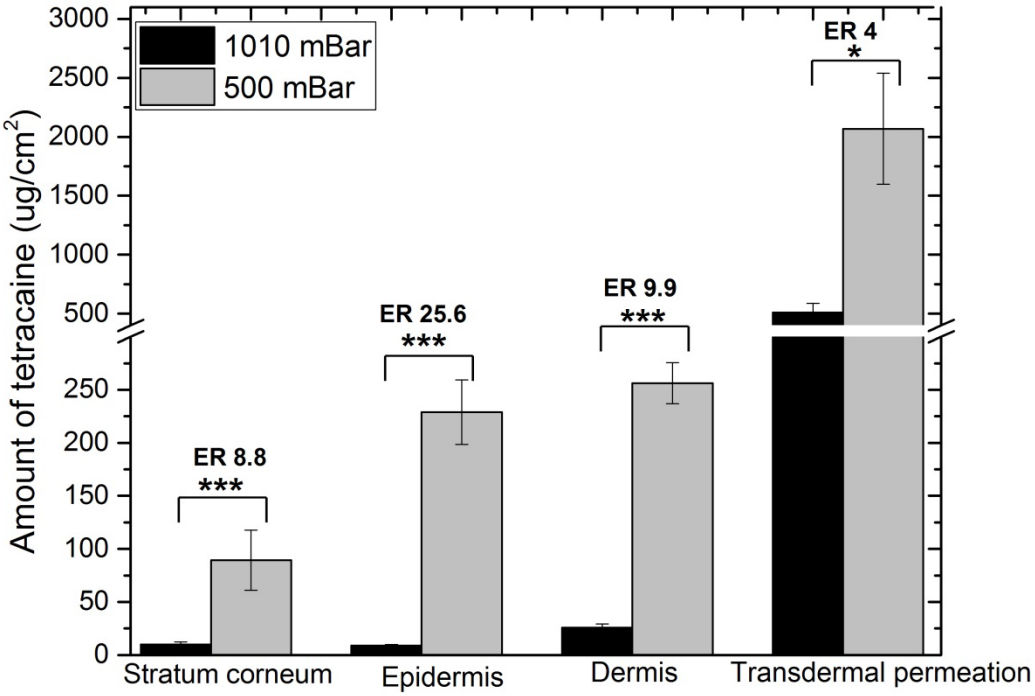

Figure 4.4. *In vitro* profile of tetracaine deposition in porcine skin layers and transdermal permeation under atmospheric (1010 mBar) and hypobaric (500 mBar) pressure conditions. Each point represents mean ± standard deviation (n = 5). ER (Enhancement ratio) represents the ratio between the amount of drug found under hypobaric and atmospheric conditions. Student's t-test with * $p < 0.05$, *** $p < 0.001$.

4.4.2 Dextran permeation studies

The application of topical hypobaric stress did not alter the amount of FDs found in the *SC*, but there was a different skin deposition of FD-4 when the barrier was challenged by mechanical stress stimuli (Figure 4.5 a). The FD-4 dextran demonstrated a 3-fold greater deposition within the dermal tissue. On the other hand, the amount of FD-10S retained in the

dermal tissue was found to be equivalent ($p < 0.05$) under both barometric conditions (Figure 4.5 b). The transdermal delivery of FDs was found to be significantly greater ($p < 0.01$) when compared to atmospheric conditions (2.9 and 19.6-fold increase, respectively) (Figure 4.5 a and b). Interestingly, the effect of hypobaric stress was more pronounced upon the transdermal delivery of the higher molecular weight dextran (10 kDa). The enhanced cutaneous and transdermal bioavailability was not thought to be attributable to chemical degradation since it has been previously shown that FDs of various molecular weights were stable after the permeation through pig, mouse and rat skin under similar experimental conditions (Ying-Zhe *et al*., 2009; Fang *et al*., 2004; Woan-Ruoh *et al*., 2008; Lombry *et al*., 2000).

The dextran permeation through rat skin was studied to investigate a possible magnification of the follicular route upon hypobaric driven delivery. Previously, permeation studies using FDs through rat skin, porcine skin and *in vitro* cultured human epidermis model suggest that the follicular route is the primary permeation pathway for dextrans between 4 - 10 kDa (Ying-zhe *et al*., 2009; Fang *et al*., 2004; Todo *et al*., 2010). This was recently confirmed in a novel follicle-plugging method, which showed that the permeation of 4 kDa dextran was dependant on the availability of "unplugged" hair follicles (Horita *et al*., 2014).

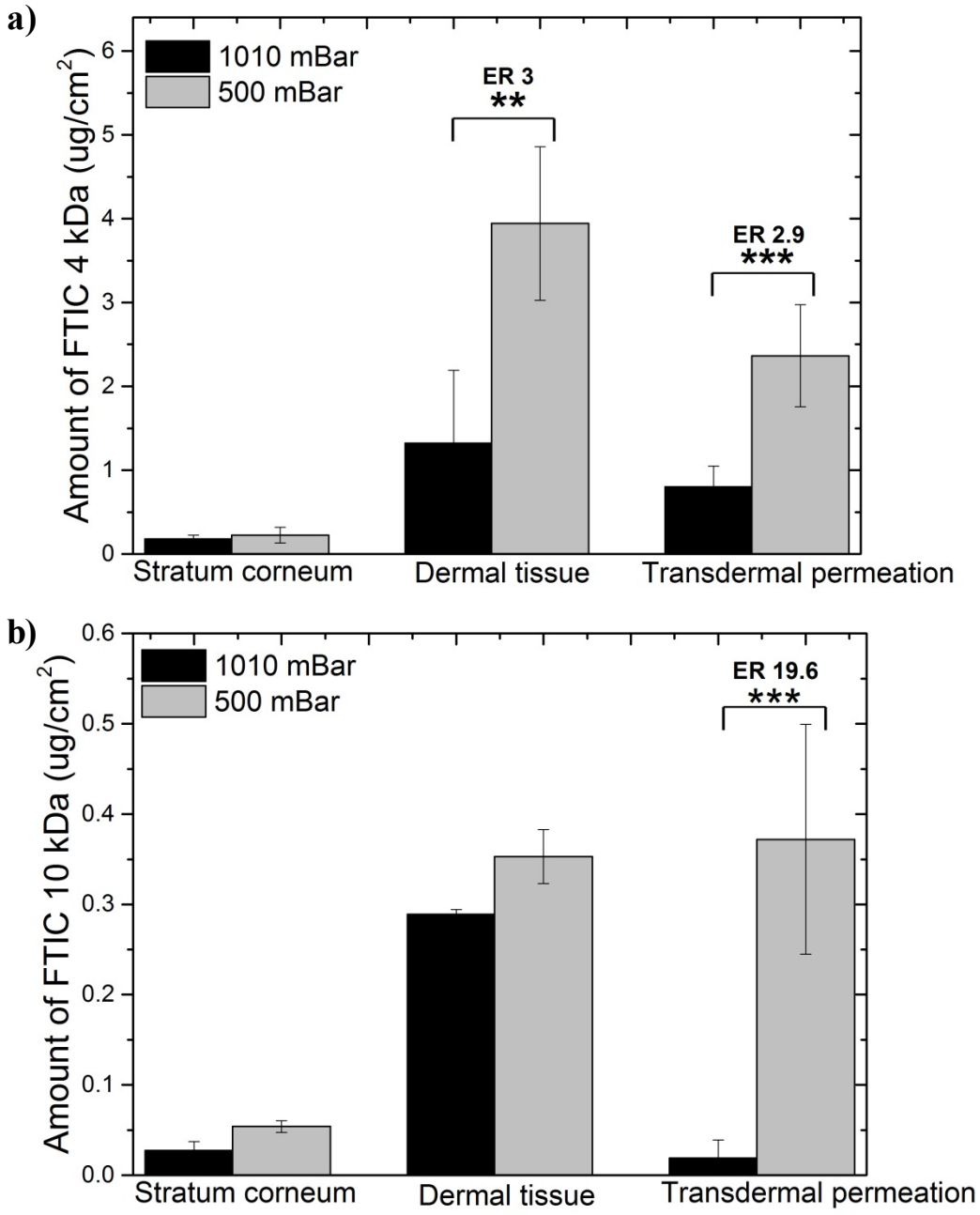

Figure 4.5. *Ex vivo* profile accumulation of FD-4 (a) and FD-10S (b) in rat skin layers and transdermal permeation under atmospheric (1010 mBar) and hypobaric (500 mBar). Each point represents mean ± standard deviation (n = 4) for atmospheric conditions and (n = 5) for hypobaric conditions. ER (Enhancement ratio) represents the ratio between the amount of drug found under hypobaric and atmospheric conditions. Student's t-test with ** $p < 0.01$ and *** $p < 0.001$.

4.4.3 Dextran permeation pathways

To evaluate the effects of hypobaric driven delivery upon dextran cutaneous diffusion routes, cryostat sections of skin with and without hypobaric treatment were viewed by fluorescence microscopy. A mounting medium with DAPI was employed to allow the visualization of cellular structures which were displayed by the blue color. Skin control samples where no dextran had been applied (Figure 4.6 a and b) exhibited some fluorescence at an excitation of 490 nm (green color) which was thought to be due to the skin's chromophores that fluoresce at this wavelength has previously shown by Hanson and Bardeen (2009). However, there was a significant increase in the fluorescence intensity in deeper skin layers exposed to hypobaric treatment (Figure 4.6 d and f) compared to the samples under atmospheric conditions (Figure 4.6 c and e). Moreover, a greater fluorescence signal was evident around the perifollicular region, which suggests that hypobaric treatment influenced drug transport across the hair follicle structures. The lower molecular weight FD dextran gave a broad and continuous band of fluorescence signal that extended from the *SC* into deeper layers of the skin (Figure 4.6 d). This may indicate that the 4 kDa dextran was transported more efficiently not only through the follicular route but also through the transcellular and/or intercellular regions. In contrast, the fluorescence signal of the 10 kDa dextran was mainly localized around the perifollicular region, suggesting that the follicular pathway was the main route utilised by this permeant to diffuse through the hypobaric stressed skin. These data suggested that the specific effects of hypobaric driven delivery were size dependant.

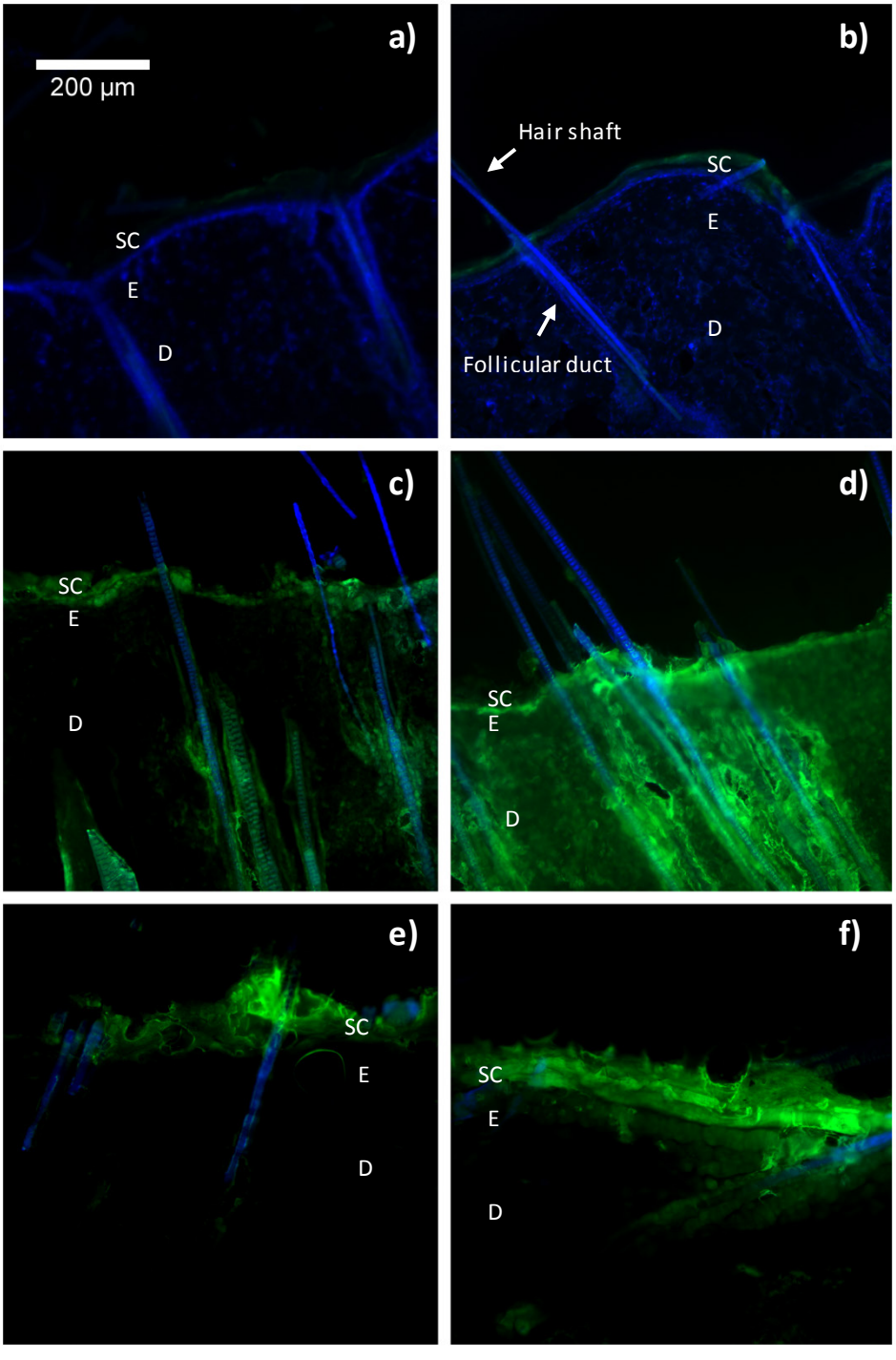

Figure 4.6. Fluorescence microscopic examination after topical administration of FD-4 and FD-10S dextran under atmospheric conditions (1010 mBar) and hypobaric stress conditions (500 mBar): control samples at atmospheric (a) and after hypobaric treatment (b); topical FD-4 delivery under atmospheric conditions (c) and upon hypobaric stress treatment (d); topical FD-10S delivery under atmospheric conditions (e) and upon hypobaric stress treatment (f). Original magnification × 10. *SC*, stratum corneum; E, epidermis and D, dermis.

4.4.4 Skin morphology and physiology

4.4.4.1 Hair follicle

Multiphoton microscopy has been widely used to analyse the skin tissue (Lin *et al.*, 2007; Hanson *et al.*, 2002; Sun *et al.*, 2003). This imaging technique was selected because is possible to rapidly obtain two dimensional reconstructions of individual hair follicles. Furthermore, no staining or mechanical sectioning is involved, since the endogenous fluorophores in the hair follicle can easily produce strong two photon excited fluorescence signals without the need of contrast agents. These signals are ideally suited to determine the size of the follicular orifice, as previously reported for mouse skin (Lyubovitsky *et al.*, 2007). In this study, the follicular infundibula was significantly longer ($p < 0.001$) upon hypobaric stress treatment. It registered an average horizontal planner length of 243 ± 23.9 μm and 151 ± 40.5 μm after hypobaric and under atmospheric conditions, respectively (Figure 4.7 c and f). In addition, there was a significantly decrease ($p < 0.01$) in the depth of the follicular structures after the application of barometric stress (159 ± 14.5 μm after hypobaric pressure conditions vs 190 ± 30.1 μm under atmospheric conditions) (Figure 4.7 c and f).

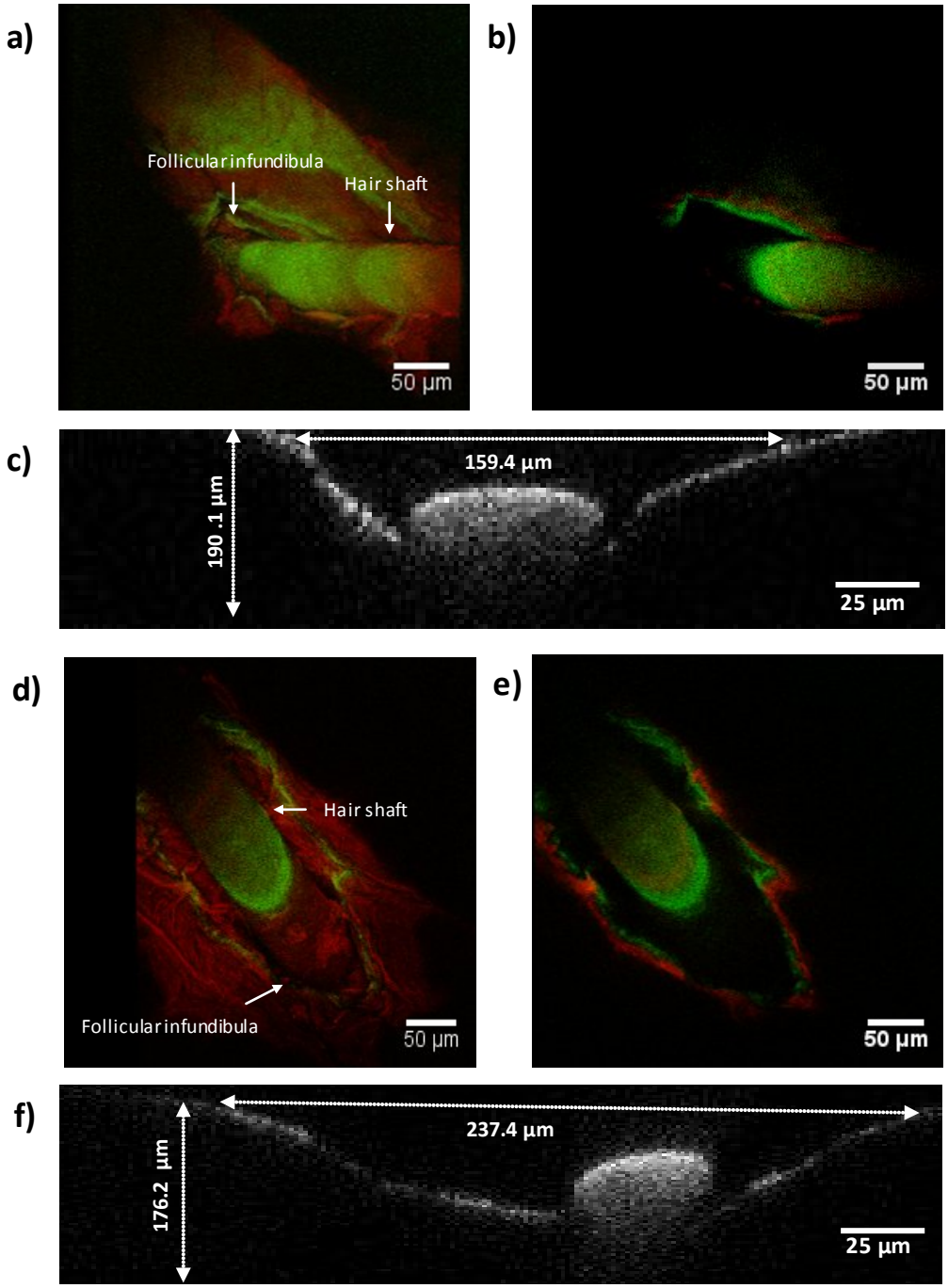

Figure 4.7. Multiphoton microscopic images of porcine follicular infundibula a) 3D reconstruction under atmospheric conditions (1010 mBar) b) top view (singe Z-stack cross-section at 1010 mBar) c) side view at 1010 mBar with an average length of 151 ± 40.5 µm and depth of 190 ± 30.1 µm d) 3D reconstruction after applying hypobaric pressure (500 mBar) e) top view after hypobaric pressure (Z-stack cross-section) f) side view after hypobaric pressure with an average length of 243 ± 23.9 µm and depth of 159 ± 14.5 µm.

A greater horizontal planner length of the follicular infundibula with concomitant decrease in the depth of the follicular structure was believed to be due to the stretching and vertical displacement of the skin when exposed to hypobaric stress. Previously, the follicular infundibula orifice was studied using cyanoacrylate porcine ear skin (Jacobi *et al*., 2007). The horizontal planner length of the follicular infundibula was reported to be between 170 and 200 μm, which is in good agreement with the values obtained under atmospheric conditions.

Several studies by Lademann *et al*., (2008 and 2001) have suggested that a large fraction of the hair follicles are not accessible to drug penetration. It was demonstrated that drug transport only occurred through the "active" (open) hair follicles that are characterized by hair growth and/or sebum production. This can be explained by the fact that plugs from shed corneocytes and dry sebum, which block some of the hair follicles, are pushed out by growing hair or flowing sebum (Otberg *et al*., 2004). Previously, mechanical peeling has been shown to open closed follicles and facilitate drug passage into the cutaneous tissue (Lademann *et al*., 2008). In a similar manner, Toll *et al*., (2004), reported that the pre-treatment of the skin with cyanoacrylate skin surface stripping resulted in drug targeting into the dermal tissue by a facilitated follicular transport of nanosized compounds. The application of hypobaric stress is commonly used to open and clean clogged hair follicles in clinical practise (Davis *et al*., 2010). This previous work and the new data derived in this PhD then suggest that hypobaric pressure may be opening up the follicles and hence facilitating xenobiotic percutaneous penetration. It is important to note in the current project, that the penetration of nanosized systems is possible via the follicular pathway through the skin has previously suggested for other nanosized delivery systems (Alvarez-Román *et al*., 2004; Vogt *et al*., 2005). As such, the increase in tetracaine permeation and deposition within the different skin layers caused by the application of barometric pressure could be attributable at least in part, to the follicular transport of the nanosized drug aggregates. It is therefore

hypothesized that hypobaric driven delivery could reverse the reduction in drug permeation induced by molecular aggregation that was an inherent property of tetracaine permeation in Chapter 3.

4.4.4.2 Corneocyte

The average size of the porcine corneocytes was significantly lower (n = 15 $p < 0.001$) upon hypobaric treatment with a length and width at 31.5 ± 8.2 μm and 26.2 ± 6.8 μm vs 41.5 ± 5.5 μm and 37.2 ± 7.2 μm under atmospheric conditions respectively (Figure 4.8). The diffusional barrier characteristics of the skin result from the properties of the lipids and the path length for diffusion. The latter depends on the number of corneocytes, their cohesion and size. Previously, a reduction in the corneocytes packing with a concomitant increase in the size of corneocytes gaps was shown to facilitate percutaneous penetration and drug deposition into deeper skin layers (Zhai *et al.*, 2011; Schafer-Korting *et al.*, 2007). In additional work, a decrease in corneocyte size was thought to result in greater drug permeation rates through the skin by a facilitated transcellular and intercellular cutaneous drug diffusion pathways (Hadgraft *et al.*, 2009). Transepidermal water loss as a measure of the water vapour flux crossing the skin to the outside environment has been previously used as an indicator of the skin barrier function. It was shown that an increase in TEWL is directly related to a decrease in corneocyte size and hence, in a shorter permeation path length through the cutaneous tissue (Rougier *et al.*, 1988; Machado *et al.*, 2010). The application of similar sub-atmospheric pressure to that employed in this study has been reported to cause an increase TEWL with concomitant morphological alteration of the corneocytes due to mechanical stretching (Pedersen *et al.*, 2006; Corcuff *et al.*, 1991).

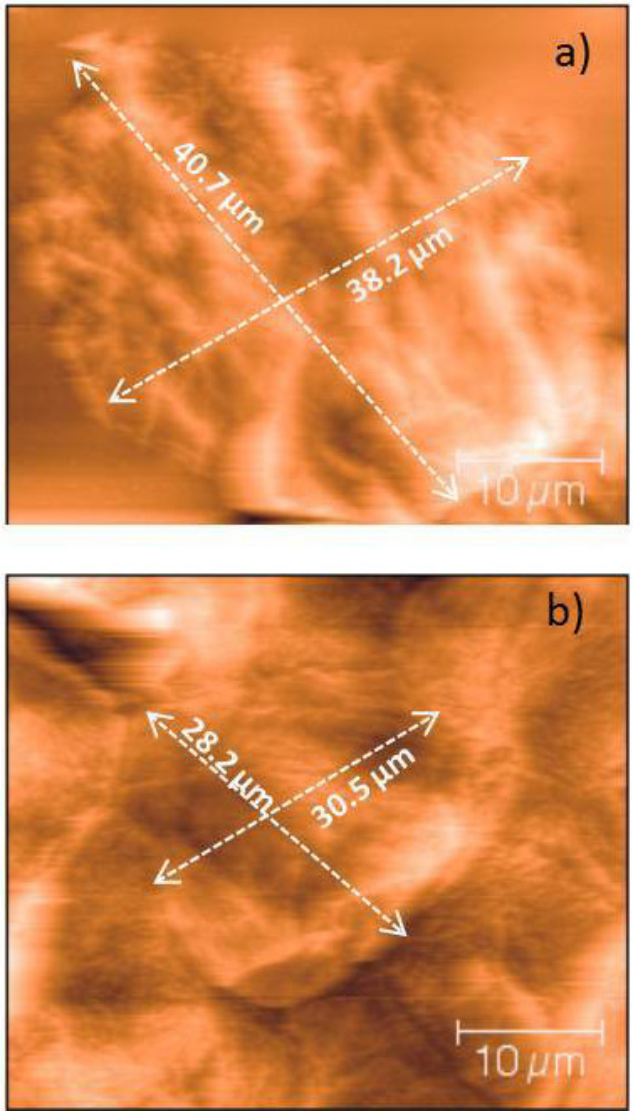

Figure 4.8. Atomic force microscopy analysis of *in vitro* porcine skin corneocytes at a) atmospheric conditions (1010 mBar) with average length of 41.5 ± 5.5 µm and width of 37.2 ± 7.2 µm and b) within 25 min of applying hypobaric pressure (500 mBar) with average length of 31.5 ± 8.2 µm and width of 26.2 ± 6.8 µm.

It can be hypothesized that the decrease in corneocyte size upon hypobaric treatment was caused by an increase in TEWL during the permeation studies and therefore a lower water content of the tissue. A shorter permeation path length may explain the facilitated dextran transport through the intercellular and transcellular route as shown by fluorescence microscopy (Figure 4.6). The intercellular route could also facilitate tetracaine delivery through the skin, but probably not via aggregate permeation as they had a size of (156.5 ± 15.5 nm) and the gaps between porcine corneocytes have been previously reported to be ca. 19 nm (van der Merwe *et al.*, 2006). It was thought unlikely that a 30% reduction in corneocyte size would lead to the transport of a large aggregate through these gaps which will have been enlarged.

4.4.4.3 Skin morphology and thickness

The hypobaric stressed porcine skin was found to be significantly thinner ($p < 0.05$) following the transport studies. A skin thickness of 0.89 ± 0.1 mm upon the application of hypobaric treatment vs 1.1 ± 0.1 mm under atmospheric pressure conditions was registered. Conversely, when rat skin was treated with the same hypobaric conditions used in the *in vitro* permeation studies and subsequent *in vivo* experiments (Chapter 6) there was no significant alteration ($p > 0.05$) in membrane thickness. Skin thinning upon the application of hypobaric stress has been previously reported in the literature. A 7% and 17% skin thickness reduction was observed upon the application of 200 and 350 mBar of sub-atmospheric pressure from a suction device (Hendricks *et al.*, 2003). The decrease in skin thickness may translate in a shorter diffusion path length across the skin and thus facilitate solute mass transport (equation 1.1). Moreover, the vertical displacement of the skin upon hypobaric treatment could result in a greater diffusional area (Figure 4.9 b, f). The change in the morphological characteristics of

the hypobaric stressed skin was shown to be reversible and the initial morphology was restored ca. 15 - 30 min after the hypobaric stress was removed (Figure 4.9 d, h). A linear stress-strain relationship up to 350 mBar has been previously demonstrated using a suction device (Childers *et al*., 2001).

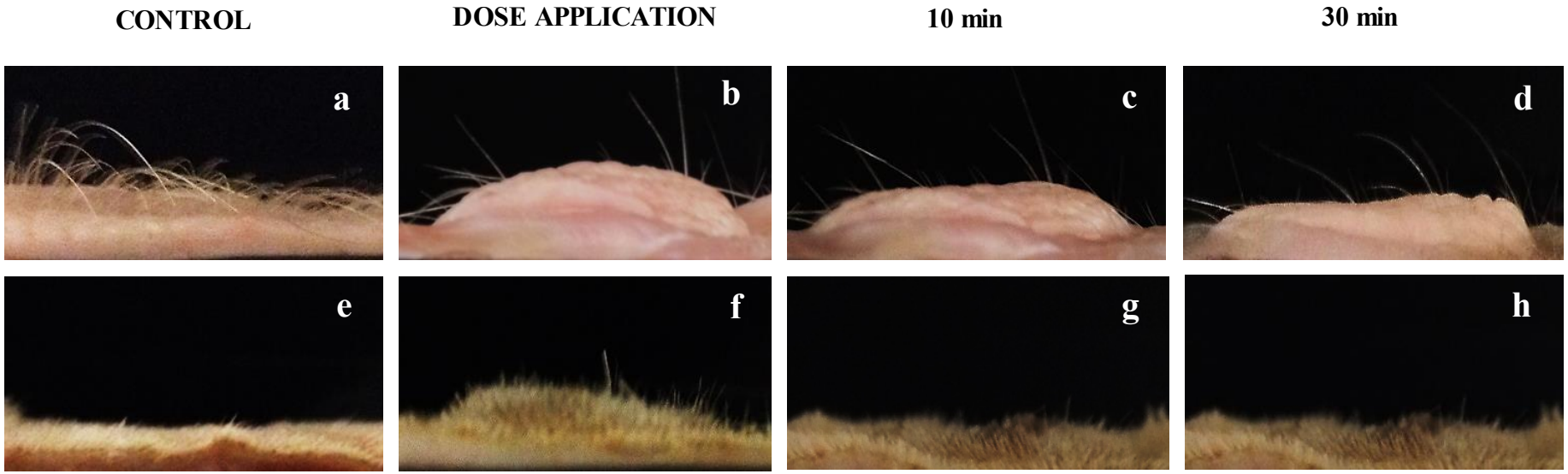

Figure 4.9. Vertical displacement of porcine (PS) and rat skin (RS) upon the application of the hypobaric conditions employed in the *in vitro* permeation studies a) PS control under atmospheric conditions (1010 mBar) e) RS control under atmospheric conditions (1010 mBar) b) PS immediately upon the application of 500 mBar for 7 h, f) RS immediately upon the application of 500 mBar for 1 h, c) and g) PS and RS after 10 min of hypobaric stress d) and h) PS and RS after 30 min of hypobaric stress.

4.4.4.4 Skin integrity

Light microscopy was used to visualize the histological changes to porcine and rat skin upon hypobaric treatment. Dermal-epidermal detachment was observed in few localized areas of both porcine (Figure 4.10 d) and rat skin samples (Figure 4.11 d). However, the majority of the skin maintained its morphological and structural characteristics (Figure 4.10 f and Figure 4.11 f) when compared to the control samples (Figure 4.10 c and 4.11 c). Minor changes were observed regarding cell cohesion, with some areas of the *SC* detaching or peeling off from the adjacent layer. However, this was most probably due to sample handling, since this was observed in the control skin samples. The small amount of dermal-epidermal detachment was thought unlikely to influence drug delivery via the skin as the *SC* seems to remain intact upon hypobaric driven delivery.

Previous *in vivo* work in human subjects has shown a rapid repair of the dermal-epidermal adherence after 2 h (Beerens *et al*., 1975; van der Leun *et al*., 1974). This process was also observed when employing porcine and rat animal models (Nanchahal and Riches, 1982; Pang *et al*., 1978). One of the major concerns when employing physical enhancement methods to deliver therapeutic agents across the cutaneous tissue is the effects upon skin integrity and reversibility. The data generated in this Chapter suggested that the enhanced topical bioavailability of the test agents was accompanied by reversible changes in the morphological and structural characteristics of the skin upon the application of hypobaric stress.

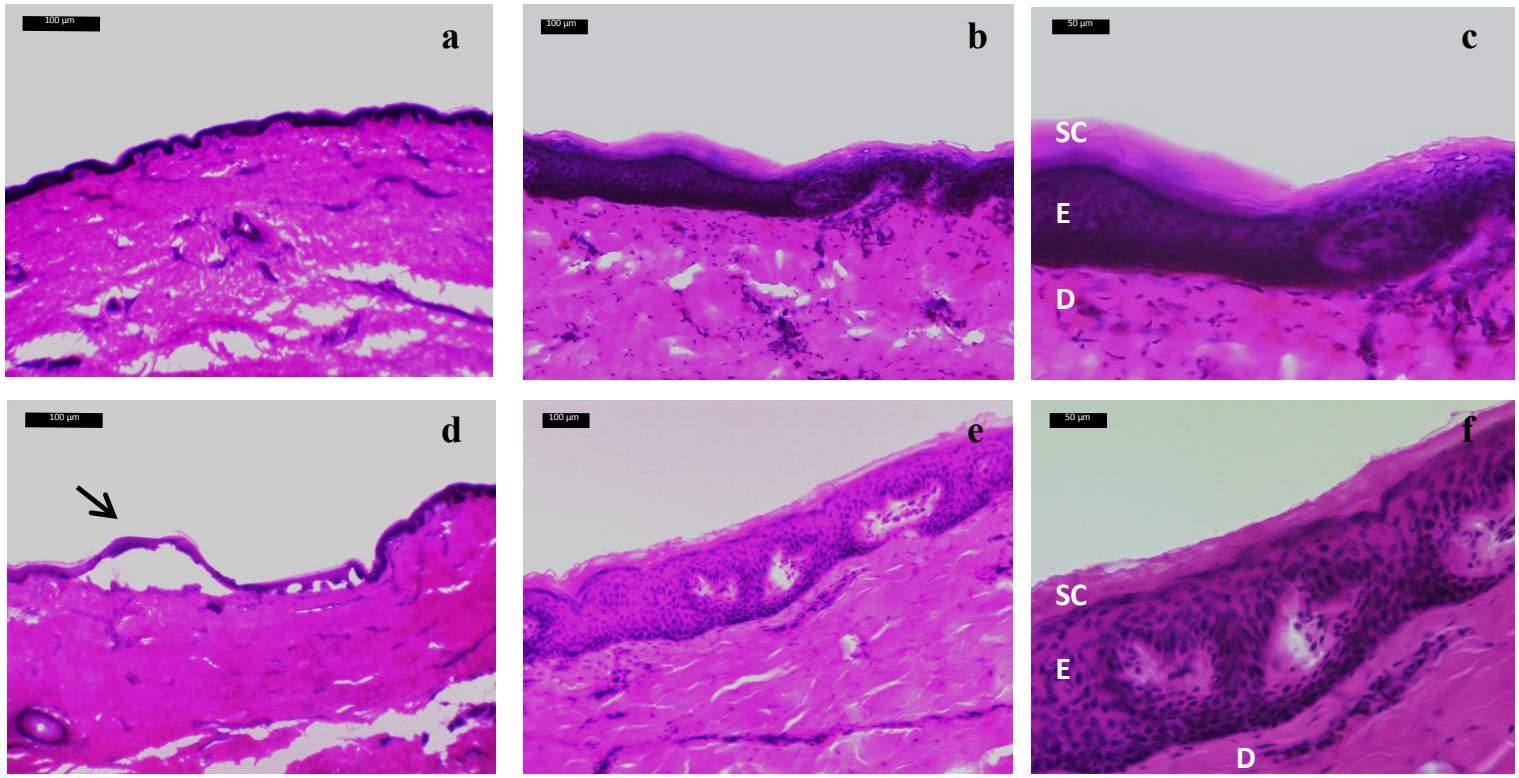

Figure 4.10. Porcine skin histology a), b) and c) control under atmospheric conditions 4 ×, 10 × and 40 × respectively d), e) and f) after hypobaric treatment of 500 mBar for 7 h at 4 ×, 10 × and 40 × respectively. SC, *stratum corneum*, E, epidermis, D, dermis and arrow indicates epidermal-dermal detachment.

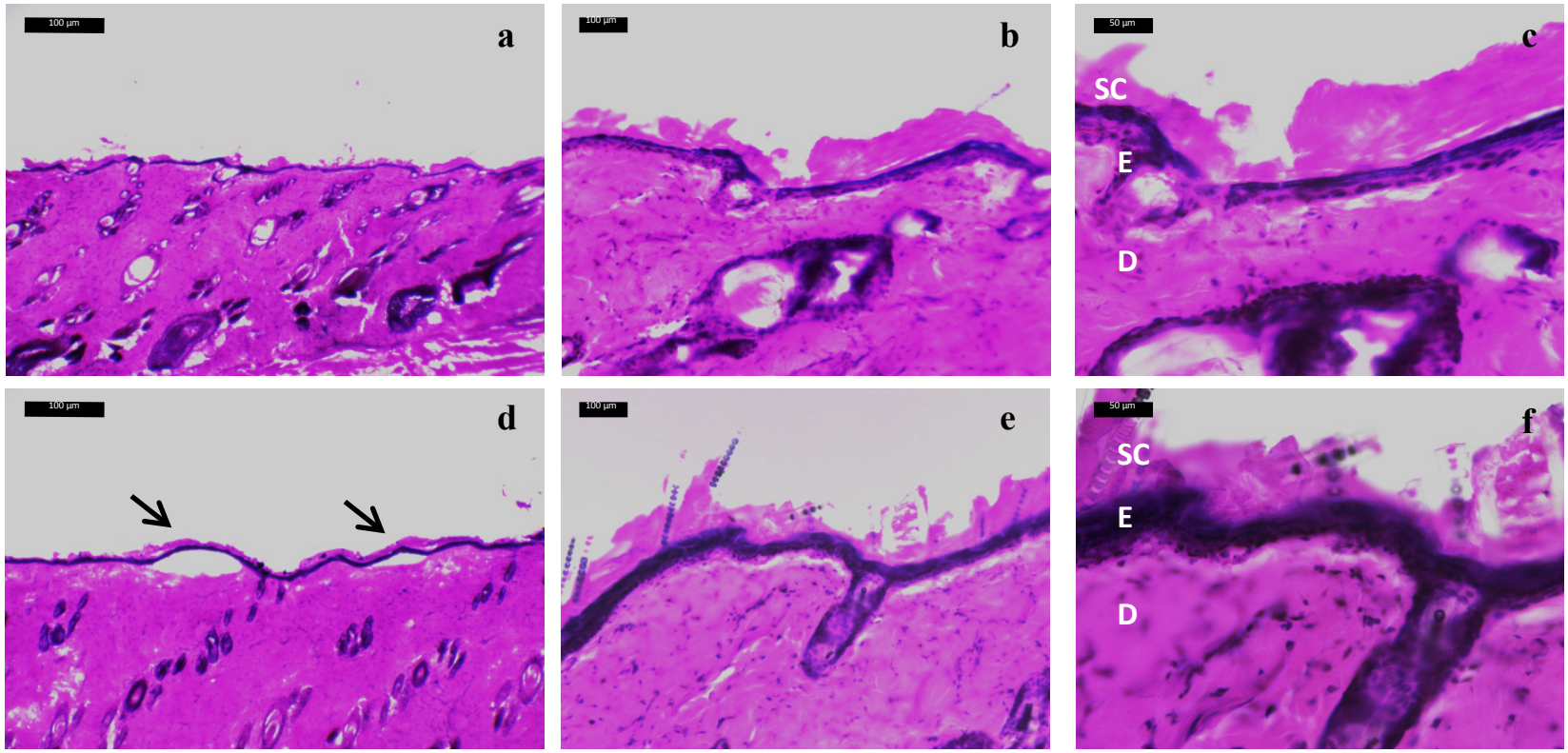

Figure 4.11. Rat skin histology a), b) and c) control under atmospheric conditions 4 ×, 10 × and 40 × respectively, d), e) and f) after hypobaric treatment of 500 mBar for 1 h at 4 ×, 10 × and 40 × respectively. *SC*, *stratum corneum*, E, epidermis, D, dermis and arrow indicates epidermal-dermal detachment.

4.5 Conclusions

This chapter has provided new insights into the effects of local hypobaric treatment upon the skin and the transport of molecules through the tissue. A novel device that can pressure seal the donor compartment of a traditional Franz diffusion cell (Franz 1975) and a 'fit for purpose' method that allowed the characterization of percutaneous penetration were developed. The use of the adapted Franz cell demonstrated that the application of topical hypobaric stress improved the delivery of both small molecular weight and macromolecular size xenobiotics. The enhanced tetracaine epidermal deposition was accompanied by an enlargement of the follicular infundibula ($p < 0.001$), reduced corneocyte size ($p < 0.001$) and skin thinning ($p < 0.05$) and this suggested that the transcellular and follicular routes of penetration could both be facilitated and therefore explain the enhanced drug penetration and/or site specific drug accumulation in the skin's strata.

It was hypothesized that hypobaric driven delivery could reverse the reduction in drug permeation of a molecular aggregated system such as tetracaine (as described in Chapter 3), by facilitating drug movement of the aggregates into the skin. Histological studies showed that these changes were accompanied by dermal-epidermal detachment in few localized areas. However, this was thought unlikely to influence drug transport as the *SC* seems to remain intact. In order to move this concept forward, a greater understanding of the relationship between cutaneous bioavailability upon hypobaric driven delivery and the drug's physicochemical properties is required. Consequently, in the next phase of this work, three model agents (tetracaine, diclofenac diethylamine and aciclovir) were employed in an aggregated/non-aggregated state and permeation studies were conducted under differential

barometric pressure to further explore this novel method to facilitate percutaneous penetration into the skin.

CHAPTER FIVE

Epidermal drug targeting upon local hypobaric stress

5.1 Introduction

In order to deposit therapeutically relevant levels of drugs within the different skin strata, complementary strategies employing chemical and physical methods have been employed (Mitragotri, 2006; Megrab *et al*., 1995; Prausnitz *et al*., 2004; Arora *et al*., 2008; Kalia *et al*., 2004). However, this needs a finely tuned approach system and at the present only limited success in retaining therapeutic molecules within the skin has been achieved (Brown *et al*., 2006). Drug localization of this type is desirable in the treatment of dermatological conditions such as skin cancer, psoriasis, eczema and microbial infections where the origin of the disease lies within the skin tissue (Brown *et al*., 2006).

One strategy that has shown encouraging results in terms of skin strata targeting is opening the follicular route. These structures circumvent the formidable barrier posed by the *SC* when passing molecules into the skin. However, despite the fact that the corneocytes of the follicular epithelium are not completely differentiated, suggesting that the skin barrier is more permeable in this area and permitting drug diffusion directly into the viable epidermis (Rancan *et al*., 2009), the follicular structure also forms a relatively tight barrier that requires open up (Knorr *et al*., 2009). This could be achieved by the application of hypobaric stress (Chapter 4). The main mechanism by which hypobaric driven delivery promotes drug localisation was thought to be due to a facilitated follicular penetration of topically applied nanosized aggregates.

The aim of this study was therefore to investigate the effects of local hypobaric treatment upon localization of actives within the cutaneous tissue and relate these findings with the presence or absence of drug aggregates in the application system. In addition, the findings of

these studies were compared to products containing the same drugs to understand the influence of the formulation components on the barometric enhanced delivery process. For this purpose, tetracaine (TC) (M.W.; 264.36, pKa 2.48 ± 0.03 and 8.56 ± 0.02 (Section 3.4.1)), diclofenac diethylamine (DDEA) (M.W.; 369.29, pKa 4 (Djordjevic *et al.*, 2005)) and aciclovir (ACV) (M.W.; 225. 21, pKa 9.25 (Freeman *et al.*, 1986)) were selected based upon their different physicochemical properties. The chemical structure of these drugs was predicted to cause molecular aggregation in solution (Miller *et al.*, 1993; Fernandez, 1980; Kitagawa *et al.*, 2004; Kriwet and Muller-Goymann, 1993; Karen *et al.*, 2001). Therefore, photon correlation spectroscopy was employed to determine the critical aggregation concentration at which nanosized aggregates were formed and zeta potential measurements provided details regarding surface potential of the supramolecular structures formed in the administration vehicle. A hydroxypropyl methylcellulose (HPMC) gel formulation was then prepared for each active with a drug load above and below the experimentally determined critical aggregation concentration. Transport studies were conducted through porcine skin under atmospheric pressure using a traditional Franz diffusion cell and hypobaric stress conditions were tested using the adapted cell described in Section 4.3.1 and cutaneous bioavailability for each drug was assessed by tape stripping and tissue homogenisation methodologies. Porcine ear skin was chosen in the current work because this barrier is especially suitable for studying follicular uptake as the ear cartilage prevents contraction of tensile fibres and closure of follicles, which greatly reduces follicular transport, when working with other animal skin sources (Patzelt *et al.*, 2008).

5.2 Materials

Acetonitrile and methanol both HPLC grade, grade A glass pipettes, clear glass HPLC vials crimpable lids and 0.45 μm nylon filter papers were purchased from Fischer Scientific (Leicester, UK). Tetracaine base and aciclovir base both BP grade (99.9%) were supplied by Sigma Aldrich (Dorset, UK). Diclofenac diethylamine BP grade (99.9%) was obtained from Chemos Group (Regenstauf, Germany). Concentrated hydrochloric acid and sodium hydroxide was from Fluka (Dorset, UK). Sodium acetate was provided by Alfa Aesar (Heysham, UK). Deionised water was obtained by purification using an Elgstat water purifier (Elga Ltd, Buckingham, UK). Hydroxypropyl methyl cellulose grade 65SH viscosity 50 cP with the brand name of Metolose was supplied by Shin-Etsu Chemical Ltd (Tokyo, Japan). Ametop® gel (tetracaine 4% w/w), Voltarol® emulgel (diclofenac diethylamine 1.16% w/w) and Zovirax® cream (aciclovir 5% w/w) were purchased from a local pharmacy.

5.3 Methods

5.3.1 Aggregation characterization

5.3.1.1 Photon correlation spectroscopy characterization

Changes in derived count rate were tracked using photon correlation spectroscopy (PCS) (Malvern Nanoseries Zetasizer, Malvern Instruments Ltd, Malvern, UK). Measurements were taken at a scattering angle of 173°. Refractive index and viscosity constants were set at 1.33 and 0.88 mPa.s, respectively. Samples were filtered through a 0.45 μm cellulose nitrate filter

prior to the analysis. The scattering information was determined in an aqueous vehicle (acetate buffer 0.1 M) at increasing molar concentrations at the pH of the commercial product: pH 9 for tetracaine (79.3% unionized) and pH 7.4 for diclofenac diethylamine (100% ionized) and aciclovir (80% unionized), respectively. In addition, studies at pH 5 (100% unionized) were performed for aciclovir. Control solutions were prepared in the same manner as for the test systems, but without the addition of drug. A discontinuity in the slope indicated the formation of a nanosized aggregate structure in the solution. The concentration at which this change occurred was assumed to be the critical aggregation concentration. The discontinuity in the linear model applied to the unattenuated derived count rate data was confirmed by the application of a second derivative function (OriginPro 9.1 Software, OriginLab, Northhampton, USA). The size of the molecular aggregates was detected by converting the light scattering signal into a hydrodynamic radius using the Stokes–Einstein equation given in Equation 3.1. The zeta potential of the aggregate containing solutions was determined in the same vehicle employed for the molecular aggregates analysis and the concentration of each drug was set above critical aggregation concentration at pH 7.4 for diclofenac diethylamine, pH 5 for aciclovir and at pH 9 for tetracaine.

5.3.1.2 Apparent distribution coefficient

The apparent drug distribution coefficients (Log D) were measured at room temperature, below and above the critical aggregation concentration in a two phase n-octanol and acetate buffer (0.1 M) system at pH 7.4 for diclofenac diethylamine, pH 5 for aciclovir and pH 9 for tetracaine as previously described (Valenta *et al*., 2000). After phase separation the aqueous phase was withdrawn and samples were centrifuged at 13.000 rpm (Biofuge, Heraeus, Germany) and aliquots of the liquid phase were then transferred into vials. The samples were

analysed using the established HPLC methods for each model agent described in Section 2.3.1. The apparent distribution coefficient was calculated using Equation 3.2.

5.3.2 HPMC gel preparation

HPMC was selected as the gelling agent because it is a non-toxic and non-ionic inert polymer, which is extensively used in the preparation of topical pharmaceutical formulations (Wu *et al.*, 1998; Wade and Weller, 1995). A 3% HPMC gel was prepared with a drug load above and below the experimentally determined critical aggregation concentration for each test active. The concentration above the critical aggregation concentration was selected to match the concentration of the commercial product where possible. A gel formulation at a concentration of 0.5 and 151 mM and 0.12 and 43 mM was prepared for tetracaine and diclofenac diethylamine, respectively. Conversely, since no significant aggregation was detected at the pH of the aciclovir commercial product (pH 7.4; 222 mM), a 0.15 and 2 mM formulation was prepared at pH 5 because it showed the presence of aggregates. The gel was prepared by heating 25 mL of distilled water up to 70 °C and 1.5 g of metolose was gradually added while stirring until complete dissolution. The required amount of drug was weighed and then dissolved in 25 mL of distilled water. Both phases were combined and then stirred homogeneously in a stirring plate. The mixture was cooled in a fridge to 0 °C – 5 °C until it became transparent. The pH was then adjusted to the required value by adding NaOH (1M) or acetic acid as required. Finally, agitation was continued for at least 30 min until room temperature was reached. The pH of the gel was then checked by diluting and dispersing it in water 10% (w/v) in a manner described elsewhere (Dhawan *et al.*, 2009). Visual inspection indicated that the formulated preparations remained physical stable for the entire duration of the experimental period and were found to be transparent and uniform in consistency.

5.3.3 Permeation studies

Adult pig ears were obtained from a local abattoir. The ears were removed from the carcass after hair removal. Any ears that were obviously damaged were discarded. The ears were cleaned with water, the residual water on the skin surface was immediately removed by blotting with tissue, visible residual hairs were trimmed carefully and the ears were stored at -20 °C. Freezing has been shown not to compromise the permeability of porcine skin (Weber, 1993). Porcine skin was defrosted and the subcutaneous fat carefully removed using a scalpel and cut into pieces of a suitable size to be mounted in the Franz diffusion cell (University of Southampton, UK) with the *SC* facing the donor compartment. For each experiment five different ears were used. The receptor phase consisted of a sponge compartment that was placed underneath the controlling barrier in intimate contact with the dermal tissue. Five diffusion cells were used for each experiment. Before the initiation of the studies an integrity test was performed, inverting each cell and visually inspecting for any signs of leakage. Leaking cells were excluded from the experiments. A 1 g aliquot of each in-house formulated gel or 1 g of the commercial product was applied to the apical surface of the porcine skin to initiate the transport studies. *In vitro* permeation experiments were conducted as method described previously in Section 4.3.1 under atmospheric pressure (1010 mBar) and under hypobaric pressure (500 mBar) using the pressure cell assembly over a period of 24 h. The samples were analysed employing the HPLC methods described in Section 2.3.1. The analysis of the chromatograms showed that matrix interference was negligible (data not shown) and drug degradation was not detected (< 2% change in peak area) for the entire duration of the experimental period.

At the end of the transport studies, the pressure cell was dismantled and skin was removed and washed with distilled water to discard any residual donor solution and excess water was absorbed with tissue paper. The *SC* of the skin was removed by tape stripping (ca. 20 strips until the skin was translucent) using adhesive tape (Scotch 845 book tape, 3M, Bracknell, UK) as reported by Primo (2008) and the first strip was considered as part of the applied formulation and hence its removal was part of the formulation wash off (Sheth *et al.*, 1987). The remaining tape strips were applied sequentially by pressing the adhesive tape onto the skin using a roller to stretch the skin surface (Surber *et al.*, 2001). Once the strips were removed they were collected together, weighted and tetracaine and diclofenac diethylamine were extracted from the adhesive tape by immersing it in a 90% MeOH and 10% NaCOOH (0.1 M at pH 4) solution for 24 h, whereas for aciclovir a 95% hydrochloric acid (0.1 M pH 3) and 5% MeOH solution was used. The adhesive tape was then removed from the drug solvent and discarded. The drug solutions were dried down and the residue was reconstituted in acetate buffer (0.1 M) at pH 7.4 for diclofenac diethylamine, pH 5 for aciclovir and in acetate buffer (0.1 M) at pH 9 for tetracaine and analysed employing the HPLC methods described in Section 2.3.1 for each model agent.

Using the specimens from the stripped skin, the epidermis was separated from the dermis using a scalpel as reported by Argenta *et al.* (2014). Both the epidermis and dermis were homogenized (Ultra Turrax, Fisher Scientific, Leicester, UK) in the extraction solutions mentioned previously and were left to equilibrate for 24 h. Samples were then centrifuged at 17000 rpm (Biofuge, Heraeus, Germany) for 15 min, the resultant supernatant was evaporated and the residue was reconstituted in acetate buffer (0.1 M) at pH 7.4 for diclofenac diethylamine, pH 5 for aciclovir and in acetate buffer (0.1 M) at pH 9 for tetracaine and analysed employing the HPLC methods described in Section 2.3.1 for each

model agent. To assess the extraction recovery efficacy, skin samples were spiked with a known amount of each drug and the extraction procedure was conducted as previously described. The extraction recovery was measured by comparing the amount of each drug added and extracted. The extraction recovery of each drug from the receptor compartment was found to be to be 95.3 ± 2.5%, 93.4 ± 1.2% and 96.1 ± 2.9% for tetracaine, diclofenac diethylamine and aciclovir, respectively. Whilst the recovery extraction at 24 h period from the tape strips and skin tissue was found to be 96.16 ± 1.3% and 93.2 ± 5.2% , 94.4 ± 3.3% and 91.9 ± 7.2% , 95.3 ± 3.9% and 95.8 ± 9.1% (n = 5) for tetracaine, diclofenac diethylamine and aciclovir, respectively. Drug extraction was within the 100 ± 15% recovery rates, which was in line with published regulatory guidelines (Health and consumer protection directorate-general, 2006). The effect of local hypobaric stress upon drug cutaneous bioavailability was represented by an enhancement ratio (ER) which was calculated according to equation 4.1. Epidermal targeting potential (TP) was calculated according to equation 5.1, where A_E and A_D were the amount of drug (μg) per cm^2 deposited within the epidermal (SC + viable epidermis) and dermal tissue under hypobaric or atmospheric pressure conditions.

$$TP = \frac{A_E}{A_D} \qquad \text{(Equation 5.1)}$$

5.3.4 Statistical analysis

All data were presented as mean ± standard deviation and statistical analysis of data was performed using SPSS version 16.0, as described previously in Section 2.3.4. In all cases, a statistically significant difference was defined as when $p < 0.05$ and denoted as: * $p < 0.05$, ** $p < 0.01$ and *** $p < 0.001$. The number of replicates was 5 in the permeation studies and

3 in the apparent distribution coefficient determination, zeta potential and light scattering studies.

5.4 Results and Discussion

5.4.1 Aggregation characterization

In order to characterize the aggregation behaviour of each model agent in the vehicles employed in the permeation studies photon correlation spectroscopy was used to track changes in the derived count rate at the pH of the commercially available product. A critical aggregation concentration of 0.62 ± 0.1 mM and 0.15 ± 0.02 mM was registered at pH 9 and 7.6 for tetracaine and diclofenac diethylamine, respectively (Figure 5.1 a and b), but no aciclovir self-association was detected at pH 7.6 of the commercial product (Figure 5.2 a). However, molecular aggregation was detected at pH 5 and a critical aggregation value of 0.3 ± 0.02 mM was recorded in this solution (Figure 5.2 b).

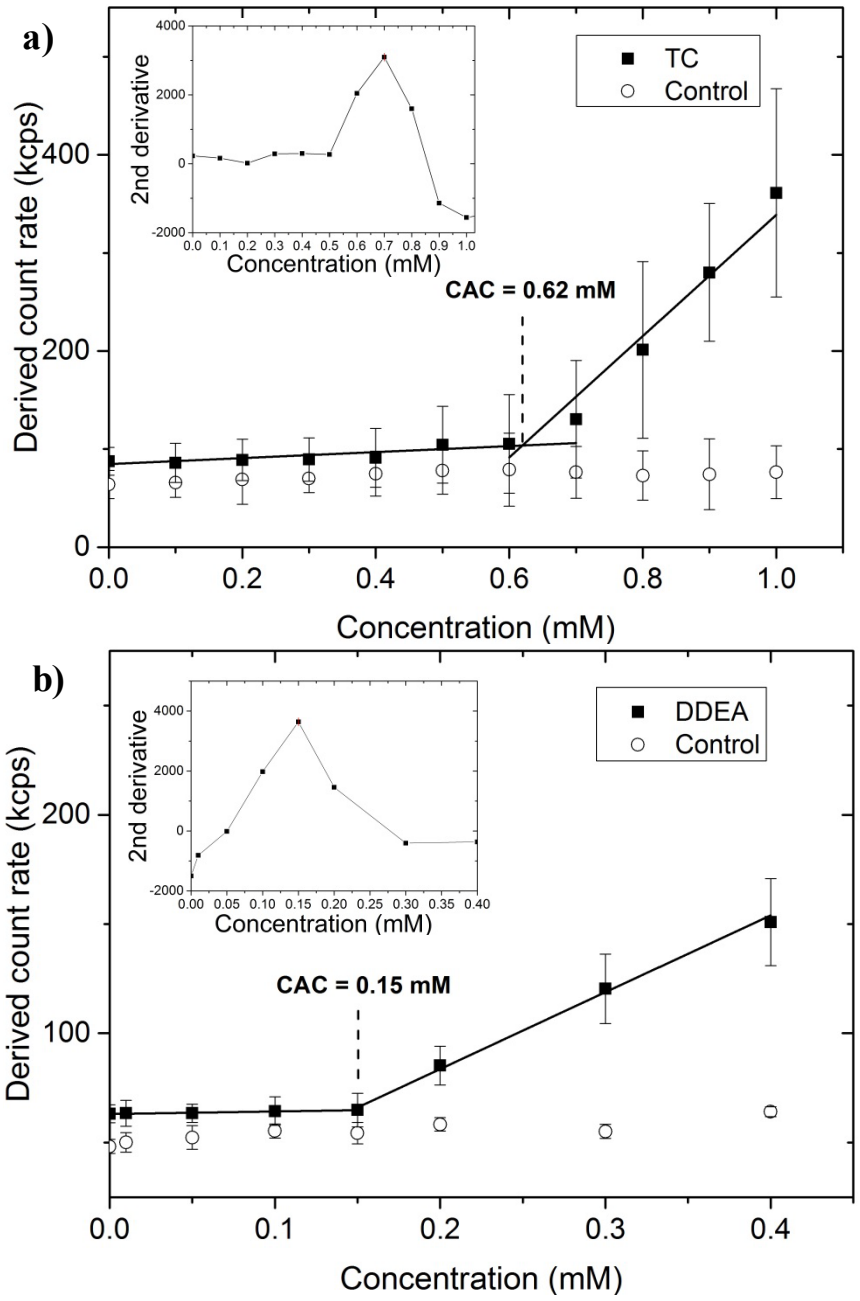

Figure 5.1. Graph depicting the changes in total light scattering in an aqueous vehicle for a) tetracaine (TC) at pH 9 and b) diclofenac diethylamine (DDEA) at pH 7.6 Each point represents mean ± standard deviation (n = 3). Inset graph represents the application of a second derivative function that confirmed the discontinuity in the slope of the derived count rate data. The critical aggregation concentration was determined to be 0.62 ± 0.1 mM and 0.15 ± 0.02 mM for TC and DDEA, respectively.

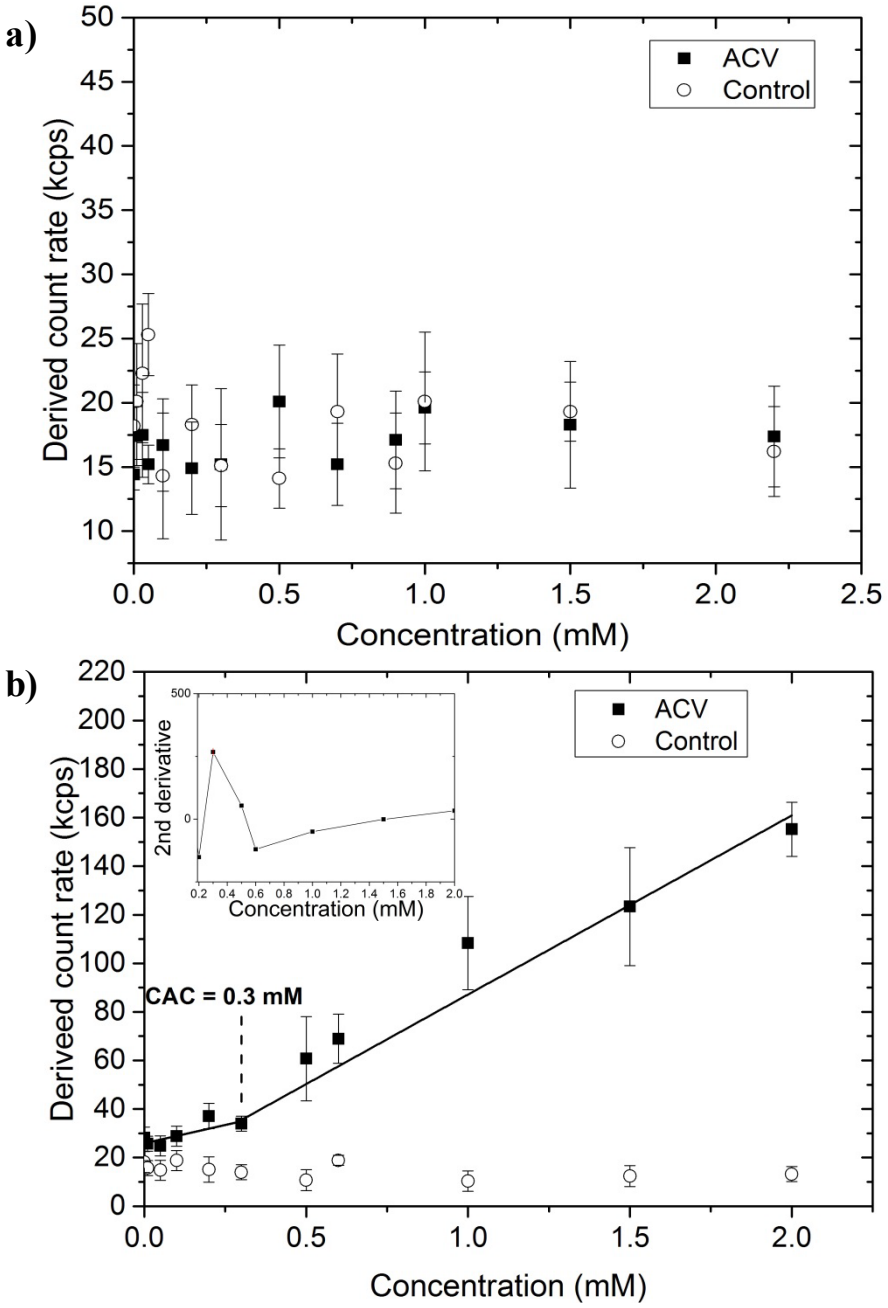

Figure 5.2. Graph depicting the changes in total light scattering in an aqueous vehicle for aciclovir a) pH 7.6 and b) pH 5 Each point represents mean ± standard deviation (n = 3). Inset graph represents the application of a second derivative function that confirmed the discontinuity in the slope of the derived count rate data. The critical aggregation concentration was determined to be 0.3 ± 0.02 mM at pH 5.

The average size of the diclofenac diethylamine molecular aggregates was significantly lower ($p < 0.001$) at 59.3 ± 10.2 nm than tetracaine at 190.2 ± 23.2 and aciclovir at 130.9 ± 17 (Table 5.1). The relatively high polydispersity index (≥ 0.28) measured for all the test systems was indicative of the presence of different sized aggregates in solution (Table 5.1). This suggests that above the experimentally determined critical aggregation concentration each drug exists in solution as several supramolecular structures of various sizes. The zeta potential values obtained for diclofenac diethylamine (-9.19 ± 0.8 mV) indicates that a negatively charged aggregate was formed, whilst the values close to neutral for tetracaine (0.98 ± 0.5 mV) and aciclovir (-0.62 ± 0.3 mV) suggests that these species are predominantly unionized in solution (Table 5.1). The experimentally determined post-aggregation distribution coefficient for tetracaine (Log D 2.1 ± 0.16) and diclofenac diethylamine (Log D 0.58 ± 0.06) were significantly lower ($p < 0.05$) when compared with the pre-aggregation values at 2.6 ± 0.12 and 0.8 ± 0.04, respectively (Table 5.1). It can be hypothesized that the aggregated species for these compounds had more favorable interactions with the aqueous vehicle in which they were dispersed. This was thought to result in a decrease in the hydrophobic characteristics of the molecules presented to the water/oil interface used to determine the distribution coefficient. The presence of an organized cluster where the polar region groups are displayed to the outer region (as suggested in Section 3.4.2) may provide a higher aqueous solubility due to a decrease in the interfacial tension between the aggregate surface and water and therefore explain the lower experimental Log D post-aggregation values compared to the pre-aggregation ones as previously reported for other molecules (Kronberg *et al.*, 2014). In contrast, the post-aggregation distribution coefficient for aciclovir (Log D -1.65 ± 0.3) was not significantly different ($p > 0.05$) when compared to the pre-aggregation value of -1.48 ± 0.7 (Table 5.1).

Table 5.1. Characteristics of tetracaine (TC), diclofenac diethylamine (DDEA) and aciclovir (ACV) molecular aggregates. [a] hydrodynamic size, [b] polydispersity index, [c] post aggregation apparent distribution coefficient and * pre aggregation apparent distribution coefficient.

Drug	pH	Size [a] (nm)	P.I. [b]	Zeta potential (mV)	Log D [c]
TC	9	190.2 ± 23.2	0.34	0.98 ± 0.5	2.1 ± 0.16 (2.6 ± 0.12)*
DDEA	7.6	59.3 ± 10.2	0.28	-9.19 ± 0.8	0.58 ± 0.06 (0.8 ± 0.04)*
ACV	5	130.9 ± 17	0.46	-0.62 ± 0.3	-1.65 ± 0.3 (-1.48 ± 0.7)*

5.4.2 Permeation studies

The data showed that drug deposition within the different skin strata and transdermal permeation under both barometric conditions was equivalent ($p < 0.05$) when tetracaine, diclofenac diethylamine and aciclovir were presented to the skin at a concentration that was below CAC (Figure 5.3). In contrast, when the drugs were applied to the skin as an aggregated system, i.e. above their CAC, the application of topical hypobaric stimuli was found to alter the cutaneous bioavailability of all three agents. Tetracaine transdermal permeation increased by 8.9-fold ($p < 0.01$) compared to the unstressed skin transport experiment, but the amount of tetracaine detected within the different cutaneous strata was found to be equivalent ($p > 0.05$) (Figure 5.3 a). All the percutaneous data recorded for diclofenac diethylamine was found to be greater ($p < 0.01$) when the porcine skin was challenged with hypobaric stress (Figure 5.3 b). There was a higher retention ($p < 0.001$) of the drug in the epidermal tissue, i.e. a 12 and 16.9-fold increase in diclofenac diethylamine was recorded in the *SC* and epidermis, respectively. In addition, diclofenac diethylamine residence in the dermal tissue and transdermal permeation was found to be enhanced by 2.8

and 2.4-fold, respectively. In a similar manner to diclofenac, all the percutaneous penetration indices recorded under barometric stress conditions were significantly different ($p < 0.01$) compared to atmospheric conditions when aggregated aciclovir was applied to porcine skin (Figure 5.3 c). More specifically, there was a 2.1 and 2.5-fold increase in the amount of aciclovir deposited in the *SC* and viable epidermis, respectively. In addition, the amount of drug detected in the receptor compartment was found to be enhanced by 2.7-fold.

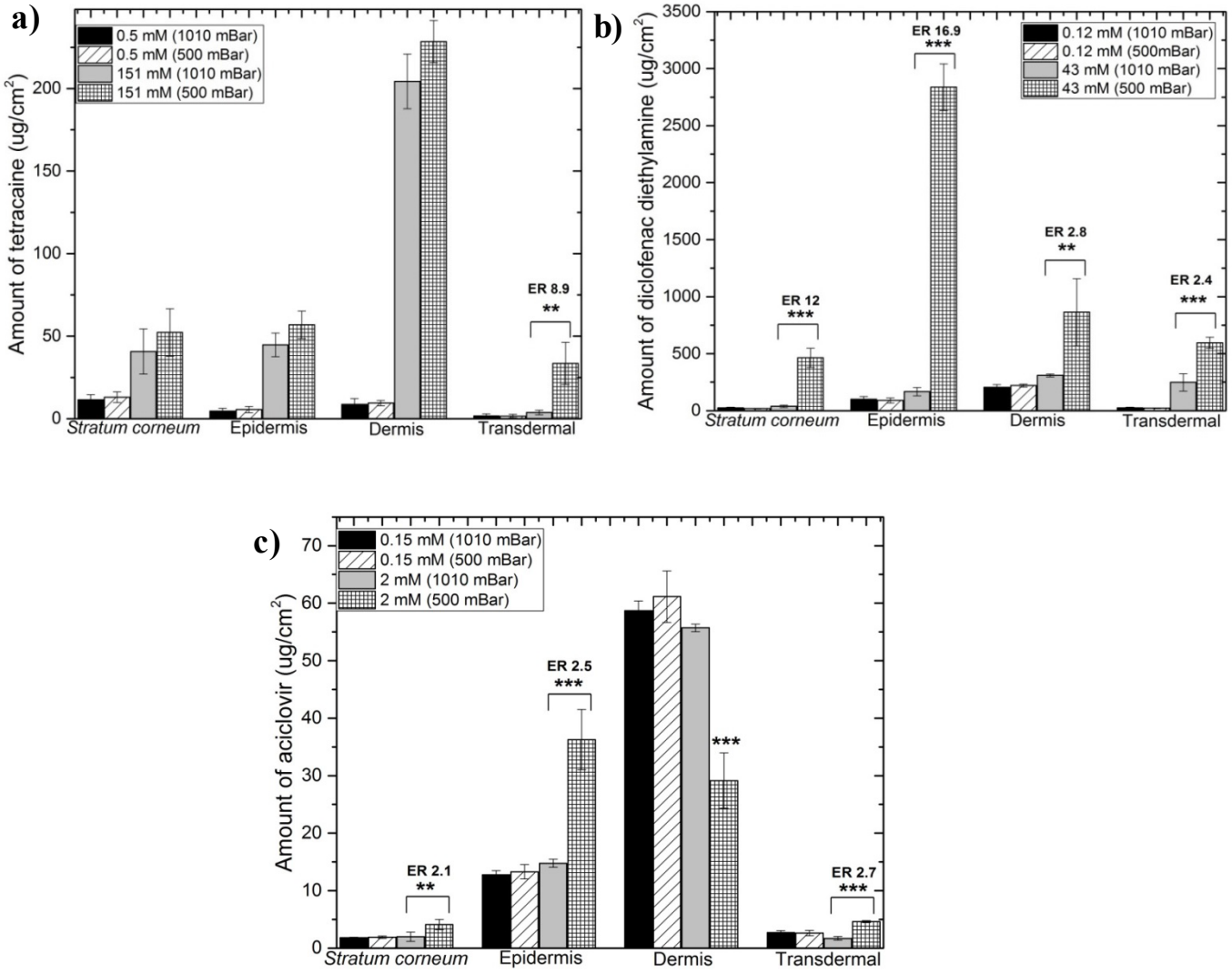

Figure 5.3. *In vitro* percutaneous penetration profile of tetracaine, diclofenac diethylamine and aciclovir in porcine skin 24 h after the application of a gel formulated with a drug load below (0.5 mM, 0.12 mM and 0.15 mM) and above (151 mM, 43 mM and 2 mM) critical aggregation concentration under atmospheric (1010 mBar) and hypobaric (500 mBar) pressure conditions, respectively. Each point represents mean ± standard deviation (n = 5).ER (Enhancement ratio) represents the ratio between the amount of drug found under hypobaric and atmospheric conditions. Student's t-test with ** $p < 0.01$ and *** $p < 0.001$.

Hypobaric driven delivery was shown to be an effective means to achieve 'targeting' of diclofenac diethylamine and aciclovir within the epidermal tissue after topical application of the aggregated agents. This effect followed the trend diclofenac diethylamine > aciclovir with a calculated 'targeting' potential of 4 and 1.4 for the two agents, respectively (Table 5.2). Drug transport into the skin can be achieved via the confluent structure presented by the cells and the pores introduced into the skin structure. However, the importance of the passage of the drug aggregates suggested that the transappendageal pathway may be the most important in terms of hypobaric pressure induced percutaneous penetration changes. Although the data generated in Chapter 4 indicated that a facilitated intercellular and transcellular route through the alteration of the corneocytes was also possible, the data in this Chapter suggested that the follicular route was being used by the drug aggregates to alter skin deposition rather than the normal passive diffusion pathway. This was shown by the fact that barometric stress only had a significant impact on drug transport in the presence of drug aggregates. The data described herein was in good agreement with previously reported studies that demonstrate a much more efficient penetration of nanosized systems through hair follicles than small molecules under mechanical stress (Lademann *et al.*, 2006).

The hydrophilic characteristics of the diclofenac diethylamine (Log D 0.58 ± 0.06) and aciclovir (Log D -1.65 ± 0.3) supramolecular structures would make them more susceptible to pass into the epidermis via the follicular route, whereas the lipophilic tetracaine molecular aggregates (Log D 2.1 ± 0.16) may reside on the skin and interact with the lipid matrix surrounding the corneocytes and/or the lipid components of the follicular structures (Meidan, 2010; Huang *et al.*, 2005; Williams, 2003; Hadgraft *et al.*, 1998).

Table 5.2. The deposition of tetracaine (TC), diclofenac diethylamine (DDEA) and aciclovir (ACV) in the epidermal (*SC* + epidermis) and dermal tissue 24 h after a gel formulated with a drug load above critical aggregation concentration was applied to porcine skin under atmospheric (1010 mBar) and hypobaric (500 mBar) pressure conditions. Epidermal targeting potential is expressed as a ratio between the amount of drug retained in the epidermal (*SC*+ viable epidermis) and dermal tissue under hypobaric and atmospheric conditions.

	Skin deposition (µg/cm^2)					
	Epidermal tissue		**Dermal tissue**		**Targeting potential**	
Drug	1010 (mBar)	500 (mBar)	1010 (mBar)	500 (mBar)	1010 (mBar)	500 (mBar)
TC	85.4 ± 2.8	109.1 ± 3.3	204.4 ± 16.5	228.4 ± 12.7	0.4	0.5
DDEA	205.9 ± 91	3301 ± 1678.5	309.8 ± 12.4	864.2 ± 293.8	0.7	4
ACV	16.8 ± 9	40.4 ± 22.6	55.7 ± 2.7	29.1 ± 4.8	0.3	1.4

The smaller size of the diclofenac diethylamine (59.3 ± 10.2 nm) and aciclovir (130.9 ± 17 nm) drug aggregates would also facilitate their more rapid passage into the skin compared to the tetracaine aggregates (190.2 ± 23.2 nm). The accumulation within the superficial layers of the *SC* of nanosized particles up to 200 nm has been previously reported through porcine and human skin (Menzel *et al.*, 2004; Lademann *et al.*, 1999) and the same mechanism may explain why only tetracaine showed an increased *SC* residence upon the formation of the aggregates even without the application of hypobaric pressure.

The follicular pathway has been shown to be the primary penetration route for nanosized systems up to 600 nm (Lademann *et al.*, 2015). As the follicular structure extend deep through the skin surface past the dermis (Delgado-Charro and Guy, 2001; Babiuk *et al.*, 2000) this allows drugs following the follicular route to access both the epidermal and dermal tissue (Rancan *et al.*, 2009). From the data in this work, it is hypothesised that the smaller and charged characteristics of the diclofenac diethylamine molecular aggregates provided a better ability of these supramolecular masses to move by passive diffusion across the follicular epithelium into the hydrophilic interfollicular epidermis, which resulted in a greater epidermal targeting potential upon hypobaric driven delivery. Interfollicular epidermal passage of nanosized systems with a similar size to that recorded for diclofenac diethylamine aggregates has been previously reported by Vogt and his colleagues (2006). On the other hand, the size of the aciclovir and tetracaine drug aggregates might limit perifollicular diffusion at some extent and result in drug transport through the follicular structures directly into the dermis with subsequent diffusion across this layer, which may explain the greater transdermal permeation.

5.4.3 The commercial product

5.4.3.1 Formulation characterization

Tetracaine is commercially available as a gel (Ametop®) that contains 4% (w/w) of the drug together with an undisclosed amount of xanthan gum as a gelling agent. The drug is presented as a two phase suspension system presumably to allow maximum thermodynamic activity to be retained throughout the entire storage and delivery process (Escribano *et al.*, 2005; Paudel *et al.*, 2010). Both the in-house produced tetracaine test system and the commercial product showed the presence of drug crystals with similar morphology when presented as a two phase suspension (Figure 5.4 a and b), hence it was assumed that the excipients in the commercial product did not significantly alter tetracaine/vehicle interactions (Higuchi, 1960). Diclofenac diethylamine is commercially available as a hydrogel (Voltarol emulgel®) that contains 1.16% (w/w) of the drug salt together with an undisclosed amount of propylene glycol as a cosolvent (Cevc *et al.*, 2001). Microscopic images revealed the presence of drug crystals in the in-house formulated diclofenac diethylamine test system (Figure 5.4 c), but this was not detected in the commercially available product (Figure 5.4 d), probably due to the use of propylene glycol as a cosolvent in the pharmaceutical preparation. Propylene glycol has been reported to enhance diclofenac diethylamine solubility (Khalil *et al.*, 2000). Aciclovir is commercially available in a cream formulation (Zovirax® cream) that contains 5% (w/w) of the drug together with an undisclosed amount of propylene glycol as a cosolvent (Cevc *et al.*, 2001). In the aciclovir product and the in-house produced aciclovir test system drug crystallization was not observed.

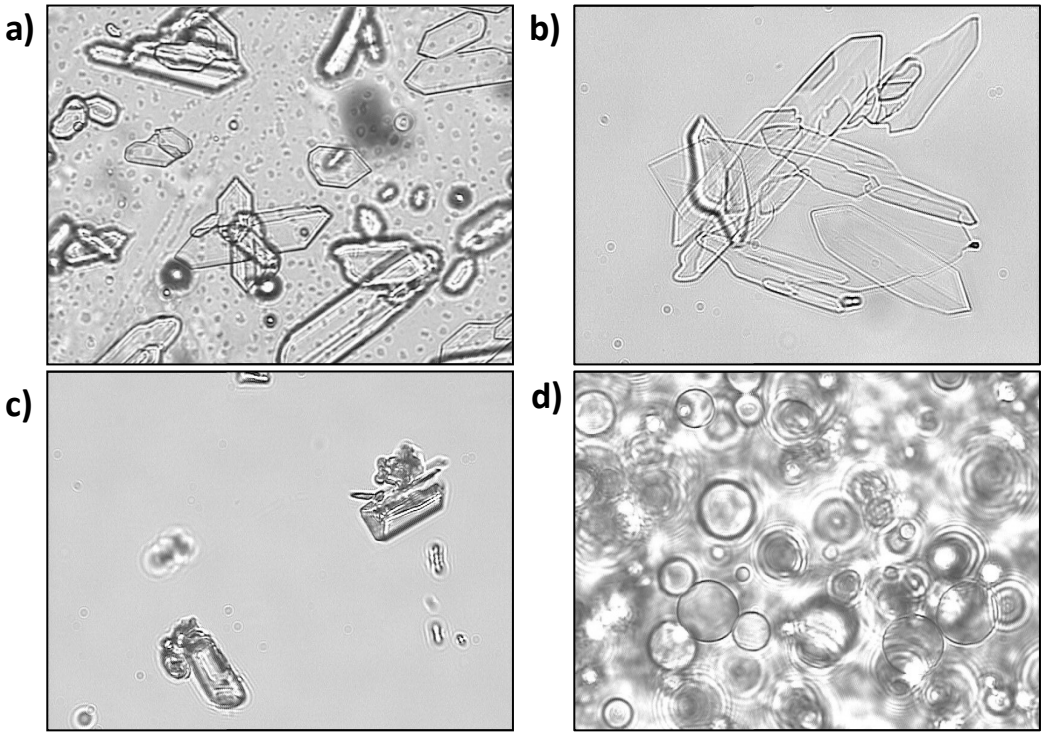

Figure 5.4. Light microscopy (Olympus BX50F, Tokyo, Japan) at a magnification of 40 × of the a) tetracaine commercial product, b) in-house tetracaine formulation above its critical aggregation concentration c) in-house diclofenac diethylamine formulation above its critical aggregation concentration and d) diclofenac diethylamine commercial product.

5.4.3.2 Permeation studies

The characteristics of the excipients and vehicles added to a formulation play a major role in determining the rate of uptake, penetration and residence of therapeutic agents through the skin (Idson, 1983). Therefore, it was of interest to assess the manner the formulation composition influenced the effects of hypobaric stress on the three model compounds. The data showed that tetracaine epidermal localisation was significantly lower ($p < 0.001$) upon

the application of hypobaric stress (Table 5.3), but the the amount of drug detected in the receptor increased by 6.5-fold compared to the unstressed skin transport experiment (Figure 5.5). The increase in tetracaine transdermal permeation was found to be similar to that recorded for the in-house formulated gel. However, the in-house formulated preparation did display an enhanced capacity ($p < 0.001$) to localise drugs within deeper skin layers (Table 5.2 and 5.3) which resulted in an enhanced transdermal permeation ($p < 0.001$) (Figure 5.3 a and Figure 5.5). This was thought to be a consequence of the use of xanthan gum in the commercial product. The negatively charged carboxyl groups presented by the hydrocolloid gum have been previously reported to alter drug/drug interactions (Salim *et al.*, 2012). In a similar manner, tetracaine-tetracaine self-association process may have been disrupted at least at some extent in the commercial vehicle product and therefore affect the ability of the drug aggregates to diffuse via the follicular route. All the percutaneous data recorded for diclofenac diethylamine was found to be greater ($p < 0.01$) when the porcine skin was challenged with hypobaric stress (Figure 5.5). There was a higher retention ($p < 0.001$) of the drug in the epidermal tissue, i.e. an 18.9 and 8-fold increase in diclofenac diethylamine was recorded in the *SC* and epidermis, respectively. In addition, diclofenac diethylamine residence in the dermal tissue and transdermal permeation was found to be enhanced by 1.54 and 5.1-fold, respectively. The ability of the commercial product formulation to deliver the drug into the skin was significantly lower ($p < 0.05$) and diclofenac diethylamine localisation in the epidermal tissue was proportionally lower when compared to that displayed by the in-house formulated gel. It was registered an epidermal targeting potential of 3.1 and 4, respectively (Table 5.2 and 5.3). This was thought to be a consequence of the use of propylene glycol in the commercial product, which may have altered drug/skin/vehicle interactions. Propylene glycol has been shown to limit the aggregation behaviour of several drug compounds and to interact with water molecules (Squillante *et al.*, 1998; Trottet *et al.*,

2004; Miller *et al.*, 1993; Dixit *et al.*, 2002). It can be hypothesised that diclofenac diethylamine self-association was limited at some extent in the commercial vehicle product and this may have resulted in a lower follicular mass transport rate under hypobaric stress. In addition, it was though that propylene glycol-water structuring in the commercial product limited diclofenac diethylamine permeating species to participate in the transport process, which resulted in a low partitioning from the delivery vehicle as previously observed by Benaouda *et al.*, (2012).

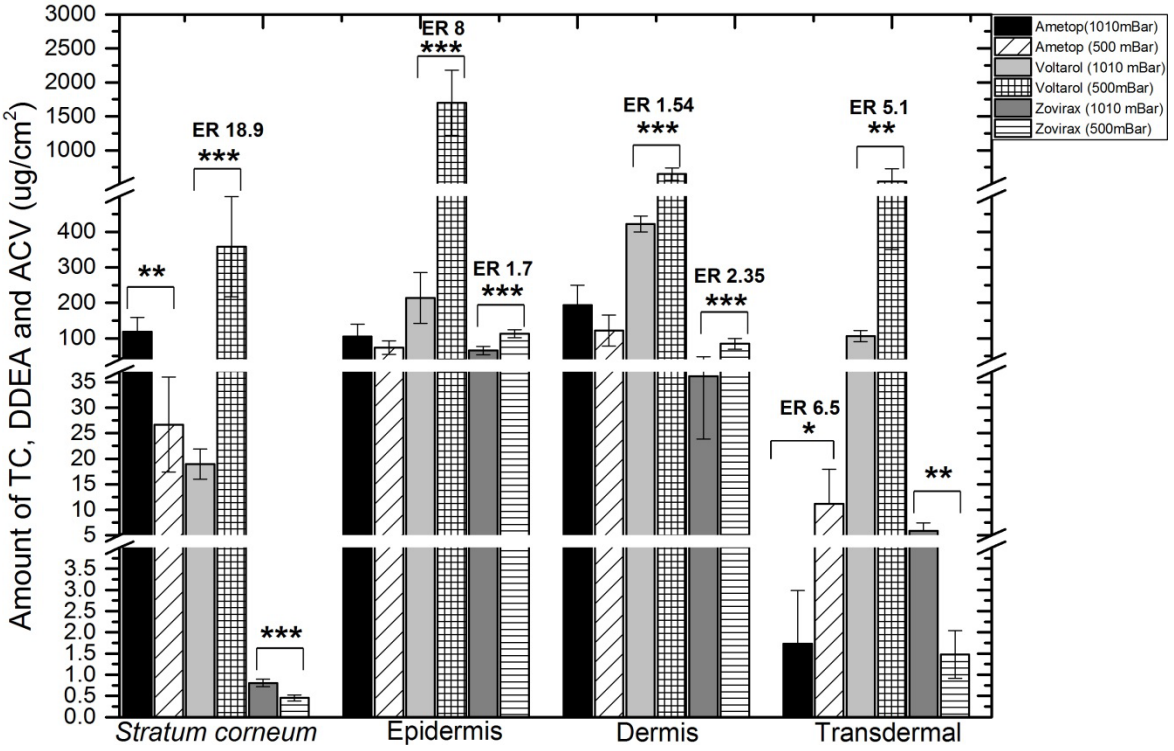

Figure 5.5. *In vitro* percutaneous penetration profile of tetracaine, diclofenac diethylamine and aciclovir in porcine skin 24 h after the application of the commercial product, Ametop® (TC), Voltarol® (DDEA) and Zovirax® (ACV) under atmospheric (1010 mBar) and hypobaric (500 mBar) pressure conditions. Each point represents mean ± standard deviation (n = 5). ER (Enhancement ratio) represents the ratio between the amount of drug found under hypobaric and atmospheric conditions. Student's t-test with * $p < 0.05$, ** $p < 0.01$, *** $p < 0.001$.

Table 5.3. The deposition of tetracaine, diclofenac diethylamine and aciclovir in the epidermal (*SC* + epidermis) and dermal tissue 24 h after the commercial product Ametop® (TC), Voltarol® (DDEA) and Zovirax® (ACV) was applied to porcine skin under atmospheric (1010 mBar) and hypobaric (500 mBar) pressure conditions. Epidermal targeting potential is expressed as a ratio between the amount of drug retained in the epidermal (*SC* + viable epidermis) and dermal tissue under hypobaric and atmospheric conditions.

	Skin deposition (µg/cm^2)					
	Epidermal tissue		**Dermal tissue**		**Targeting potential**	
Drug	1010 (mBar)	500 (mBar)	1010 (mBar)	500 (mBar)	1010 (mBar)	500 (mBar)
TC	223.2 ± 9.3	100.9 ± 33.6	193.8 ± 56.2	122.2 ± 43.9	1.1	0.8
DDEA	232.9 ± 37.9	2057. 6 ± 248.5	422 ± 22.8	650.8 ± 91.2	0.6	3.1
ACV	66.9 ± 46.1	113.1 ± 79.3	36.1 ± 12.3	84.9 ±15.1	1.8	1.3

In a similar manner to diclofenac all the percutaneous penetration indices recorded under barometric stress conditions were significantly different ($p < 0.01$) compared to atmospheric conditions when aciclovir was applied to porcine skin (Figure 5.5). More specifically there was a 1.7 and 2.35-fold increase in the amount of aciclovir deposited in the viable epidermis and dermal tissue, respectively. The ability of the commercial product formulation to deliver the drug into the skin was significantly enhanced ($p < 0.05$), but aciclovir localisation in the epidermal tissue was similar when compared to that displayed by the in-house formulated gel. It was registered an epidermal targeting potential of 1.3 and 1.4 respectively (Table 5.2 and 5.3). It can be hypothesised that a better ability of the commercial product to deliver greater amounts of aciclovir into the cutaneous tissue was due to the higher concentration of the drug in the application vehicle (222 mM vs 2 mM in the in-house formulated gel), which was thought to result in more aciclovir permeating species available to participate in the transport process.

5.5 Conclusions

The results from this investigation suggested that the application of local hypobaric stress was effective in targeting and retaining topically applied therapeutic agents within the epidermal tissue. However, this effect was only observed when the drug was presented to the skin as an aggregated system. It was thought that an enhanced follicular transport was the main mechanism that hypobaric driven delivery used to promote epidermal localisation. The epidermal targeting potential was calculated to be 4, 1.4 and 0.5 for diclofenac diethylamine, aciclovir and tetracaine, respectively. The smaller size ($p < 0.001$) and more hydrophilic characteristics (Log D 0.58 ± 0.06) of the diclofenac drug aggregates was believed to facilitate drug movement into the interfollicular epidermis, which resulted in the formation of

an epidermal depot of the drug. The use of propylene glycol as a cosolvent in the commercial product was thought to decrease drug epidermal localization due to its ability to alter drug/skin/vehicle interactions.

The *in vitro* data generated in this Chapter supports the hypothesis from Chapter 4 that the ability to alter cutaneous drug diffusion paths upon hypobaric treatment could potentially represent a new means to enhance topical bioavailability of therapeutic agents in medical practice. To validate this, *in vivo* studies were required and hence, the next phase of this work aimed to satisfy this need using both a drug aggregate and a macromolecule.

CHAPTER SIX

In vivo percutaneous penetration studies

6.1 Introduction

One of the major limitations of the *in vitro* transport data presented in Chapter 4 and 5 specially when considering the application of barometric stress is the absence of the cutaneous microvascular flow, which has been shown to have a significant impact upon drug diffusion and distribution within the skin tissue and systemic circulation (Wojciechowski *et al*., 1985). Early studies by Schaefer and Stuttgen (1978) showed the importance of blood flow upon skin absorption by comparing *in vitro* and *in vivo* dermal levels of topically applied hydrocortisone. These workers reported a significantly higher amount of the drug in the dermal tissue in the *in vitro* studies. The co-administration of vasoactive agents (known to alter drug absorption into the systemic circulation) has provided further knowledge of the function of the local vasculator in drug penetration and distribution (Riviere *et al*., 1991; Singh *et al*., 1994). Theoretically, vasodilatation should allow a greater absorption of drug into the systemic circulation due to an efficient clearance of the penetrant by the skin microcirculation and vasoconstriction is expected to have a contrary effect. This hypothesis has been experimentally confirmed for a variety of drugs including lidocaine and flurbiprofen when co-administered with vasoactive agents (Riviere *et al*., 1991; Sugibayashi *et al*., 1999). In addition, faster drug uptake and distribution below the site of topical application and at contralateral sites due to vasodilation (Cross *et al*., 1999) and the opposite effect due to vasoconstriction (Higaki *et al*., 2005) have also been reported. It is believed that upon drug movement through the epidermis, the permeant is removed by the local blood supply once it reaches the dermal tissue or is transported into deeper tissues by diffusion, perfusion or a combination of both (Roberts, 1991; Cross and Roberts, 1999; Roberts *et al*., 2002). The orientation of the blood vessels has also been suggested to play a pivotal role in the rapid distribution of drugs from the epidermal-dermal interface to deeper cutaneous tissues

(Roberts and Cross, 1999). It has been proposed that the orientation of the microvascular networks produces a "convective force" that generates a localized deep tissue mechanism, which is believed to result in a deeper tissue penetration at the site of application and away from the site of application for several compounds (Cross and Roberts, 1999; McNeill *et al.*, 1992; Monteiro-Riviere *et al.*, 1993). However, how hypobaric pressure driven delivery affects *in vivo* drug diffusion through the skin and subsequent clearance by the systemic circulation is at the present not well characterised.

There is conflicting evidence concerning the effects of hypobaric stress upon the local vasculature. Skagen *et al.*, (1983) applied between 13 mBar and 330 mBar to the skin using a suction device and found that sub-atmospheric pressure changes of 53 mBar or more induced pronounced vasoconstriction and a corresponding increase in vascular resistance of about 90% using a ^{133}Xe wash-out technique. These findings were further supported by Kairinos and his colleagues (2009) who found a decrease in blood flow upon the application of local hypobaric stress to human tissue using radioisotope perfusion imaging. Conversely, an increase in blood flow has been reported when laser Doppler flowmetry was employed to investigate the cutaneous haemodynamic vascular responses to hypobaric stress stimuli. A continuous application of sub-atmospheric pressures between 166 to 660 mBar to the skin was reported to significantly increase cutaneous blood flow when compared to baseline measurements (Morykwas *et al.*, 1997; Timmers *et al.*, 2005). In addition, it has been shown a temporary and controlled dilation of the dermal blood vessels upon the application of sub-atmospheric pressure between 170 and 510 mBar generated from a suction cup (Aguilar *et al.*, 2005). In a follow up study, Childers *et al.*, (2007) demonstrated that the application of a hypobaric pressure of 500 mBar resulted in a two-fold dilation of the dermal blood vessels with concomitant displacement towards the skin surface. However, a link between cutaneous

blood flow changes induced by barometric pressure alteration and the penetration of xenobiotics into the cutaneous tissue has not been reported and hence this field warrants further investigation.

The aim of this Chapter of the PhD thesis was to assess the effects of locally applied hypobaric stress upon skin microvascular flow and relate these findings with drug diffusion behavior across the skin and subsequent clearance by the systemic circulation. In order to achieve this aim Full-Field Laser Perfusion Imaging (FLPI) was used to determine the cutaneous haemodynamic vascular responses to hypobaric stress stimuli as previously carried out by Leutenegger and colleagues (2011). A radiolabelled (carboxyl-^{14}C) dextran with a molecular weight of 10 kDa was selected as the model compound for *in vivo* permeation studies since the follicular route is the main pathway taken by this permeant to access the skin tissue (Section 4.4.3). In addition, it was anticipated that a greater understanding of the effects of the local vasculature upon skin permeation could be attained by comparing the results with the previously *in vitro* data collected for this agent (Section 4.4.2). Rat was chosen as the model for skin permeation due to its good accessibility and common use for *in vivo* permeation studies (Jung and Maibach, 2015; Godin and Touitou, 2007). Although, rat skin is more permeable than human skin, the permeation absorption kinetic parameters are generally comparable (Jung and Maibach, 2015; Godin and Touitou, 2007; Roberts and Mueller, 1990; Sato *et al.*, 1991). Tape stripping and tissue homogenisation methodologies permitted the assessment of cutaneous bioavailability and tissue distribution profile by scintillation counting (Tsai *et al.*, 1999; Schwarb *et al.*, 1999; Wester *et al.*, 1998). In order to investigate if the greater epidermal localization of diclofenac diethylamine upon hypobaric driven delivery (Section 5.4.2) would translate in a better anti-inflammatory efficacy a rat carrageenan-induced paw oedema model was used. For this purpose an in-house

hydroxypropyl methylcellulose gel formulated with a diclofenac diethylamine drug load above critical aggregation concentration (Section 5.3.2) was selected as the test model. This allowed the formation of diclofenac diethylamine nanosized molecular aggregates with an average size of ca. of 59.3 ± 10.2 (Section 5.4.1).

6.2 Materials

Dextran (carboxyl-^{14}C) with an average M.W. of 10 kDa and specific activity of 0.00006 Ci/mmol was obtained from American Radiolabeled Chemicals, Inc. (St. Louis, USA). Diclofenac diethylamine BP grade (99.9%) was obtained from Chemos Group (Regenstauf, Germany). Concentrated hydrochloric acid and sodium hydroxide was from Fluka (Dorset, UK). Deionised water was obtained by purification using an Elgstat water purifier (Elga Ltd., Buckingham, UK). Hydroxypropyl methyl cellulose grade 65SH viscosity 50 cP with the brand name of Metolose was supplied by Shin-Etsu Chemical Ltd (Tokyo, Japan). Heparin sodium salt from porcine intestinal mucosa grade (I-A) 1800 USP units/mg, urethane, 0.7% (v/v) glacial acetic acid, isopropanol, λ carrageenan were purchased from Sigma Aldrich (Dorset, UK). Scintillation vials and hydrogen peroxide 30% were obtained from VWR International (Leicestershire, UK). Optiphase scintisafe gel was from Fischer Scientific (Leicester, UK). Soluene® 350 was provided by Perkin Elmer (Bucks, UK). Isoflurane 100% (w/v) inhalation vapour liquid was obtained from Animalcare Ltd. (York, UK).

6.3 Methods

6.3.1 Animals

All procedures were conducted in accordance with the U.K. Animal Scientific Procedures Act (1986) and Amendments Regulations (2012) and approved by the King's College London Animal Care and Ethics Committee. Sprague Dawley male rats (6 - 9 weeks old, ca. 220 - 250 g; Charles River, Kent, UK) were caged in groups of 4 with free access to water and food. A temperature of 19 - 22 °C was maintained, with a relative humidity of 45 – 65%, and a 12 h light/dark cycle. Animals were acclimatized for 7 days before each experiment.

6.3.2 Cutaneous blood flow measurements

Rats were anaesthetized by inhalation of (1 - 3%) isoflurane / (1 – 3%) O_2 and cutaneous blood flow was assessed in the whole plantar hind paw area using the Full-Field Laser Perfusion Imager (FLPI, Moor Instruments, Axminster, UK). Baseline blood flow in both hind paws was recorded prior to the application of hypobaric stress to ensure the haemodynamic vascular responses were stabilized following the induction of anaesthesia. The ipsilateral hind paw was subsequently exposed to 500 mBar for 7 min (group 1 n = 6) and 250 mBar for 28 min (group 2 n = 6) employing the adapted pressure cell described in Section 4.3.1 that was modified for *in vivo* purposes to fit the rat's hind paw (Figure 6.1). The contralateral paw was untreated and served as a control. Changes in blood flow after these treatments were followed for 15 min. Rats were placed on a heating mat (Harvard Apparatus, Cambridge, UK) in the ventral position maintained at 36 °C for blood flow measurements. All animals were culled by a schedule 1 method upon termination of the experiment. Results

were expressed as a measure of % change in blood flow from baseline for the entire recording period for 15 min following hypobaric treatment or maximum % increase in blood flow (representing maximum vasodilatation from baseline recorded to 0 – 2 min following local hypobaric treatment). The mathematical equation 6.1 was used to drive % change in blood flow and equation 6.2 to calculate maximum vasodilatation.

$$\%\ Change\ in\ blood\ flow = \frac{(Blood\ flow - Baseline)}{Baseline} \times 100 \qquad \text{Equation 6.1}$$

$$Maximum\ vasodilatation = \frac{(Peak\ vasodilatation - Baseline)}{Baseline} \times 100 \qquad \text{Equation 6.2}$$

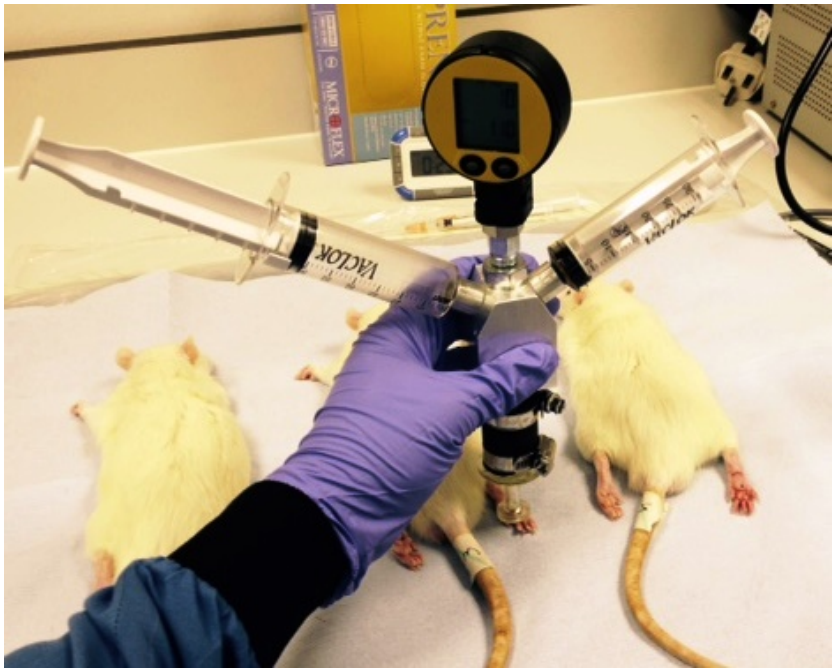

Figure 6.1. Adapted pressure cell for cutaneous blood flow measurements.

6.3.3 Pharmacokinetic studies

Animals were anaesthetized by intraperitoneal injection of urethane (0.175 g/100 g) and placed on a heating mat (Harvard Apparatus, Cambridge, UK) in the ventral position maintained at 36 °C for the duration of the experiments. The dorsal fur was carefully removed (to avoid any damage to the skin) with an animal hair clipper and the donor compartment of a Franz cell with an available area of 2.1 ± 0.2 cm^2 was attached to the shaved skin with glue, as previously described (Jing *et al.*, 2011; Woan-Ruoh *et al.*, 2008; Ren-Jiunn *et al.*, 2007). Rats were bled by tail veil puncture and ca. 100 µL of blood was collected to a heparinized tube. To initiate the finite dose studies (Howes *et al.*, 1996) a 300 µL of ^{14}C- labeled dextran in phosphate buffer (0.79 µCi equivalent to 1.428 pM) was added to the donor compartment. Permeation studies were conducted under atmospheric pressure (1010 mBar) for 7 h (n = 5). The same procedure was followed for the hypobaric pressure

condition studies, but in this case the assembled pressure cell (Section 4.3.1) was immediately attached to the top of the donor compartment (Figure 6.2) and a sub-atmospheric pressure of 500 mBar was applied for the first hour (n = 5) of the experimental period. At different time points the rats were bled by tail vein puncture and ca. 100 µL of blood was collected to a heparinized tube. Blood withdrawn did not exceed 10% of the 6.86 ± 0.53 mL/100 g rat blood volume per day as previously determined by Probst *et al.*, (2006). All animals were culled by a schedule 1 method upon termination of the experiment. Blood samples were transferred to 20 mL scintillation vials and solubilized with 1 mL of tissue solubilizer and shaken overnight at 55 °C. Before adding the scintillation cocktail, samples were decolorized by adding 0.3 mL of 30% H_2O_2 and isopropanol as an antifoaming agent. Samples were shaken at 55 °C for at least 3 h to expel H_2O_2 content and then mixed with 20 mL of scintillation cocktail acidified with 0.7% (v/v) glacial acetic acid to eliminate any chemiluminescence and kept in the dark for 24 h before counting (Al-Jamal *et al.*, 2012). ^{14}C radioactivity was quantified for each sample using a LS6500 multi-purpose scintillation counter (Beckman Coulter, Brea, USA) with a defined limit of detection of 3 × background level measurements. Total radioactivity in the blood was calculated based on the total blood volume of 6.86 ± 0.53 ml/100 g previously reported for Sprague Dawley male rats (Probst *et al.*, 2006). The results were expressed as amount of ^{14}C- dextran (fg) per mL of blood (n = 5).

Figure 6.2. Adapted pressure cell for *in vivo* permeation studies.

6.3.4 Cutaneous bioavailability and tissue distribution

At the end of the transport studies, the dorsal skin underneath the Franz cell donor compartment and organs (heart, bladder, kidneys, liver and spleen) were collected, rinsed with distilled water and weighed. The *SC* was removed by tape stripping using adhesive tape (Scotch 845 book tape, 3M, Bracknell, UK). Each tape strip was weighted prior to application onto the skin and after removal in order to guarantee that the collected amount of *SC* was uniform throughout the samples (Weigmann *et al*., 1999; Marttin *et al*., 1996). The first strip was discarded (Sheth *et al*., 1987) and the adhesive tape was pressed onto the skin using a roller to stretch the skin surface and ensure a constant pressure during the procedure (Surber *et al*., 2001). The tape strips were dissolved in 15 mL of tissue solubilizer and left at room temperature for 2 days, as previously conducted by Rougier and Lotte (1993). A 2 mL aliquot

was then transferred to 20 mL scintillation vials and mixed with 15 mL of scintillation cocktail acidified with 0.7% (v/v) glacial acetic acid to eliminate any chemiluminescence (Al-Jamal *et al.*, 2012). The stripped skin and whole organs were homogenized using a tissue homogenizer (Ultra Turrax, Fisher Scientific, Leicester, UK) in phosphate buffer (0.2 mL per 100 mg of tissue). An aliquot of 200 µL was transferred using a positive displacement pipette to 20 mL scintillation vials and 1 mL of tissue solubilizer was added and samples were shaken overnight at 55 °C. Samples were then processed as described in section 6.3.3. The extraction recovery of ^{14}C-labeled dextran from the process was found to be 95.6 ± 3.3%. Drug extraction was within the 100 ± 15% recovery rates, which was in line with published regulatory guidelines (Health and consumer protection directorate-general, 2006). The results were expressed as amount of ^{14}C- dextran (fM) per cm^2 or per gram of tissue (n = 5). The effect of local hypobaric stress upon ^{14}C-labeled dextran cutaneous bioavailability was represented by an enhancement ratio (ER) which was calculated according to equation 4.1.

6.3.5 Anti-inflammatory assay

The anti-inflammatory activity of diclofenac diethylamine formulated in a hydroxypropyl methylcellulose gel with a drug load above critical aggregation concentration (Section 5.3.2) was studied in a rat carrageenan-induced paw oedema under atmospheric (1010 mBar) and hypobaric (500 mBar) pressure conditions. Rats were randomly divided in 6 groups (n = 5) and the experimenter was blinded towards the different barometric pressure conditions applied to the ipsilateral hind paw at the time of the study. The contralateral paw was untreated for the duration of the experiments. Animals were anaesthetized by inhalation of (1 - 3%) isoflurane / (1 – 3%) O_2 and placed on a heating mat (Harvard Apparatus, Cambridge, UK) in the ventral position maintained at 36 °C for the duration of the anaesthesia. The

contralateral and ipsilateral hind paw thickness in the dorsal plantar axis was measured with a caliper (Mitutoyo, Kanagawa, Japan) and the point of measurement was pre-marked as reference for subsequent measurements (Morris, 2000). The first and the second groups served as control and 1 g of in-house formulated gel (no drug was added) was topically applied under atmospheric and hypobaric pressure conditions (500 mBar for 30 min using the adapted pressure cell described in Section 6.3.1). In the third and fourth groups, 1 g of the formulated gel containing diclofenac diethylamine was topically applied to the hind paw glabrous skin under both barometric conditions whereas in the fifth and sixth groups the same formulation was delivered to the paw non glabrous skin. Carrageenan paw oedema was induced by sub-plantar injection (0.1 mL of 1% w/v carrageenan in 0.9% saline) after 30 min of topical application of the formulated gel and anaesthesia was interrupted. Animals were allowed to recover and changes in paw thickness were determined by three replicate measurements carried out at 60 min intervals. All animals were culled by a schedule 1 method upon termination of the experiment. The results were expressed as paw swelling % (PS) which was calculated according to equation 6.3, where T_e is the mean paw edema thickness at a specific time point after carrageenan induced inflammatory response and T_i is the initial paw thickness (basal value).

$$PS = \frac{T_e - T_i}{Ti} \times 100 \qquad \text{(Equation 6.3)}$$

6.3.6 Statistical analysis

Statistical evaluation was carried out using a statistical package for social sciences software (SPSs version 16.0, SPSS Inc., Chicago, USA). All data were checked in terms of normality

(Kolmogorov-Smirnov test) and homogeneity of variances (Levene's test) prior to analysis. Data statistical analysis was performed using Student's *t*-test, Mann-Whitney *U*-test or two-way analysis of variance followed by Bonferroni's comparison post-hoc test. In all cases, a statistically significant difference was defined as when $p < 0.05$ and denoted as: * $p < 0.05$, ** $p < 0.01$ and *** $p < 0.001$. The number of replicates was 6 in the cutaneous blood flow measurements and 5 in the transport studies, cutaneous bioavailability, tissue distribution and anti-inflammatory assay.

6.4 Results and Discussion

6.4.1 Cutaneous blood flow measurements

Following baseline blood flow measurements, the ipsilateral hind paw was subjected to hypobaric treatment (500 and 250 mBar for 7 and 28 min, respectively) whilst the contralateral paw remained untreated under atmospheric pressure. It was anticipated that the application of different barometric dose treatments to the skin would allow a broader understanding of the effects of hypobaric upon the cutaneous microvascular flow. The cutaneous vascular response to hypobaric stress treatment was assessed immediately after the application of local sub-atmospheric pressure for 15 min using full-field laser perfusion imaging, to allow dynamic measurement, at a time period chosen to ensure that the response to hypobaric treatment was complete (return to base line levels) (Figure 6.3 a). The haemodynamic response to hypobaric stress stimuli resulted in significant increase in blood flow ($p < 0.001$) under both barometric stress conditions. The increase in local blood flow declined at ca. 3 min, which was in good agreement with previously reported maximum haemodynamic response period under hypobaric stress (Morykwas *et al.*, 1997). Furthermore,

maximum vasodilation was observed between 0 to 2 min following application of sub-atmospheric pressure to the ipsilateral hind paw (peak vasodilatation, Figure 6.3 a) and determined as the % maximum increase in blood flow from the baseline line obtained under atmospheric pressure conditions (Figure 6.3 b). This response was not significantly different ($p > 0.05$) under both hypobaric conditions, but there was a 51 ± 14.3 and 42.3 ± 8.5% increase in the ipsilateral hind paw blood flow from baseline upon treatment with 250 mBar and 500 mBar pressure conditions, respectively. The data suggest that haemodynamic response was time dependent and did not significantly change with a greater amount of mechanical stress as demonstrated elsewhere (Borgquist *et al.*, 2010). Moreover, the application of hypobaric stress resulted in an increased blood flow at the contralateral sites of hypobaric treatment, as shown in Figure 6.4. The increase in cutaneous blood flow upon the application of sub-atmospheric pressures has been attributed to a pressure gradient between the surrounding tissues and the site of topical mechanical stress, with blood flow surging to the latter to increase perfusion pressure of the tissue, which originates an increase in the capillaries volume and opening of the capillary beds (Koller and Kaley, 1991; Ohno *et al.*, 1993).

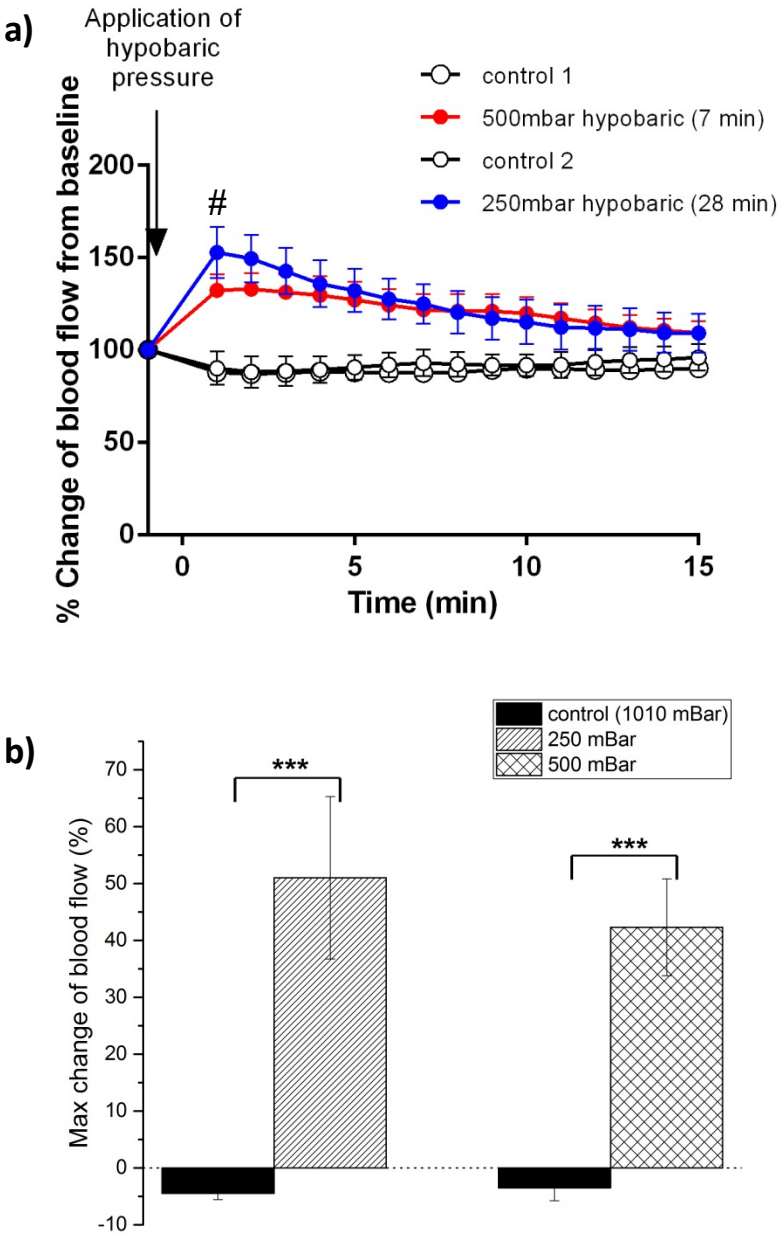

Figure 6.3. Hypobaric stress induced vascular response a) representative % change in ipsilateral and contralateral (control) hind paw blood flow from baseline to 0 - 15 min following hypobaric stress treatment, # peak vasodilatation b) % change in ipsilateral and contralateral (control) paw blood flow from baseline to 0 - 2 min following hypobaric treatment (maximum vasodilatation). Student's *t*-test with *** $p < 0.001$.

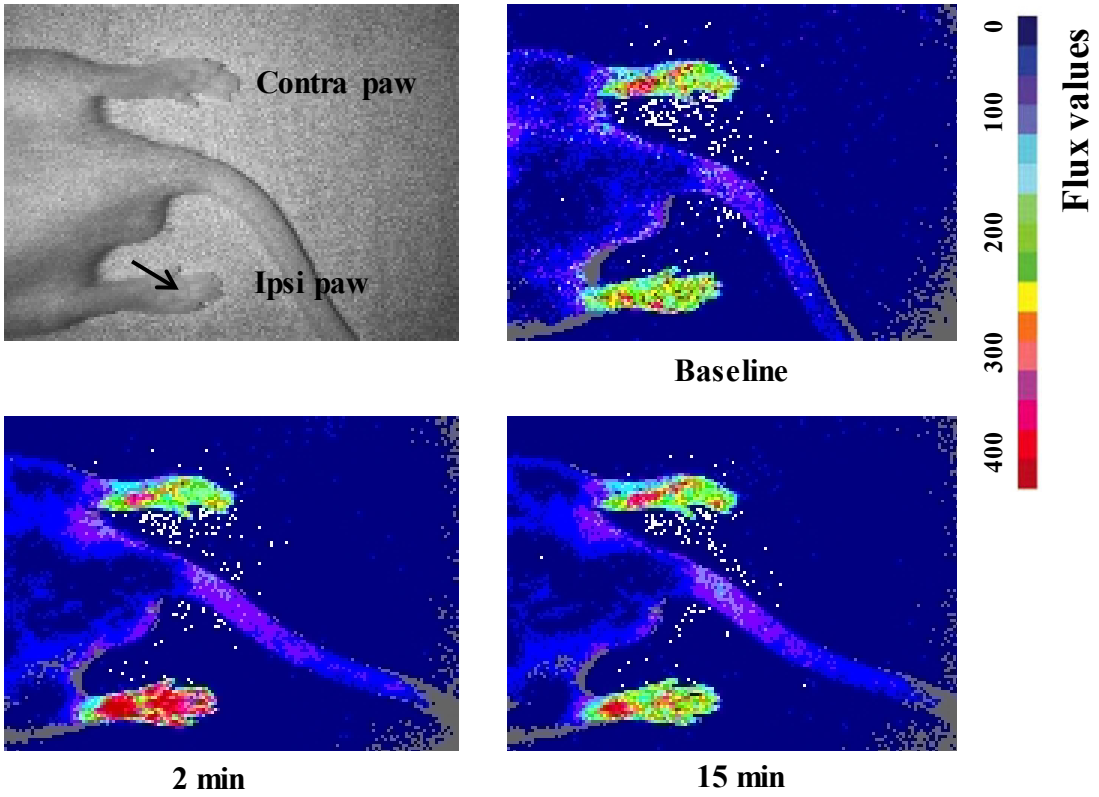

Figure 6.4. Representative full-field laser perfusion imaging pictures alongside grey scale picture showing blood flow at baseline, 2 and 15 min in hypobaric stress treated (500 mBar for 7 min) ipsilateral hind paw. Arrow indicates site of topical hypobaric treatment.

6.4.2 Pharmacokinetic studies

Topical application of local barometric stress resulted in a rapid appearance of the dextran in the systemic circulation after 1 h (Figure 6.5) with a detected concentration of 7.2 ± 2.81 $fg.mL^{-1}$ of blood. However, as the systemic levels of the rest of the experimental were found to be too low to be accurately quantified by liquid scintillation counting (values were below the defined limit of detection) parameters such as C_{max} and T_{max} could not be derived. One interpretation of this data was that the *in vivo* transdermal delivery of the 10 kDa dextran was enhanced during topical application of mechanical stress, i.e. for the 1 h duration of mechanical stimuli, but the effect was reversed by the re-establishment of atmospheric conditions at the surface of the skin.

The *in vivo* and *in vitro* transdermal permeation upon hypobaric driven delivery (Section 4.4.2) was compared through the analysis of the percentage of applied dose that reached the systemic circulation and receptor compartment as described elsewhere (Bronaugh and Maibach, 1985; Bronaugh and Franz, 1986; Wester *et al.*, 1992; Dick *et al.*, 1995; Dick *et al.*, 1997; Cnubben *et al.*, 2002; Mavon *et al.*, 2007; Griffin *et al.*, 1999; Griffin *et al.*, 2000). The detected amount of dextran corresponded to 0.004 ± 0.001% and 0.051 ± 0.002% of the applied dose in the *in vitro* and *in vivo* studies, respectively. The *in vivo* transdermal delivery was found to be significantly higher ($p < 0.001$) when compared to that observed *in vitro* (Figure 6.7) and resulted in a 13-fold increase in the amount of drug that permeated through the skin when the cutaneous microcirculation was present.

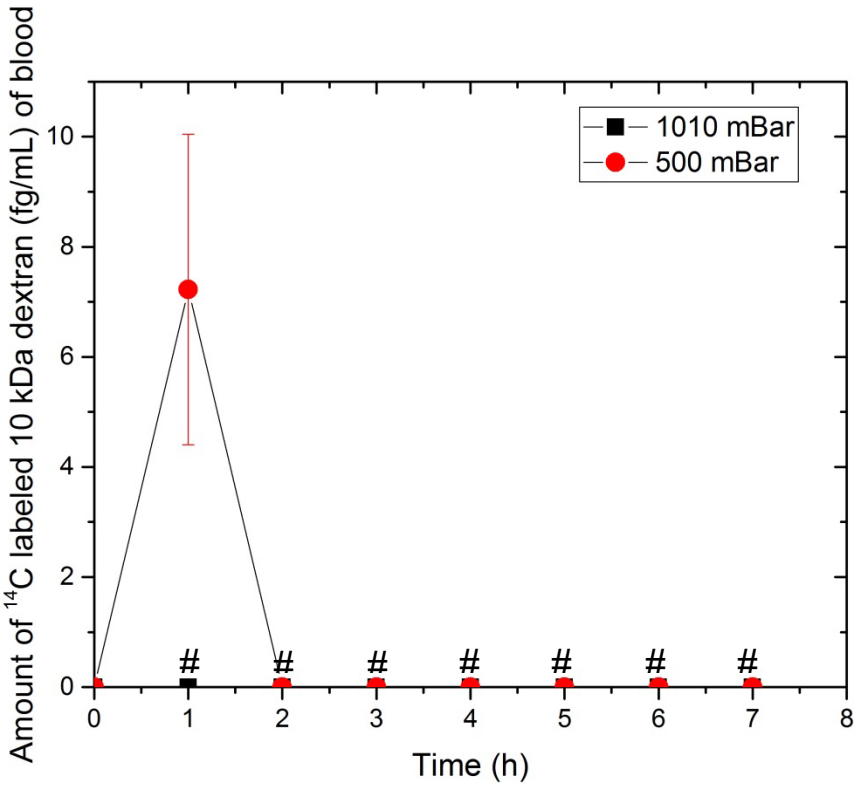

Figure 6.5. Blood concentration vs time profile of ^{14}C- labeled 10 kDa dextran in phosphate buffer (0.79 µCi equivalent to 1.428 pM) applied topically under atmospheric (1010 mBar) and hypobaric conditions (500 mBar). Each point represents mean ± standard deviation (n = 5). # Values below limit of detection (< 3 × background level measurements).

This was believed to be due to the barometric pressure opening of the follicular pathway (as demonstrated in Chapter 4), which combined with an increase in cutaneous blood flow resulted in a greater *in vivo* transdermal permeation. The significant role played by the heavily vascularized follicular structures upon rapid transdermal permeation has been previously reported when a vasodilator was topically applied in areas with varied follicle density (Jepps *et al.*, 2013; Jacobi *et al.*, 2006). It should be noted that urethane anaesthesia has been previously reported to decrease blood flow (Iwamoto *et al.*, 1987; Sakaeda *et al.*,

1997) and hence clearance of the penetrant by the systemic circulation under both barometric conditions may potentially be reduced by the anaesthetic employed in this work.

Compared to existing strategies to enhance percutaneous penetration of macromolecules, the transdermal delivery of the dextran in this work was found to be 125 and 19-fold higher when compared to *in vitro* rat skin data that applied iontophoresis delivery and *SC* removal respectively (Wu *et al.*, 2007; Wu *et al.*, 2006). In addition, the amount of absorbed dose under hypobaric stress was found to be 7-fold higher to that detected upon *in vitro* skin electroporation delivery of a similar molecular weight dextran (Lombry *et al.*, 2000). Conversely, highly invasive methods such as the ablation of the *SC* by argon-fluoride laser were found to be more effective in delivering a 10 kDa dextran through the skin (Fujiwara *et al.*, 2005). It is noteworthy that in some cases this comparison may be over exaggerated due to the absence of skin microcirculation and hence efficient clearance of the drug from the cutaneous tissue in the *in vitro* studies. Nevertheless, hypobaric pressure was shown to be a competitive efficient manner to push macromolecules into the skin.

6.4.3 Cutaneous bioavailability and tissue distribution

At the end of the transport studies, the dorsal skin and organs (heart, bladder, kidneys, liver and spleen) were collected and the amount of ^{14}C labeled 10 kDa dextran was quantified in the different layers of the skin and tissues in order to determine cutaneous bioavailability and organ uptake under differential barometric pressure. The data showed that cutaneous bioavailability was significantly greater ($p < 0.01$) under hypobaric pressure conditions and this effect was more pronounced upon dextran localization in deeper skin tissues. The amount of dextran found in the *SC* and dermal tissue was 4.3 and 5.7-fold higher, respectively (Figure

6.6). The enhanced drug deposition within deeper cutaneous tissues was believed to be due to an increase in blood flow volume that has been previously reported to allow deeper tissue distribution below the site of topical application (Cross *et al*., 1999; Singh and Roberts, 1993; Singh and Roberts, 1996). In addition, the different anatomical configuration of the cutaneous vasculature under differential barometric pressure could have a significant role in the distribution of drugs from the epidermal-dermal interface to deeper cutaneous tissues (Roberts and Cross, 1999). The application of mechanical stress to the skin (ca. 500 mBar) has been shown to result in vertical displacement of dermal blood vessels towards the skin surface (Childers *et al*., 2007). It can be hypothesised that a close proximity of the microvascular network to the epidermal-dermal layer combined with an increase in blood flow volume produced a "convective force" that generated a localized deep tissue mechanism that resulted in a deeper tissue penetration at the site of application, as previously shown by other researchers (Cross and Roberts, 1999; McNeill *et al*., 1992; Monteiro-Riviere *et al*., 1993).

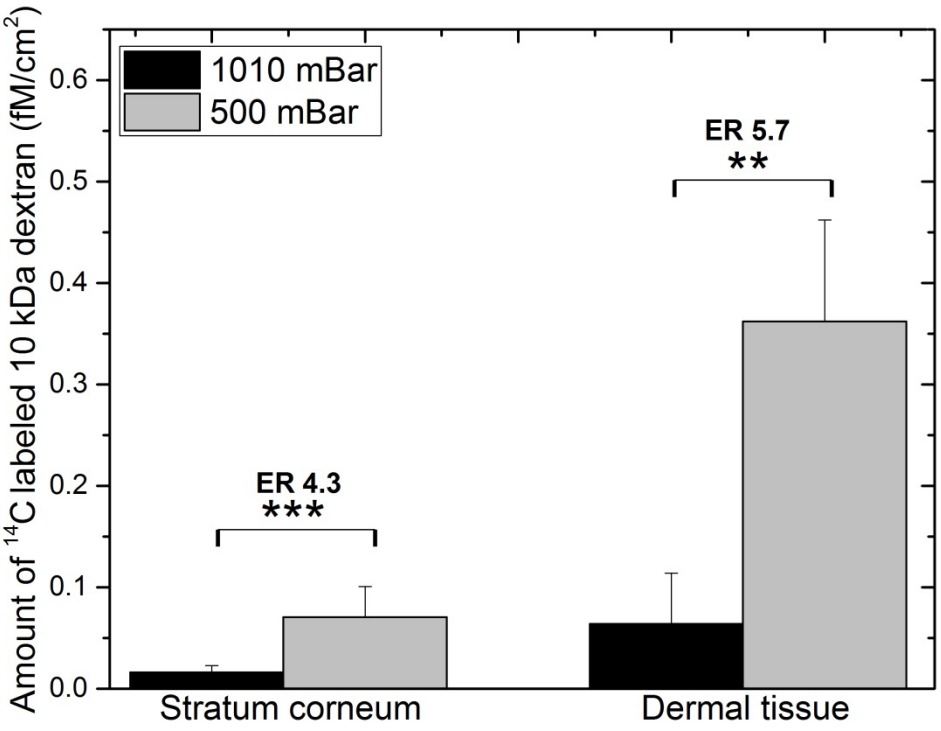

Figure 6.6. *In vivo* profile of ^{14}C labeled 10 kDa dextran cutaneous bioavailability in rat skin layers under atmospheric (1010 mBar) and hypobaric (500 mBar) pressure conditions. Each point represents mean ± standard deviation (n = 5). ER (Enhancement ratio) represents the ratio between the amount of drug found under hypobaric and atmospheric conditions. Students t-test with ** $p < 0.01$, *** $p < 0.001$.

The *in vivo* and *in vitro* cutaneous bioavailability upon hypobaric driven delivery (Section 4.4.2) was compared through the analysis of the percentage of applied dose that reached the different layers of the cutaneous tissue (Figure 6.7). The detected amount of dextran within the *SC* layer corresponded to $5.76 \times 10^{-4} \pm 6.8 \times 10^{-6}$% and $4.9 \times 10^{-3} \pm 2 \times 10^{-3}$% of the applied dose in the *in vitro* and *in vivo* studies, respectively. In addition, the determined amount deposited within the dermal tissue was equivalent to $3.7 \times 10^{-3} \pm 3 \times 10^{-4}$% and 2.5 ×

$10^{-2} \pm 7 \times 10^{-3}$% of the applied dose *in vitro* and *in vivo*, respectively. The *in vivo* cutaneous bioavailability was found to be significantly higher ($p < 0.01$) when compared to that observed *in vitro* (Figure 6.7). It was registered a 9 and 7-fold increase in the amount of drug that was detected in the *SC* and dermal tissue, respectively. This data underpinned again the pivotal role of the cutaneous microcirculation in the diffusion partition process across the skin tissue that was not necessarily captured in traditional *in vitro* excised skin transport studies (Cross and Roberts, 1999; McNeill *et al.*, 1992; Monteiro-Riviere *et al.*, 1993).

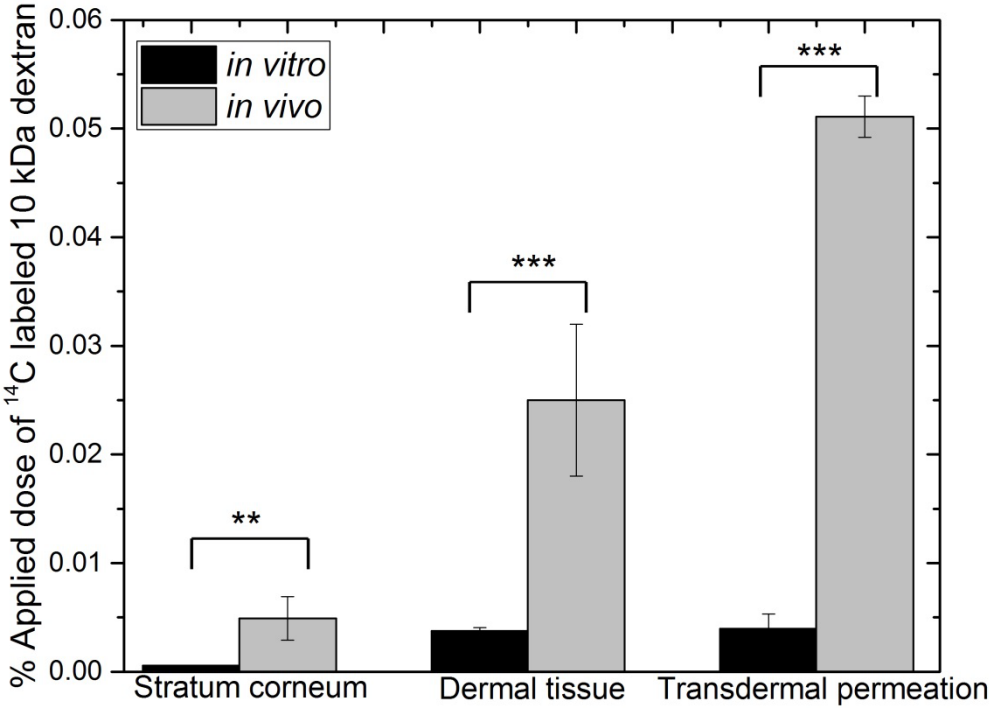

Figure 6.7. *In vitro vs in vivo* profile 10 kDa dextran cutaneous bioavailability in rat skin layers and transdermal permeation under atmospheric (1010 mBar) and hypobaric (500 mBar) pressure conditions. Each point represents mean ± standard deviation ($n = 5$). Students *t*-test with ** $p < 0.01$, *** $p < 0.001$.

Organ uptake of the ^{14}C-labeled 10 kDa dextran following topical delivery is shown in Figure 6.8. The overall biodistribution trend under both barometric conditions was in good agreement. There was a higher accumulation ($p < 0.01$) of the radiolabeled dextran in the heart, bladder and spleen with lower amounts detected in the kidneys and liver. However, a greater tissue uptake ($p < 0.05$) under hypobaric driven delivery was observed in all the collected organs, which was suggested to be attributable to a greater dextran uptake into the systemic circulation due to vasodilatation. A higher dextran systemic level may therefore explain the 64.4-fold increase in the amount found in the heart. The greater amount of dextran detected in the kidneys and bladder ($p < 0.01$) when compared to the low liver uptake under both barometric conditions suggest that the elimination of the 10 kDa dextran is dependent on the renal excretion rather than hepatic accumulation. A minimal dextran accumulation in the liver with a significantly higher ($p < 0.001$) amount detected in the urine following intravenous injection of a 4 kDa dextran has been previously described by Mehvar and his colleagues (1995). It has been reported in the literature that dextrans with a hydrodynamic radius < 2 nm (M.W. < 10 kDa) undergo significant renal clearance due to their ability to permeate through the glomerular wall pores (Chang *et al*., 1975; Chouinard-Pelletier *et al*., 2012). Tissue distribution profile has been demonstrated to be dependent on the chemical structure of a molecule (van de Water *et al*., 2006; Li and Liang, 2010). These findings suggest that dextran chemical stability in this study was not compromised upon topical administration (i.e. presence of cutaneous metabolic systems) under both barometric conditions as demonstrated by the similar tissue uptake to that reported in the literature following intravenous administration of similar molecular weight dextrans.

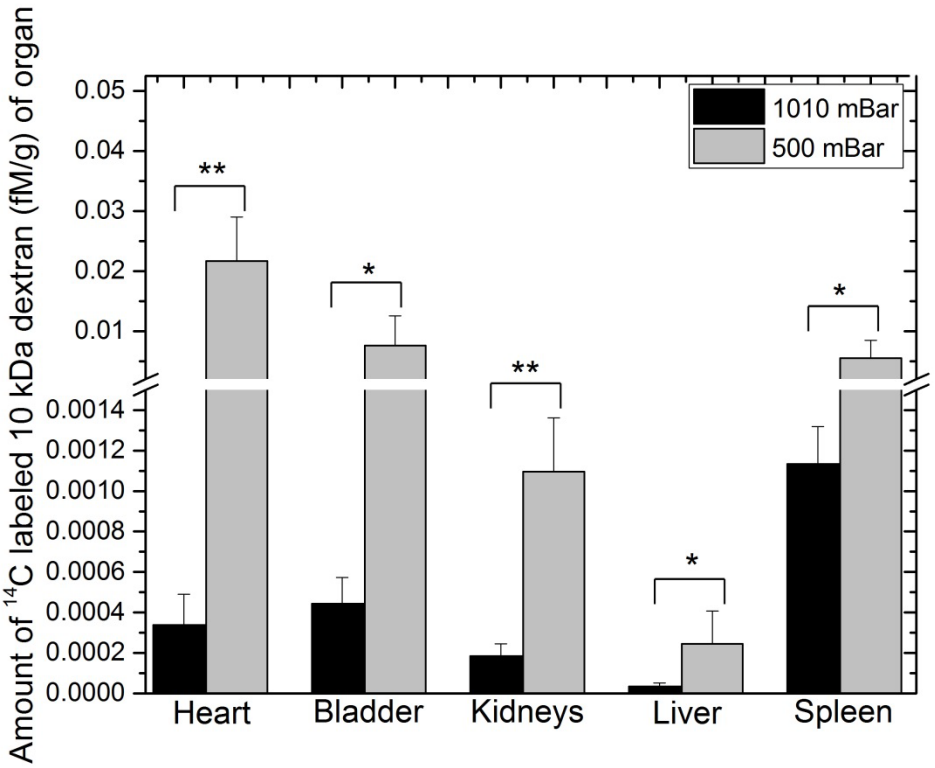

Figure 6.8. Biodistribution of ^{14}C labeled 10 kDa dextran following topical application under atmospheric (1010 mBar) and hypobaric (500 mBar) pressure conditions. Each point represents mean ± standard deviation (n = 5). Students t-test with * $p < 0.05$, ** $p < 0.01$.

6.4.4 Anti-inflammatory assay

Carrageenan-induced paw oedema is a well-established model to evaluate the anti-inflammatory activity of diclofenac (Halici *et al.*, 2007; Manosroi *et al.*, 2008; Moncada *et al.*, 1973). Its pharmacologic action upon topical application is believed to be dependent upon tissue localization rather than a systemic effect (Nair and Taylor-Gjevre, 2010; Reiss *et al.*, 1986; Cross *et al.*, 1998). Therefore, in order to investigate if a greater epidermal localization upon hypobaric driven delivery (Section 5.4.2) would translate in a better anti-inflammatory efficacy; diclofenac diethylamine was presented to the skin as a nanosized aggregated system

(Section 5.3.2.). In addition, to elucidate the possible contribution of the follicular route upon nanosized cutaneous transport the in-house formulated gel was applied in the glabrous (plantar) and non glabrous skin (dorsal).

Intraplantar injection of carrageenan in rats led to a time-dependent increase in paw oedema (Figure 6.9 a, b and c). The oedema was significantly reduced ($p < 0.01$) over the duration of the experiment when diclofenac diethylamine was applied under atmospheric pressure both in glabrous and non glabrous paw skin. On the other hand, significant oedema decrease ($p < 0.001$) was only observed upon 240 min and 180 min when the in house gel was topically applied under hypobaric stress to the glabrous and non glabrous skin, respectively. These findings suggest that a more rapid onset of anti-oedematous effect was achieved upon topical application under atmospheric conditions. To simplify data analysis between topically administration to the glabrous and non glabrous skin under differential barometric pressure, the area under the curve (AUC) of the % increase in paw swelling effect-time curve was calculated by the trapezoidal method (Figure 6.9 d) (Rowland and Tozer, 1995).

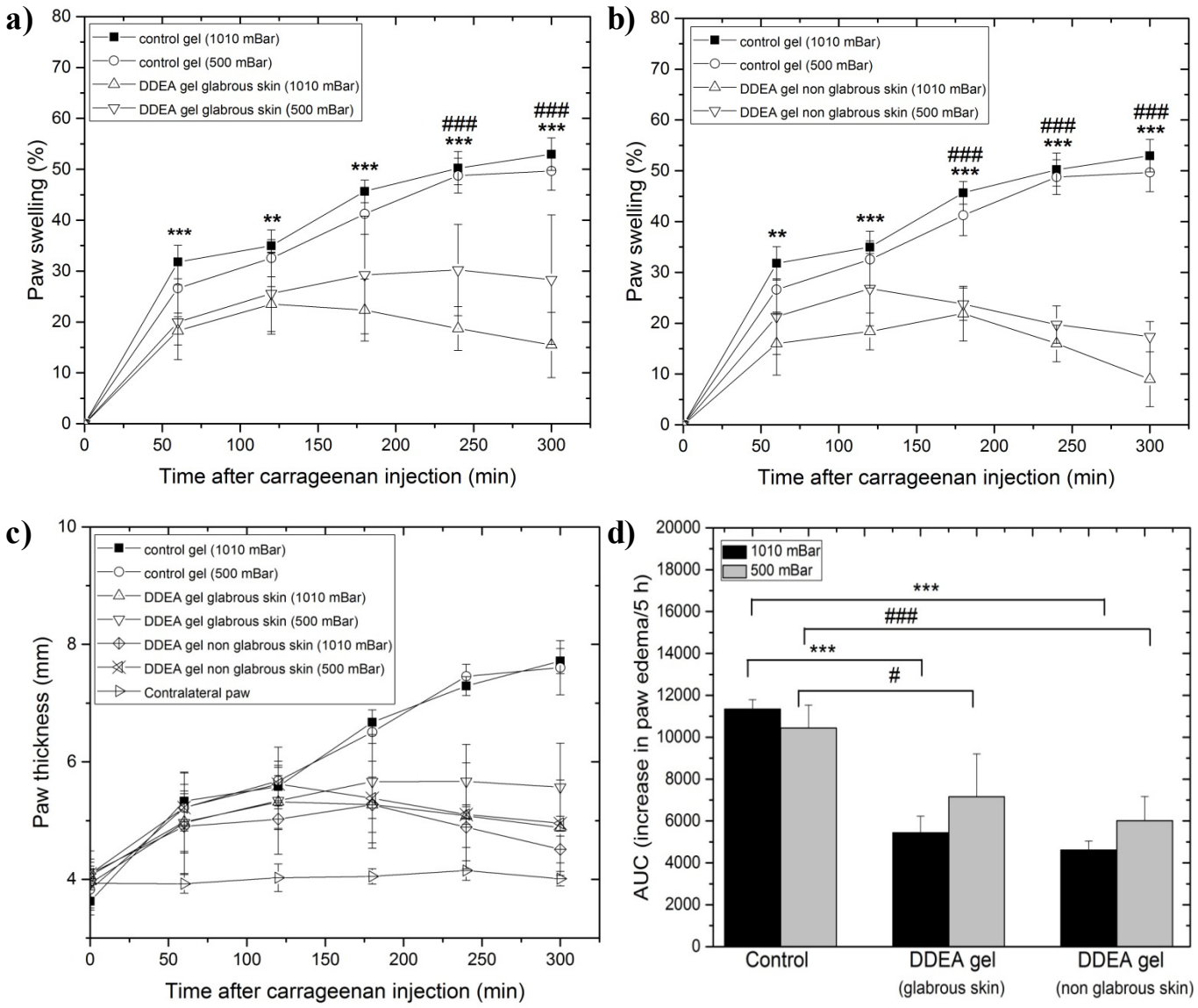

Figure 6.9. Time course for the anti-inflammatory activity of diclofenac diethylamine formulated in a hydroxypropyl methylcellulose gel (43 mM) on rat carrageenan-induced paw oedema under atmospheric (1010 mBar) and hypobaric (500 mBar) pressure conditions. Oedema was measured at 1, 2, 3, 4 and 5 h after the inflammatory challenge on the ipsilateral hind paw and is expressed as mean ± standard deviation (n = 5), a) paw swelling (%) upon topical administration in ipsilateral hind paw glabrous skin, b) paw swelling (%) upon topical administration in ipsilateral hind paw non glabrous skin, c) paw thickness (mm) over the time course of the study, d) area under the curve determined using the trapezoidal rule (arbitrary units). ** $p < 0.01$, *** $p < 0.001$ atmospheric vs control, $^{\#}$ $p < 0.05$, $^{\#\#\#}$ $p < 0.001$ hypobaric vs control (Mann-Whitney U-test or analysis of variance, Bonferroni post-hoc test).

Area under the curve analysis showed that despite of a more rapid onset of action upon topical application at atmospheric conditions, diclofenac diethylamine anti-oedematous effect was statistically equivalent ($p > 0.05$) to that observed under hypobaric stress over the time course of the anti-inflammatory assay when topically applied to both glabrous and non glabrous skin. The results suggest that diclofenac diethylamine had a significant anti-inflammatory effect on carrageenan-induced paw oedema regardless of topical barometric conditions or skin physiology. Edema formation results as a consequence of a synergism between inflammatory mediators that increase vascular permeability and/ or mediators that increase blood flow (Ialenti *et al*., 1995). The data suggest that the cutaneous haemodynamic response to hypobaric stress did not alter the inflammatory process since the increase in paw oedema in the control was not significantly different ($p > 0.05$) throughout the experimental period at both barometric conditions. Although diclofenac diethylamine has been shown to provide a good permeation rate across the skin (Sengupta *et al*., 2015; Fini *et al*., 1999), it was expected that the rate of mass transfer across glabrous skin would be significantly lower when compared to non glabrous skin as was observed in previous studies for other molecules (Prausnitz *et al*., 2012; Jacobi *et al*., 2006). This lack of difference suggests that an excessive dose may have been applied to the skin which could have reduced the assay sensitivity.

6.5 Conclusions

The results presented herein demonstrated the significant role played by the cutaneous microcirculation upon drug localization within the cutaneous tissue and subsequent uptake by the systemic circulation under barometric stress. The haemodynamic response to topical hypobaric pressure led to a significant increase in skin blood flow at the site of hypobaric treatment, which was thought to result in a significant higher dextran cutaneous and systemic

bioavailability. The *in vivo* and *in vitro* data comparison further supported the importance of vasodilatation upon hypobaric driven delivery. The anti-inflammatory study showed that diclofenac diethylamine had a significantly anti-inflammatory effect on carrageenan-induced paw oedema regardless of topical barometric conditions or skin physiology. In conclusion, hypobaric driven delivery was shown to be competitive compared to the most prominent strategies to deliver drugs into the skin. Whereas these systems target the cutaneous tissue by changes in the penetration rate of the agents, the application of hypobaric stress can potentially alter cutaneous drug diffusion paths and blood flow which could represent a compelling prospect as a means to deliver therapeutic agents in medical practice. It may perhaps be more efficient however to use this strategy to enhance the percutaneous penetration of macromolecules rather than small molecular weight drugs.

CHAPTER SEVEN

General discussion

For many therapeutic agents, percutaneous drug delivery presents many advantages when compared to other major routes of administration including oral and parenteral (Guy and Hadgraft, 2003; Williams, 2003; Prausnitz *et al*., 2004; Bronaugh and Maibach, 2005). These include the avoidance of first-pass metabolism, the provision of a drug reservoir that can be removed from the body and the possibility of a convenient and pain free means to provide controlled release of a drug over 24 h from a single application (Joshi and Raje, 2002; Roberts *et al*., 2002). However, drug deliver via the skin has yet to fully achieve its potential as an alternative route when compared to oral and parenteral administration because the selective permeability of the skin only allows relatively small lipophilic molecular weight drugs to penetrate into lower layers (Naik *et al*., 2000; Barry, 1983). As such, the greatest challenge is to widen the range of drugs that can be administered via this route to achieve a clinical relevant dose in the body.

The administration of hydrophilic drugs via the skin has been difficult to achieve and the delivery of peptides, nano-particulate systems and macromolecules, including new genetic treatment employing DNA or small-interfering RNA has posed particular challenges (Prausnitz and Langer, 2008). Nevertheless, a variety of chemical and physical methods have proved successful in delivering large molecules into the cutaneous tissue, but an ideal system has yet to be produced (Arora *et al*., 2008; Prausnitz and Langer, 2008). Many of the challenges related with the strategies already developed are associated with achieving an appropriate balance between safety and cost-effectiveness. Their clinical success can be limited by their lack of reversibility and cost. Moreover, they usually involve the use of cumbersome devices that require the need of trained personnel and hence pose problems regarding patient self-administration and compliance. The application of topical barometric

stress as a strategy to improve percutaneous drug delivery has received little attention and this study wanted to explore this enhancement technology further.

The exposure of humans to barometric changes is becoming more common in the modern world. For example, the modern jet engine operates most efficiently at altitudes above 30 000 ft. The atmospheric pressure outside a commercial aircraft with a flight altitude of 35 000 ft is 3.4 psi (235 mBar), whereas the atmospheric pressure at sea level is 14.7 psi (1010 mBar). A standard aircraft is typically pressurized to maintain a cabin altitude of around 5500 ft and the passengers in this situation would be expose to a hypobaric pressure of 830 mBar. Whilst activities such as deep sea diving and hyperbaric medicine, both of which are becoming more popular, can expose the body to pressures of up to 8000 mBar. Physiological changes in blood circulation and respiration under hyperbaric and hypobaric pressures have been well documented, but the effects on xenobiotic entry into the body have not been systematically investigated. Whole body exposure to barometric pressure changes would be expected to have very different effects to local pressure changes induced by methods such as suction because the latter generates a pressure differential which could draw molecules across the barrier and have less profound effects on whole body physiology.

Local barometric pressure changes at the apical surface of the skin have been previously reported to alter the mechanical and physiological properties of the cutaneous tissue. Topical application of hypobaric pressure generated from a suction cup device has been shown to result in a marked increase in TEWL, disorganization of the intercellular lipid bilayers, rupture of the corneosomes and thinning of the epidermis (Childers *et al.* 2007; Pedersen and Jemec 2006; Rawlings *et al.*, 1995; Leveque *et al.*, 2002). Furthermore, the application of mechanical stress to the skin has been demonstrated to alter cutaneous microcirculation and

orientation of the local vasculature, albeit with conflicting evidence. Whereas a decrease in blood flow has been reported using radioisotope perfusion imaging (Skagen *et al*., 1983; Kairinos *et al*., 2009), a contrary effect was shown when laser Doppler flowmetry was employed to investigate the cutaneous haemodynamic vascular responses to hypobaric stress stimuli (Morykwas *et al*., 1997; Timmers *et al*., 2005). Further, a vertical displacement of the local vasculature towards the skin surface upon the application of a sub-atmospheric of 500 mBar has been previously reported by Childers *et al*., (2001). However, a link between skin changes induced by barometric pressure alteration and xenobiotic percutaneous penetration is less predictable and at the present unknown. As such, the aim of this PhD was to investigate the effects of local barometric pressure changes upon cutaneous drug delivery with a view to understand if such an approach could be used to design a novel medicinal product.

In order to accomplish this aim three relevant agents (tetracaine, diclofenac diethylamine and aciclovir) were selected based upon their different physicochemical properties. This was anticipated to allow a broader understanding of the effects of hypobaric driven delivery by establishing a relationship between the drug characteristics and the diffusion partition behavior through the cutaneous tissue. Thereby, an analytical method for each needed to be established and the transport methodology adapted for the specific application to this work overall aim. HPLC with ultraviolet detection was selected as the method to be implemented for each of the selected actives since their quantification by HPLC was reported to be reproducible, accurate and sensitive (Wang *et al*., 2003; Vemula *et al*., 2013; Boulieu *et al*., 1997). The experimental transport setup was designed to investigate the parameters where tetracaine permeation could be determined under equilibrium conditions that allowed ‘free diffusion’ through the membrane (Section 1.4.2). Three different set of method parameters were optimised 1) the degree of ionization of tetracaine in the donor solution, which was

achieved by tightly controlling the pH of the drug-saturated vehicles, 2) the effect of membrane thickness and 3) the influence of tetracaine donor solution pre-equilibration time. This was considered important to access before designing an optimal method for diffusion testing due to the complex solution state behavior shown by this active (Menon and Norris, 1980; Guerin *et al*., 1980; Umemura *et al*., 1981; Zhang *et al*., 2007).

The three verified HPLC methods for each model agent were shown to be 'fit for purpose', which was underpinned by a sound calibration curve linearity, specificity, repeatability and precision in accordance with ICH guideline recommended values (ICH, 1995). Tetracaine chemical stability assessment showed that tetracaine was prone to hydrolytic degradation in both acidic and basic environments. The analysis of the chromatograms revealed that the verified HPLC method was able to detect tetracaine chemical degradation and this was suggested to be attributable to the formation of p-n–butylaminobenzoic acid in solution as previously described by Menon and Norris, (1980).

Only the permeation data through a 0.25 mm thick silicone membrane was thought to provide a suitable representation of tetracaine permeation behaviour across a hydrophobic controlling barrier. Changing the pH of the delivery vehicle and thus the degree of ionisation of the molecule was found to have a large influence on membrane permeation. A comparison of the steady-state flux from the drug saturated vehicles at pH 4 (predominantly ionised form in solution) and pH 10 (unionised form dominates in solution) demonstrated a better ability of the molecule to cross the barrier when it was presented as a unionised microspecies. This was believed to be due to the different degree of ionisation of tetracaine in the vehicles employed in the permeation studies. The hydrophobic characteristics of the molecule at pH 10 suggested a facilitated drug movement across the lipophilic silicone barrier when compared

to that registered at pH 4, which was in agreement with the pH-partition hypothesis (Shore *et al.*, 1957). Surprisingly, lag time was significantly greater ($p < 0.01$) despite the better diffusion and partition characteristics of the unionised form when compared to that observed at pH 4. In addition, an increase in the application system pre-equilibration time was observed to result in slower drug diffusion through the membrane at pH 4. The data indicated that tetracaine permeation through a confluent barrier could not be explained by Higuchi's equation of mass transport (Section 1.4.1). It was hypothesised that the decrease in permeation with an increase in donor solution pre-equilibration time and the differences in lag time at both pHs was due to drug-drug interactions in solution (Guerin *et al.*, 1980; Umemura *et al.*, 1981). A different molecular arrangement in solution of the drug was thought to alter tetracaine diffusion behavior through the barrier. This initial part of the work provided a suitable testing methodology that was not limited by drug depletion, spent receiver saturation or chemical degradation, which was deemed critical for the assessment of the effects of hypobaric driven delivery upon drug transport permeation. In addition, it demonstrated the importance of molecular aggregation in the transport of tetracaine.

Molecular aggregation in solution was expected to have a significant influence on the pharmacological action of a drug since it can change the passive diffusion process through the cutaneous tissue and hence altering localisation at a receptor site (Schreier *et al.*, 2000; Rossetti *et al.*, 2011; Ueda *et al.*, 2012). This is believed to happen due to intermolecular bonding in solution that generates a cluster of molecules that display different physicochemical properties to their monomeric counterparts (Florence and Attwood, 1998; Potts and Guy, 1995). It was thought that tetracaine self-association could explain the deviation from the Higuchi model of mass transport (Section 1.4.1) observed in the transport methodology development, albeit further investigations were necessary to confirm this

hypothesis. For this purpose, a series of aqueous vehicles where the degree of ionization of both the tertiary and secondary amine was varied were utilised to understand the properties of tetracaine molecular aggregates that may form in topical preparations. These findings were linked to drug passive diffusion through a model synthetic membrane and porcine skin.

The aggregation process was found to be more favourable at increasing pH when only the tertiary amine was protonated (i.e. at pH 9 of the commercially available formulation) whereas drug solutions containing species with some proportion of both the tertiary and secondary amine ionized (i.e. pH 4) displayed a significantly greater ($p < 0.05$) critical aggregation concentration. It should be noted that due to the analytical sensitivity of the assay, critical aggregation values reported in this work could be challenged since the presence of supramolecular structures in solution was only detected when drug aggregates displayed a hydrodynamic radius greater than 2 nm. However, in this case it was assumed that the data collected in this work provided a good indication of tetracaine molecular structure changes in solution. This assumption was supported by comparing the experimentally determined critical aggregation values recorded herein with previous reported literature, which suggested a better analytical sensitivity of light scattering when compared to other analytical methods. A favourable environment for drug-drug interactions was found to result in larger molecular aggregates in solution, which exhibited a zeta potential close to neutrality. This was suggested to be a result of the uncharged drug microspecies being in majority and these species migrating to the surface of the molecule to minimize its surface energy as was observed in previous studies for other molecules (Tanford, 1980; Israelachvili, 1985). This assumption was underpinned by molecular dynamic studies that suggested that upon self-association, the protonated tertiary amine is positioned to the outer region of the supramolecular structure at pH 4 and hence, when a lower proportion of these species were

present at a higher pH it makes sense that the drug aggregates would display lower electrostatic repulsion. Moreover, the appearance of 'new' vibrational bands in the FTIR spectra and NMR spectroscopy data further supported this hypothesis.

The analysis of the permeation data suggested that when tetracaine was presented to the silicone membrane as an aggregated system, drug diffusion behavior was in good agreement with the pH-partition hypothesis (Shore *et al.*, 1957). Wherein, the greater steady-state flux was determined at pH 10 when the unionised fraction accounted for ca. 95% of the total microspecies in solution. Conversely, the highest rate of mass transfer through porcine skin was registered at pH 7.6 when the unionised fraction represented only 9.88% of the tetracaine species in solution. The pH of the delivery vehicle was thought to have a negligible influence on skin permeability (i.e. *SC* isoelectric point 4.8 - 6) since the barrier characteristics of the cutaneous tissue have been previously reported to remain unchanged when exposed to delivery vehicles with pHs between 3.5 and 11 (Thune *et al.*, 1988; Sznitowska *et al.*, 2001; Zatz, 1991). This was believed to be due, at least at some extent, to stronger tetracaine/skin lipid interactions when the unionised species dominated in solution (Zhang *et al.*, 2007), which may have limited percutaneous permeation through the biological membrane. An increase in lag time at higher pHs was surprising and it was thought to be a consequence of the presence of larger and more strongly bonded drug aggregates in the donor solution. It can be hypothesised that large hydrophobic masses (i.e. pH 9 Log D 2.1 ± 0.16; 188 ± 20.4 nm) may have difficulty in passing through or leaving a hydrophobic barrier like a silicone membrane or the skin despite the ability of the individual molecules to partition into the membrane. On the other hand, at lower pHs, the smaller size of the hydrophilic masses (i.e. pH 4 Log D -0.9 ± 0.03; 114 ± 8.3 nm) may result in a facilitated passage across the *SC* and/or through the pores introduced into the skin tissue compared to the basic pHs as

previously reported for other local anaesthetics molecules (Horita *et al.*, 2014). The properties of the supramolecular structures appeared an elegant means to explain the changes in diffusion speed through the controlling barrier at the different delivery vehicle pHs (Figure 7.1). The findings from the study highlight the relevance of the complex drug-drug interactions upon transcutaneous permeation and how this process may change the topical bioavailability of therapeutic agents.

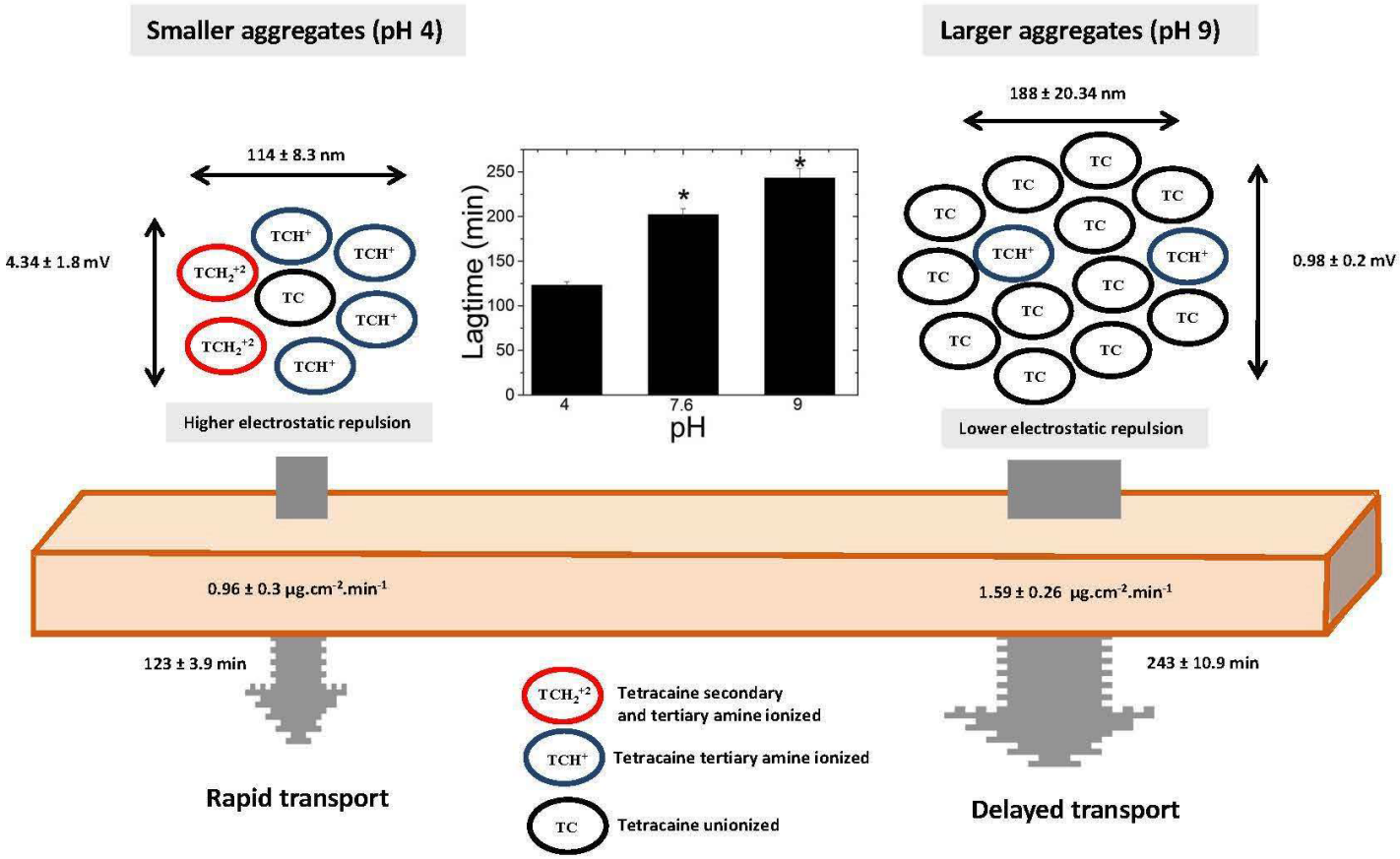

Figure 7.1. Diagram representing the effects of molecular aggregation upon tetracaine skin transport at different pHs. The presence of larger hydrophobic uncharged masses when only the tertiary amine (TCH^+) was ionized (at pH 9 of the commercially available formulation) was coupled with a significantly slower diffusion rate (243 ± 10.9 min) through the controlling barrier. Whereas when both the secondary (TCH_2^{+}) and tertiary amine (TCH^+) where ionized (pH 4) smaller hydrophilic charged masses were shown to diffuse more rapidly through the skin tissue (123 ± 3.9 min) despite a lower rate of mass transport ($p < 0.001$).

The primary focus of this study was to investigate the influence of locally applied hypobaric stress upon drug delivery into the skin. To accomplished this aim, the work adapted one of the most widely used test systems for studying *in vitro* skin permeability, the Franz diffusion cell (Franz, 1975), in order to generate a pressure differential at the apical surface of the skin. It was anticipated that the application of topical hypobaric pressure could potentially reverse the reduction in the permeation of topically applied aggregated systems through changes to the mechanical and morphological properties of the skin. Therefore, the experimental setting previously shown to result in optimal self-assembly configuration of tetracaine and hence allow a rapidly diffusing species available for transport through the skin was employed in the study. It was predicted that the balance between the ionic form (TCH^+) and non ionised form of the drug (TC) at pH 7.6 allowed the molecule to pass into the skin via the transcellular, intercellular and follicular route, thus any changes in these routes induced by local barometric stress could potentially be picked up using tetracaine as the test species. Drug movement across the skin under hypobaric driven delivery was understood by relating the changes in the mechanical and morphological properties of the hypobaric stressed skin and the cutaneous deposition profile of tetracaine.

The in-house designed pressure cell system was shown to be 'fit for purpose'. The transport method limited data collection to a single time point and hence, other permeation parameters such as lag time and steady-state flux could not be derived from the experimental data. However, knowledge that tetracaine established steady-state transport through the skin after 1h and that its diffusion process was linear for up to 7 h, strengthened the findings presented from this method. The use of the adapted cell demonstrated that topical application of hypobaric pressure improved drug delivery into the skin in the presence of the nanosized aggregates and this resulted in a significantly increase in cutaneous bioavailability ($p <$

0.001). Furthermore, drug deposition within the epidermis was found to be proportional higher to that found in the *SC* and dermal tissue (25.6-fold vs 8.8 and 9.9-fold increase, respectively). In addition, tetracaine transdermal permeation was improved when hypobaric stress was applied to the skin; however with proportionally lower levels of drug crossing all the way through the barrier (4-fold higher) when compared to the amount retained within the cutaneous tissue.

The mechanical and morphological changes in the hypobaric stressed skin suggested that the 'targeted' tetracaine deposition to the epidermal layer was driven by the enlargement of the follicular infundibula ($p < 0.001$), reduced corneocyte size ($p < 0.001$) and skin thinning ($p < 0.05$). The data suggested that an improved follicular transport and/or a facilitated transcellular and intercellular drug diffusion could be possible causes of the enhanced cutaneous bioavailability. Although, it was thought that the intercellular pathway could not be accessed by the tetracaine supramolecular structures (156.5 ± 15.5 nm) formed in the aggregated drug solutions used to administer the active, since the lateral and vertical gaps between porcine corneocytes have been previously reported to be ca. 19 nm (van der Merwe *et al*., 2006). The nanosized aggregate systems could have passed into the skin tissue by the follicular pathway. This was further supported by fluorescence micrograph pictures that revealed that the penetration of dextran nanosized molecules (4 kDa (0.45 nm); 10 kDa (1.9 nm)) into the hypobaric stressed skin resulted in a greater fluorescence signal around the perifollicular area, which suggested that hypobaric treatment affects the performance of the hair follicles and hence increased drug transport into the tissue. It is important to note that due to the size of the molecular aggregates, drug transport via other pores introduced into the skin tissue (i.e. sebaceous and sweat glands) may also provide an effective means to circumvent the formidable barrier posed by the *SC*. However, these structures were difficult

to visualise by fluorescence spectroscopy and hence their contribution to drug transport under hypobaric stress is at the present less clear and therefore should be investigated in further studies.

One of the main challenges when developing new means to deliver drugs into the cutaneous tissue is the conservation of the skin's barrier function upon treatment; hence skin integrity and the reversibility of any damage should be one of the primary concerns during this process. Histological and morphological studies indicated that the enhanced topical bioavailability of nanosized drug aggregates and macromolecules was accompanied by reversible changes in the mechanical properties of the skin and that the *SC* remained intact upon hypobaric treatment. This was considered to be the major advantage of this means to enhance xenobiotic penetration into the tissue compared to technologies such as laser ablation and tape stripping of the *SC*.

Once mechanical stress was shown to be effective in delivering both small and large molecules into the skin, it was thought important to investigate how a drug's physicochemical properties influenced the skin tissue distribution upon hypobaric driven delivery. In order to achieve this aim three model agents (tetracaine, diclofenac diethylamine and aciclovir) were formulated in a gel preparation in an aggregated/non aggregated state. The physicochemical characteristics of the drug aggregates and monomeric species was then related to their ability to diffuse through the hypobaric stressed skin.

The penetration and permeation profile of the three drugs when it was thought that only the monomeric species was applied to the skin was found to be statistically equivalent ($p > 0.05$) under atmospheric and hypobaric pressure conditions. However, when topically applied as an

aggregated system, hypobaric driven delivery altered the cutaneous bioavailability of each active, albeit at a different extent. This provided a strong basis to suggest that barometric delivery was mainly functioning via the opening of the follicular transport route. Hypobaric driven delivery seemed to have an effect of 'targeting' diclofenac diethylamine and aciclovir within the epidermal tissue and this effect was most significant for diclofenac diethylamine then aciclovir. The calculated epidermal 'targeting' was found to be 4 and 1.4 for each model agent respectively, when considering the drug levels in the different layers of the tissue. Interestingly, the transdermal permeation followed the opposite trend in terms of the three compounds with highest amounts of tetracaine reaching the receptor compartment when compared to that registered for aciclovir and diclofenac diethylamine (8.9 vs 2.7 and 2.4-fold increase in drug permeation, respectively).

These results might be attributable to the different physicochemical characteristics of each active in the delivering vehicle employed in the transport studies. The hydrophilic characteristics of the diclofenac diethylamine (Log D 0.58 ± 0.06) and aciclovir (Log D -1.65 ± 0.3) supramolecular structures would make them more susceptible to pass into the epidermis via the follicular route, whereas the lipophilic tetracaine molecular aggregates (Log D 2.1 ± 0.16) may interact with the lipid matrix surrounding the corneocytes and/or the lipid components of the follicular epithelium (Meidan, 2010; Huang *et al.*, 2005; Williams, 2003; Hadgraft *et al.*, 1998). It was hypothesised that the smaller and charged diclofenac diethylamine molecular aggregates allowed drug movement into the hydrophilic interfollicular epidermis most readily, as previously reported for nanosized compounds with a similar size (Rancan *et al.*, 2009; Vogt *et al.*, 2006), which resulted in a higher epidermal drug localisation upon hypobaric driven delivery (Figure 7.2). On the other hand, the size of the aciclovir and tetracaine drug aggregates might limit, at least at some extent, perifollicular

diffusion into the epidermal tissue. This could have resulted in drug transport through the follicular structures directly into the dermis with subsequent diffusion across this layer, which may explain the greater transdermal permeation of these actives (Figure 7.2). It is important to note that other factors such as cutaneous drug metabolism and binding to cellular components of the epidermal tissue (Liu *et al.*, 1991; Hikima *et al.*, 2002; Roberts *et al.*, 2005) may have limited diclofenac diethylamine permeation into the underlying dermal tissue and therefore contribute to the epidermal residence of this agent under hypobaric driven delivery.

The effect of the commercial product composition upon topical bioavailability was considered important to determine since the excipients added to a formulation play a major role in determining the rate of uptake, penetration, and residence of therapeutic agents through the skin (Idson, 1983). Therefore, it was of interest to assess the manner the formulation composition influenced the effects of hypobaric stress on drug transport. The presence of excipients known to alter drug/skin/vehicle interactions was shown to have a significant effect upon cutaneous bioavailability under hypobaric stress. For example, the epidermal localization of diclofenac diethylamine following topical application of the commercial product was proportionally lower to that obtained from the in-house formulated gel. This was suggested to be attributable to the use of propylene glycol in the Voltarol emulgel® preparation. Propylene glycol may have interacted with water molecules and/or created a less favourable environment for drug-drug interaction in the delivery vehicle (Squillante *et al.*, 1998; Trottet *et al.*, 2004; Miller *et al.*, 1993; Shigeta *et al.*, 2000; Benaouda *et al.*, 2012) and hence reducing the amount of diclofenac permeation species able permeate into the skin via the follicular route. This again highlighted the role of the drug

aggregates and suggested this enhancement technique was best employed with macromolecules.

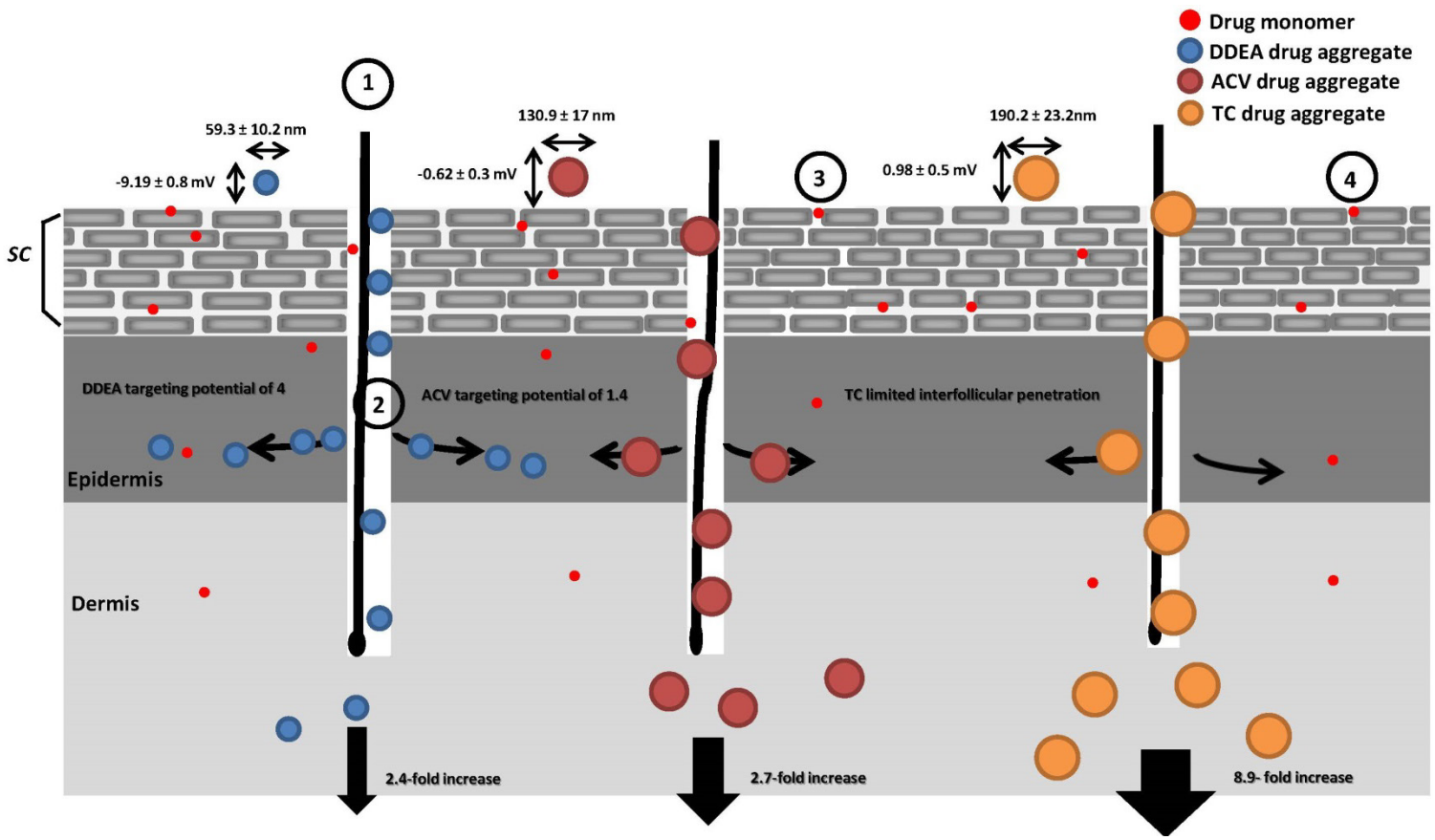

Figure 7.2. Diagram representing the postulated mechanism of diclofenac diethylamine (DDEA), aciclovir (ACV) and tetracaine (TC) enhanced topical bioavailability when administered as an aggregated system under hypobaric pressure conditions. A higher DDEA epidermal 'targeting' potential was thought to result from a greater transport of the aggregated species through the follicular route (1) followed by drug diffusion into the perifollicular epidermis (2). A greater TC and ACV transdermal permeation was thought to result from a facilitated follicular route (1) which led to drug transport directly into the dermis. It was believed that the intercellular (3) and transcellular (4) routes were mainly accessed by the monomeric species since drug aggregate diffusion via these pathways was limited by the size of the supramolecular structures. SC, *stratum corneum*.

The 10 kDa dextran was selected as the model compound for the *in vivo* transport studies since this allowed a greater understanding of the effects of the local vasculature upon skin permeation of a nanosized structure (10 kDa dextran has a reported size of 1.9 nm (Chouinard-Pelletier *et al.*, 2012)). In addition, the activity of diclofenac diethylamine, the agent best localised in the epidermal tissue, was evaluated under differential barometric pressure in a rat carrageenan-induced paw oedema to assess if the epidermal localization upon *in vitro* hypobaric driven delivery would translate in an improved anti-inflammatory efficacy. These *in vivo* studies were considered important because the effects of the changes in cutaneous microvascular flow could be combined with the changes in skin penetration profile caused by hypobaric pressure.

The application of sub-atmospheric pressure induced a haemodynamic response which was significantly greater ($p < 0.001$) compared to atmospheric conditions. This change in skin blood flow in combination with the opening of the follicular structures resulted in an improved transdermal bioavailability upon hypobaric treatment (Figure 7.3). The pharmacokinetic profile suggested that the transdermal delivery was only enhanced during topical application of mechanical stress and it was reversible upon re-establishment of atmospheric conditions at the surface of the skin. The higher dextran systemic levels resulted in a greater tissue uptake ($p < 0.05$) in the collected organs (Figure 7.3). The biodistribution data suggest that topical delivery did not compromise dextran chemical stability as it mimicked organ uptake following intravenous administration of a similar molecular weight dextran (Chang *et al.*, 1975; Chouinard-Pelletier *et al.*, 2012). In addition, cutaneous tissue availability was found to be statistically greater ($p < 0.01$) under hypobaric pressure conditions with proportionally higher amounts of drug found in deeper skin tissues (Figure 7.3). It can be hypothesised that a different organization of the local vasculature network

under hypobaric stress with concomitant increase in blood flow allowed deeper tissue distribution below the site of topical application as previously reported by other researchers (Cross *et al.*, 1999; Singh and Roberts, 1993; Singh and Roberts, 1996). Evidence that the changes in local blood flow induced by barometric stress had a role to play in the enhanced percutaneous delivery under hypobaric pressure was provided by an *in vitro-in vivo* data comparison. The presence of the cutaneous microvascular flow resulted in a 13-fold increase in the amount of dextran that was able to cross all the way through the cutaneous tissue. Moreover, it was registered a 9 and 7-fold increase in the amount of drug that was detected in the *SC* and dermal tissue, respectively. It is important to note that changes in tissue integrity could have occurred between *in vitro* and *in vivo* assays and hence histological examinations of *in vivo* hypobaric stressed skin should be conducted in further studies.

The diclofenac diethylamine anti-inflammatory assay that utilised a carrageenan-induced paw oedema model employed two different experimental settings in order to establish if the follicular route did have an influence upon diclofenac drug aggregates cutaneous transport. It was expected that due to the absence of follicular structures and lower permeability of the glabrous skin this would result in a lower anti-oedematous efficacy. However, the data suggest that diclofenac diethylamine was effective in reducing oedema formation over the experimental period regardless of topical barometric conditions or skin physiology. It can be hypothesised that the maximum therapeutic effect was achieved at the drug concentration used in this work. There was not the time or resources to tailor the applied dose to optimise the model. It is therefore suggested that lower concentrations of the drug should be employed to further these investigations.

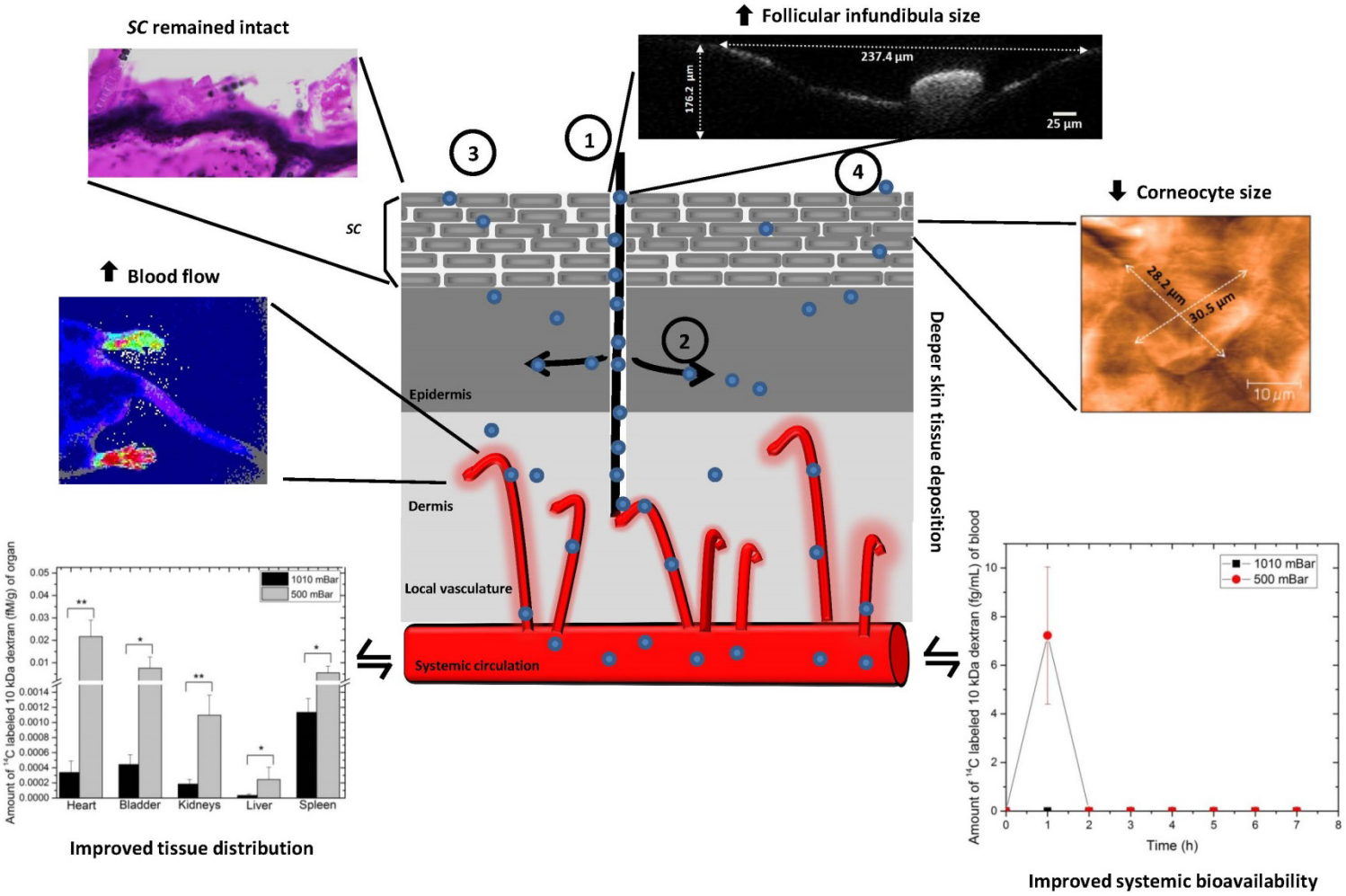

Figure 7.3. Diagram representing the effects of topical hypobaric stress upon skin barrier properties and local vasculature. An enhanced cutaneous and systemic bioavailability of 10 kDa dextran with concomitant improvement in tissue distribution under hypobaric pressure conditions (500 mBar) was coupled with an increase in skin blood flow and facilitated cutaneous drug diffusion paths. An enhanced follicular transport (1 and 2) into the epidermal and dermal tissue was thought to be the main pathway for drug entry into the cutaneous tissue rather than intercellular (3) and transcellular (4) diffusion. SC, *stratum corneum*.

The data obtained from the PhD suggested that hypobaric driven delivery was an effective means to enhance percutaneous penetration. In addition, the data generated suggested that hypobaric stress was competitive with some of the most prominent alternatives (e.g. iontophoresis and electroporation). Whereas the clinical success of such approaches is usually restricted due to the disruption of the mechanical integrity of the skin, the application of hypobaric pressure was shown to only induce reversible effects and hence it may potentially represent a cost-effective means of delivering therapeutic agents in medical practise. However, clinical application will be dependent upon the ability of such a novel means to deliver relevant drug dose levels to human skin that are able to exert a topical and/or systemic pharmacological effect. It is important to note that both animal membranes employed in this project display different anatomical and morphological characteristics to that of human cutaneous tissue (e.g. larger diameter of the follicular opening in porcine skin and greater hair follicle density in rat skin) and hence drug transport upon the application of hypobaric stress may be over exaggerated in the studies presented herein. Therefore, further investigations employing human skin and using a wide range of hypobaric treatment doses would be valuable in order to find the optimal conditions for increasing permeation in medical practise. In addition, the use of other skin sources with varied hair follicle density (e.g. hairless rat skin and rabbit skin) may be useful to understand in greater detail the contribution of the follicular pathway upon hypobaric driven delivery.

In the first part of the project it was demonstrated that molecular aggregation could modify the rate of mass transport through the skin and hence change the topical bioavailability of therapeutic agents. The data suggested that the presence of tetracaine unionized microspecies in the delivery vehicle led to the formation of larger supramolecular structures that resulted in a delayed diffusion through the skin. It can be hypothesised that this could be one possible

reason that may contribute to tetracaine slow onset of topical anaesthesia when using the commercially available formulation (Ametop®). Therefore, it is proposed that a compromise between aggregate formation and the permeation rate for this molecule is required or a strategy to modulate this process should be sought to improve its clinical efficiency. This work is of particular relevance since the concept of optimising drug delivery to the skin by controlling drug aggregation has received little attention to date. Nevertheless, drug-drug interactions are known to occur in topical pharmaceutical preparations intended to be administered to the skin (Walters, 2002) and a large majority of pharmaceutical active compounds display amphiphilic properties that can lead to molecular aggregation (Berge *et al.*, 1977). It is therefore suggested that this process should be studied while developing topical pharmaceutical preparations and the feasibility of adding compounds known to modulate drug aggregation such as electrolytes (Attwood and Udeala, 1975), surfactants (Rossetti *et al.*, 2011; Shao *et al.*, 1993) or polymers (Pygall *et al.*, 2011) to the delivery vehicle should be investigated in greater detail.

In the later part of the study, the application of topical hypobaric treatment has been demonstrated to improve the delivery of large molecules to the skin. The delivery of peptides, proteins and antigens via the skin is an attractive proposal when considering the treatment and prevention of diseases (Glen *et al.*, 2000). The findings from this part of the project could have a significant clinical impact in the treatment of chronic diseases, such as diabetes, osteoporosis and growth hormone deficiency. The glycaemic control required to attenuate associated complications of diabetes mellitus often involves several daily subcutaneous injections of peptides such as insulin (5.8 kDa) or enenatide (4.1 kDa) that can result in poor patient compliance (Shivanand, 2010). The required daily dose of exenatide (10 μg) compares to the transdermal permeation of the 4 kDa dextran reported herein whilst insulin

recommended systemic levels (272 ug) are considerably greater (Section 4.4.2). Likewise, parathyroid hormone (9.4 kDa) recommended systemic therapeutic levels (40 μg) for the treatment of osteoporosis are significantly higher compared to the transdermal permeation of a 10 kDa dextran registered in this study (Section 4.4.2). However, the development of a patch based formulation that can operate under differential barometric pressure may obviate this problem due to avoidance of peptide gastrointestinal degradation and first pass metabolism as reported elsewhere (Bastaki, 2005). In addition, an increased surface area available for drug diffusion and duration of hypobaric treatment might result in improved therapeutic systemic levels. Moreover, a patch-based formulation provides a needle free alternative that could improve patient adherence and compliance. It is anticipated that patient control over hypobaric treatment dose could result in a modulated rate of delivery which could be beneficial in glycaemic control. Other applications are also feasible, such as the topical delivery of human growth hormone (22 kDa), but further investigations using higher molecular weight dextrans would be needed in order to examine "cut-off" value of these technology.

Vaccine delivery via the skin is a very attractive approach because it targets the cutaneous antigen-presenting cells (APCs) that may generate a strong immune response at much lower doses when compared to deeper injection (Prausnitz and Langer, 2008). It has been reported that cutaneous vaccination can allow antigen dilution up to one fifth and hence may provide the possibility to reduce vaccine cost (Nasir, 2008) and increase availability (Nel *et al*., 2006). However, designing a cost-effective product to deliver a vaccine to the cutaneous tissue remains a challenge. There have been a number of devices engineered to deliver vaccines, but these tend to be costly due to the complexities of depositing large molecules to the skin. Recently, trans-follicular vaccination has been shown to be a promising approach to

vaccine delivery (Mittal *et al*., 2013; Mittal *et al*., 2015; Combadiere *et al*., 2010; Baleeiro *et al*., 2013). The main aim of such a technology is to deliver antigens to the abundant perifollicular APCs without compromising the *SC* barrier function (Fan *et al*, 1999). Nanosized systems have been shown to be ideal vehicles for trans-follicular delivery, since they preferentially accumulate and penetrate deeper into hair follicles than conventional formulations (Lademann *et al*., 2015). Some experiments suggest that vaccination via this route may favor a $CD8^+$ preferred response which would be appealing for developing vaccines against intracellular pathogens, cancer or virus infection (Combadiere *et al*., 2010). Thereby, a facilitated follicular route of nanosized compounds under hypobaric driven delivery could represent a compelling prospect as a novel means do induce skin vaccination. It is anticipated that the possibility of administering hypobaric driven vaccine patches by minimally trained personnel or patients themselves could not only facilitate compliance but also eliminate the risks involved with the use of hypodermic needles (Prausnitz and Langer, 2008). In addition, such a novel means could become a simple, low-cost solution to the current challenges to transdermal vaccination.

This research project has examined the potential of hypobaric driven delivery as a means to enhance percutaneous delivery of therapeutic agents. It was shown that hypobaric stress significantly improved the delivery of large molecules into the skin. The assessment of the mechanical and physiologic properties of hypobaric stressed skin not only provided a better understanding of the effects of topical mechanical stress upon the local vasculature and cutaneous diffusion paths but also allowed to gain a mechanistic insight into the contribution of such processes upon hypobaric driven delivery. The findings from this project could assist in the development of a novel pressure induced transdermal patch that could potentially be applied for the treatment of chronic diseases and for vaccine delivery.

8.References

Abraham, M.H.; Martins, F. and Mitchell, R.C. Algorithms for skin permeability using hydrogen bond descriptors: The problem of steroids. Journal of Pharmacy and Pharmacology. 49 (1997), 858-865.

Aguilar, G.; Svaasand, L.O. and Nelson, J.S. Effects of hypobaric pressure on human skin: feasibility study for port wine stain laser therapy (part I). Lasers in Surgery and Medicine. 36 (2005), 124-129.

Akrill, P.; Cocker, J. and Dixon, S. Dermal exposure to aqueous solutions of N-methyl pyrrolidone. Toxicology Letters. 134 (2002), 265–269.

Alderighi, L.; Gans, P.; Ienco, A.; Peters, D.; Sabatini, A. and Vacca, A. Hyperquad simulation and speciation (HySS): a utility program for the investigation of equilibria involving soluble and partially soluble species. Coordination Chemistry Reviews. 184 (1999), 311-318.

Al-Jamal, W.T.; Al-Ahmady, Z.S. and Kostarelos, K. Pharmacokinetics and tissue distribution of temperature-sensitive liposomal doxorubicin in tumor-bearing mice triggered with mild hyperthermia. Biomaterials. 33 (2012), 4608-4617.

Al-Otaibi, F., Ghazaly, E., Johnston, A. and Perrett, D. Development of HPLC-UV method for rapid and sensitive analysis of topically applied tetracaine: its comparison with a CZE method. Biomedical Chromatography. 28 (2014), 826-830.

Al-Otaibi, F.; Tucker, A.T.; Johnston, A. and Perrett, D. Rapid analysis of tetracaine for a tape stripping pharmacokinetic study using short-end capillary electrophoresis. Biomedical Chromatography. 23 (2008) 488-491.

Alvarez-Román, R.; Naik, A.; Kalia, Y.N.; Guy, R.H. and Fessi, H. Skin penetration and distribution of polymeric nanoparticles. Journal of Controlled Release. 99 (2004), 53–62.

Andrade, A.L.; Melich, K. and Karpen, J. Cyclic nucleotide-gated channel block by hydrolysis-resistant tetracaine derivatives. Journal of Medicinal Chemistry. 54 (2011), 4904-4912.

Anissimov, Y.G. and Roberts, M.S. Diffusion modelling of percutaneous absorption kinetics. Effects of flow rate, receptor sampling rate, and viable epidermal resistance for a constant donor concentration. Journal of Pharmaceutical Science. 88 (1999), 1201-1209.

Argenta, D.F.; Mattos, C.B.; Misturini, F.D.; Koester, L.S.; Bassani, V.L.; Simões, C.M.O. and Teixeira, H.F. Factorial design applied to the optimization of lipid composition of topical antiherpetic nanoemulsions containing isoflavone genistein. International Journal of Nanomedicine. 9 (2014), 4737–4747.

Arora, A.; Prausnitz, M.R. and Mitragotri, S. Micro-scale devices for transdermal drug delivery. International Journal of Pharmaceutics. 364 (2008), 227-236.

Attwood, D. and Udeala, O. Aggregation of antihistamines in aqueous solution. Self-association of some pyridine derivatives. The Journal of Physical Chemistry. 79 (1975), 889-892.

Aungst, B.J.; Blake, J.A. and Hussain, M.A. Contributions of drug solubilization, partitioning, barrier disruption, and solvent permeation to the enhancement of skin permeation of various compounds with fatty-acids and amines. Pharmaceutical Research. 7, (1990) 712-718.

Ayub, A.C.; Gomes, A.D.M.; Lima, M.V.C.; Vianna-Soares, C.D. and Ferreira, L.A.M. Topical Delivery of Fluconazole: in vitro skin penetration and permeation using emulsions as dosage forms. Drug Development and Industrial Pharmacy. 33 (2007), 273-280.

Babiuk, S.; Baca-Estrada, M.; Babiuk, L.A.; Ewen, C. and Foldvari, M. Cutaneous vaccination: the skin as an immunologically active tissue and the challenge of antigen delivery. Journal of Controlled Release. 66 (2000), 199-214.

Baisch, F.; Beck, L.; Blomqvist, G.; Wolfram, G.; Drescher, J.; Rome, J.L. and Drummer, C. Cardiovascular response to lower body negative pressure stimulation before, during, and after space flight. European Journal of Clinical Investigation. 30 (2000), 1055-1065.

Baleeiro, R.B.; Wiesmuller, K-H.H.; Reiter, Y.; Baude, B.; Dähne, L.; Patzelt, A.; Lademann, J.; Barbuto, J.A. and Walden, P. Topical vaccination with functionalized particles targeting dendritic cells. Journal of Investigative Dermatology. 133 (2013), 1933–1941.

Banga, A.K. Electrically-assisted transdermal and topical drug delivery. London: Taylor & Francis, 1998.

Banga, A.K. Transdermal and intradermal delivery of therapeutic agents: application of physical technologies. Boca Raton, FL: CRC Press, 2011.

Bangaru, R.; Bansal, Y.; Rao, A. and Gandhi, T. Rapid, simple and sensitive high-performance liquid chromatographic method for detection and determination of acyclovir in human plasma and its use in bioavailability studies. Journal of Chromatography B. 739 (2000), 231-237.

Barratt, M.D. Quantitative structure-activity relationships for skin permeability. Toxicology In Vitro. 9 (1995), 27-37.

Barry, B.W. Topical formulations. Churchill Livingstone, New York, 1988.

Barry, B.W. Dermatological formulations percutaneous absorption. Marcel Dekker, New York, 1983.

Barry, B.W. Mode of action of penetration enhancers in human skin. Journal of Controlled Release. 6 (1987), 85-97.

Barry, B.W. Transdermal drug delivery. Churchill Livingstone, London, 2007.

Barry, B. W. and Woodford, R. Proprietary hydrocortisone creams - vasoconstrictor activities and bio-availabilities of 6 preparations. British Journal of Dermatology. 95 (1976), 423-425.

Basavaiah, K.; Prameela, H.C. and Chandrashekar, U. Simple high-performance liquid chromatographic method for the determination of acyclovir in pharmaceuticals. Il Farmaco. 58 (2003), 1301-1306.

Bastaki, S. Diabetes mellitus and its treatment. Journal of Diabetes and Metabolism. 13 (2005), 111–134.

Batheja, P.; Thakur, R. and Michniak, B. Transdermal iontophoresis. Expert Opinion Drug Delivery. 3 (2006), 127-38.

Bazzoni, G. and Dejana, E. Keratinocyte junctions and the epidermal barrier: how to make a skin-tight dress. Journal of Cell Biology. 156 (2002), 947-949.

Bebawy, L. Stability-indicating method for the determination of meloxicam and tetracaine hydrochloride in the presence of their degradation products. Spectroscopy Letters. 31 (1998), 797-820.

Beerens, E.G.J.; Slot, J.W. and van der Leun, J.C. Rapid regeneration of the dermal-epidermal junction after partial separation by vacuum: an electron microscopy study. Journal of Investigative Dermatology. 65 (1975), 513-521.

Benaouda, F.; Brown, M.B.; Shah, B.; Martin, G.P. and Jones, S.A. The influence of self-assembling supramolecular structures on the passive membrane transport of ion-paired molecules. International Journal of Pharmaceutics. 439 (2012), 434-441.

Benson, H.E. Transdermal drug delivery: Penetration enhancement techniques. Current Drug Delivery. 2 (2005), 23-33.

Berge, S.M.; Bighley, L.D. and Monkhouse, D.C. Pharmaceutical salts. Journal of Pharmaceutical Sciences. 66 (1977), 1-19.

Bhatt, V.D.; Soman, R.S.; Miller, M.A. and Kasting, G.B. Permeation of tecnazene through human skin in vitro as assessed by HS-SPME and GC-MS. Environmental Science and Technology. 42 (2008), 6587-6592.

Bilal, Y.; Asci, A. and Palabiyik, S. HPLC method for determination of diclofenac in human plasma and its application to a pharmacokinetic study in turkey. Journal of Chromatography Science. 49 (2011), 422-427.

Blank, I.B; Moloney, J.; Alfred, G.E.; Simon, I. and Charles, A. The diffusion of water across the stratum corneum as a function of its water content. The Journal of Investigative Dermatology. 82 (1984), 188-194.

Borenstein, M.R.; Xue, Y.; Cooper, S. and Tzeng, T.B. Sensitive capillary gas chromatographic mass spectrometric selected ion monitoring method for the determination of diclofenac concentrations in human plasma. Journal of Chromatography. 685 (1996), 59-66.

Borgquist, O.; Ingemansson, R. and Malmsjo, M. Wound edge microvascular blood flow during negative-pressure wound therapy: examining the effects of pressures from –10 to –175 mmHg. Plastic Reconstructive Surgery. 125 (2010), 502–509.

Bos, J.D. and Meinardi, M.M.H.M. The 500 Dalton rule for the skin penetration of chemical compounds and drugs. Experimental Dermatology. 9 (2000), 165-169.

Boulieu, R.; Gallant, C. and Silberstein, N. Determination of acyclovir in human plasma by high-performance liquid chromatography. Journal of Chromatography B. 693 (1997), 233-236.

Boutsiouki, P.; Thompson, J.P. and Clough, G.F. Effects of local blood flow on the percutaneous absorption of the organophosphorus compound malathion: a microdialysis study in man. Archives of Toxicology. 75 (2001), 321-328.

Bouwstra, J.A.; Honeywell-Nguyen, P.L.; Gooris, G.S. and Ponec, M. Structure of the skin barrier and its modulation by vesicular formulations. Progress in Lipid Research. 42 (2003), 1-36.

Bouwstra, J.A.; Thewalt, J.; Gooris, G.S. and Kitson, N. A model membrane approach to the epidermal permeability barrier: an X-ray diffraction study. Biochemistry. 36 (1997), 7717-7725.

Brain, K.R.; Walters, K.A. and Watkinson. A.C. Methods for studying percutaneous absorption. Marcel Dekker, New York, 2002.

Brand, G.; Schiavano, G.F.; Balestra, E.; Tavazzi, B.; Perno, C.F. and Magnani, M. The potency of acyclovir can be markedly different in different cell types. Life Sciences. 69 (2001), 1285-1290.

Brandner, J.M.; Kief, S.; Wladykowski, E.; Houdek, P. and Moll, L. Tight junction proteins in the skin. Skin Pharmacology and Physiology. 19 (2006), 71-77.

Braveman, I.M.; Keh, A. and Goldminz, D. Correlation of laser Doppler wave patterns with underlying microvascular anatomy. Journal of Investigative Dermatology. 95 (1990), 283-286.

Bronaugh. A. Methods for in vitro percutaneous absorption studies II. Animal models for human skin. Toxicology and Applied Pharmacology. 62 (1982), 481-488.

Bronaugh, R.L. and Franz, T.J. Vehicle effects on percutaneous absorption: in vivo and in vitro comparisons with human skin. British Journal of Dermatology. 115 (1986), 1-11.

Bronaugh, R.L. and Maibach, H.I. Percutaneous absorption: drugs cosmetics mechanisms methodology. Marcel Dekker, New York, 2005.

Brooke, I.; Cocker, J.; Delic, J.I.; Payne, M.; Jones, K. and Gregg, N.C. Dermal uptake of solvents from the vapour phase: an experimental study in humans. The Annals of Occupational Hygiene. 42 (1998), 531–540.

Brown, M.B.; Hanpanitcharoen, M. and Martin, G.P. An in vitro investigation into the effect of glycosaminoglycans on the skin partitioning and deposition of NSAIDs. International Journal of Pharmaceutics. 225 (2001), 113-121.

Brown, M. B.; Marriott, C. and Martin, G.P. The effect of hyaluronan on the in vitro deposition of diclofenac within the skin. International Journal of Tissue Reactions. 17, (1995), 133-140.

Brown, M.B.; Martin, G.P; Jones, S.A. and Akomeah, F.K. Dermal and transdermal drug delivery systems: current and future prospects. Drug Delivery. 13 (2006), 175-187.

Buchwald, P. and Bodor, N. A simple, predictive, structure-based skin permeability model. Journal of Pharmacy and Pharmacology. 53 (2001), 1087-1098.

Burkoth, T.L.; Bellhouse B.J.; Hewson, G.; Longridge, D.J.; Muddle, A.J and Sarphie, D.F. Transdermal and transmucosal powdered drug deliver. Critical Reviews in Therapeutic Drug Carrier Systems. 16 (1999), 331-384.

Caspers, P.J.; Williams, A.C.; Carter, E.A.; Edwards, H.G.M.; Barry, B.B.; Bruining, H.A.; Puppels, G.J. Monitoring the penetration enhancer dimethyl sulfoxide in human stratum corneum in vivo by confocal Raman spectroscopy. Pharmaceutical Research. 19 (2002), 1577-1580.

Cevc, G. Drug delivery across the skin. Expert Opinion on Investigational Drugs. 6 (1997), 1887-1937.

Cevc, G. and Blume, G. New, highly efficient formulation of diclofenac for the topical, transdermal administration in ultradeformable drug carriers, Transfersomes. Biochimica et Biophysica Acta. 1514 (2001), 191-205.

Chang, R.L.S.; Ueki, I.F.; Troy, J.L.; Deen, W.M.; Robertson, C.R. and Brenner, B.M. Permselectivity of the glomerular capillary wall to macromolecules II. Experimental studies in rats using neutral dextran. Biophysical Journal. 15 (1975), 887-906.

Chao, F.; Yi, L.; Xun, Y.; Zheng-xing, R.; Xue-mei, F.; Chan-bing, J. and Hong-zhuan, C. Synergistically enhanced transdermal permeation and topical analgesia of tetracaine gel containing menthol and ethanol in experimental and clinical studies. European Journal of Pharmaceutics and Biopharmaceutics. 68 (2008), 735-740.

Chekirou, N.L.; Benomrane, I.; Lebsir, F. and Krallafa, A.M. Theoretical and experimental study of the tetracain/β-cyclodextrin inclusion complex. Journal of Inclusion Phenomena and Macrocyclic Chemistry. 74 (2012), 211–221.

Chen, Y.P.; Shen, Y.Y.; Guo, X.; Zhang, C.S.; Yang, W.J.; Ma, M.L.; Liu, S.; Zhang, M.B. and Wen, L.P. Transdermal protein delivery by a co-administered peptide identified via phage display. Nature Biotechnology. 24 (2006), 455–460.

Chilcott, R.; Barai, N.; Beezer, A.; Brain. S.; Brown, M. and Bunge, A. Inter- and intra-laboratory variation of in vitro diffusion cell measurements: an international multi-centre study using quasi standardised methods and materials. Journal of Pharmaceutical Sciences. 94 (2005), 632–638.

Childers, M.; Walfre, F.; Nelson, J. and Aguilar, G. Laser surgery of port wine stains using local vacuum pressure: changes in skin morphology and optical properties (part I). Lasers in Surgery and Medicine 39 (2007), 108-117.

Chien, Y.W.; Chien, T.Y.; Bagdon, R.E.; Huang, Y.C. and Bierman, R.H. Transdermal dual-controlled delivery of contraceptive drugs: formulation development, in vitro and in vivo evaluations, and clinical performance. Pharmaceutical Research. 6 (1989), 1000-1010.

Chouinard-Pelletier, G.; Leduc, M.; Guay, D.; Coulombe, S.; Leask, R.L. and Jones, E.A.V. Use of inert gas jets to measure the forces required for mechanical gene transfection. BioMedical Engineering Online. 11 (2012), 67-79.

Clough, G.F.; Boutsiouki, P.; Church, M.K. and Michel, C.C. Effects of blood flow on the in vivo recovery of a small diffusible molecule by microdialysis in human skin. Journal of Pharmacology and Experimental Therapeutics. 302 (2002), 681-686.

Cnubben, N.H.; Elliott, G.R.; Hakkert, B.C.; Meuling, W.J. and van de Sandt, J.J. Comparative in vitro-in vivo percutaneous penetration of the fungicide ortho-phenylphenol. Regulatory Toxicology and Pharmacology. 35 (2002), 198-208.

Combadiere, B.; Vogt, A.; Mahe, B.; Costagliola, D.; Hadam, S.; Bonduelle, O.; Sterry, W.; Staszewski, S.; Schaefer, H.; van der Werf, S.; Katlama, C.; Autran, B. and Blume-Peytavi, U. Preferential amplification of CD8 effector-Tcells after transcutaneous application of an inactivated influenza vaccine: a randomized phase I trial. PLoS ONE. 5 (2010) e10818.

Corcuff, P.; de Lacharriere, O. and Leveque, J. Extension-induced changes in the microrelief of the human volar forearm. Variations with age. Journal of Gerontology. 46 (1991), 223-227.

Cordero, J.A.; Alarcon, L. and Escribano, E. A comparative study of the transdermal penetration of a series of nonsteroidal anti-inflammatory drugs. Journal of Pharmaceutical Sciences. 86 (1997), 503-508.

Cormier, M.; Trautman, J.; Kim, H. L.; Samice, A.P.; Ermans, A.P.; Edwards, B.P.; Lim, W.L. and Poutiatine, A . Skin treatment apparatus for sustained transdermal drug delivery. Patent (serial number WO 01/41864 A1), 2001.

Cosman, F.; Lane, N.E.; Bolognese, M.A.; Zanchetta, J.R.; Garcia-Hernandez, P.A.; Sees, K.; Matriano, J.A.; Gaumer, K. and Daddona, P.E. Effect of transdermal teriparatide administration on bone mineral density in postmenopausal women. The Journal of Clinical Endocrinology and Metabolism. 95 (2010), 151-158.

Crank, J. The mathematics of diffusion. Clarendon Press, Oxford, 1975.

Cross, S.E.; Anderson, C. and Roberts, M.S. Topical penetration of commercial salicylate esters and salts using human isolated skin and clinical microdialysis studies. British Journal of Clinical Pharmacology. 46 (1998), 29–35.

Cross, S.E.; Megwa, S.A.; Benson, H.A. and Roberts, M.S. Self-promotion of deep tissue penetration and distribution of methylsalicylate after topical application. Pharmaceutical Research. 16 (1999), 427-433.

Cross, S.E. and Roberts, M.S. Targeting local tissues by transdermal application: understanding drug physicochemical properties that best exploit protein binding and blood flow effects. Drug Development Research. 46 (1999), 309–315.

Cross, S.E. and Roberts, M.S. Physical enhancement of transdermal drug application: is delivery technology keeping up with pharmaceutical development?. Current Drug Delivery. 1 (2004), 81-92.

Darville, J.M.; Lovering, A.M. and MacGowan, A.P. Development, evaluation and application of an isocratic high-performance liquid chromatography (HPLC) assay for the simultaneous determination of aciclovir and its metabolite 9-carboxymethoxymethylguanine in human serum and cerebrospinal fluid. International Journal of Antimicrobial Agents. 30 (2007), 30-33.

Davis, A.F. and Hadgraft, J. Effect of supersaturation on membrane transport. International Journal of Pharmaceutics. 76 (1991), 1-8.

Davis, E. and Callender, V. A review of acne in ethnic skin pathogenesis, clinical manifestations and management strategies. Journal of Clinical and Aesthetic Dermatology. 3 (2010), 24-38.

Delgado-Charro, M.B. and Guy, R.H. Transdermal drug delivery. Taylor & Francis Group, Florida, 2001.

Denet, A.R.; Vanbever, R. and Preat, V. Skin electroporation for transdermal and topical delivery. Advanced Drug Delivery Reviews. 56 (2004), 659-674.

Desai, P.; Patlolla, R.R. and Singh, M. Interaction of nanoparticles and cell-penetrating peptides with skin for transdermal drug delivery. Molecular Membrane Biology. 27 (2010), 247-259.

Dhawan, S.; Medhi, B. and Chopra, S. Formulation and evaluation of diltiazem hydrochloride gels for the treatment of anal fissures. Scientia Pharmaceutica. 77 (2009), 465-482.

Dias, M.; Raghavan, S.L. and Hadgraft, J. ATR-FTIR spectroscopic investigations on the effect of solvents on the permeation of benzoic acid and salicylic acid through silicone membranes. International Journal of Pharmaceutics. 216 (2001), 51-59.

Dick, D.; Ng, K.M.; Sauder, D.N. and Chu, I. In vitro and in vivo percutaneous absorption of 14C-chloroform in humans. Human and Experimental Toxicology. 14 (1995), 260-265.

Dick, I.P.; Blain, P.G.; Williams, F.M. The percutaneous absorption and skin distribution of lindane in man. II. In vitro studies. Human and Experimental Toxicology. 16 (1997), 652-657.

Dick, I.P. and Scott, R.C. Pig ear skin as an in vitro model for human skin permeability. Journal of Pharmaceutical Pharmacology. 44 (1992), 640-645.

Dixit, S.; Crain, J.; Poon, W.C.K.; Finney, J.L. and Soper, A.K. Molecular segregation observed in a concentrated alcohol–water solution. Nature. 416 (2002), 829-832.

Djordjevic, L.; Primorac, M. and Stupar, M. In vitro release of diclofenac diethylamine from caprylocaproyl macrogolglycerides based microemulsions. International Journal of Pharmaceutics. 296 (2005), 73-79.

Doliwa, A.; Santoyo, S. and Ygartua, P. Effect of passive and iontophoretic skin pretreatments with terpenes on the in vitro skin transport of piroxicam. International Journal of Pharmaceutics. 229 (2001), 37-44.

Doukas, A.G. and Kollias, N. Transdermal drug delivery with a pressure wave. Advanced Drug Delivery Reviews. 56 (2004), 559-579.

Down, J. and Harvey, N. G. Minimally invasive systems for transdermal drug delivery. In Transdermal Drug Delivery. Marcel Dekker, New York, 2003.

Elias, P. Stratum corneum defensive functions: an integrated view. Journal of Investigative Dermatology. 125 (2005), 183-200.

Ellis, R.A. Vascular patterns in the skin. Advances in Biology of the Skin. Pergamon Press, New York, 1961.

Ellis, R., 2010. Ellis Hematoxylin and Eosin (H&E) Staining Protocol, 2010. Available from http://www.ihcworld.com/_protocols/special_stains/h&e_ellis.htm.

El-Sayed, Y.M.; Abdel-Hameed, M.E.; Suleiman, M.S. and Najib, N.M. A rapid and sensitive high-performance liquid chromatographic method for the determination of diclofenac sodium in serum and its use in pharmacokinetic studies. Journal of Pharmacy and Pharmacology. 40 (1998), 727-790.

Escribano, E.; Obach, M.; Arevalo, M.I.; Calpena, A.C.; Domenech, J. and Queralt, J. Rapid human skin permeation and topical anaesthetic activity of a new amethocaine microemulsion. Skin Pharmacology and Physiology. 18 (2005), 294-300.

Essa, E.; Bonner, M. and Barry, B. Human skin sandwich for assessing shunt route penetration during passive and iontophoretic drug and liposome delivery. Journal of Pharmacy and Pharmacology. 54 (2002), 1481–1490.

Fabin, B. and Touitou, E. Localization of lipophilic molecules penetrating rat skin in vivo by quantitative autoradiography. International Journal of Pharmacy. 74 (1991), 59–65.

Fan, H.; Lin, Q.; Morrissey, G.R. and Khavari, P.A. Immunization via hair follicles by topical application of naked DNA to normal skin. Nature Biotechnology.17 (1999), 870–872.

Fang, J.; Lee, W.; Shen, S.; Wang, H.; Fang, C. and Hu, C. Transdermal delivery of macromolecules by erbium:YAG laser. Journal of Controlled Release. 100 (2004), 75-85.

Feather, J.W.; Haijizadeh-Saffar, M.; Leslie, G. and Dawson, J.B. A portable scanning reflectance spectrophotometer using visible wavelengths for the rapid measurement of skin pigmentation. Physics in Medicine and Biology. 34 (1989), 807–820.

Feldmann, R.J. and Maibach, H.I. Percutaneous penetration of 14C hydrocortisone in man Effect of certain bases and pretreatments. Archives of Dermatology. 94 (1966), 649.

Feldmann, R.J. and Maibach, H.I. Regional variation in precutaneous penetration of 14C cortisol in man. Journal of Investigative Dermatology. 48 (1967), 181.

Feldstein, M.M.; Raigorodskii, I.M.; Iordanskii, A.L. and Hadgraft, J. Modeling of percutaneous drug transport in vitro using skin-imitating Carbosil membrane. Journal of Controlled Release. 52 (1998), 25-40.

Fernandez, M. Formation of micelles and membrane action of the local anesthetic tetracaine hydrochloride. Biochimica et Biophysica Acta. 597 (1980), 83-91.

Ferreira, L.A.M.; Doucet, J.; Seiller, M.; Grossiord, J.L.; Marty, J.P. and Wepierre, J. In vitro percutaneous absorption of metronidazole and glucose: comparison of w/o, w/o/w and w/o systems. International Journal of Pharmaceutics. 112 (1995), 169–179.

Fini, A.; Fazio, G.; Gonzalez-Rodriguez, M.; Cavallari, C.; Passerini, N. and Rodriguez, L. Formation of ion-pairs in aqueous solutions of diclofenac salts. International Journal of Pharmaceutics. 187 (1999), 163–173.

Florence, A.T. and Attwood, D. Drug absorption and routes of administration. Macmillan Press, Hampshire, 1998.

Flynn, G.; Yalkowsky, S.H and Roseman, T.J. Mass transport phenomena and models. Journal of Pharmaceutical Sciences. 63 (1974), 479-510.

Foldvari, M. In vitro cutaneous and percutaneous delivery and in vivo efficacy of tetracaine from liposomal and conventional vehicles. Pharmaceutical Research. 11 (1994), 1593-1598.

Franz, T. J. The finite dose technique as a valid in vitro model for the study of percutaneous absorption in man. Current Problems in Dermatology. 7 (1978), 58-68.

Franz, T. J. Percutaneous absorption - relevance of in vitro data. Journal of Investigative Dermatology. 64 (1975), 190-195.

Fredonnet, J.; Gasc, G.; Serre, G.; Severac, C. and Simon, M. Topographical and nano-mechanical characterization of native corneocytes using atomic force microscopy. Journal of Dermatological Science. 75 (2014), 63-65.

Freeman, D.J.; Sheth, N.V. and Spruance, S.L. Failure of topical acyclovir in ointment to penetrate human skin. Antimicrobial Agents and Chemotherapy. 29 (1986), 730 -732.

Frezzatti, W.; Toselli, W. and Schreier, S. Phase separation of the uncharged form and bilayer micellization by the charged form of tetracaine. Biochimica et Biophysica Acta. 860 (1986), 531-538.

Friberg, S.E.; Kayali, I.; Beckerman, W.; Rhein, L.D. and Simion, A. Water permeation of reaggregated sratum-corneum with model lipids. Journal of Investigative Dermatology. 94 (1990), 377-380.

Frum, Y.; Eccleston, G.M. and Meidan. V.M. Evidence that drug flux through synthetic membranes is associated with normally distributed permeability coefficients. European Journal of Pharmaceutics and Biopharmaceutics. 67 (2007), 434–439.

Fuji, M.; Yamanouchi, S. and Hori, N. Evaluation of Yucatan micropig skin for use as an in vitro model for skin permeation study. Biological and Pharmaceutical Bulletin. 20 (1997), 249-254.

Fujiwara, A.; Hinokitani, T.; Goto, K. and Arai, T. Partial ablation of porcine stratum corneum by argon-fluoride excimer laser to enhance transdermal drug permeability. Lasers in Medical Science. 19 (2005), 210-217.

Gans, P.; Sabatini, A. and Vaca, A. Determination of equilibrium constants from spectrophotometric data obtained from solutions of known pH: the program pHab. Annali di Chimica. 89 (1999), 45–49.

Gehl, J. Electroporation for drug and gene delivery in the clinic: doctors go electric. Methods Molecular Biology. 423 (2008), 351-359.

Giuliano, F. and Warner, T. Ex vivo assay to determine the cyclooxygenase selectivity of non- steroidal anti-inflammatory drugs. British Journal of Pharmacology. 126 (1999), 1824-1830.

Glenn, G.M.; Taylor, D.N.; Li, X.; Frankel, S.; Montemarano, A. and Alving, C.R. Transcutaneous immunization: a human vaccine delivery strategy using a patch. Nature Medicine. 6 (2000), 1403–1406.

Grams, Y.; Whitehead, L.; Cornwell, P. and Bouwstra, J. Time and depth resolved visualization of the diffusion of a lipophilic dye into the hair follicle of fresh unfixed human scalp skin. Journal of Controlled Release. 98, (2004) 367–378.

Godbillon, J.; Gauron, S. and Metayer, J.P. High-performance liquid chromatographic determination of diclofenac and its monohydroxylated metabolites in biological fluids. Journal of Chromatography. 338 (1985), 151–159.

Godin, B. and Touitou, E. Transdermal skin delivery: predictions for humans from in vivo, ex vivo and animal models. Advanced Drug Delivery Reviews. 59 (2007), 1152-1161.

Grams, Y.Y. and Bouwstra, J.A. Penetration and distribution in human skin focusing on the hair follicle. Taylor and Francis, Boca Raton, 2005.

Gray, G.M. and Yardley, H.J. Lipid compositions of cells isolated from pig human, and rat epidermis. Journal of Lipid Research. 16 (1975), 434–440.

Gregory, A.E.; Titball, R. and Williamson, D. Vaccine delivery using nanoparticles. Frontiers in Cellular and Infection Microbiology. 3 (2013), 3-20.

Griffin, P.; Mason, H.; Heywood, K. and Cocker, J. Oral and dermal absorption of chlorpyrifos: a human volunteer study. Occupational and Environmental Medicine. 56 (1999), 10-13.

Griffin, P.; Payne, M.; Mason, H.; Freedlander, E.; Curran, A.D. and Cocker, J. The in vitro percutaneous penetration of chlorpyrifos. Human Experimental Toxicology. 19 (2000), 104-107.

Guerin, M.; Dumas, J. and Sandorfy, C. Vibrational spectroscopic studies of molecular associations by local anesthetics, Canadian Journal of Chemistry. 58 (1980), 2080-2088.

Gupta, S.; Shroff, S. and Gupta, S. Modified technique of suction blistering for epidermal grafting in vitiligo. International Journal of Dermatology. 38 (1999), 306-309.

Gupta, S.K.; Southam, M.; Gale, R. and Hwang, S.S. System functionality and physicochemical model of fentanyl transdermal delivery. Journal of Pain and Symptom Management. 7 (1992), 17-26.

Guy, R.H. and Hadgraft, J. Physicochemical aspects of percutaneous penetration and its enhancement. Pharmaceutical Research. 5 (1988), 753-758.

Guy, R.H. and Hadgraft, J. Transdermal drug delivery. Marcel Dekker, New York, 2004.

Hadgraft, J. Recent developments in topical and transdermal delivery. European Journal of Drug Metabolism and Pharmacokinetics. 21 (1996), 165-173.

Hadgraft, J. Passive enhancement strategies in topical and transdermal drug delivery. International Journal of Pharmaceutics. 184 (1999), 1-6.

Hadgraft, J. and Guy, R.H. Transdermal Drug Delivery. Developmental Issues and Research Initiatives. Marcel Dekker, New York, 1989.

Hadgraft, J. and Lane, M. Transepidermal water loss and skin site: a hypothesis. International Journal of Pharmaceutics. 373 (2009), 1-3.

Hadgraft, J. and Pugh, W.J. The selection and design of topical and transdermal agents: a review. Journal of Investigative Dermatology Symposium Proceedings. 3 (1998), 131-135.

Halici, Z.; Dengiz, G.O.; Odabasoglu, F.; Suleyman, H.; Cadirci, E. and Halici, M. Amiodarone has anti-inflammatory and anti-oxidative properties: An experimental study in rats with carrageenan-induced paw edema. European Journal of Pharmacology. 566 (2007), 215–221.

Hanson, K.M. and Bardeen, C.J. Application of nonlinear optical microscopy for imaging skin. Photochemistry and Photobiology. 85 (2009), 33–44.

Hanson, K.; Behne, M.; Barry, N.; Mauro, T.; Gratton, E. and Clegg, R. Two photon fluorescence lifetime imaging of the skin stratum corneum pH gradient. Biophysical Journal. 83 (2002), 1682–1690.

Hata, T.; Matsuki, H. and Kaneshina, S. Effect of local anesthetics on the bilayer membrane of dipalmitoylphosphatidylcholine: interdigitation of lipid bilayer and vesicle-micelle transition. Biophysical Chemistry. 87 (2002), 25–36.

Health and consumer protection directorate-general. Basic criteria for in vitro assessment of dermal absorption of cosmetic ingredients. European commission (2006), SCCP/0970/06.

Heavner, J.E. Pharmacology of Local Anesthesia, Longnecker's Anesthesiology. McGraw-Hill, 2008.

Hendriks, F.M.; Brokken, D.; van Eemeren, J.T.; Oomens, C.W.; Baaijens, F.P. and Horsten, J.B. A numerical-experimental method to characterize the non-linear mechanical behaviour of human skin. Skin Research Technology. 9 2003), 274–283.

Heyneman, C.; Cara. L. and Geoffrey, W. Oral versus topical NSAIDs in rheumatic diseases. Drugs. 60 (2012) 555-574.

Higaki, K.; Nakayama, K.; Suyama, T.; Amnuaikit, C.; Ogawara, K. and Kimura, T. Enhancement of topical delivery of drugs via direct penetration by reducing blood flow rate in the skin. International Journal of Pharmaceutics. 288 (2005), 227-233.

Higuchi, T. Physical chemical analysis of percutaneous absorption process from creams and ointments. Journal of the Society of Cosmetic Chemists. 11(1960), 85-97.

Higuchi, T. Rate of release of medicaments from ointment bases containing drugs in suspension. Journal of Pharmaceutical Sciences. 50 (1961), 874-875.

Hikima, T.; Yamada, K.; Kimura, T.; Maibach, H.I. and Tojo, K. Comparison of skin distribution of hydrolytic activity for bioconversion of beta-estradiol 17-acetate between man and several animals in vitro. European Journal of Pharmaceutics and Biopharmaceutics. 54 (2002), 155-160.

Hinedi, Z.R.; Johnston, C.T. and Erickson, C. Chemisorption of benzene on cu-montmorillonite as characterized by FTIR and ^{13}C MAS NMR. Clays and Clay Mineral. 41 (1993), 87-94.

Hoppert, M. Microscopic techniques in biotechnology. Microscopic techniques in biotechnology. Wiley-VCH, Veinheim, 2003.

Horita, D.; Yoshimoto, M.; Todo, H. and Sugibayashi, K. Analysis of hair follicle penetration of lidocaine and fluorescein isothiocyanate- dextran 4 kDa using hair follicle-plugging method. Drug Development and Industrial Pharmacy. 40 (2014), 345-351.

Houk, J. and Guy, R. H. Membrane models for skin penetration studies. Chemical Reviews. 88 (1988), 455-471.

Howes, D., Guy, R., Hadgraft, J., Heylings, J., Hoeck, U., Kemper, F., Maibach, H., Marty, J. P., Merk, H., Parra, J., Rekkas, D., Rondelli, I., Schaefer, H., Tauber, U., and Verbiese, N. Methods for assessing percutaneous absorption - The report and recommendations of ECVAM workshop 13. Atla-Alternatives to Laboratory Animals. 24 (1996), 81-106.

Huang, S.Y.; Chen, N.F.; Chen, W.F.; Hung, H.C.; Lee, H.P.; Lin, Y.Y.; Wang, H.M.; Sung, P.J.; Sheu, J.H. and Wen, Z.H. Sinularin from indigenous soft coral attenuates nociceptive responses and spinal neuroinflammation in carrageenan-induced inflammatory rat model. Marine Drugs. 10 (2012), 1899–1919.

Huang, X.; Tanojo, H.; Lenn, J.; Deng, C.H. and Krochmal, L. A novel foam vehicle for delivery of topical corticosteroids. Journal of the American Academy of Dermatology. 53 (2005), S26-S38.

Hunter, C; Lawson, K; Perkins, J. and Urch, C. Aromatic interactions. Journal of Chemical Society. 2 (2001), 651-669.

Hurley, H.J. The eccrine sweat glands: structure and function. The Biology of the Skin. Parthenon, New York, 2001.

Ialenti, A.; Ianaro, A.; Moncada, S. and Di Rosa, M. Modulation of acute inflammation by endogenous nitric oxide. European Journal of Pharmacology. 211 (1995), 177–182.

ICH Q2A: text on validation of analytical procedures: definitions and terminology. Proceedings of the International Conference on Harmonisation (ICH) 60. 1995, US FDA Federal Register.

Idson, B. Vehicle effects in percutaneous absorption. Drug Metabolism Reviews. 14 (1983), 207–222.

Iervolino, M.; Cappello, B.; Raghavan, S.L. and Hadgraft, J. Penetration enhancement of ibuprofen from supersaturated solutions through human skin. International Journal of Pharmaceutics. 212 (2001), 131-141.

Iglesias-Garcia., I., Brandariz, I. and Iglesias, E. Fluorescence study of tetracaine–cyclodextrin inclusion complexes. Fluorescence study of tetracaine–cyclodextrin inclusion complexes. Supramolecular Chemistry. 22 (2010), 228–236.

Israelachvili, J.N. Intermolecular and surface forces. Academic Press, 1985.

Ito, Y.; Ise, A.; Sugioka, N. and Takada, K. Molecular weight dependence on bioavailability of FITC-dextran after administration of self-dissolving micropile to rat skin. Drug Development and Industrial Pharmacy. 36(2010) 845-851.

Iwamoto, K.; Watanabe, J. and Atsumi, F. Effects of urethane anesthesia and age on organ blood flow in rats measured by hydrogen gas clearance method. Journal of Pharmaco-biodynamics. 10 (1987), 280-284.

Jacobi, U.; Kaiser, M. and Sterry, W. Kinetics of blood flow after topical application of benzyl nicotinate on different anatomic sites. Archives of Dermatological Research. 298 (2006), 291-300.

Jacobi, U.; Kaiser, M.; Sterry, W. and Lademann, J. Kinetics of blood flow after topical application of benzyl nicotinate on different anatomic sites. Archives of Dermatological Research. 298 (2006), 291-300.

Jacobi, U.; Kaiser, M.; Toll, R.; Mangelsdorf, S.; Audring, H.; Otberg, N.; Lademann, W. Porcine ear skin: an in vitro model for human skin. Skin Research Technology. 13 (2007), 19–24.

Jakubovic, H.R. and Ackerman, A.R. Structure and function of the skin: development, morphology and physiology. W.B. Saunders, Philadelphia, 1992.

Jansen, L.H.; Hojyo-Tomodo, M.T and Kligman, A.M. Improved fluorescence staining for estimating turnover of the human stratum corneum. British Journal of Dermatology. 90 (1974), 9–12.

Jean, Y.H.; Chen, W.F.; Duh, C.Y.; Huang, S.Y.; Hsu, C.H.; Lin, C.S.; Sung, C.S.; Chen, I.M. and Wen, Z.H. Inducible nitric oxide synthase and cyclooxygenase-2 participate in anti-inflammatory and analgesic effects of the natural marine compound lemnalol from formosan soft coral Lemnalia cervicorni. European Journal of Pharmacology. 578 (2008), 323–331.

Jepps, O.G.; Dancik, Y.; Anissimov, Y.G. and Roberts, M.S. Modeling the human skin barrier-Towards a better understanding of dermal absorption. Advanced Drug Delivery Reviews. 65 (2013), 152-168.

Jiang, X.; Ortiz, C. and Hammond, P. Exploring the rules for selective deposition: interactions of model polyamines on acid and oligoethylene oxide surfaces. Langmuir. 18 (2002), 1131-1143.

Jing, Yu.; Dhaval, R. K. and Yogeshvar, N.K. Erbium:YAG fractional laser ablation for the percutaneous delivery of intact functional therapeutic antibodies. Journal of Controlled Release. 156 (2011), 53-59.

Joshi, A. and Raje, J. Sonicated transdermal drug transport. Journal of Controlled Release. 83 (2002), 13-22.

Jung, E.C. and Maibach, H.I. Animal models for percutaneous absorption. Journal of Applied Toxicology. 35 (2015), 1-10.

Jung-Hwan. P.; Jeong-Woo, L., Yeu-Chun, K. and Prausnitz, M.R. The effect of heat on skin permeability. International Journal of Pharmacy. 359 (2008), 94-103.

Kairinos, N.; Voogd, A.M.; Botha, P.H.; Kotze, T.; Kahn, D.; Hudson, D.A. and Solomons, M. Negative-pressure wound therapy II: negative-pressure wound therapy and increased perfusion. Just an illusion?. Plastic and Reconstructive Surgery. 123 (2009), 601–612.

Kalia, Y.N.; Naik, A.; Garrison, J. and Guy, R.H. Iontophoretic drug delivery. Advanced Drug Delivery Reviews. 56 (2004), 619-658.

Kammerau, B.; Zesch, A. and Schaefer, H. Absolute concentrations of dithranol and triacetyl-dithranol in the skin layers after local treatment: in vivo investigations with four different types of pharmaceutical vehicles. Journal of Investigative Dermatology. 64 (1975), 145–149.

Kang, L.; Poh, A.L.; Fan, S.K.; Ho, P.C.; Chan, Y.W. and Chan, S.Y. Reversible effects of permeation enhancers on human skin. European Journal of Pharmaceutics and Biopharmaceutics. 67 (2007), 149-55.

Kaplun-Frischoff, Y. and Touitou, E. Testosterone skin permeation enhancement by menthol through formation of eutectic with drug and interaction with skin lipids. Journal of Pharmaceutical Sciences. 86 (1997), 1394-1399.

Kashibuchi, N.; Hirai, Y.; O'Goshi, K. and Tagami, H. Three-dimensional analyses of individual corneocytes with atomic force microscope: morphological changes related to age, location and to the pathologic skin conditions. Skin Research and Technology. 8 (2002), 203–211.

Kasim, N.; Whitehouse, M.; Ramachandran, C.; Bermejo, M. and Lennernas, H. Molecular properties of WHO essential drugs and provisional biopharmaceutical classification. Molecular Pharmaceutics. 1 (2004), 85-96.

Kezic, 2008. Methods for measuring in-vivo percutaneous absorption in humans. Human and Experimental Toxicology. 27 (2008), 289–295.

Khalil, E.; Najjar, S. and Sallam, A. Aqueous solubility of diclofenac diethylamine in the presence of pharmaceutical additives: a comparative study with diclofenac sodium. Drug Development and Industrial Pharmacy. 26 (2000), 375-381.

Khan, G.; Frum, Y.; Sarheed, O.; Eccleston, G.M. and Meidan, V.M. Assessment of drug permeability distribution in two different model skins. International Journal of Pharmaceutics. 303 (2005), 81–7.

Kim, Y.; Ludovice, P.J. and Prausnitz, M.R. Transdermal delivery enhanced by magainin pore-forming peptide. Journal of Controlled Release. 122 (2007), 375–383.

Kim, Y.; Late, S.; Banga, A.K.; Ludovice, P.J. and Prausnitz, M.R. Biochemical enhancement of transdermal delivery with magainin peptide: modification of electrostatic interactions by changing pH. International Journal of Pharmaceutics. 362 (2008), 20-28.

Kitade, T.; Kitamura, K.; Hayakawa, J.; Nakamoto, E. and Kishimoto, N. Poly(vinyl alcohol) as solid substrate material for room-temperature phosphorimetry. Analytical Chemistry. 67 (1995), 3806-3808.

Kitagawa, N.; Oda, M. and Totoki, T. Possible mechanism of irreversible nerve injury caused by local anesthetics. Anesthesiology. 100 (2004), 962-967.

Klimich, H.M. and Chandra, G. Use of Fourier transform infrared spectroscopy with alternate total reflectance for in vivo quantification of polydimethylsiloxanes on human skin. Journal of the Society of Cosmetic Chemists. 37 (1986), 73–87.

Kling, W. and Lange, H. Proceedings of the 2nd International Congress of Surface Activity. 1957, 295.

Knorr, F.; Lademann, J.; Patzelt, A.; Sterry, W.; Blume-Peytavi, U. and Vogt, A. Follicular transport route. Research progress and future perspectives. European Journal of Pharmaceutics and Biopharmaceutics. 71 (2009), 173-180.

Koller, A. and Kaley, G. Endothelial regulation of wall shear stress and blood flow in skeletal muscle microcirculation. American Journal of Physiology. 260 (1991), 862-868.

Kolmel, K.; Sennhen, B. and Giese, K. Evaluation of drug penetration into the skin by photoacoustic measurement. Journal of the Society of Cosmetic Chemists. 37 (1986), 375–385.

Koyama, Y.; Bando, H.; Yamashita, F.; Takakura, Y.; Sezaki, H. and Hashida, M. Comparative analysis of percutaneous absorption enhancement by d-limonene and oleic acid based on a skin diffusion model. Pharmaceutical Research. 11 (1994), 377-383.

Kreilgard, M. Assessment of cutaneous drug delivery using microdialysis. Advanced Drug Delivery Reviwes. 54 (2000), 99–121.

Kreyden, O.P. Iontophoresis for palmoplantar hyperhidrosis. Journal of Cosmetic Dermatology. 3 (2004), 211-214.

Kroneberg, B.; Holmberg, K. and Lindman, B. Surface chemistry of surfactants and polymers. John Wiley & Sons, West Sussex, 2014.

Kunta, J.R.; Goskonda, V.R.; Brotherton, H.O.; Khan, M.A. and Reddy, I.K. Effect of menthol and related terpenes on the percutaneous absorption of propranolol across excised hairless mouse skin. Journal of Pharmaceutical Sciences. 86(1997), 1369-1373.

Lademann, J.; Jacobi, U.; Surber, C.; Weigmann, J.-H. and Fluhr, J.W. The tape stripping procedure – evaluation of some critical parameters. European Journal of Pharmaceutics and Biopharmaceutics. 72 (2009), 317-323.

Lademann, J.; Knorr, F.; Richter, H.; Blume-Peytavi, U.; Vogt, A. and Antoniou, C. Hair follicles – an efficient storage and penetration pathway for topically applied substances. Skin Pharmacology and Physiology. 21 (2008), 150–155.

Lademann, J.; Knorr, F.; Richter, H.; Jung, S.; Meinke, M.C.; Rühl, E.; Alexiev, U.; Calderon, M. and Patzelt, A. Hair follicles as a target structure for nanoparticles. Journal of Innovative Optical Health Sciences. 8 (2015), 1-8.

Lademann, J.; Otberg, N.; Richter, H.; Jacobi, U.; Schaefer, H. and Blume-Peytavi, U. Follikulare penetration- ein entscheidender penetrationsweg von topisch applizierten substanzen. Hautarzt. 54 (2003), 321-323.

Lademann, J.; Otberg, N.; Richter, H.; Weigman, H.J.; Lindemann, U.; Schaefer, H. and Sterry, W. Investigation of follicular penetration of topically applied substances. Skin Pharmacology and Applied Skin Physiology. 14 (2001), 17–22.

Lademann, J.; Weigmann, H.; Rickmeyer, C.; Barthelmes, H.; Schaefer, H.; Mueller, G. and Sterry, W. Penetration of titanium dioxide microparticles in a sunscreen formulation into the horny layer and the follicular orifice. Skin Pharmacology and Applied Skin Physiology. 12 (1999), 247-256.

Lee, W.R.; Shen, S.C.; Al-Suwayeh, S.A.; Yang, H.H.; Yuan, C.Y. and Fang, J.Y. Laser-assisted topical drug delivery by using a low-fluence fractional laser: imiquimod and macromolecules. Journal of Controlled Release. 153 (2011), 240-248.

Lee, W.R.; Shen, S.C.; Lai, H.H.; Hu, C.H. and Fang, G.Y. Transdermal drug delivery enhanced and controlled by erbium:YAG laser: a comparative study of lipophilic and hydrophilic drugs. Journal of Controlled Release. 75 (2001), 155-166.

Lehman, P.A. and Malany, A.M. Evidence for percutaneous absorption of isotretinoin from the photo-isomerization of topical tretinoin. Journal of Investigative Dermatology. 93 (1989), 595–599.

Lehman, P.A.; Slattery, J.T. and Franz, T.J. Percutaneous absorption of retinoids: influence of vehicle light exposure, and dose. Journal of Investigative Dermatology. 91 (1988), 56–61.

Leutenegger, M.; Martin-Williams, E.; Harbi, P.; Thatcher, T.; Raffoul, W.; Andre, M.; Lopez, A.; Lasser, P. and Lasser, T. Real-time full field laser Doppler imaging. Biomedical Optics Express. 2 (2011), 1470-1477.

Leveque, J.; Halllegot, P.; Doucet, J. and Pierard, G. Structure and function of human stratum corneum under deformation. Dermatology. 205 (2002), 353-357.

Li, J. and Liang, Z. The consideration of synthetic short interfering RNA for therapeutic use. Basic Clinical Pharmacology & Toxicology. 106 (2010), 22-29.

Lim, C.W.; Fujiwara, S.; Yamashita, F. and Hashida, M. Prediction of human skin permeability using a combination of molecular orbital calculations and artificial neural network. Biological and Pharmaceutical Bulletin. 25 (2002), 361-366.

Lin, S.; Jee, S. and Dong, C. Multiphoton microscopy: a new paradigm in dermatological imaging. European Journal of Dermatology. 17 (2007), 361–366.

Liu, H.; Li, S.; Wang, Y.; Yao, H. and Zhang, Y. Effect of vehicles and enhancers on the topical delivery of cyclosporin A. International Journal of Pharmaceutics. 311 (2006), 82-86.

Liu, P.; Higuchi, W.; Song, W.Q.; Kurihara-Bergstrom, T. and Good, W.R. Quantitative evaluation of ethanol effects on diffusion and metabolism of beta-estradiol in hairless mouse skin. Pharmaceutical Research. 8 (1991), 865-872.

Liu, Y.; Ye, X.; Feng, X.; Zhou, G.; Rong, Z.; Fang, C. and Chen, H. Menthol facilitates the skin analgesic effect of tetracaine gel. International Journal of Pharmaceutics. 305 (2005), 31–36.

Lombry, C.; Dujardin, N. and Preat, V. Transdermal delivery of macromolecules using skin electroporation. Pharmaceutical Research. 17 (2000), 32-37.

Lubens, H.; Ausdenmoore, R.; Shafer, A. and Reece, R. Anesthetic patch for painful procedures such as minor operations. American Journal of Diseases of Children. 128 (1974), 192-194.

Lyubovitsky, J.; Krasieva, T.; Xu, X.; Andersen, B. and Tromberg, B. In situ multiphoton optical tomography of hair follicles in mice. Journal of Biomedical Optics. 12 (2007), 404-411.

Machado, M.; Salgado, T.M.; Hadgraft, J. and Lane, M.E. The relationship between transepidermal water loss and skin permeability. International Journal of Pharmaceutics. 384 (2010), 73-77.

Macrae, C.F.; Bruno, I.J.; Chishom, J.A.; Edgington, P.R.; McCabe, P.; Pidcock, E.; Rodriguez-Monge, L.; Taylor, R.; van de Streek, J. and Wood, P.A. Mercury CSD 2.0 - new features for the visualization and investigation of crystal structures. Journal of Applied Crystallography. 41 (2008), 466-470.

Maddock, W.G. and Coller, F.A. The role of the extremities in the dissipation of heat. American Journal of Physiology. 106 (1993), 589-596.

Mckenzie, A.W. and Stoughton, R.B. Method for comparing percutaneous absorption of steroids. Archives of Dermatology. 86 (1962), 608-610.

Magnusson, B.M.; Anissimov, Y.G.; Cross, S.E. and Roberts, M.S. Molecular size as the main determinant of solute maximum flux across the skin. Journal of Investigative Dermatology. 122 (2004), 993-999.

Manosroi, A.; Jantrawuta, P. and Manosroi, J. Anti-inflammatory activity of gel containing novel elastic niosomes entrapped with diclofenac diethylammonium. International Journal of Pharmaceutics. 260 (2008), 156-163.

Marjukka Suhonen, T.; Bouwstra, J.A. and Urtti, A. Chemical enhancement of percutaneous absorption in relation to stratum corneum structural alterations. Journal of Controlled Release. 59 (1999), 149-61.

Marttin, E.; Neelissen-Subnel, M.T.A.; De Haan, F.H.N. and Bodde, H.E. A critical comparison of methods to quantify stratum corneum removed by tape stripping. Skin Pharmacology and Applied Skin Physiology. 9 (1996), 69–77.

Matsukawa, S. and Ando, I. Study of self-diffusion of molecules in polymer gel by pulsed-gradient spin-echo 1H NMR. 2. Intermolecular hydrogen-bond interaction. Macromolecules. 30 (1997), 8310.

Mavon, A.; Miquel, C.; Lejeune, O.; Payre, B. and Moretto, P. In vitro percutaneous absorption and in vivo stratum corneum distribution of an organic and a mineral sunscreen. Skin Pharmacology and Physiology. 20 (2007), 10-20.

Mayes, S. and Ferrone, M. Fentanyl HCL patient-controlled iontophoretic transdermal system for the management of acute postoperative pain. Annals of Pharmacotherapy. 40 (2006), 2178-2186.

McAllister, D.V.; Wang, P.M.; Davis, S.P.; Park, J.H.; Canatella, P.J.; Allen, M.G. and Prausnitz, M.R. Microfabricated needles for transdermal delivery of macromolecules and nanoparticles: fabrication methods and transport studies. Proceedings of the National Academy of Sciences, USA. 100 (2003), 13755-13760.

McCafferty, D.; Woolfson, A.; McClelland, K. and Boston, V. Comparative in vivo and in vitro assessment of the percutaneous absorption of local anesthetics. British Journal of Anaesthesia. 60 (1988), 64-69.

McNeill, S.C.; Potts, R.O. and Francoeur, M.L. Local enhanced topical delivery (LETD) of drugs: does it truly exists?. Pharmaceutical Research. 9 (1992), 1422-1427.

Megrab, N.A.; Williams, A.C. and Barry, B.W. Oestradiol permeation through human skin and silastic membrane: effects of propylene glycol and supersaturation. Journal of Controlled Release. 36 (1995), 277-294.

Mehvar, R.; Robinson, A. and Reynolds, J.M. Dose dependency of the kinetics of dextrans in rats: effect of molecular weight. Journal of Pharmaceutical Sciences. 84 (1995), 815-818.
Meidan, V.M. Methods for quantifying intrafollicular drug delivery: a critical appraisal. Expert Opinion on Drug Delivery.7 (2010), 1095-1108.

Menon, G.K. New insights into skin structure: scratching the surface. Advanced Drug Delivery Reviews. 54 (2002), S3-S17.

Menon, G.N. and Norris, B.J. Simultaneous determination of tetracaine and its degradation product, p-n- butylaminobenzoic acid, by high-performance liquid chromatography. Journal of Pharmaceutical Sciences. 70 (1981), 569-570.

Menzel, F.; Reinert, T.; Vogt, J. and Butz, T. Investigations of percutaneous uptake of ultrafine TiO2 particles at the high energy ion nanoprobe LIPSION. Nuclear Instruments and Methods in Physics Research, Section B: Beam Interactions with Materials and Atoms. 220 (2004), 82-86.

Meyer, V.R. Practical high-performance liquid chromatography. John Wiley and Sons Ltd, Chichester, 2005.

Michaels, A.S.; Chandrasekaran, S.K. and Shaw, J.E. Drug permeation through human skin - Theory and in vitro experimental measurement. Aiche Journal. 21 (1975), 985-996.

Miller, K.J.; Goodwin, S.R.; Westermann-Clark, G.B. and Shah, D.O. Importance of molecular aggregation in the development of a topical local anesthetic. Langmuir. 9 (1993), 105-109.

Mittal, A.; Raber, A.S.; Schaefer, U.F.; Weissmann, S.; Ebensen, T.; Schulze, K.; Guzmán, C.A.; Lehr, C.M. and Hansen, S. Non-invasive delivery of nanoparticles to hair follicles: a perspective for transcutaneous immunization. Vaccine. 31 (2013), 3442–3451.

Mittal, A.; Schulze, K.; Ebensen, T.; Weißmann, S.; Hansen, S.; Lehr, C.M. and Guzmán, C.A. Efficient nanoparticle-mediated needle-free transcutaneous vaccination via hair follicles requires adjuvantation. Nanomedicine: Nanotechnology, Biology and Medicine. 11 (2015), 147-154.

Mittal, K.L. and Fendler, E.J. Solution behaviour of surfactants, theoretical and applied aspects. Plenum Press, New York, 1982.

Mitragotri, S. Healing sound: the use of ultrasound in drug delivery and other therapeutic applications. Nature Reviews Drug Discovery. 4 (2005), 255-60.

Mitragotri, S. Temperature dependence of skin permeability to hydrophilic and hydrophobic solutes. Journal of Pharmaceutical Sciences. 96 (2006), 1832-1839.

Mitragotri, S.; Edwards, D.; Blankschtein, D. and Langer, R. A mechanistic study of ultrasonically-enhanced transdermal drug delivery. Journal of Pharmaceutical Sciences. 84 (1995), 697-706.

Moncada, S.; Ferreira, S.H. and Vane, J.R. Prostaglandins, aspirin-like drugs and the edema of inflammation. Nature. 246 (1973), 217–219.

Montagna, W.; Kligman, A.M. and Carslile, K.S. Atlas of Normal Human Skin. Springer-Verlag, New York, 1992.

Monteiro-Riviere, N.A.; Bristol, D.; Manning, T.; Rodgers, R. and Riviere, J. Interspecies and interregional analysis of the comparative histologic thickness and laser Doppler blood flow measurements at five cutaneous sites in nine species. Journal of Investigative Dermatology. 95 (1990), 582-586.

Monteiro-Riviere, N.A.; Inman, A.O.; Riviere, J.E.; McNeill, S.C. and Francoeur, M.L. Topical penetration of piroxicam is dependent on the distribution of the local vasculature. Pharmaceutical Research. 10 (1993), 1326-1331.

Moore, A.R. and Willoughby, D.A. Hyaluronan as a drug delivery system for diclofenac: a hypothesis for mode of action. International Journal of Tissue Reactions. 17 (1995), 153-156.

Morgan, C.J.; Renwick, A.G. and Friedmann, P.S. The role of stratum corneum and dermal microvascular perfusion in penetration and tissue levels of water-soluble drugs investigated by serum levels and tissue content in microdialysis. British Journal of Dermatology. 148 (2003), 434–443.

Morris, C.J. Carrageenan-induced paw edema in the rat and mouse. Inflammation protocols. Methods in Molecular Biology. 225 (2003), 115-121.

Morykwas, M.J.; Argenta, L.C.; Shelton-Brown, E.I. and McGuirt, W. Vacuum-assisted closure: a new method for wound control and treatment: animal studies and basic foundation. Annals of Plastic Surgery. 38 (1997), 553–562.

Moser, K.; Kriwet, K.; Naik, A.; Kalia, Y.N. and Guy, R.H. Passive skin penetration enhancement and its quantification in vitro. European Journal of Pharmaceutics and Biopharmaceutics. 52 (2001), 103-112.

Muhm, J.M.; Rock, P.B.; McMullin, D.L.; Jones, S.P.; Lu, I.L.; Eilers, K.D.; Space, D.R. and McMullen, A. Effect of aircraft-cabin altitude on passenger discomfort. The New England Journal of Medicine. 356 (2007), 18-27.

Mura, P.; Maestrelli, F.; Gonzalez-Rodriguez, M.L.; Michelacci, I.; Ghelardini, C. and Rabasco, A.M. Development, characterization and in vivo evaluation of benzocaine-loaded liposomes. European Journal of Pharmaceutics and Biopharmaceutics. 67 (2007), 86-95.

Murtaza, R.; Jackman, H.; Alexander, B.; Lleshi, T.; Winnie, A. and Igic, R. Simultaneous determination of mepivacaine, tetracaine, and p-butylaminobenzoic acid by high-performance liquid chromatography. Journal of Pharmacological and Toxicological Methods. 46 (2002), 131-136.

Naik, A.; Kalia, Y.N. and Guy, R.H. Transdermal drug delivery: overcoming the skin's barrier function. Pharmaceutical Science & Technology Today. 3 (2000), 318-326.

Naik, A.; Pechtold, L.A.R.M.; Potts, R.O. and Guy, R.H. Mechanism of oleic acid-induced skin penetration enhancement in vivo in humans. Journal of Controlled Release. 37 (1995), 299–306.

Nair, B. and Taylor-Gjevre, R. A review of topical diclofenac use in musculoskeletal disease. Pharmaceuticals. 3 (2010), 1892-1908.

Nanchahal, J. and Riches, D.J. The healing of suction blisters in pig skin. Journal of Cutaneous Pathology. 9 (1982), 303-315.

Nasir, A. Dermatologic toxicity of nanoengineered materials. Archives of Dermatology. 144 (2008), 253–254.

Nel, A.; Xia, T.; Mädler, L. and Li, N. Toxic potential of materials at the nanolevel. Science. 311 (2006), 622–7.

Netzlaff, F.; Lehr, C.M.; Wertz, P.W. and Schaefer, U.F. The human epidermis models EpiSkin®, SkinEthic® and EpiDerm®: an evaluation of morphology and their suitability for testing phototoxicity, irritancy, corrosivity, and substance transport. European Journal of Pharmaceutics and Biopharmaceutics. 60 (2005), 167-178.

Neubert, R.H.; Mrestani, Y.; Schwarz, M. and Colin, B. Application of micellar electrokinetic chromatography for analysing antiviral drugs in pharmaceutical semisolid formulations. Journal of Pharmaceutical and Biomedical Analysis. 16 (1998), 893-897.

Nevado, J.J.; Pulgarin, J.A. and Escudero, O.I. Determination of procaine and tetracaine in cocaine samples by variable-angle synchronous fluorimetry. Applied Spectroscopy. 54 (2000), 1678-1683.

Neukermans, A.P.; Poutiatine, A.I.; Sendelbeck, S.; Trautman, J.; Wai, L.L.; Edwards, B.P.; Eng, K.P.; Gyory, J.R.; Hyunok, K.L.; Lin, W.Q. and Cormier, M. Device and method for enhancing microprotrusion skin piercing. Patent (serial number WO 0141863), 2001.

Nicoli, S.; Padula, C.; Aversa, V.; Vietti, B.; Wertz, P.W.; Millet, A.; Falson, F.; Govoni, P. and Santi, P. Characterization of rabbit ear skin as a skin model for in vitro transdermal permeation experiments: histology, lipid composition and permeability. Skin Pharmacology and Physiology. 21 (2008), 218-226.

Nokhodchi, A.; Shokri, J.; Dashbolaghi, A.; Hassan-Zadeh, D.; Ghafourian, T. and Barzegar-Jalali, M. The enhancement effect of surfactants on the penetration of lorazepam through rat skin. International Journal of Pharmaceutics. 250 (2003), 359-69.

Norlen, L. The physical structure of the skin barrier. Dermal Absorption and Toxicity Assessment. Informa Healthcare, New York, 2008.

Nowell, H.; Attfield, J.P.; Cole, J.C.; Cox, P.J.; Shankland, K.; Maginn, S.J. and Motherwell, W.D. Structure solution and refinement of tetracaine hydrochloride from X-ray powder diffraction data. New Journal of Chemistry. 26 (2002), 469-472.

O'Brien, L.; Taddio, A.; Lyszkiewicz, D. and Koren, G. A critical review of the topical local anesthetic amethocaine (AmetopTM) for pediatric pain. Paediatric Drugs.7 (2005), 41–54.

O'Connor, K. and Corrigan, O. Comparison of the physicochemical properties of the N-(2-hydroxyethyl) pyrrolidine, diethylamine and sodium salt forms of diclofenac. International Journal of Pharmaceutics. 222 (2001), 281-293.

Ohno, M.; Gibbons, G.H.; Dzau, V.J.; Cooke, J.P. Shear stress elevates endothelial cGMP. Role of a potassium channel and G protein coupling. Circulation. 88 (1993), 193-197.

Ongpipattanakul, B.; Burnette, R.R.; Potts, R.O. and Francoeur, M.L. Evidence that oleic acid exists in a separate phase within stratum corneum lipids. Pharmaceutical Research. 8 (1991), 350-354.

Pang, S.C.; Daniels, W.H. and Buck, R.C. Epidermal migration during the healing of suction blisters in rat skin: a scanning and transmission electron microscopic study. The American Journal of Anatomy. 153 (1978), 177-191.

Pasekova, H. and Polasek, M. Determination of procaine, benzocaine and tetracaine by sequential injection analysis with permanganate-induced chemiluminescence detection. Talanta. 52 (2000), 67-75.

Patzelt, A.; Richter, H.; Knorr, F.; Schafer, U.; Lehr, C.M.; Dahne, L.; Sterry, W. and Lademann, J. Selective follicular targeting by modification of the particle sizes. Journal of Controlled Release. 150 (2011), 45-48.

Paudel, K.; Milewski, M.; Swadley, C.; Brogden, N.; Ghosh, P. and Stinchcomb, A. Challenges and opportunities in dermal/transdermal delivery. Therapeutic Delivery. 1 (2010), 109-131.

Pedersen, L. and Jemec, G.B. Mechanical properties and barrier function of healthy human skin. Acta Dermato-Venereologica. 86 (2006), 308-311.

Pellett, M.A; Roberts, M.S. and Hadgraft, J. Supersaturated solutions evaluated with an in vitro stratum corneum tape stripping technique. International Journal of Pharmaceutics. 151 (1997), 91-98.

Pershing, L.K.; Bakhtian, S.; Poncelet, C.E.; Corlett, J.L. and Shah, V.P. Comparison of skin stripping, in vitro release, and skin blanching response methods to measure dose response and similarity of triamcinolone acetonide cream strengths from two manufactured sources. Journal of Pharmaceutical Sciences. 91 (2002), 312-1323.

Pershing, L.K.; Corlett, J. and Jorgensen, C. In vivo pharmacokinetics and pharmacodynamics of topical ketoconazole and miconazole in human stratum corneum. Antimicrobial Agents and Chemotherapy. 38 (1994), 90-95.

Pershing, L.K.; Lambert, L.D. and Knutson, K. Mechanisms of ethanol-enhanced estradiol permeation across human skin in vivo. Pharmaceutical Research. 7 (1990), 170-175.

Pierre, M.B.; Ricci, E. Jr.; Tedesco, A.C and Bentley, M.V. Oleic acid as optimizer of the skin delivery of 5-aminolevulinic acid in photodynamic therapy. Pharmaceutical Research. 23 (2006), 360-366.

Piret, J., Desormeaux, A. and Gourde, P. Efficacies of topical formulations of foscarnet and acyclovir and of 5-percent acyclovir ointment (Zovirax) in a murine model of cutaneous herpes simplex virus type 1 infection. Antimicrobial Agents and Chemotherapy. 44 (2000), 30-38.

Popova, A.V. and Hincha, D.K. Intermolecular interactions in dry and rehydrated pure and mixed bilayers of phosphatidylcholine and digalactosyldiacylglycerol: a Fourier Transform Infrared spectroscopy study. Biophysical Journal. 85 (2003), 1682-1690.

Potts, R.O. and Francoeur, M.L. The influence of stratum corneum morphology on water permeability, Journal Investigative Dermatology. 96 (1991), 495-499.

Potts, R.O. and Guy, R.H. Predicting skin permeability. Pharmaceutical Research. 9 (1992), 663-669.

Potts, R.O. and Guy, R.H. A predictive algorithm for skin permeability: the effects of molecular size and hydrogen bond activity. Pharmaceutical research. 12 (1995), 1628-1633.

Prausnitz, M.R.; Bose, V.G.; Langer, R. and Weaver, J.C. Electroporation of mammalian skin: a mechanism to enhance transdermal drug delivery. Proceedings of the National Academy of Sciences, USA. 90 (1993), 10504-10508.

Prausnitz, M.R.; Elias, P.M.; Franz, T.J.; Schmuth, M.; Tsai, J.; Menon, G.K.; Walter, M.H. and Feingold, K.R. Skin Barrier and Transdermal Drug Delivery. Saunders, Philadelphia, 2012.

Prausnitz, M.R. and Langer, R. Transdermal drug delivery. Nature Biotechnology. 26 (2008), 1261-1268.

Prausnitz, M.R.; Mitragotri, S. and Langer, R. Current status and future potential of transdermal drug delivery. Nature Reviews Drug Discovery. 3 (2004), 115-124.

Primo, F.; Rodrigues, M.; Simioni, A.; Bentley, M.; Morais, P. and Tedesco, A. In vitro studies of cutaneous retention of magnetic nanoemulsion loaded with zinc phthalocyanine for synergic use in skin cancer treatment. Journal of Magnetism and Magnetic Materials. 320 (2008), 211-214.

Probst, R.J.; Lim, J.M.; Bird, D.N.; Pole, G.L.; Sato, A.K. and Claybaugh, J.R. Gender differences in the blood volume of conscious Sprague-Dawley rats. Journal of the American Association for Laboratory Animal Science. 45 (2006), 49-52.

Pugh, W. J.; Hadgraft, J. and Roberts, M. S. Dermal Absorption and Toxicity Assessment. Marcek Dekker, New York, 1998.

Pygall, S.R.; Griffiths, P.C.; Wolf, B.; Timmins, P. and Melia, C.D. Solution interactions of diclofenac sodium and meclofenamic acid sodium with hydroxypropyl methylcellulose (HPMC). International Journal of Pharmaceutics. 405 (2011), 55-62.

Qin, M.; Liu, S.; Liu, Z. and Hu, X. Resonance Rayleigh scattering spectra, non-linear scattering spectra of tetracaine hydrochloride–erythrosin system and its analytical application. SpectroChimica Acta Part A. 71 (2009), 2063-2068.

Qin, W.; Jiao, Z.; Zhong, M.; Shi, X.; Zhang, J.; Li, Z. and Cui, X. Simultaneous determination of procaine, lidocaine, ropivacaine, tetracaine and bupivacaine in human plasma by high-performance liquid chromatography. Journal of Chromatography B. 878 (2010), 1185-1189.

Racansky, V.; Bederova, E. and Piskova, L. The influence of local anesthetics on the gel-liquid crystal phase transition in model dipalmitoylphosphatidylcholine membranes. General Physiology and Biophysics. 7 (1988), 217–221.

Rancan, F.; Papakostas, D.; Hadam, S.; Hackbarth, S.; Delair, T.; Primard, C.; Verrier, B.; Sterry, W.; Blume-Peytavi, U. and Vogt, A. Investigation of polylactic acid (PLA) nanoparticles as drug delivery systems for local dermatotherapy. Pharmaceutical Research. 26 (2009), 2027-2036.

Rawlings, A.; Watkinson, A.; Harding, C.; Ackerman, C.; Banks, J.; Hope, J. and Scott, I. Changes in stratum corneum lipid and desmosome structure together with water barrier function during mechanical stress. Journal Society Cosmetic Chemists. 46 (1995), 141-151.

Reid, M.L.; Brown, M.B.; Moss, G.P. and Jones, S.A. An investigation into solvent-membrane interactions when assessing drug release from organic vehicles using regenerated cellulose membranes. Journal of Pharmacy and Pharmacology. 60 (2008), 1139-1147.

Reiss, V.W.; Schmid, K.; Botta, L.; Kobayashi, K.; Moppert, J.; Schneider, W.; Sioufi, A.; Strusberg, A. and Tomasi, M. Die perkutane resorption von diclofenac. Arzneim Forsch. 36 (1986), 1092–1096.

Ren-Jiunn, W.; Yaw-Bin, H.; Pao-Chu, W.; Jia-You, F. and Yi-Hung, T. The effects of iontophoresis and electroporation on transdermal delivery of indomethacin evaluated in vitro and in vivo. Journal of Food and Drug Analysis. 15 (2007), 126-132.

Riviere, J.E.; Monteiro-Riviere, N.A. and Inman, A.O. Determination of lidocaine concentrations in skin after transdermal iontophoresis: effects of vasoactive drugs. Pharmaceutical Research. 9 (1992), 211-214.

Riviere, J.E.; Sage, B. and Williams, P.L. Effects of vasoactive drugs on transdermal lidocaine iontophoresis. Journal of Pharmaceutical Sciences. 80 (1991), 615-620.

Richter, T.; Muller, J.; Schwarz, U.; Wepf, R. and Wiesendanger, R. Investigation of the swelling of human skin cells in liquid media by tapping mode scanning force microscopy. Applied Physics A. 72 (2001), 125–128.

Ritschel, W.A. and Hussain, A.S. The principles of permeation of substances across the skin. Methods and Findings in Experimental and Clinical Pharmacology. 10 (1988), 39-56.

Robert, ML.; Gang, D.; Peishu, Z. and George, FM. Hairless micropig skin. American Journal of Pathology. 138 (1991), 687-697.

Roberts, M.E. and Mueller, K.R. Comparisons of in vitro nitroglycerin (TNG) flux across Yucatan pig, hairless mouse, and human skin. Pharmaceutical Research. 7 (1990), 673-676.

Roberts, M.S. Percutaneous absorption of phenolic compounds. Ph.D. Thesis, University of Sidney, Australia (1976).

Roberts, M.S. Structure-permeability considerations in percutaneous absorption. IBC Technical Services, London, 1991.

Roberts, M. S. and Cross, S. E. A physiological pharmacokinetic model for solute disposition in tissues below a topical application site. Pharmaceutical Research. 16 (1999), 1392-1398.

Roberts, M.S.; Cross, S.E. and Anissimov, Y.G. The skin reservoir for topically applied products, Taylor and Francis, Boca Raton, 2005.

Roberts, M.S.; Cross, S.E. and Pellett, M.A. Skin transport. Dermatological and transdermal preparations. Informa Healthcare, New York, 2002.

Roberts, M.S.; Pugh, W.J. and Hadgraft, J. Epidermal permeability: penetrant structure relationships. 2. The effect of H-bonding groups in penetrants on their diffusion through the stratum corneum. International Journal of Pharmaceutics. 132 (1996), 23-32.

Rossetti, F.C.; Lopes, L.B.; Carollo, A.R.; Thomazini, J.A.; Tedesco, A.C. and Bentley, M.V. A delivery system to avoid self-aggregation and to improve in vitro and in vivo skin delivery of a phthalocyanine derivative used in the photodynamic therapy. Journal of Controlled Release. 155 (2011), 400-408.

Rothbard, J.B.; Garlington, S.; Lin, Q.; Kirschberg, T.; Kreider, E.; McGrane, P.L.; Wender, P.A. and Khavari, P.A. Conjugation of arginine oligomers to cyclosporin a facilitates topical delivery and inhibition of inflammation. Nature Medicine. 6 (2000), 1253–1257.

Rougier, A.; Dupuis, D.; Lotte, C.; Roguet, R. and Schaefer, H. In vivo correlation between stratum corneum reservoir function and percutaneous absorption. Journal of Investigative Dermatology. 81 (1983), 275-278.

Rougier, A. and Lotte, C. Predictive approaches I, the stripping technique. Plenum Press, New York, 1993.

Rougier, A.; Lotte, C.; Corcuff, P. and Maibach, H.I. Relationship between skin permeability and corneocyte size according to anatomic site, age and sex in man. Journal of the Society of Cosmetic Chemists. 39 (1988), 15–26.

Rowland, M. and Tozer, T.N. Assessment of AUC. Clinical Pharmacokinetics: Concepts and Applications. Lippincott Williams and Wilkins, Philadelphia, 1995.

Roy, S.D.; Fujiki, J. and Fleitman, J.S. Permeabilities of alkyl p-aminobenzoates through living skin equivalent and cadaver skin. Journal of Pharmaceutical Sciences. 82 (1993), 1266-1268.

Russell, L.M. and Guy, R.H. Measurement and prediction of the rate and extent of drug delivery into and through the skin. Expert Opinion on Drug Delivery. 6 (2009), 355-369.

Sakaeda, T.; Fukumura, K.; Takahashi, K.; Matsumura, S.; Matsuura, E. and Hirano, K. Blood flow rate in normal and tumor-bearing rats in conscious state, under urethane anesthesia and during systemic hypothermia. Journal of Drug Targeting. 6 (1998), 261-272.

Salim, N.; Basri, M.; Rahman, M.; Abdullah, D.K. and Basri, H. Modification of palm kernel oil esters nanoemulsions with hydrocolloid gum for enhanced topical delivery of ibuprofen. International Journal of Nanomedicine. 7 (2012), 4739–4747.

Sang-Chul, S.; Cheong-Weon, C. and Jung-Shik, C. Development of the bioadhesive tetracaine gels for enhanced local anesthetic effects. Drug Development and Industrial Pharmacy. 9 (2004), 931–936.

Sassi, A.; Beltran, S.; Hooper, H.; Blanch, H.; Prausnitz, J. and Siegel, R. Monte Carlo simulations of hydrophobic weak polyelectrolytes: Titration properties and pH-induced structural transitions for polymers containing weak electrolytes. Journal of Chemical Physics. 97 (1992), 8767-8774.

Sato, K.; Sugibayashi, K. and Morimoto,Y. Species differences in percutaneous absorption of nicorandil. Journal of Pharmaceutical Sciences. 80 (1991), 104–107.

Scf-online [homepage on the Internet]. Daniels R. [cited 2007 June 15]. Available from: http://www.scf-online.com/english/37_e/skinpenetration37_ e.htm.

Schaefer, H. and Lademann, J. The role of follicular penetration. A differential view. Skin Pharmacology and Applied Skin Physiology. 14 (2001), 23-27.

Schaefer, H. and Stuttgen, G. Absolute concentrations of an antimycotic agent, econazole, in the human skin after local application. Drug Research. 26 (1976), 432–435.

Schaefer, H.; Stuttgen, G.; Zesch. A.; Schalla,W. and Gazith, J. Quantitative determination of percutaneous absorption of radiolabeled drugs in vitro and in vivo by human skin. Current Problems in Dermatology. 7 (1978), 80-94.

Schäfer-Korting, M.; Mehnert, W. and Korting, H.C. Lipid nanoparticles for improved topical application of drugs for skin diseases, Advanced Drug Delivery Reviews. 59 (2007), 427-430.

Scheuplein, R.J. Mechanism of percutaneous absorption. Transient diffusion and relative importance of various routes of skin penetration. Journal of Investigative Dermatology. 48 (1967), 79.

Scheuplein, R.J and Blank, I.H. Permeability of the skin. Physiological Reviews. 51 (1971), 702-747.

Scheuplein, R.J.; Blank, I.H.; Brauner, G. and MacFarlane, D. Percutaneous absorption of steroids. Journal of Investigative Dermatology. 52 (1969), 63-70.

Schmook, F.P.; Meingassner, J.G. and Billich, A. Comparison of human skin or epidermis models with human and animal skin in in vitro percutaneous absorption. International Journal of Pharmacy. 215 (2001), 51-56.

Schneider, W. and Degen, P.H. Simultaneous determination of diclofenac sodium and its metabolites in plasma by capillary column gas chromatography with electron-capture detection. Journal of Chromatography. 383 (1986), 412-418.

Schnetz, E. and Fartasch, M. Microdialysis for the evaluation of penetration through the human skin barrier–a promising tool for future research?. European Journal of Pharmaceutical Sciences. 12 (2001), 165–174.

Schreier, S.; Malheiros, S. and Paula, E. Surface active drugs: self-association and interaction with membranes and surfactants. Physicochemical and biological aspects. Biochimica et Biophysica. 1508 (2000), 210-234.

Schwarb, F.P.; Gabard, B.; Rufli, T. and Surber, C. Percutaneous absorption of salicylic acid in man after topical administration of three different formulations. Dermatology. 198 (1999), 44-51.

Scott, D.B.; Jebson, P.R. and Braid, D.P. Factors affecting plasma levels of lignocaine and prilocaine. British Journal of Anaesthesia. 44 (1972), 1040-1049.

Sekkat, N. and Guy, R.H. Biological models to study skin permeation. Pharmacokinetic optimization in drug research. Wiley-VCH and VHCA, Zurich, 2001.

Sengupta, S.; Banerjee, S.; Sinha, B. and Mukherjee, B. Improved skin penetration using in situ nanoparticulate diclofenac diethylamine in hydrogel systems: in vitro and in vivo studies. AAPS PharmSci Tech, 2015.

Sennhenn, B.; Giese, K.; Plamann, K.; Harendt, N. and Kolmel, K. In vivo evaluation of the penetration of topically applied drugs into human skin by spectroscopic methods. Skin Pharmacology. 6 (1993), 152–160.

Shah, V.P. Bioequivalence of topical dermatological dosage forms- methods of evaluation of bioequivalence. Skin Pharmacology and Applied Skin Physiology. 11 (1998), 117-124.

Shah, V.P.; Flynn, G.L.; Yacobi, A.; Maibach, H.I.; Bon, C.; Fleischer, N.M.; Franz, T.J.; Kaplan, S.A.; Kawamoto, J.; Lesko, L.J.; Marty, J.-P.; Pershing, L.K.; Schaefer, H.; Sequeira, J.A.; Shrivastava, S.P.; Wilkin, J. and Williams, R.L. Bioequivalence of topical dermatological dosage forms-methods of evaluation of bioequivalence. Pharmaceutical Research. 15 (1998), 167-171.

Shao, Z.; Li, Y.; Krishnamoorthy, R.; Chermak, T. and Mitra, A.K. Differential effects of anionic, cationic, nonionic, and physiologic surfactants on the dissociation, α-chymotryptic degradation, and enteral absorption of insulin hexamers. Pharmaceutical research. 10 (1993), 243-251.

Sheth, N.; McKeogh, S. and Spruance, S. Measurement of the stratum corneum drug reservoir to predict the therapeutic efficacy of topical iododeoxyuridine for herpes simplex virus infection. Journal of Investigative Dermatology. 89 (1987), 598-602.

Shigeta, K.; Olsson, U. and Kunieda, H. Effect of alcohols (propanol, propylene glycol, and glycerol) on cloud point and micellar structure in long-poly(oxyethylene)n oleyl ethers systems. Proceedings of the International Conference on Colloid and Surface Science. 5 (2000), 93-96.

Shinoda, K.; Yamagushi, T. and Hori, R. The surface tension and the critical micelle concentration in aqueous in aqueous solution of β-D-alkyl glucosides and their mixtures. Bulletin of the Chemical Society of Japan. 34 (1961), 237.

Shivanand, P. Various emerging technologies in insulin delivery system. International Journal of Pharmaceutical Sciences Review and Research. 2 (2010), 14–16.

Shomaker, T.S.; Zhang, J. and Ashburn, M.A. Assessing the impact of heat on the systemic delivery of fentanyl through the transdermal fentanyl delivery system. Pain Medicine. 1 (2000), 225-230.

Shore, P.A.; Brodie, B.B. and Hogben, C.A.M. The gastric secretion of drugs - a pH partition hypothesis. Journal of Pharmacology and Experimental Therapeutics. 119 (1957), 361-369.

Simon, G.A. and Maibach, H.I. Relevance of hairless mouse as an experimental model of percutaneous penetration in man, Skin Pharmacology and Applied Skin Physiology. 11 (1998), 80–86.

Singh, P. and Roberts, M.S. Dermal and underlying tissue pharmacokinetics of salicylic-acid after topical application. Journal of Pharmacokinetics and Biopharmaceutics. 21 (1993), 337-373.

Singh, P. and Roberts, M.S. Effects of vasoconstriction on dermal pharmacokinetics and local tissue distribution of compounds. Journal of Pharmaceutical Sciences. 83 (1994), 783-791.

Singh, P. and Roberts, M.S. Local deep tissue penetration of compounds after dermal application: structure-tissue penetration relationships. Journal of Pharmacology and Experimental Therapeutics. 27 (1996), 908–917.

Singh, S.; Zhao, K. and Singh , J. In vitro permeability and binding of hydrocarbons in pig ear and human abdominal skin. Drug and Chemical Toxicology. 25 (2002), 83-92.

Sintov, A.C.; Krymberk, I.; Daniel, D.; Hannan, T.; Sohn, Z. and Levin, G. Radiofrequency-driven skin microchanneling as a new way for electrically assisted transdermal delivery of hydrophilic drugs. Journal of Controlled Release. 89 (2003), 311-20.

Skagen, K. and Henriksen, O. Changes in subcutaneous blood flow during locally applied negative pressure to the skin. Acta Physiologica Scandinavica. 117 (1983), 411-414.

Smith, K.L. Penetrant characteristics influencing skin absorption. Methods for skin absorption. CRC Press, Boca Raton, 1990.

Spiliopoulos, S.; Katsanos, K.; Diamantopoulos, A.; Karnabatidis, D. and Siablis, D. Does ultrasound-guided lidocaine injection improve local anaesthesia before femoral artery catheterization?. Clinical Radiology. 66 (2011), 449-455.

Spruance, S.L.; Nett, R. and Marbury, T. Acyclovir cream for treatment of herpes simplex labialis: results of two randomized, double-blind, vehicle controlled, multicenter clinical trials. Antimicrobial Agents and Chemotherapy. 46 (2002), 2238-43.

Squillante, E.; Needham, T.; Maniar, A.; Kislalioglu, S. and Zia, H. Co-diffusion of propylene glycol and dimethyl isosorbide in hairless mouse skin. European Journal of Pharmaceutics and Biopharmaceutics. 46 (1998), 265-271.

Stinchcomb, A.L.; Pirot, F.; Touraille, G.D.; Bunge, A.L. and Guy, R.H. Chemical uptake into human stratum corneum in vivo from volatile and non-volatile solvents. Pharmaceutical Research. 16 (1999), 1288-1293.

Stuttgen, G. The present status of anti-inflammatory agents in dermatology. Drugs. 36 (1998), 49-50.

Sugibayashi, K.; Yanagimoto, G.; Hayashi, T.; Seki, T.; Juni, K. and Morimoto, Y. Analysis of skin disposition of flurbiprofen after topical application in hairless rats. Journal of Controlled Release. 62 (1999), 193-200.

Surber, C.; Schwarb, F.P. and Smith, E.W. Tape-stripping technique. Journal of Toxicology, Cutaneous and Ocular Toxicology. 20 (2001), 461–474.

Surber, C.; Wilhelm, K.P.; Bermann, D. and Maibach, H.I. In-vivo skin penetration of acitretin in volunteers using 3 sampling techniques. Pharmaceutical Research. 10 (1993), 1291-1294.

Surber, C.; Wilhelm, K.P. and Maibach, H.I. In-vitro skin pharmacokinetics of acitretin: percutaneous absorption studies in intact and modified skin from three different species using different receptor solutions. Journal of Pharmacy and Pharmacology. 43 (1991), 836–840.

Svedman, P. Transdermal perfusion of fluids. Patent (serial number U.S. 5,441,490), 1995.

Svedman, P.; Lundin, S.; Hoglund, P.; Hammarlund, C.; Malmros, C. and Pantzar, N. Passive drug diffusion via standardized skin mini-erosion; methodological aspects and clinical findings with new device. Pharmaceutical Research. 13 (1996), 1354–1359.

Svedman, P.; Lunin, S. and Svedman, C. Administration of antidiuretic peptide (DDVAP) byway of suction de-epithelialised skin. Lancet. 337 (1991), 1506– 1509.

Swayer, J.; Febbraro, S.; Masud, S.; Ashburn, M. and Campbell, J. Heated lidocaine/tetracaine patch (SyneraTM, RapydanTM) compared with lidocaine/prilocaine cream (EMLAw) for topical anaesthesia before vascular access. British Journal of Anesthesia. 102 (2009), 210-15.

Sznitowska, M.; Janicki, S. and Baczek, A. Studies on the effect of pH on the lipoidal route of penetration across stratum corneum. Journal of Controlled Release. 76 (2001), 327-335.

Tanford, C. The hydrophobic effect: formation of micelles and biological membranes. Wiley-Interscience, New York, 1980.

Tanner, T. and Marks, R. Delivering drugs by the transdermal route: review and comment. Skin Research and Technology. 14 (2008), 249-260.

Thomas, B.J. and Finnin, B.C. The transdermal revolution. Drug Discovery Today. 9 (2004), 697–703.

Thomas, I.R.; Bruno, I.J.; Cole, J.C.; Macrae, C.F.; Pidcock, E. and Wood, P.A. WebCSD: the online portal to the Cambridge Structural Database. Journal of Applied Crystallography. 43 (2010), 362-366.

Thune, P.; Nilsen, T.; Hanstad, I.K.; Gustavsen, T. and Dahl, H.L. The water barrier function of the skin in relation to water content of stratum corneum, pH and skin lipids. Acta Dermato-Venereologica. 68 (1988), 277–283.

Tiemessen, H. Percutaneous absorption: animal skin models versus in vitro models using human skin. Dermal and transdermal drug delivery. Wissenschaftliche Verlagsgesellschaft, Stuttgart, 1993.

Timmers, M.S.; Le Cessie, S.; Banwell, P. and Jukema, G.N. The effects of varying degrees of pressure delivered by negative-pressure wound therapy on skin perfusion. Annals of Plastic Surgery. 55 (2005), 665-671.

Todo, H.; Kimura, E.; Yasuno, H.; Tokudome, Y.; Hashimoto, F. and Ikarashi, Y. Permeation pathway of macromolecules and nanospheres through skin. Biological and Pharmaceutic Bulletin. 33 (2010), 1394-1399.

Toll, R.; Jacobi, U.; Richter , H.; Lademann, J.; Schaefer, H. and Blume-Peytavi, U. Penetration profile of microspheres in follicular targeting of terminal hair follicles. Journal of Investigative Dermatology. 123 (2004), 168–176.

Torrez-Lopez, J.E.; Robles, M.B.; Perez-Urizar, J. and Forsh, Arzneim. Determination of diclofenac in micro-whole blood samples by high-performance liquid chromatography with electrochemical detection. Application in a pharmacokinetic study. Drug Research. 47 (1997), 1040-1043.

Treffèl, P.; Panisset, F.; Humbert, P.; Remoussenard, O.; Bechtel, Y. and Agache, P. Effèct of pressure on in vitro percutaneous absorption of caffèine. Acta Dermato-Venereologica. 73 (1993), 200-202.

Trommer, H. and Neubert, R.H. Overcoming the stratum corneum: the modulation of skin penetration. A review. Skin Pharmacology and Physiology. 19 (2006), 106-21.

Trottet, L.; Merly, C.; Mirza, M.; Hadgraft, J. and Davis, A.F. Effèct of finite doses of propylene glycol on enhancement of in vitro percutaneous permeation of loperamide hydrochloride. International Journal of Pharmaceutics. 274 (2004), 213-219.

Tsai, J.C.; Chuang, S.A.; Hsu, M.Y. and Sheu, H.M. Distribution of salicylic acid in human stratum corneum following topical application in vivo: a comparison of six different formulations. International Journal of Pharmaceutics. 188 (1999), 145-153.

Twist, J.N. and Zatz, J.L. Influence of solvents on paraben permeation through idealized skin model membranes. Journal of the Society of Cosmetic Chemists of Japan. 37 (1986), 429-444.

Tzanavaras, P. and Themelis, D. High-throughput HPLC assay of acyclovir and its major impurity guanine using a monolithic column and a flow gradient approach. Journal of Pharmaceutical and Biomedical Analysis. 43 (2007), 1526-1530.

Ueda, K.; Hihashi, K.; Limwikrant, W.; Sekine, S.; Horie, T.; Yamamoto, K. and Moribe, K. Mechanistic differences in the permeation behaviour of supersaturated and solubilized solutions of carbamazepine revealed by nuclear magnetic resonance measurements. Molecular Pharmaceutics. 9 (2012), 3012-3033.

Umeda, Y.; Fukami, T.; Furuishi, T.; Suzuki, T.; Makimura, M. and Tomono, K. Molecular complex consisting of two typical external medicines: intermolecular interaction between indomethacin and lidocaine. Chemical and Pharmaceutical Bulletin. 55 (2007), 832-836.

Valenta, C.; Siman, U.; Kratzel, M. and Hadgraft, J. The dermal delivery of lignocaine: influence of ion pairing. International Journal of Pharmaceutics. 197 (2000), 77-85.

Valiveti, S.; Wesley, J. and Lu, G.W. Investigation of drug partition property in artificial sebum. International Journal of Pharmaceutics. 346 (2008), 10-16.

van den Akker, J.T.; Iani, V.; Star, W.M.; Sterenborg, H.J and Moan, J. Topical application of 5-aminolevulinic acid hexyl ester and 5-aminolevulinic acid to normal nude mouse skin: differences in protoporphyrin IX fluorescence kinetics and the role of the stratum corneum. Photochemistry and Photobiology. 72 (2000), 681-689.

Van der Leun, J.C.; Beerens, E.G.J.; Lowe, L.B.J. Repair of dermal-epidermal adherence: a rapid process observed in experiments on blistering with interrupted suction. Journal of Investigative Dermatology. 63 (1974), 397-401.

van der Merwe, D.; Brooks, J.D.; Gehring, R.; Baynes, R.E.; Monteiro-Riviere, N.A. and Riviere, J.E. A Physiologically based pharmacokinetic model of organophosphate dermal absorption. Toxicological Sciences. 89 (2006), 188-204.

van den Merwe, E. and Ackermann, C. Physical changes in hydrated skin. International Journal of Cosmetic Science. 9 (1987), 237-247.

van der Molen, R.G.; Spies, F.; van't Noordende, J.M.; Boelsma, E.; Mommaas, A.M. and Koerten, H.K. Tape stripping of human stratum corneum yields cell layers that originate from various depths because of furrows in the skin. Archives of Dermatological Research. 289 (1997), 514–518.

van de Water, F.M.; Boerman, O.C.; Wouterse, A.C.; Peters, J.G.; Russel, F.G. and Masereeuw, R. Intravenously administered short interfering RNA accumulates in the kidney and selectively suppresses gene function in renal proximal tubules. Drug metabolism and disposition: the final fate of chemicals. 34 (2006), 1393-1397.

Vemula, V. and Sharma, P. RP-HPLC method development and validation for simultaneous estimation of diclofenac and tolperisone in tablet dosage form. Asian Journal of Pharmaceutical and Clinical Research. 6 (2013), 186-189.

Verbiese, N. Methods for assessing percutaneous absorption- The report and recommendations of ECVAM workshop 13. Atla-Alternatives to Laboratory Animals. 24 (1996), 81-106.

Vogt, A.; Combadiere, B.; Hadam, S.; Stieler, K.M.; Lademann, J.; Schaefer, H.; Autran, B.; Sterry, W. and Blume-Peytavi, U. 40 nm, but not 750 or 1,500 nm, nanoparticles enter epidermal CD1a+ cells after transcutaneous application on human skin. Journal of Investigative Dermatology. 126 (2006), 1316–1322.

Vogt, A.; Mandt, N.; Lademann, J.; Schaefer, H. and Blume-Peytavi, U. Follicular targeting-A promising tool in selective dermatotherapy. Journal of Investigative Dermatology Symposium Proceedings. 10 (2005), 252–255.

Wade, A. and Weller, P. Handbook of Pharmaceutical Excipients. American Pharmaceutical Association,Washington D.C, 1995.

Walters, K.A. Dermatological and transdermal formulations. Marcel Dekker, New York, 2002.

Wang, C.Y.; Hu, X.Y.; Jin, G.D. and Leng, Z.Z. Differential pulse adsorption voltammetry for determination of procaine hydrochloride at a pumice modified carbon paste electrode in pharmaceutical preparations and urine. Journal of Pharmaceutical and Biomedical Analysis. 30 (2002), 131-139.

Wang, J., Lu, J., Zhang, Li., Hu, Y. Determination of cetylpyridinium chloride and tetracaine hydrochloride in buccal tablets by RP-HPLC. Journal of Pharmaceutical and Biomedical Analysis. 32 (2003), 381-386.

Washington, N. Transdermal drug delivery. Taylor & Francis Group, London, 2001.

Weber, L. The penetration of 2,3,7,8-tetrachlorodibenzo-p-dioxin into viable and non-viable porcine skin in vitro. Toxicology. 84 (1993), 125-140.

Weigmann, J.-H.; Lademann, J.; Meffert, H.; Schaefer, H. and Sterry, W. Determination of the horny layer profile by tape stripping in combination with optical spectroscopy in the visible range as a prerequisite to quantify percutaneous absorption. Skin Pharmacology and Applied Skin Physiology. 12 (1999), 34–45.

Wepierre, J. Actualites Pharmacologiques. Masson, Paris, 1979.

Wermeling, D.P.; Banks, S.L.; Hudson, D.A.; Gill, H.S.; Gupta, J.; Prausnitz, M.R. and Stinchcomb, A. Microneedles permit transdermal delivery of a skin-impermeant medication to humans. Proceedings of the National Academy of Sciences, USA. 105 (2008), 2058-2063.

Wester, R.C.; Maibach, H.I.; Melendres, J.; Sedik, L.; Knaak, J. and Wang, R. In vivo and in vitro percutaneous absorption and skin evaporation of isofenphos in man. Fundamental and Applied Toxicology. 19 (1992), 521-526.

Wester, R.C.; Melendres, J.; Sedik, L.; Maibach, H.I. and Riviere, J.E. Percutaneous absorption of salicylic acid, theophylline, 2,4-dimethylamine, diethyl hexyl phthalic acid, and p-aminobenzoic acid in the isolated perfused porcine skin flap compared to man in vivo. Toxicology and Applied Pharmacology. 151 (1998), 159-165.

Wiechers, J.W. The barrier function of the skin in relation to percutaneous absorption of drugs. Pharmaceutisch Weekblad. Scientific Edition. 11 (1989), 85-98.

Wilke, K.; Wepf, R.; Keil, F.J.; Wittern, K.P.; Wenck, H. and Biel, S.S. Are sweat glands an alternate penetration pathway? Understanding the morphological complexity of the axillary sweat gland apparatus. Skin Pharmacology and Physiology. 19 (2006), 38-49.

Williams, A.C. Transdermal and topical drug delivery. Pharmaceutical Press, London, 2003.

Williams, A.C. and Barry, B.W. Terpenes and the lipid-protein-partitioning theory of skin penetration enhancement. Pharmaceutical Research. 8 (1991), 17-24.

Winter, C.A.; Risley, E.A. and Nuss, G.W. Carrageenin-induced edema in hind paw of the rat as an assay for anti-inflammatory drugs. Proceedings of the Society for Experimental Biology and Medicine. 111 (1962), 544–547.

Woan-Ruoh, L.; Tai-Long, P.; Pei-Wen, W.; Rou-Zi, Z.; Chun-Ming, H. and Jia-You, F. Erbium:YAG laser enhances transdermal peptide delivery and skin vaccination. Journal of Controlled Release. 128 (2008), 200-208.

Wojciechowski, Z.J., Burton, S.A.; Petelenz, T.J. and Krueger, G.G. Role of microcirculation in percutaneous absorption. Clinical Research. 33 (1985), 696 A.

Wu, P.; Huang, Y.; Fang, J. and Tsai, Y. Percutaneous absorption of captopril from hydrophilic cellulose derivatives through excised rabbit skin and human skin. Drug Development and Industrial Pharmacy. 24 (1998), 179–182.

Wu, X-M.; Todo, H. and Sugibayashi, K. Effects of pretreatment of needle puncture and sandpaper abrasion on the in vitro skin permeation of fluorescein isothiocyanate (FTIC)-dextran. International Journal of Pharmaceutics. 316 (2006), 102-108.

Wu, X-M.; Todo, H. and Sugibayashi, K. Enhancement of skin permeation of high molecular compounds by a combination of microneedle pretreatment and iontophoresis. Journal of Controlled Release. 118 (2007), 189-195.

Wuon-Ruoh, L.; Tai-Long, P.; Pei-Wen, W.; Rou-Zi, Z.; Chun-Ming, H. and Jia-You, F. Erbium:YAG laser enhances transdermal peptide delivery and skin vaccination. Journal of Controlled Release. 128 (2008) 200–208.

Yang, M.; Zou, Y.; Yu, S. and Li, X. A novel chemiluminescent system of acyclovir-H_2O_2-Co(II) and its application. Fenxi Huaxue. 9 (2004), 1237-1239.

Yeo, J.M. and Fiddian, A.P. Acyclovir in the management of herpes labialis. Journal of Antimicrobial and Chemotherapy. 12 (1983), 95-103.

Ying-Zhe, L.; Ying-shu, Q.; Lei, Z.; Mei-na, J.; Fumio, K.; Hidemasa, K.; Sadami, T. and Akira, Y. Trypsin as a novel potential absorption enhancer for improving the transdermal delivery of macromolecules. Journal of Pharmacy and Pharmacology. 61 (2009), 1005-1012.

Yotsuyanagi, T. and Higuchi, W.I. A two phase series model for the transport of steroids across the fully hydrated stratum corneum. Journal of Pharmacy and Pharmacology. 24 (1972), 934-941.

Yuan, Y. Cross flow filtration of natural organic matter (NOM), polysaccharides and silica colloids: transport, fouling and mixture effects. Rensselaer Polytechnic Institute, 2007.

Zatz, J. Assessment of vehicle factors influencing percutaneous absorption. In Vitro Percutaneous Absorption: Principles, Fundamentals and Applications. CRC Press, Boca Raton, 1991.

Zecca, L.; Ferrario, P. and Costi, P. Determination of diclofenac and its metabolites in plasma and cerebrospinal fluid by high-performance liquid chromatography with electrochemical detection. Journal of Chromatography. 567 (1991), 425–432.

Zhai, H. and Maibach, H.I. Effects of skin occlusion on percutaneous absorption: an overview. Skin Pharmacology and Applied Skin Physiology. 14 (2001), 1-10.

Zhang, J.; Hadlock, T.; Gent, A. and Strichartz, G.R. Tetracaine membrane interactions: effects of lipid composition and phase on drug partitioning, location and ionization. Biophysical Journal. 92 (2007), 3988-4001.

Zhang, Q.; Grice, J.; Li, P.; Jepps, O.; Wang, G. and Roberts, M. Skin solubility determines maximum transepidermal flux for similar size molecules. Journal of Pharmaceutical Research. 26 (2009), 1974-1985.

Zhang, S.S.; Yuan, Z.B.; Liu, H.X.; Zou, H.; Xiong, H. and Wu, Y.J. Analysis of acyclovir by high performance capillary electrophoresis with on-column amperometric detection. Electrophoresis. 14 (2000), 2995-2998.